# Influence of polyunsaturated fatty acids on fluconazole susceptibility and drug efflux in *Candida krusei*

by

**Abdullahi Temitope Jamiu**

Submitted in fulfilment of the requirements for the degree

**Magister Scientiae**

In the

Department of Microbial, Biochemical and Food Biotechnology

Faculty of Natural and Agricultural Sciences

University of the Free State

Bloemfontein

South Africa

**February 2021**

**Supervisor: Prof. C.H. Pohl-Albertyn**

**Co-Supervisors: Prof. J. Albertyn**

**Mr. E. Bisschoff**

UNIVERSITY OF THE FREE STATE
UNIVERSITEIT VAN DIE VRYSTAAT
YUNIVESITHI YA FREISTATA

UFS·UV
NATURAL AND AGRICULTURAL SCIENCES
NATUUR- EN LANDBOUWETENSKAPPE
MICROBIAL, BIOCHEMICAL AND FOOD BIOTECHNOLOGY
MIKROBIESE, BIOCHEMIESE EN VOEDSELBIOTEGNOLOGIE

Globally, fungal infections affect more than one billion people annually, with an estimated mortality of approximately two million people. The genus *Candida* is a highly heterogeneous group containing several opportunistic pathogens responsible for the increasing number of life-threatening mycoses, especially in immunocompromised subjects, including cancer patients, human immunodeficiency virus (HIV) positive patients, and organ transplant recipients. Compared to antibacterial counterparts, the number of available antifungals is limited, and the increase in antifungal resistance further complicates this. Resistance or tolerance towards all the available classes of antifungals has been reported. Strikingly, *Candida krusei* exhibits innate resistance to fluconazole (FLC) and rapid adaptive resistance to other antifungal drugs. Moreover, the role of efflux pumps (e.g. ATP-binding cassette 1, Abc1p) in this inherent FLC resistance remains unclear. This yeast also forms biofilms, which are potentially more resistant to antifungal drugs than planktonic counterparts. Additionally, there is paucity of information on the ability of exogenous polyunsaturated fatty acids (PUFAs) to overcome intrinsic antifungal resistance, such as in the case of *C. krusei*.

In order to address this lack of knowledge, we firstly determined the susceptibility profiles of biofilms of *C. krusei* strains (and a *C. albicans* reference strain) towards FLC and five PUFAs [i.e. oleic acid (OA), linoleic (LA), gamma-linolenic acid (GLA), arachidonic acid (AA), and eicosapentaenoic (EPA)]. Our results showed that the antifungal activity of FLC against these strains is concentration-dependent, with *C. krusei* UFS Y-0277 displaying the least susceptibility. Moreover, the antifungal effect of the PUFAs is dependent on the strain, as well as on the chain length and dose of the fatty acid, with LA and GLA showing the most favourable activity. Upon combination therapy assay, we found that either of the two superior PUFAs (LA or GLA) potentiates the action of FLC towards the biofilms of the most-resistant strain of *C. krusei*. An initial attempt to examine the mechanism responsible for this revealed that the combination treatments induce the production of extracellular vesicles, cell membrane damage, and cell rupture. A subsequent membrane integrity assay confirmed this deleterious impact on the cell membrane. Our results also showed that antioxidants are capable of protecting *C. krusei* biofilms from the deleterious effects of the combination treatments. Additionally, these treatments had an inhibitory influence on the activity of efflux pumps, which was directly proportional to the concentration of PUFA used. Furthermore, our *in vitro* findings were corroborated by *in vivo* assays in a *Caenorhabditis elegans* infection model, which demonstrated that the combination treatments promote the overall survival and significantly reduce the intestinal fungal burden of infected nematodes. These observations may reiterate the combination of fatty acids with conventional antifungal drugs as a favourable therapeutic strategy deserving of increased traction and research for resistance reversal and infection

control.

We also aimed to establish a Clustered Regularly Interspaced Short Palindromic Repeats-Cas associated protein 9 (CRISPR-Cas9)-mediated gene-editing system for *C. krusei* since the absence of such system has impeded genome engineering, resistance, and virulence studies in this yeast. This was performed through the adaptation of a previously designed *C. albicans*-specific, CRISPR-Cas9 system (HIS-FLP type). This system's efficacy for gene-editing was validated by the successful homozygous deletion of two auxotrophic marker genes, *URA3* and *ADE2*, in this yeast. Using the adapted system, we attempted to construct a Green Fluorescent Fusion (GFP) fusion of Abc1p to assess the influence of AA and FLC on the localisation, expression, and activity of Abc1p – in order to gain better insights into the role of this efflux pump in FLC resistance. However, this was unsuccessful, possibly due to the failure of the yeast to incorporate the supplied *ABC1*-GFP fusion donor DNA (dDNA). Hence, we resorted to using western blot analysis and efflux pump assay. Results obtained demonstrate that FLC increases the expression and functionality of Abc1p, suggesting that this transporter plays a role in FLC resistance. However, AA reduces the expression of Abc1p, and abrogates its activity in a dose-dependent manner, even in the presence of FLC. These findings highlight AA as a potential inhibitor of Abc1p and lent credence to the role of this transporter in FLC resistance.

Taken together, this study demonstrates the FLC-potentiating activity of PUFAs against an intrinsically-resistant *C. krusei in vitro* and *in vivo* in a *C. elegans* infection model – which may pave the way for future studies into novel therapeutic strategies. It also establishes a successful development of a CRISPR-Cas9 system for *C. krusei*. Although preliminary findings demonstrate the involvement of Abc1p in FLC resistance and show the potential of AA as an inhibitor of this transporter, further studies are necessary for a definitive assertion.

**Keywords:** *Candida krusei*, biofilm, antifungal resistance, polyunsaturated fatty acids, fluconazole susceptibility, combination therapy, *Caenorhabditis elegans*, CRISPR-Cas9 system, Abc1p

Every year, fungal infections, although less studied compared to bacterial infections, kill up to two million people. More worrisome is that many fungi are becoming increasingly resistant due to the extended and indiscriminate use of the limited available antifungals. For example, *Candida krusei*, a yeast (fungus) displays a natural resistance to FLC (fluconazole) – the most commonly used antifungal due to its affordability, low toxicity, and excellent efficacy. This yeast also develops an acquired (secondary) resistance to other antifungal drugs. Such resistance increases the risks of treatment failures, resulting in long-term hospitalisation, increased economic burden, and reduced quality of lives. Hence, there is an urgent need to develop effective therapeutic options and the complementary usage of antifungals (e.g. FLC) with natural compounds, such as polyunsaturated fatty acids (PUFAs), might offer more effective therapy. Hence, we evaluated the effect of the combination of FLC and PUFAs on FLC resistance of *C. krusei*. We found that when combined with FLC, either of two PUFAs (linoleic acid or gamma-linolenic acid) potentiates the susceptibility of *C. krusei* biofilms to FLC (i.e. combination of a PUFA with FLC enhanced the killing of *C. krusei* compared to when FLC is used alone). Furthermore, we designed a gene-editing tool (CRISPR-Cas9 system) for *C. krusei*, a system which was previously absent in this yeast. Our study also demonstrated that Abc1p transporter is vital for FLC-resistance in *C. krusei* and that arachidonic acid (a type of PUFA) is a potential inhibitor of this transporter. Together, this study provides answers to some key research questions and sets the pace for future investigations into overcoming antifungal resistance.

## *DECLARATIONS*

I, Abdullahi Temitope Jamiu, declare that the Master's degree dissertation or interrelated, publishable manuscripts/published articles, or coursework Master's degree mini-dissertation that I herewith submit for the Master's degree qualification in Microbiology at the University of the Free State is my independent work and that I have not previously submitted to any faculty or institution of higher education for the attainment of any qualification.

I, Abdullahi Temitope Jamiu, hereby declare that all royalties regarding intellectual property that was developed during the course of, and/or in connection with the study at the University of the Free State, will accrue to the University.

---

**Abdullahi T. Jamiu**

abdullahijamiu45@gmail.com

## *DEDICATION*

*In the Name of Allah, the most Beneficent, the entirely Merciful. All praises and adorations are due the Lord of all worlds.*

**This work is dedicated to**

ALLAH (SWT) for bestowing me with the wellbeing, knowledge, and tenacity to complete this dissertation; HIS BELOVED PROPHET MUHAMMAD (peace and blessing be upon him, his household and companions), the quintessential role model and a mercy to mankind; and ALL SINCERE SEEKERS OF BENEFICIAL KNOWLEDGE in all realms of life.

"*This is a favour of Allah. He grants it to whomever He wills. And Allah is the Lord of infinite bounty*."
(Qur'an 62 vs 4)

***I would like to express my heartfelt gratitude to the following persons and institutions:***

- **Prof. Carolina Pohl-Albertyn**, for her unmatched guidance, support, motivation, and confidence throughout this study. For wonderfully unleashing my potential. I am truly grateful.
- **Prof. Jacobus Albertyn**, for his stellar mentorship, valuable input and everyday support
- **Mr. Eduvan Bisshoff**, for his brilliant input and guidance with the molecular aspect of this study
- **Prof. Olihile Sebolai**, for his assistance and everyday support
- **Dr. Oluwasegun Kuloyo**, for being a fantastic mentor and wingman
- **Dr. Ruan Fourie**, for his valuable discussions and pace-setting
- **Dr. Sabiu Saheed**, for his kindness, motivation, and moral support
- **Ms Nthabiseng Mokoena**, for her help with the nematodes
- **Mrs Aurelia Jansen**, at the UFS Yeast Culture Collection
- **Everyone in the Pathogenic Yeast Research Group**, for the great moments shared together
- **Ms Hanlie Grobler,** for her assistance with electron microscopy
- **Dr. Obinna Ezeokoli**, for his assistance with protein analyses
- **Dr. Wunmi Ogundeji**, for her help with fluorescence microscopy
- **Ms Toluwase Adedoja** and **Ms Gloria Kankam**, for their kindness and support
- **Dr. Samuel Folorunso**, for his support
- **The Department of Microbial, Biochemical and Food Biotechnology**, thank you for the enabling environment

## Financial assistance:

The financial assistance of the **National Research Foundation (**NRF) towards this research is hereby acknowledged (grant number 117435). Opinions expressed and conclusions arrived at, are those of the author and are not necessarily to be attributed to the NRF.

The financial assistance of the **South African Fryer Oil Initiative** (SAFOI) is also acknowledged.

## Personal Acknowledgements:

***A very special thank you to the following people:***

- My parents, ALHAJI ISHAQ JAMIU and ALHAJA KHADIJAH JAMIU, for their unwavering love, kindliness, prayer, and support. Most importantly, thank you for always believing in me!
- My uncles, MR. KUNLE ADEDIGBA and MR. RAHMAN OLARINDE, for their altruism, support, and guidance.
- MY SIBLINGS, thank you for your affection and never-ending support.
- THE SPECIAL ONE, thank you for being a wonderful backroom supporter!
- MY ENTIRE FAMILY**,** I thank you for your support.
- MUSA AKANBI, for leading the way!
- ALL DEAR FRIENDS, BROTHERS, AND SISTERS IN FAITH**,** you guys are amazing!
- TO OTHERS FAR AND WIDE**,** thank you for being part of this story "I am, because we are''.

This research was approved by the Biosafety & Environmental Research Ethics Committee of the University of the Free State with ethical clearance number: **UFS-ESD2019/0029**

- **Symposia & Conferences:**

  **AT Jamiu**, J Albertyn, OM Sebolai, CH Pohl. Polyunsaturated fatty acids potentiate the susceptibility of *Candida krusei* to fluconazole via the distortion of membrane integrity and efflux pump activity. World Antimicrobial Awareness Week (WAAW) 2020 Virtual Symposium. 19 – 20 November 2020 [Oral presentation].

  **AT Jamiu**, J Albertyn, OM Sebolai, O Kuloyo, N Mokoena, CH Pohl. Arachidonic acid increases the susceptibility of *Candida krusei* to fluconazole. American Society for Microbiology (ASM) Microbe 2020 Conference. 18 – 22 June 2020 [ePoster].

  **AT Jamiu**, O Kuloyo, N Mokoena, J Albertyn, CH Pohl. Anti-biofilm activity of unsaturated fatty acids with fluconazole. Canadian Fungal Research Network 2020. 29 – 30 July 2020 [Oral presentation].

  **AT Jamiu**, O Kuloyo, N Mokoena, J Albertyn, CH Pohl. Influence of polyunsaturated fatty acids on fluconazole susceptibility of *Candida krusei*. University of the Free State Postgraduate Academic Conference. 20 September 2019 [Oral presentation].

  **AT Jamiu**, O Kuloyo, N Mokoena, J Albertyn, CH Pohl. Influence of polyunsaturated fatty acids on fluconazole susceptibility of *Candida krusei*. Young Scientist Symposium on Infectious Diseases. 27 – 28 May 2019 [Poster].

- **Publication:**

  **AT Jamiu**, **J Albertyn**, **OM Sebolai**, **CH Pohl** (2020) Update on *Candida krusei*, a potential multidrug-resistant pathogen, *Medical Mycology*, 59:14-30, https://doi.org/10.1093/mmy/myaa031

## Chapter 1



## Chapter 2

## Chapter 3

## Chapter 4

# LIST OF TABLES

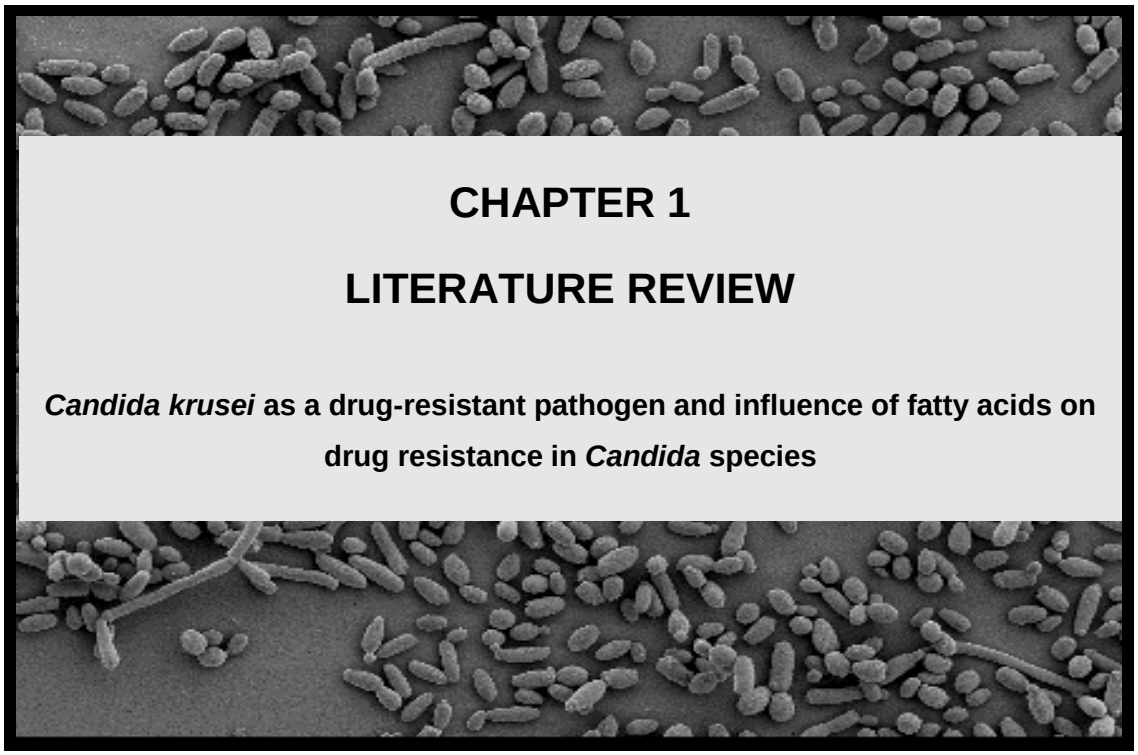

# CHAPTER 1

# LITERATURE REVIEW

***Candida krusei* as a drug-resistant pathogen and influence of fatty acids on drug resistance in *Candida* species**

## Motivation

Some members of the *Candida* genus are part of the commensal microbiota of humans; they colonise the gastrointestinal and urogenital tracts, oral cavity, mucosal as well as cutaneous surfaces in healthy individuals (Filler and Sheppard 2006; Bizerra et al. 2008). These yeasts are typically innocuous, with their growth and spread well controlled by coexisting microbiota, intact epithelial barriers and defences of the innate immune system (Kabir and Ahmad 2013). However, under certain circumstances, such as mucosal barrier disruption, immune system impairment, usage of broad-spectrum antibiotics, or a combination thereof, *Candida* spp. may proliferate and multiply to cause various opportunistic infections, ranging from self-limiting topical diseases to life-threatening systemic infections (Samaranayake and MacFarlane 1990; Dixon et al. 1996). The incidence of life-threatening candidal infections has markedly increased over the years due to the increasing population of immunosuppressed patients, such as HIV/AIDS and cancer patients, premature neonates, and organ transplant recipients (Pfaller and Diekema 2007). *Candida albicans* remains the primary cause of invasive candidiasis; however, the epidemiology has changed in recent years, with 35 to 65% of all cases of infections attributed to non-*albicans Candida* (NAC) species (i.e. *C. krusei*, *C. tropicalis, C. parapsilosis*, and *C. glabrata*) (Trick et al. 2002; Poikonen et al. 2010; Chi et al. 2011; da Silva et al. 2013; Sadeghi et al. 2018).

To date, fungal infections are mainly treated with either azole, echinocandin or polyene antifungals. Among these, azoles such as posaconazole, fluconazole (FLC), voriconazole, and itraconazole are the most commonly used in the treatment and prevention of mycoses, due to their broad-spectrum activity (Falci and Pasqualotto 2013). These compounds inhibit lanosterol 14α-demethylase (Erg11p), an enzyme important for ergosterol biosynthesis (Kathiravan et al. 2012). Its inhibition results in the depletion of ergosterol and accumulation of toxic methylated sterols, which ultimately result in the arrest of cell growth (Sheehan et al. 1999; Weete et al. 2010). Fluconazole remains the most widely used azole for the treatment of candidiasis; however, its fungistatic nature, as well as widespread and extended use, has led to the development of resistance among fungi (Shukla et al. 2016). More worrisome, *Candida krusei*, a member of the highly heterogeneous *Candida* genus, exhibits innate resistance to this drug, with more than 97% of isolates displaying resistance (Whaley et al. 2017). Many studies have attributed the mechanism of inherent FLC resistance in this yeast to the low affinity of Erg11p for FLC (Venkateswarlu et al. 1997; Orozco et al. 1998; Fukuoka et al. 2003). The role of efflux pump transporters, including Abc1p, in this inherent resistance remains controversial and warrants further studies.

Additionally, like other common *Candida* spp., *C. krusei* forms recalcitrant biofilms with higher antifungal resistance compared to planktonic cells (Hacioglu et al. 2018). This enhanced resistance could be explained by the inherent complexity of biofilm owing to its sophisticated structures and functions (Finkel and Mitchell 2011; Ramage et al. 2012). Moreover, their presence on medical implants increases the risks of systemic infections, seeds recurrent infections, and results in treatment failures, increased economic burden, and reduced quality of lives (Ramage et al. 2006). This highlights an urgent need to develop novel antifungal treatment approaches and combination therapy may be one such option.

The study of putative antifungal-resistance related genes, for example, *ABC1* and *ERG11*, using molecular tools would provide valuable insights into the roles of these genes in antifungal resistance. These insights may consequently guide the preservation of current antifungal drugs and inspire the development of novel therapeutic strategies. However, such molecular study is impeded in *C. krusei* by the absence of a facile, precise, and efficient genome engineering tool like CRISPR technology.

Furthermore, although polyunsaturated fatty acids (PUFAs) have been reported to increase the sensitivity of intrinsically-susceptible *C. albicans* and *C. dubliniensis* biofilms to antifungal drugs such as clotrimazole, amphotericin B, and FLC (Ells et al. 2009; Thibane et al. 2012b; Kuloyo et al. 2020), whether exogenous PUFAs could reverse intrinsic antifungal resistance in *C. krusei* remains to be investigated. This study was, therefore, conducted to address the aforementioned knowledge gaps.

# *SECTION B*

**This section was published in *Medical Mycology*; the writing and reference style of the journal was followed.**

The candidate, Abdullahi Temitope Jamiu, conducted the literature study and wrote the manuscript. The supervisor and co-authors reviewed and provided constructive feedbacks on the manuscript.

Citation: **AT Jamiu**, **J Albertyn**, **OM Sebolai**, **CH Pohl** (2020) Update on *Candida krusei*, a potential multidrug-resistant pathogen, *Medical Mycology*, 59:14-30, https://doi.org/10.1093/mmy/myaa031

ISHAM INTERNATIONAL SOCIETY FOR HUMAN AND ANIMAL MYCOLOGY

*Medical Mycology*, 2020, 0, 1–17
doi:10.1093/mmy/myaa031
Advance Access Publication Date: 0 2020
Review Article

Review Article

# Update on *Candida krusei*, a potential multidrug-resistant pathogen

**A. T. Jamiu, J. Albertyn, O. M. Sebolai, and C. H. Pohl***

Pathogenic Yeast Research Group, Department of Microbial, Biochemical and Food Biotechnology, University of the Free State, Bloemfontein, South Arica, 9301

*To whom correspondence should be addressed. C. Pohl, PhD. E-mail: PohlCH@ufs.ac.za

Received 16 December 2019; Revised 9 April 2020; Accepted 14 April 2020; Editorial Decision 12 April 2020

## Abstract

Although *Candida albicans* remains the main cause of candidiasis, in recent years a significant number of infections has been attributed to non-*albicans Candida* (NAC) species, including *Candida krusei*. This epidemiological change can be partly explained by the increased resistance of NAC species to antifungal drugs. *C. krusei* is a diploid, dimorphic ascomycetous yeast that inhabits the mucosal membrane of healthy individuals. However, this yeast can cause life-threatening infections in immunocompromised patients, with hematologic malignancy patients and those using prolonged azole prophylaxis being at higher risk. Fungal infections are usually treated with five major classes of antifungal agents which include azoles, echinocandins, polyenes, allylamines, and nucleoside analogues. Fluconazole, an azole, is the most commonly used antifungal drug due to its low host toxicity, high water solubility, and high bioavailability. However, *C. krusei* possesses intrinsic resistance to this drug while also rapidly developing acquired resistance to other antifungal drugs. The mechanisms of antifungal resistance of this yeast involve the alteration and overexpression of drug target, reduction in intracellular drug concentration and development of a bypass pathway. Antifungal resistance menace coupled with the paucity of the antifungal arsenal as well as challenges involved in antifungal drug development, partly due to the eukaryotic nature of both fungi and humans, have left researchers to exploit alternative therapies. Here we briefly review our current knowledge of the biology, pathophysiology and epidemiology of a potential multidrug-resistant fungal pathogen, *C. krusei*, while also discussing the mechanisms of drug resistance of *Candida* species and alternative therapeutic approaches.

**Key words:** *Candida krusei*, biotechnology, pathogenicity, antifungal resistance, alternative therapy.

## Introduction

The incidence of fungal infections has escalated dramatically in recent years due to an increased number of immunocompromised patients, which include premature neonates, human immunodeficiency virus (HIV) positive patients, cancer patients and those using immunosuppressive therapy, such as patients with organ transplant and autoimmune disease.[1] Although often neglected, more than 300 million people suffer from serious mycoses worldwide, with an associated mortality of over 1.5 million (1.5 to 2 m) yearly. This mortality is similar to or more than that of tuberculosis or malaria.[2,3] Most of this mortality is caused by pathogenic yeasts of the genus *Candida*, *Cryptococcus*, and *Pneumocystis*, and filamentous fungi belonging to the genus *Aspergillus*,[4] with *Candida* spp. being the most common cause of invasive mycoses.[5] Some members of the genus *Candida* are commensals of the oral cavity, urogenital and gastrointestinal tracts as well as mucosal and cutaneous surfaces in healthy individuals.[6] The growth and spread of these yeasts are kept in check by coexisting microbiota, defenses of the innate immune system and intact epithelial barriers. However, under certain circumstances, such as when broad-spectrum antibiotics are used, when mucosal barriers are disrupted due to chemotherapy, radiotherapy and surgery or when the immune system is compromised, *Candida* spp. can cause a variety of opportunistic infections ranging from superficial diseases to life-threatening systemic infections.[7,8] *Candida* spp. remain the fourth leading cause of hospital-acquired infections and the leading cause of nosocomial fungemia with more than 250,000 infections and 50,000 deaths annually attributed to candideamia.[9–11]

*Candida albicans* no doubt remains the predominant cause of candidiasis, however, this has changed in recent years with a significant number of infections being attributed to non-*albicans Candida* (NAC) species. This epidemiological shift may be partly explained by the increased resistance of NAC species to antifungal agents.[12,13] Among these NAC species is *Candida krusei*, which is a diploid, dimorphic ascomycetous yeast that belongs to the family *Pichiaceae*. It is a transient commensal, and it inhabits the mucosal membrane of healthy individuals.[14] It is not a member of the CTG clade, unlike *C. albicans*[15] and differs from other pathogenic *Candida* spp. in morphology.[16]

Fungal infections are usually treated with five major classes of antifungal agents which include azoles, echinocandins, polyenes, allylamines, and nucleoside analogues. Amongst these, only azoles, echinocandins, and polyenes are available for the treatment of systemic candidal infections. While nucleoside analogues, allylamines, and morpholines are usually used for topical treatment or as adjuvants with other antifungal drugs. The widespread use and misuse of this limited antifungal arsenal have resulted in increased resistance of fungal pathogens to the available antifungal agents.[17] This resistance can either be intrinsic (primary) or acquired (secondary). Primary resistance occurs inherently in some fungal strains without prior exposure to antifungal drugs, while secondary resistance occurs in previously susceptible strains after exposure to antifungal agents.[18,19]

Azoles are the most commonly used antifungals for the treatment of fungal infection due to their extended-spectrum activity.[20] These agents disrupt ergosterol biosynthesis via the inhibition of lanosterol-14$\alpha$-demethylase (encoded by *ERG11*), an important enzyme in ergosterol biosynthesis.[21] Among these agents, fluconazole is the most commonly used azole for the treatment of candidiasis because it is highly water-soluble, highly bioavailable with lesser host toxicity.[22,23] However, its fungistatic nature, widespread and extended use has led to remarkable resistance development to it.[24] *C. krusei* is a potential multidrug-resistant yeast because of its intrinsic resistance to fluconazole (with more than 97% isolates displaying resistance)[25] as well as its rapid acquired resistance development to other antifungal drugs. The mechanisms of antifungal resistance of this yeast may be due to, but not limited to: (i) alteration of target enzyme (e.g., ERG11, FKS1); (ii) overexpression of target enzyme; (iii) reduction in intracellular drug concentration due to efflux pump activity (e.g., CDR1, CDR2), and (iv) development of bypass pathway for biosynthesis of sterols to replace ergosterol in the cell membrane.[26,27]

This review provides an update on the biology, pathophysiology and epidemiology of a potential multidrug-resistant fungal pathogen, *C. krusei,* while also discussing the mechanisms of drug resistance of *Candida* species and alternative therapeutic approaches.

## Brief history and taxonomy of *Candida krusei*

*C. krusei* was discovered in 1839 when it was first isolated from the buccal epithelial layer of a typhus patient; however, at this time, it was not regarded as a human pathogen. The name *Saccharomyces krusei* was proposed for this yeast by Castellani; this and other names were used until 1923 when *C. krusei* was proposed by Berkhout.[28,29]

In 1960, Kudryavtsev suggested the name *Issatchenkia orientalis* under the genus *Issatchenkia* for a yeast he isolated from fruit juice and berries.[30] One of the distinctive features of members of this group is their ability to form spherical ascospores. This classification was disregarded by Kreger-van Rij, who transferred this species to *Pichia* as *Pichia orientalis*. Unknown to Kreger-van Rij, a different organism had already been named *Pichia orientalis*, and this led to the proposal of the name *Pichia kudriavzevii*.[31] The genus *Issatchenkia* was revived after the re-examination of circumscription of yeast genera with emphasis on ascospore morphology as the defining feature, and this prompted the species to be moved back to this genus as *Issatchenkia orientalis*.[32] This name was used until 1998 when an analysis of D1/D2 LSU rRNA gene sequences suggested that the species grouped in *Issatchenkia* were members of *Pichia membranifaciens* clade.[33] This was further consolidated and affirmed by multigene analysis, and this resulted in the return of this species to *Pichia* as *P. kudriavzevii*.[34] The features of members of this genus include multilateral budding, ovoid, spherical or short elongate cells, ascospores formation, which may be spherical or hat-shaped, and presence or absence of septate hyphae and pseudohyphae.

In 1980, Kurtzman and colleagues proposed *C. krusei* as the anamorph (asexual form) of *P. kudriavzevii* based on mating tests and DNA reassociation.[35] This was further confirmed when the D1/D2 sequences of the 26S ribosomal RNA (rRNA) of *C. krusei* and *P. kudriavzevii* type strains were found to be identical.[34] More recently, the whole genome sequence study of the type strains of *C. krusei* (CBS573$^T$) and *P. kudriavzevii* (CBS5147 $^T$) showed that there is no genetic distinction between the two yeasts, and their genomes are completely collinear with 99.6% nucleotide identity, thus confirming that these yeasts are conspecific.[36] Thus, *C. krusei* (anamorph / imperfect form) and *P. kudriavzevii* (teleomorph / perfect form) are the same species. To avoid using multiple names and to abide by ''One Fungus, One Name" principle, the usage of *P. kudriavzevii* (sexual form) has been suggested but has not yet been enacted.[36] In this review, *C. krusei* would be used throughout, while *P. kudriavzevii* would only be used specifically to refer to the environmental and teleomorphic isolate.

This yeast is an ascomycetous fungus that belongs to the class *Saccharomycetes*, order *Saccharomycetales*. However, phylogenetic analysis of rRNA and other genes (e.g., *MDN1* gene) indicates that it is only distantly related to *C. albicans*.[36] Moreover,

**Table 1.** Comparisons of some features of *Candida krusei* with other pathogenic *Candida* species.[15,16,36,67,202,203]

| Organism | Genome size (Mb) | GC content (%) | CTG clade | Ploidy | Pseudohyphae | Hyphae | Reproduction |
|---|---|---|---|---|---|---|---|
| *C. krusei* | 11.40 | 38.42 | No | Diploid or aneuploid | Yes | No | Asexual or sexual |
| *C. albicans* | 14.28 | 33.48 | Yes | Diploid | Yes | Yes | Asexual or parasexual |
| *C. glabrata* | 12.62 | 38.62 | No | Haploid | Yes | No | Asexual |
| *C. tropicalis* | 14.63 | 33.20 | Yes | Diploid | Yes | Yes | Asexual |
| *C. parapsilosis* | 13.03 | 38.30 | Yes | Aneuploid or diploid | Yes | No | Asexual |

unlike members of *Candida* CTG clade, it translates CUG codon as leucine rather than serine.[15]

## Biology of *Candida krusei*

### Morphology and colony characteristics

*C. krusei* is a dimorphic fungus that usually exists as single-cell yeasts or pseudohyphae. The two morphological forms may be present at the same time in growing cultures, but are difficult to separate.[29] Unlike most members of the genus, *C. krusei* cells are elongated and resemble long grains of rice with a dimension of 2.2–5.6 µm by 4.3–15.2 µm. Asexual reproduction in *C. krusei* is by budding.[16]

*C. krusei* (anamorph) does not produce ascospores, however its ascosporic and teleomorphic form, *P. kudriavzevii* was regarded to be able to sporulate (forming one spore per ascus) when it was first described. However, cultures of its type strain were later found to be unable to sporulate or conjugate.[37] Just like other pathogenic *Candida* species, *C. krusei* exhibits dimorphic transition which contributes to its virulence because of the invasive nature of the pseudohyphae.[38] Table 1 summarizes some important features of *C. krusei* and other pathogenic *Candida* spp.

On malt extract agar, *C. krusei* colonies are butter-like to light-cream in color.[39] It grows as spreading colonies with rough and whitish-yellow surface on Sabouraud's dextrose agar, distinguishing it from other *Candida* spp.[7] *C. krusei* colonies appear rough on Pal's agar, making it indistinguishable from *C. parapsilosis* and *C. dubliniensis*.[40] However, its colonies appear pink and rough-textured on CHROMagar Candida medium supplemented with Pal's agar, thus distinguishing it from a mixed culture of *C. albicans* and other pathogenic NAC species.[41] This is similar to what is observable on CHROMagar *Candida* medium without Pal's agar supplementation, where *C. krusei* colonies appear pale pink, flat, dry and rough-textured with white edges.[42] This yeast also forms a pellicle or adherent film on the surface of liquid culture, and this feature distinguishes it from other pathogenic *Candida* species.[43]

### Habitat

*C. krusei* is a facultative saprophyte, widely distributed in nature, and is generally considered as a transient human commensal and a mucosal inhabitant in healthy individuals.[14] However, it can be responsible for self-limiting candidiasis in non-immunocompromised and life-threatening infections in immune-compromised patients. The teleomorph form of *C. krusei* is usually found in soil in warmer regions and on fruit, vegetables and food products such as fruit juices and fermented milk.[44] The transformation between the two (asexual and sexual) forms is determined by the environmental conditions but, it is usually unclear.[45]

### Growth and metabolism

*C. krusei* cells grow optimally at 24–26°C; however, they can also survive at a maximum temperature of 43–45°C and pH as low as 2. *C. krusei,* unlike many other *Candida* spp., does not require biotin or any other vitamins for optimal growth.[29] Some strains of *C. krusei* can assimilate sorbose, galactose, citrate, and inositol; however, all known isolates of *C. krusei* can utilize glucose, glycerol, succinate, D-glucosamine, ethanol, DL-lactate, and *N*-acetylglucosamine.[46] *C. krusei* can ferment glucose but not galactose, maltose, sucrose, lactose, and trehalose. It is also one of the most effective producers of ethanol from glucose under aerobic and facultative aerobic conditions.[47] Moreover, this yeast produces acetoin, which it can use when carbon sources are depleted in the culture medium.[48] In addition, *C. krusei* produces intracellular phytase, an enzyme capable of releasing inorganic phosphate via the catalytic hydrolysis of phytate (phytic acid).[49]

### Interaction with other microbes

Biofilms are microbial populations embedded in a self-produced extracellular polymer matrix (polysaccharides and glycoprotein) and are usually adhered to a surface.[50] Although biofilms can competently adhere to abiotic surfaces such as catheters, dentures, and prostheses with their presence increasing the risk of infections, they also exist on biotic surfaces such as the tooth surfaces, urinary and respiratory tract.[51,52]

*Candida* species can form a biofilm, which is one of their major virulence factors because of the reduced susceptibility of biofilm cells to antifungal drugs and host defenses compared to their planktonic counterpart.[53,54] *C. krusei* forms monospecies biofilms as well as polymicrobial biofilms with other fungi and bacteria.[55] This interaction could be beneficial or antagonistic

and may have a direct influence on the growth and survival of microorganisms, depending on the microbes involved in the interaction.[56] *C. krusei* has been reported to inhibit *Pseudomonas aeruginosa* population within a mixed biofilm.[57] Moreover, antagonistic interaction has also been observed in a polymicrobial biofilm of *C. albicans* and *C. krusei*, where the latter was reported to inhibit the growth and filamentation of the former.[58,59] Similar findings were observed by Rossoni and colleagues,[60] who reported that *C. albicans* caused a more intense oral cavity infection in mice singly than when in a mixed population with *C. krusei*. Furthermore, in two other studies by Barros and colleagues,[61,62] this yeast was also reported to reduce the filamentation of *C. albicans* via decreasing the expression of hyphal wall protein 1 (*HWP1*) gene, which is important in hyphal development, cell wall assembly, intracellular signaling and adherence in *C. albicans*. *C. krusei* interaction with other NAC species has also been studied, and this yeast has been observed to grow better in a polymicrobial biofilm with *C. glabrata* than in a single species biofilm.[63] Moreover, *C. krusei* also inhibited *C. glabrata* growth and colonization of mice oral cavity. The reason(s) behind *C. krusei* inhibition and suppression of *C. albicans* and *C. glabrata* growth could be due to competitive adhesion, competition for food and space and/or due to the synthesis of inhibitory chemicals and molecular messengers by *C. krusei*.[62,64]

In addition, in a study conducted by Fleischmann and coworkers,[65] *C. krusei* plated in parallel streaks with itself and two other *Candida* species (*C. albicans* and *C. glabrata*) was able to detect the presence of itself as well as that of *C. albicans* and *C. glabrata* by forming mycelia towards itself and the other yeasts. However, neither of the latter two reacted to *C. krusei* nor themselves. Although the quorum sensing compounds farnesol, tyrosol, and tryptophol were detected on the agar surfaces, they were not responsible for the response and the cause of this remains unknown.

### Genome sequence

The majority of *C. krusei* isolates are diploid, however rare cases of aneuploidy (possibly as a response to environmental stress) have been reported.[36,66] This yeast contains five chromosomes; three large chromosomes (2.7–3.5 Mb) and two smaller ones with a size of approximately 1.4 Mb each.[36,67] To date, two genome sequences are available for clinical strains of *C. krusei*. Genome sequence of *C. krusei* strain 81-B-5 and CBS573$^T$ (type strain) was reported by Cuomo and co-workers[67] and Douglass and co-workers,[36] respectively. These clinical strains have genome sizes between 10.8 to 11.4 Mb, with 4949 to 5154 protein-coding genes and a GC content between 38.25% and 38.42%.[36,67] Genes encoding for drug efflux pumps belonging to the ABC transporter family such as *ABC1*, *ABC2*, *ABC11*, and *ABC12* have been identified in the genome of the clinical isolates of this yeast.[36,66,68] The genome sequence of the clinical strain CBS573$^T$ is the only available annotated genome for this yeast.[36] Genome sequences of five environmental strains of *C. krusei* have also been reported. The draft genome of an environmental isolate, *P. kudriavzevii* M12, was published by Chan and colleagues[69] and was reported to be approximately 10.5 Mb in size with a GC content of 38.32%. The strain was predicted to contain 4863 protein-encoding genes, which include three genes coding for phytases and genes coding for xylose reductase, xylulokinase, and xylitol dehydrogenase, which are essential for ethanol production from xylose.[69] A draft genome sequence of another environmental strain, *P. kudriavzevii* 129, isolated from fermented Masau fruits in Zimbabwe, revealed a genome size of 11.7 Mb with a GC content of 38.5% and 5470 genes.[70] Furthermore, Park and colleagues,[71] published a draft genome of a multi stress-tolerant strain, *P. kudriavzevii* NG7, with a genome size of 10.6 Mb, GC content of 38.27%, and 4001 predicted protein-coding genes. The genome sequence of the environmental type strain CBS5147$^T$ with genome size of 10.78 Mb and GC content of 38.34% has also been reported.[36] Most recently, the complete genome sequence of an environmental strain, *P. kudriavzevii* SJP-SNU, isolated from fermented plants, was reported by Hong and co-workers.[72] The complete genome consists of approximately 10.9 Mb with GC content of 38.2%.

## Biotechnological applications

*C. krusei*, in its teleomorphic form, *P. kudriavzevii,* has various biotechnological potentials ranging from food production to industrial applications. This yeast has been isolated from an array of food products including fruit juices, fermented foods, and milk products. Moreover, it has been given the Generally Regarded as Safe status by the US Food and Drug Administration (FDA).[44] However, due to the fact that members of the *Candida* genus, including *C. krusei*, have pathogenic potential, this genus (except for *C. cylindracea*) is excluded from consideration for Qualified Presumption of Safety (QPS) status in Europe.[73]

*Pichia kudriavzevii* has been reported to play an important role in the fermentation of milk and addition of flavors to milk products such as Suusac (Kenya), Kefir, Armada, and acid curd cheese (North Spain).[74–76] Moreover, this yeast is also involved in the fermentation of cocoa to chocolate, while also ensuring aroma development and obviation of bitter taste in chocolate.[77,78] *Pichia kudriavzevii* is involved in cassava fermentation for fufu,[79] garri,[80] ogi,[81] and agbelima[82] (types of food in western Africa). Furthermore, elubo (yam flour) is also produced in west Africa from yam through a fermentative procedure that involves *P. kudriavzevii*.[83]

In addition to its applications in food production, this yeast has also been documented to have a possible application in biofertilization, bioremediation as well as glycerol and ethanol synthesis. *Pichia kudriavzevii* produces phytases, which degrade phytate in soil to release phosphorus; this process improves

phosphorus availability and acquisition in soil. This also reduces the need for phosphorus fertilizer, thus making it a potential biofertiliser.[69] In addition, *P. kudriavzevii* is also an effective producer of glycerol from glucose.[84,85] as well as an effective ethanol producer. As such it offers various advantages over other ethanol-producing yeasts.[16] It can produce ethanol at a temperature above 40°C, reducing the risk of contamination.[86] It also produces ethanol without succinic acid as a by-product. This is advantageous as succinic acid damages silicon rubber-coated silicate membranes used during ethanol separation by pervaporation.[47,87] Furthermore, this yeast has the ability to bioremediate xenobiotic synthetic dyes such as basic violet 3 (triphenylmethane dye), azo dye, and reactive brilliant red dye.[88,89]

## Pathogenicity of *C. krusei*

### Pathophysiology

*Candida* species can be members of the commensal microbiota of human gastrointestinal and genitourinary tracts, oral cavities as well as mucosal and cutaneous surfaces.[6] These yeasts are typically harmless, with their growth kept in check by coexisting microbiota, intact epithelial barriers and defenses of the innate immune system. However, in the event of disruption of the mucosal barrier (due to surgery or chemo/radiotherapy), use of broad-spectrum antibiotics or compromised immune system (due to cancer or AIDS), *Candida* spp. can cause a variety of opportunistic infections ranging from superficial diseases to life-threatening systemic infections.[7,8] Fungal infections are generally classified based on the mode of entry of the fungal pathogen and the degree of tissue involvement.[16] Infections caused by *Candida* spp. are known as candidiasis, and the three forms of candidiasis include cutaneous, mucosal and systemic candidiasis.[13]

Although invasive candidiasis and candidemia are used interchangeably to describe candidal infection of the bloodstream, a more strict definition defines invasive candidiasis as a form of candidiasis that affects all body parts, including heart, brain, eyes, bone, and blood, and it comprises both candidemia and deep-tissue candidiasis. Deep-tissue candidiasis are candidal infections involving the internal organs and could either occur via hematogenous dissemination or direct introduction of the yeast to a sterile site.[11]

*C. krusei* is responsible for, among others, endophthalmitis, onycholysis, endocarditis, and osteomyelitis, and the type of disease developed by patients depends on the health status of the patient (Table 2).

**Table 2.** A summary of infections caused by *Candida krusei*.[43,113,187,204–212]

| Disease | Susceptible patient |
|---|---|
| Candidemia | Neutropenia; allogeneic marrow transplant |
| Soft tissue abscess | Osteoarthritis |
| Osteomyelitis | Leukemia; neutropenia |
| Pneumonia | Post-transplantation |
| Vaginitis | Older age |
| Onycholysis | Healthy |
| Endophthalmitis | Neutropenia |
| Endocarditis | Heart surgery; heart disease |
| Oral candidiasis | Leprosy |
| Pyelonephritis | Cancer |
| Spondylodiscitis | Acute myeloid leukemia |

### Virulence factors

*C. krusei* produces an array of virulence factors. Similar to *C. albicans*, the dimorphic transition of *C. krusei* is one of its virulence traits. Unlike the yeast form, the pseudohyphae are invasive, thus conferring it the ability to invade host tissues. However, studies have shown that *C. albicans* hyphae colonize tissues and also penetrate deep tissue more effectively than pseudohyphae of *C. krusei*.[38,90]

Phenotypic switching, which is a reversible phenotypic change that involves the spontaneous emergence of colonies with an altered phenotype at a higher rate than that of somatic mutation rates, is another virulence factor utilized by *C. krusei*.[91] Phenotypic switching of a cell may result in the adjustment of antigenicity of the cell surface, cell physiology and composition of molecules such as lipid, sugar, and protein to allow adaptation to adverse environments.[92] This allows the yeast to adapt rapidly to various environmental conditions.[93] The switched forms of *C. krusei* exhibit a wrinkled and mycelial appearance with higher adherence capacity and lower sensitivity to chlorhexidine than the unswitched form.

Since phospholipids and proteins are the major chemical constituents of the host cell membrane, pathogenic *Candida* spp. secrete phospholipases and proteinases. Phospholipases act to hydrolyse phospholipids and are classified as phospholipases A, B, C, and D based on the ester bonds cleaved. Proteinases (e.g., secreted aspartyl proteinases, SAPs) degrade human proteins such as keratin, immunoglobulin A (IgA), hemoglobin and albumin,[94,95] thus enhancing the yeasts ability to colonize host tissues and evade the host immune system.[96] As such, these enzymes are considered to play critical roles in the virulence of *Candida* species. However, unlike *C. albicans*, *C. krusei* has lower exoenzyme secretions, correlating to lower virulence compared to *C. albicans*.[97,98] *C. krusei* has also been reported to be more hydrophobic than *C. albicans*, and this facilitates its adherence to its host cells and inert surfaces.[93] Unlike *C. albicans* that already has many of its virulence genes identified and characterized, only a few virulence genes have been identified in *C. krusei*. Some of these virulence genes in *C. krusei* include aspartyl proteases, phospholipase B, and oligopeptide transporter genes.[67]

## Epidemiology of *Candida krusei*

From 1970 to 1990, NAC species were only responsible for 10–40% cases of systemic candidiasis. However, this has changed in the last two decades with about 35–65% of all cases of candidemia attributed to NAC species.[12,13,99–101] This epidemiological shift may be partly explained by the increased intrinsic or acquired resistance of NAC species to antifungal agents.[13,102] Improvements in diagnostic techniques, such as the use of Matrix Assisted Laser Desorption/Ionization Time of Flight Mass Spectrometry (MALDI-TOF MS) and routine diagnosis with molecular techniques may also explain the increased prevalence of NAC species.[13]

The four most common NAC species in descending order of prevalence include *C. glabrata* (18.7%), *C. parapsilosis* (15.9%), *C. tropicalis* (9.3%), and *C. krusei* (2.8%).[103] Among these common NAC species, *C. krusei* is the predominant species in patients with hematologic malignancies and others receiving prolonged azole prophylaxis.[104,105] Moreover, infection by this yeast results in the lowest 90-day survival rate when compared to other common *Candida* spp. This could due to the extensive comorbidities in patient population affected by this yeast.[106] This yeast is also gaining increasing attention due to its inherent resistance to the triazole antifungal, fluconazole, which is complicated by the increased use of fluconazole and other triazoles to treat fungal infections.[15]

## Distribution

Some factors, such as individual patient risk factors, antifungal usage patterns and outbreaks of healthcare-associated *Candida* strains, usually determine the prevalence of NAC species in different regions.[107] In the United States, France, Australia, Denmark, Canada, and northern Europe, *C. glabrata* has emerged as the most encountered species, especially among recipients of solid organ transplants and people older than sixty years, whereas, *C. tropicalis* and/or *C. parapsilosis* are much more prominent than *C. glabrata* and *C. krusei* in southern Europe, Latin America, Japan, Iran, Pakistan, and India.[105] In a study by Pfaller and colleagues,[108] *C. krusei* was found to be more prevalent in Europe and North America (3.1–3.4%), and lowest prevalence was recorded in Asia-Pacific (1.2%) (Table 3).

Moreover, a more recent study by Pfaller and colleagues[103] reported a similar trend in *C. krusei* geographic distribution between 2006 and 2016, where the species distribution in Europe, North America, Latin America, and Asia-Pacific was 3.0%, 2.9%, 2.0%, and 1.8%, respectively. Furthermore, Europe, which has the highest *C. krusei* distribution, also happens to harbor the highest *C. krusei* isolates displaying resistance to fluconazole. Conversely, isolates from Latin America which showed the lowest resistance to fluconazole, exhibited the highest resistance to voriconazole (Table 4).[108]

**Table 3.** Geographic distribution of *C. krusei* and other common *Candida* spp. from 2001 to 2007.[108]

| | *Candida* species distribution by region (%) | | | | |
|---|---|---|---|---|---|
| Species | Africa and Middle East | Europe | Asia-Pacific | Latin America | North America |
| *C. krusei* | 1.6 | 3.4 | 1.2 | 1.4 | 3.1 |
| *C. glabrata* | 8.8 | 11.3 | 12.6 | 7.4 | 21.1 |
| *C. tropicalis* | 6.6 | 4.9 | 11.7 | 13.2 | 7.3 |
| *C. parapsilosis* | 6.0 | 4.2 | 7.4 | 10.3 | 13.6 |
| *C. albicans* | 67.1 | 67.9 | 64.4 | 51.8 | 48.9 |
| Others | 9.9 | 8.3 | 2.7 | 15.9 | 6.0 |

**Table 4.** Geographical distribution of azole-resistant isolates of *C. krusei* between 2001 and 2007.[108]

| | Azole resistant isolates by region (%) | |
|---|---|---|
| Region | Fluconazole | Voriconazole |
| Africa and Middle East | 72.4 | 4.5 |
| Europe | 80.8 | 7.7 |
| Asia-Pacific | 73.5 | 5.0 |
| Latin America | 66.8 | 14.0 |
| North America | 74.0 | 5.5 |

**Table 5.** Distribution of azole-resistant isolates of *C. krusei* by specimen type.[108]

| | Azole-resistant isolates by specimen (%) | |
|---|---|---|
| Specimen | Fluconazole | Voriconazole |
| Blood | 74.5 | 8.5 |
| NSBF | 80.5 | 4.5 |
| Urine | 80.1 | 11.4 |
| Respiratory tract | 79.2 | 7.8 |
| Skin/soft tissue | 81.7 | 8.0 |
| Genital tract | 71.9 | 6.9 |

In addition, variation exists in the resistance profile of *C. krusei* isolates to azoles among different specimen types. Highest resistance to fluconazole (80.5%) and voriconazole (11.4%) was observed in isolates from normally sterile body fluid (NSBF) and urine respectively, while the lowest resistance to fluconazole (71.9%) and voriconazole (4.5%) was recorded in isolates from the genital tract and NSBF (Table 5). It is noteworthy that resistance to fluconazole does not usually imply voriconazole resistance or cross-resistance to other members of azoles, as observed in NSBF specimen, with isolates displaying highest resistance to fluconazole, but highest susceptibility to voriconazole.[108]

A recent 5-year South African case study (January 2012 – December 2016),[109] regarding the incidence of candidemia among

neonates in a university-affiliated hospital in Gauteng Province, South Africa, reported a total of 262 cases of candidemia caused by 10 different *Candida* spp. The most prevalent species during this study was *C. krusei*, followed by *C. albicans* and then *C. parapsilosis*. Interestingly, only a single case of candidemia was attributed to *C. krusei* (October 2012) before the onset of the first *C. krusei* candidemia outbreak in July 2014. However, during the first outbreak between July and October 2014, most cases of candidemia were due to *C. krusei* with an incidence of 8.2 cases per 100 admissions. Furthermore, a second *C. krusei* candidemia outbreak occurred between April and July 2015. *C. krusei* candidemia was probably transmitted among neonates via contact with healthcare workers and fomites, with infants with low birth weight (<1.5 kg), total parenteral nutrition (TPN) administration, blood transfusion, lower gestational age, and necrotizing enterocolitis at higher risk. The major cause of the candidemia outbreaks was due to the improper adherence to infection prevention and control practices. Other causes include delayed outbreak recognition, disrupted water supply, poor ventilation, overcrowding, and structural problems of the hospital.

### Risk factors

Although there are several specific risk factors for individual NAC species, they generally tend to be more prevalent in cancer patients, especially those with hematological malignancies (e.g., leukemia) or bone marrow transplant (BMT) recipients. The risk factors of *C. krusei* candidiasis include antifungal prophylaxis (especially fluconazole), long-term use of broad-spectrum antibiotics, neutropenia, immunocompromised system (especially blood cancer), and increased use of medical devices.[110] *C. krusei* risk factors are akin to that of *C. tropicalis*, and it is mostly associated with adult neutropenic cancer patients, mainly those with leukemia or BMT recipient receiving fluconazole prophylaxis, responsible for the high incidence of 13–25% in leukemic patients.[111,112] However, *C. krusei* is less common in neonates and intensive care unit (ICU) patients with an incidence rate between 1–3% and 2–4%, respectively.[113] Interestingly, HIV-positive patients frequently receiving prolonged low dose fluconazole therapy, expected to be at high risk of *C. krusei* candidemia, are actually at a lower risk. The reason behind this and for the high prevalence in cancer patients remains unknown.[113,114]

### Prevention and therapeutic approach

Although there is no specific preventive measure for candidiasis, avoiding antibiotics misuse and unnecessary antifungal (fluconazole) prophylaxis, as well as adherence to infection prevention and control practices, could help decrease the occurrence of infection.[113] Amphotericin B can be administered for empirical treatment of candidiasis. Azoles or polyenes (amphotericin B) can be administered for infections caused by NAC species such as *C. parapsilosis* and *C. tropicalis*, which are susceptible to both azoles and polyenes, while amphotericin B can be administered for fluconazole-resistant isolates of *C. glabrata* and other *Candida* spp.[113,115] Although reduced susceptibility of *C. krusei* to amphotericin B and flucytosine has been documented, amphotericin B is still largely effective for the treatment of *C. krusei* associated candidiasis.[116–119] Itraconazole, voriconazole, and the newer triazoles, such as posaconazole and isavuconazole, are usually active against *C. krusei*.[113,120–122] Although rare, resistance to these agents has also been reported in *C. krusei*.[123,124] This, coupled with severe nephrotoxicity and infusion-related toxicity associated with amphotericin B, makes the echinocandins, a newer generation antifungal with fungicidal and broad-spectrum activity, a better and safer option for candidiasis treatment.[125]

Echinocandins such as caspofungin, anidulafungin, and micafungin are also very effective against *C. krusei,* due to their fungicidal activity. Reduced susceptibility to echinocandins has also been reported, however, this is very rare and generally falls in the range of 0–1% of isolates tested.[126,127] A combination of different antifungal drugs, or antifungal drugs and other compounds may be investigated for improved therapeutic options.[128]

### Antifungal drug resistance

Antifungal drug resistance can either be clinical or microbiological. Clinical resistance refers to the recalcitrance of a fungal infection despite the administration of an appropriate antifungal agent. In contrast to clinical resistance, microbiological resistance is defined as the nonsusceptibility of a fungus to an antifungal agent as determined by an *in vitro* antifungal susceptibility test. Microbiological resistance can either be intrinsic (primary) or acquired (secondary). Primary resistance occurs inherently in some fungal strains without prior exposure to antifungal drugs, while secondary resistance occurs in previously susceptible strains after exposure to antifungal agents, and it is usually a product of altered gene expression.[18,19] Although microbiological resistance can contribute to clinical resistance development, factors such as patient's underlying condition(s), reduced drug bioavailability, increased drug metabolism, and impaired immune function also play important roles.[129] Resistance development in bacteria is faster than in fungi, possibly due to the lack of horizontal gene transfer and longer generation times in fungi. However, once drug resistance is acquired in fungi, it is maintained even in the absence of an antifungal drug.[130] Amongst *Candida* spp., in comparison to *C. albicans*, NAC species are usually less susceptible to antifungal drugs; with 97% of *C. krusei* isolates, 35% of *C. glabrata,* and 10–25% of *C. tropicalis* isolates displaying either primary or secondary resistance to fluconazole.[25] Table 6 summarizes the various mechanisms of

**Table 6.** Mechanisms of resistance of *Candida* spp. to antifungal drugs.[158]

| Drug class | Major mode of action | Mode of resistance | | Gene | Species | Comment |
|---|---|---|---|---|---|---|
| Azoles (fluconazole, voriconazole, posaconazole, itraconazole, ketoconazole) | Inhibition of lanosterol 14α-demethylase = depletion of ergosterol | Drug target alteration = decreased susceptibility of lanosterol-14α-demethylase to azoles | | *ERG11* | *C. krusei*<br>*C. albicans*<br>*C. parapsilosis*<br>*C. tropicalis*<br>*C. auris* | Point mutation in *ERG11* gene |
| | | Drug target overexpression = overproduction of lanosterol-14α-demethylase | | *ERG11* | *C. krusei*<br>*C. albicans*<br>*C. parapsilosis*<br>*C. tropicalis*<br>*C. glabrata* | GOF mutation in *UPC2* |
| | | Overexpression of efflux pumps = reduced intracellular concentration of azoles | ABC | *ABC1*, *ABC2*, *ABC11*, *ABC12* | *C. krusei* | GOF mutation in *TAC1* |
| | | | | *CaCDR1*/*CaCDR2* | *C. albicans* | GOF mutation in *TAC1*, *PDR1* |
| | | | | *CpCDR1*<br>*CgCDR1*/*CgCDR2*<br>*CauCDR1*<br>*CdCDR1* | *C. parapsilosis*<br>*C. glabrata*<br>*C. auris*<br>*C. dubliniensis* | |
| | | | MFS | *MDR1* | *C. albicans*,<br>*C. parapsilosis*,<br>*C. tropicalis*,<br>*C. auris* | GOF mutation in *MRR1* |
| | | | | *TPO3* | *C. glabrata* | GOF mutation in *MRR1* |
| | | Compensatory pathway | | *ERG3* | *C. albicans*,<br>*C. tropicalis* | Toxic sterol synthesis is prevented |
| | | Aneuploidy | | *ERG11*, *UPC2*, *TAC1* | *C. albicans* | Amplified resistance |
| | | Loss of heterozygosity | | *ERG11*, *TAC1*, *MRR1* | *C. albicans* | Amplified resistance |
| Polyenes (amphotericin B, nystatin, natamycin) | Binding and extraction of ergosterol | Point mutation = decreased ergosterol content | | *ERG3*, *ERG5*, *ERG11*<br>*ERG2*, *ERG6* | *C. albicans*<br>*C. glabrata* | Cross resistance to azoles |
| Echinocandins (caspofungin, anidulafungin, micafungin) | Inhibition of β-1,3-D-glucan synthase | Drug target alteration = decreased affinity of β-1,3-D-glucan synthase | | *FKS1*, *FKS2* | *C. krusei*<br>*C. albicans*<br>*C. parapsilosis*<br>*C. tropicalis*<br>*C. glabrata* | Rare |
| Pyrimidine analogue (flucytosine) | Inhibition of nucleic acid/protein synthesis | Point alteration in cytosine permease = alteration in drug uptake | | *FCY2* | *C. glabrata* | Cross-resistance to fluconazole |
| | | Point alteration in cytosine deaminase = alteration in 5-flucytosine metabolism | | *FCY1* | *C. glabrata* | |
| | | Point alteration in uracil phosphoribosyl transferase gene = alteration in 5-fluorouracil metabolism | | *FUR1* | *C. albicans* | |

resistance of fungi to antifungal agents with emphasis on *C. krusei* and other *Candida* spp.

## Mechanisms of drug resistance

### Resistance to azoles

The survival of the fungal population in the presence of azoles (due to their fungistatic nature, worsened by their extensive use as prophylaxis and misuse), has resulted in the widespread resistance to azoles.[26,27] The mechanisms of resistance to azoles include alteration of the target enzyme; overexpression of the target enzyme; reduction in intracellular drug concentration; development of bypass pathway for biosynthesis of sterols to replace ergosterol in the cell membrane.

The primary target of azoles is lanosterol-14$\alpha$-demethylase (ERG11) encoded by *ERG11*. One of the most prevalent mechanisms of azole resistance in *Candida* spp. is the alteration of ERG11 protein.[131] *Candida* spp. can obtain resistance to azoles via nonsynonymous point mutation in the *ERG11* gene. This mutation leads to amino acid substitutions and altered conformation of the ERG11 protein formed. This will consequently reduce the susceptibility of the target enzyme to inhibition by azoles without affecting the cellular function of the enzyme.[132–134] In *C. krusei*, the reduced affinity of ERG11 to azoles due to *ERG11* gene mutation is the main mechanism of resistance to azoles.[135] Moreover, the reduced susceptibility of ERG11 is the chief mechanism of intrinsic fluconazole resistance,[121,135,136] together with constitutive but low expression of *ABC1*.[137]

Resistance to azole can also occur due to the increased expression of *ERG11*. This overexpression results in insufficient azole activity due to the overproduction of the target enzyme.[138] Although *ERG11* overexpression has been reported in azole-resistant NAC species, including *C. krusei*, the mechanism behind the overexpression remains unknown.[139,140]

Another mechanism of azole resistance is via the decreased intracellular accumulation of azole. This can be due to efflux pump activity or changes in the cell membrane. Drug efflux pumps belong to either major facilitator superfamily (MFS) class or ATP-binding cassette (ABC) family of transporters. Each of these protein functions to pump out toxic compounds across the cell membrane, and their overexpression results in multidrug resistance phenotype in pathogenic microbes.[137] In contrast to members of the MFS class that are powered by electrochemical proton-motive force, ABC family members rely on the hydrolysis of ATP for energy.[141,142] Furthermore, while the induction of *CDR*-encoded efflux pumps of the ABC family can confer resistance to all azoles, *MDR*-encoded efflux pumps of the MFS class are only selective for fluconazole efflux.[143] In *C. albicans*, the ABC transporters involved in azole resistance include CDR1 and CDR2.[139] Although no MFS transporter protein has been identified yet in *C. krusei*, it possesses CkABC1 and CkABC2 which are homologous to CDR1 and CDR2 proteins found in *C. albicans*, and their overexpression results in resistance to azoles.[68] Other ABC transporters such as ABC11 and ABC12 have also been identified in *C. krusei*.[36,66]

The overexpression of both ERG11 and efflux pump ABC2 has been reported to be involved in itraconazole resistance in *C. krusei*.[139,140] However, an unusual transient or stable resistance of *C. krusei* to fungicidal voriconazole has also emerged. Overexpression of ABC2 and ERG11, as observed in itraconazole resistance, imparts a transient resistance to voriconazole, while a more stable resistance was observed due to the overexpression of ABC1 and point mutation in *ERG11*.[145]

### Resistance to polyenes

Resistance to amphotericin B is very rare, possibly because it directly targets a vital cellular component, and resistance development attempts against this drug may present a fitness cost of increased sensitivity of mutants to host-relevant stresses.[146] However, there have been reports of increasing minimum inhibitory concentration (MIC) of amphotericin B in *C. krusei* isolates. Resistance to amphotericin B in *Candida* spp. is usually associated with decreased ergosterol content of the cell membrane.[17] The inactivation of ERG3 will result in low ergosterol levels and replacement of 14$\alpha$-methylfecosterol with ergosterol. This results in insufficient ergosterol for the action of polyenes.[147,148] Several other mutations in the ergosterol biosynthetic genes such as *ERG2*, *ERG5*, *ERG6*, *ERG11,* and *ERG24* can also result in polyene resistance.[149–153]

### Resistance to echinocandins

Although echinocandins possess fungicidal activities against all *Candida* spp. including azole and polyene-resistant strains,[154] the resistance of some isolates of *C. krusei*, to echinocandins has been reported.[155] The main mechanism of resistance to echinocandins is via point mutations within the conserved regions of *FKS1* and *FKS2* genes.[149,156] Mutations in these conserved regions, hotspot 1 (HS1) and hotspot 2 (HS2), within these genes, especially *FKS1,* result in amino-acid substitution and altered conformation of the resulting $\beta$-1,3-D-glucan synthase (FKS). As a result, the $\beta$-1,3-D-glucan synthase has diminished sensitivity to inhibition by echinocandins.[157,158] Acquired *FKS* point mutation has been reported in *Candida* spp. including *C. krusei.* However, the impact of each mutation on echinocandin susceptibility is determined by the position and type of the mutation and individual *Candida* spp.[155,159,160] For example, in *C. krusei,* amino acid D to Y substitution at the eighth codon in HS1 of *FKS1* results in a much higher MIC than in *C. albicans*.[161] Just as highlighted in polyene resistance, resistance to echinocandins may also confer reduced fitness, and this is because some mutations in *FKS* genes can result in FKS protein with reduced

catalysis of glucan synthesis, thus resulting in decreased synthesis of glucan. This fitness cost makes resistant strains to compete poorly with their wild-type counterparts, and this explains why they are seldom transmitted among patients.[162,163]

The initiation of adaptive stress response to counteract the toxic effect of echinocandins by fungi is another potential mechanism of echinocandin-resistance. Moreover, this is also a mechanism used to circumvent the decreased glucan content of resistant strains. This allows the stressed cell to increase the production of one or more components of the cell wall when another is inhibited.[19] *In vitro* studies have shown that *Candida* spp. increase chitin synthesis in response to inhibition of glucan synthesis by echinocandins. This increase is initiated by high-osmolarity glycerol response, protein kinase C and $Ca^{2+}$ calcineurin signaling pathways.[164,165]

### Other resistance mechanisms

Biofilms are microbial populations embedded in a self-produced extracellular polymer matrix and are usually adhered to either biotic or abiotic surfaces.[50] Biofilms play important roles in virulence, antifungal resistance, and protection against host defences.[53,54] Biofilm formation has been reported in many fungi, including *Candida* spp., such as *C. albicans* and *C. krusei*. Biofilms are known to reduce the effective drug concentration and to increase the non-susceptibility of these fungal species to antifungal drugs, especially azoles, polyenes and nucleoside analogues.[166,167] Biofilms are able to confer these benefits due to production of extracellular polymer matrix, which comprises polysaccharides, carbohydrates, proteins, and signaling molecules that decreases the penetration of drugs; dense population of fungal cells within the biofilm; enhanced activity of efflux pumps; alterations in sterol content of the fungal membrane via mutation or modified expression of ergosterol biosynthetic genes and presence of phenotypic variants known as persisteror dormant cells that are tolerant to drugs.[166,168]

The ability of fungi to adapt and survive various environmental stresses is partially due to their genomic flexibility.[27] Various genetic alterations such as aneuploidies (segmental or complete chromosomal) and loss of heterozygosity (LOH) have been linked to azole resistance in *C. albicans*.[162] Aneuploidy is rare under physiological conditions; however, it can be induced through various laboratory stress conditions and genetic manipulations.[169,170] Chromosomal abnormalities in the form of increased copy number of *ERG11* and formation of segmental/complete chromosomal aneuploidy have also been reported in NAC species, including *C. krusei*.[137]

## Alternative therapy

Due to antifungal resistance menace discussed above, complicated by the paucity of available antifungal arsenal and host toxicity, it is imperative to find novel antifungal drugs (including through drug repurposing) and exploit alternative treatment approaches. These alternative options include combination of antifungal drugs, the use of natural compounds, either alone or in combination with antifungal drugs, immunotherapeutic approaches, photodynamic inactivation and laser therapy.[171] Some of these approaches have been applied to *C. krusei*.

### Novel antifungal drugs

The lack of new antifungal drugs is made starkly clear by the fact that only one new antifungal (isavuconazole) and two posaconazole formulations were marketed over the last ten years.[172] This demonstrates the difficulties in commercializing new antifungals. A drug that is currently undergoing clinical evaluation is rezafungin, a structural analogue of anidulafungin. As an echinocandin, it also inhibits $\beta$-1,3-glucan synthesis and has increased stability and solubility. Other advantages include long half-life, limited toxicity, extensive tissue distribution and quick penetration into abscesses.[173–175] Tóth and colleagues[176] compared the *in vitro* activity of rezafungin with that of anidulafungin, caspofungin, micafungin, amphotericin B, and fluconazole against several *Candida* spp., including *C. krusei* and found that it displayed excellent activity against all *C. krusei* strains with a $MIC_{90}$ value of 0.06 mg/l.

Another inhibitor of $\beta$-1,3-glucan synthase is SCY-078. It is the first member of a new subclass of glucan synthase inhibitor, the triterpenoid antifungals. Although it shares a target with the echinocandins, the two classes differ in chemical structure and interaction with the target enzyme.[177] This compound has good oral bioavailability, Caco-2 cell monolayer permeability and extensive tissue distribution. It is also highly soluble in acidic media. Scorneaux and colleagues[178] found that SCY-078 had a MIC (1 $\mu$g/ml) against *C. krusei* comparable to the reference range of caspofungin (0.125–1 $\mu$g/ml).

### Drug repurposing

Drug repurposing (or repositioning) involves the application of drugs already approved for or undergoing clinical trials for the treatment of other diseases for a new purpose, such as antifungals. This approach may reduce the time, effort, and money required to develop new antifungals.[179] It often involves screening of large libraries of approved off-patent drugs to find drugs with antifungal activity. This has led to the identification of ebselen (currently undergoing clinical trials for various conditions), as an antifungal compound, effective against several *Candida* species, including *C. krusei*.[180] The proposed target for its antifungal activity is the thioredoxin system,[181] and it has been associated with the induction of reactive oxygen species and the depletion of intracellular glutathione levels.[182,183] Auranofin, an anti-inflammatory antirheumatic drug, has also shown anti-fungal

activity against *C. krusei*.[179] Interestingly, this drug also targets the thioredoxin system, indicating that these enzymes may be a possible target for novel antifungal drugs.[181]

The repurposing of serotonin reuptake inhibitors has shown potential as novel antifungals against *Candida* and *Aspergillus* species, and in a study by Kang and colleagues,[184] the serotonin receptor antagonist, metergoline, showed potent antifungal activity against fluconazole-resistant clinical *C. krusei* isolates. This drug also inhibited the production of extracellular phospholipases by this yeast, in a dose-dependent manner.

## Combination therapy

Combination therapy is usually more effective and provides more significant benefits than monotherapy. Its benefits include increased efficacy due to the complementary effects of both agents; reduction/decrease in resistance evolution rate; dosage reduction, which translates to decreased host toxicity and cidal activity, may results from two fungistatic agents.[185,186]

While an antagonistic effect is sometimes possible, the synergistic effects of various antifungal combinations have been reported. Examples are the combination of amphotericin B and caspofungin to treat a leukemic patient with fluconazole-resistant *C. krusei* fungemia, after he failed to respond to amphotericin B alone[118] as well as the successful treatment of a patient with *C. krusei* vertebral osteomyelitis with a combination of caspofungin and posaconazole after he failed to respond to caspofungin alone.[187] Katragkou and colleagues[188] studied the *in vitro* interactions of isavuconazole with amphotericin B or micafungin against strains of several *Candida* species, including *C. krusei* and found that the interaction of isavuconazole and micafungin was synergistic against *C. albicans*, *C. parapsilosis*, and *C. krusei*. However, the combination of isavuconazole and amphotericin B was either indifferent or antagonistic.

Antifungal drugs can also be combined with other drugs/compounds not traditionally considered to be antifungal. An example of such a strategy that may be effective against *C. krusei,* is the combination of calcineurin inhibitors and drugs targeting ergosterol synthesis. Although Cruz and colleagues[189] showed that the combination of fluconazole and the calcineurin inhibitors (cyclosporine A and FK506) is effective in inhibiting *C. albicans*, but not the more resistant *C. krusei*, combining calcineurin inhibitors with other drugs targeting ergosterol synthesis (such as terbinafine and fenpropimorph) can inhibit *C. krusei*.[190] A synergistic effect was also seen against clinical strains of *C. krusei in vitro*, when metergoline was combined with amphotericin B[184] as well as with a combination of tyrosol and amphotericin B.[191] Another compound shown to act in synergism with known antifungals is the triterpene, menthol.[192] It increased the effectiveness of itraconazole as well as nystatin against *C. krusei*. Moraes and colleagues[193] also demonstrated a synergistic interaction between the water-insoluble fraction from *Uncaria tomentosa* (cat's claw) bark and fluconazole or terbinafine against *C. krusei*. They determined that intermolecular interactions took place between the *U. tometosa* fraction and either fluconazole or terbinafine, and speculated that the synergism might be due to these interaction events, occurring outside the cell. The mechanism of action may then be targeted at the cell wall, without involvement of the ABC efflux pumps.

## Natural compounds and extracts

Plants are invaluable sources of pharmaceutical products, including potential antifungal compounds. Many articles on natural products claim to have discovered antifungal activities, but the methods used to test natural compounds for antifungal activity vary between groups and are often adapted to specific samples.[194] This makes it very difficult to impossible to compare results directly. Scorzoni and colleagues[194] tested various Brazilian plants for antifungal activity using different methods. Although they found that several extracts showed moderate antifungal activity against *C. krusei,* by the microdilution test, none of them showed any activity with the agar diffusion method. This method was thus less sensitive than the microdilution method in these antifungal tests.

Using the CLSI M27-A3 broth microdilution method, Marcos-Arias and colleagues[195] determined the activity of 10 pure constituents of essentials oils as well as farnesol and tyrosol against various *Candida* isolates. All the essential oil components were active against the *Candida* strains, including fluconazole-resistant *C. krusei*, with the lowest MIC for this strain at 0.06% (v/v) for terpinen-4-ol. The same method was used by Faria and colleagues[196] to test several phenolics found in edible plants. Compared to the other *Candida* spp. tested, *C. krusei* was generally less susceptible. However, several compounds (i.e., cinnamic, benzoic and salicylic acids, thymol, 2,3-dihydroxybenzaldehyde and 2,5-dihydroxybenzaldehyde) could inhibit growth by at least 90% at a concentration of 5 mmol/l.

Another group of natural products with *in vitro* antifungal activity are anthraquinones, found in many plants. Purpirin is a natural anthraquinone pigment, used as a food coloring agent and for cotton dye. This compound has also shown *in vitro* antifungal activity against several *Candida* spp., notably with a low MIC of 1.28 mg/ml against fluconazole-resistant *C. krusei*.[197]

## Photodynamic inactivation

Photodynamic inactivation requires a photosensitizing compound (generally macrocyclic compounds with no or minimal inherent toxicity), a light source and the presence of oxygen. This combination results in the excitation of the photosensitizer. The interaction between the excited photosensitizer and oxygen leads to the formation of highly reactive singlet oxygen, which can interact with cellular polymers such as DNA, proteins, and

**Table 7.** Effective combinations for photodynamic inactivation of *Candida krusei*.[198–201]

| Photosensitizer (concentration) | Light source (fluence) | Inhibitory effect |
|---|---|---|
| Photogem (50 mg/l) | Blue LED (18 J/cm$^2$) | 50% reduction in viability |
| Hyperin (40 $\mu$M) | Yellow LED (18 J/cm$^2$) | 3 $\log_{10}$ fold reduction in viability |
| Photofrin (1 $\mu$g/ml) | Broadband visible light (9 J/cm$^2$) | 50% reduction in viability |
| Methylene blue (100 $\mu$g/ml) | Red laser (28 J/cm$^2$) | 91.6% reduction in cfu |

lipids.[198,199] Although a blue light-emitting diode (LED) (predominantly 455 nm) and the photosensitizer, Photogem®, was able to inhibit *C. albicans*, *C. dubliniensis*, and *C. tropicalis*, it was unable to kill *C. krusei*, but a reduction in viability was observed.[199] In contrast, the photosensitizing agent, Photofrin was effective at inhibiting *C. krusei* in the presence of broadband visible light.[198] Another photosensitizing agent that was effective in inhibiting *C. krusei* by more than 90%, is methylene blue.[200] This was used with a red laser (685 nm). Hypericin, a naturally occurring polycyclic aromatic compound found in *Hypericum* spp., was tested in combination with a yellow LED (predominantly 602 nm) on a number of *Candida* spp.[201] Of the tested species, *C. krusei* was the least susceptible, requiring higher dosages of hypericin and more light to reduce viability, than *C. albicans* or *C. parapsilosis*. The different parameters used to obtain the best results are given in Table 7.

The epidemiology of candidiasis has changed with a shift to non-*albicans Candida* (NAC) species including *C. krusei*. This epidemiological shift is partly explained by the increased resistance of NAC species to antifungal drugs. *C. krusei* can cause life-threatening infections in immune-compromised patients, with hematologic malignancies patients and those using prolonged azole prophylaxis being at higher risk. The teleomorph of this yeast (*P. kudriavzevii*) has been given the Generally Regarded as Safe status by the US FDA, and it is used for the production of various food products including chocolate. However, this needs to be revisited given the pathogenic potential of *C. krusei*. The widespread use and misuse of the limited antifungal arsenal, as a result of the increased number of fungal infections due to the rise in the number of immunocompromised and terminally ill individuals, have resulted in increased resistance of fungal pathogens. Understanding the mechanisms of antifungal resistance of these pathogens is crucial for the effective management of their infections, effective use of the limited antifungals while also aiding in future drug development; for example, drugs or adjuvants that are efflux pump inhibitors can be developed to tackle drug resistance due to overexpression of efflux pumps. The paucity of antifungal agents coupled with the problem of antifungal resistance, host toxicity as well as difficulty in antifungal drug development partially due to the eukaryotic nature of both fungi and humans have left researchers to exploit alternative therapeutic options. Although *C. krusei* may also be more resistant to them than *C. albicans*, they provide avenues worthy of further investigation to find effective novel antifungal drugs, even in the face of several hurdles on the way to marketing of new antifungal therapies.

## Funding

The financial support of the National Research Foundation of South Africa is acknowledged (grant number 117435 to A.T.J.; grant number 115566 to C.H.P.).

## Declaration of interest

The authors report no conflict of interest. The authors alone are responsible for the content and the writing of the paper.

## References

1. Denning DW, Bromley MJ. How to bolster the antifungal pipeline. *Science*. 2015; 347: 1414–1416.
2. Brown GD, Denning DW, Gow NAR, Levitz SM, Netea MG, White TC. Hidden killers: human fungal infections. *Sci Transl Med*. 2012; 4: 165rv13.
3. Schmiedel Y, Zimmerli S. Common invasive fungal diseases: an overview of invasive candidiasis, aspergillosis, cryptococcosis, and *Pneumocystis* pneumonia. *Swiss Med Wkly*. 2016; 146: w14281.
4. Perfect JR, Hachem R, Wingard JR. Update on epidemiology of and preventive strategies for invasive fungal infections in cancer patients. *Clin Infect Dis*. 2014; 59: S352–S355.
5. Bassetti M, Peghin M, Timsit J-F. The current treatment landscape: candidiasis. *J Antimicrob Chemother*. 2016; 71: ii13–ii22.
6. Filler SG, Sheppard DC. Fungal invasion of normally non-phagocytic host cells. *PLoS Pathog*. 2006; 2: e129.
7. Samaranayake LP MacFarlane TW. (eds). *Oral Candidosis*. London: Wright-Butterworth, 1990.
8. Dixon DM, McNeil MM, Cohen ML, Gellin BG, La Montagne JR. Fungal infections: a growing threat. *Public Health Rep*. 1996; 111: 226–235.
9. Pfaller MA, Diekema DJ. Epidemiology of invasive candidiasis: A persistent public health problem. *Clin Microbiol Rev*. 2007; 20: 133–163.
10. Leroy O, Gangneux J-P, Montravers P et al. Epidemiology, management, and risk factors for death of invasive *Candida* infections in critical care: a multicenter, prospective, observational study in France (2005–2006). *Crit Care Med*. 2009; 37: 1612–1618.
11. Kullberg BJ, Arendrup MC. Invasive candidiasis. *N Engl J Med*. 2015; 373: 1445–1456.
12. da Silva CR, de Andrade Neto JB, Sidrim JJ et al. Synergistic Effects of amiodarone and fluconazole on *Candida tropicalis* resistant to fluconazole. *Antimicrob Agents Chemother*. 2013; 57: 1691–1700.
13. Sadeghi G, Ebrahimi-Rad M, Mousavi SF, Shams-Ghahfarokhi M, Razzaghi-Abyaneh M. Emergence of non-*Candida albicans* species: epidemiology, phylogeny and fluconazole susceptibility profile. *J Mycol Med*. 2018; 28: 51–58.
14. Odds FC. *Candida and Candidosis*, 2nd edn. London: Bailliere Tindall, 1988.
15. Butler G, Rasmussen MD, Lin MF et al. Evolution of pathogenicity and sexual reproduction in eight *Candida* genomes. *Nature*. 2009; 459: 657–662.

16. Yadav JSS, Bezawada J, Yan S, Tyagi RD, Surampalli RY. *Candida krusei*: biotechnological potentials and concerns about its safety. *Can J Microbiol*. 2012; 58: 937–952.
17. Scorzoni L, de Paula E, Silva ACA, Marcos CM et al. Antifungal therapy: new advances in the understanding and treatment of mycosis. *Front Microbiol*. 2017; 8: 36.
18. Kanafani ZA, Perfect JR. Resistance to antifungal agents: mechanisms and clinical impact. *Clin Infect Dis*. 2008; 46: 120–128.
19. Sanguinetti M, Posteraro B, Lass-Flörl C. Antifungal drug resistance among *Candida* species: mechanisms and clinical impact. *Mycoses*. 2015; 58: 2–13.
20. Falci DR, Pasqualotto A. Profile of isavuconazole and its potential in the treatment of severe invasive fungal infections. *Infect Drug Resist*. 2013; 22: 163–174.
21. Kathiravan MK, Salake AB, Chothe AS et al. The biology and chemistry of antifungal agents: a review. *Bioorg Med Chem*. 2012; 20: 5678–5698.
22. Grant SM, Clissold SP. Fluconazole. *Drugs*. 1990; 39: 877–916.
23. Andriole VT. Current and future antifungal therapy: new targets for antifungal therapy. *Int J Antimicrob Agents*. 2000; 16: 317–321.
24. Shukla PK, Singh P, Yadav RK, Pandey S, Bhunia SS. Past, present, and future of antifungal drug development. In: Saxena A. (ed). *Communicable Diseases of the Developing World. Topics in Medicinal Chemistry*, vol 29. Cham: Springer, 2016: 125–167.
25. Whaley SG, Berkow EL, Rybak JM, Nishimoto AT, Barker KS, Rogers PD. Azole antifungal resistance in *Candida albicans* and emerging non-*albicans Candida* species. *Front Microbiol*. 2017; 7: 2173.
26. Pappas PG, Kauffman CA, Andes DR et al. Executive summary: clinical practice guideline for the management of candidiasis: 2016 update by the infectious diseases society of America. *Clin Infect Dis*. 2016; 62: 409–417.
27. Robbins N, Caplan T, Cowen LE. Molecular evolution of antifungal drug resistance. *Annu Rev Microbiol*. 2017; 71: 753–775.
28. Castellani A. Observations on the fungi found in tropical bronchomycosis. *The Lancet*. 1912; 179: 13–15.
29. Samaranayake YH, Samaranayake LP. *Candida krusei*: biology, epidemiology, pathogenicity and clinical manifestations of an emerging pathogen. *J Medical Microbiol*. 1994; 41: 295–310.
30. Kudryavtsev VI. *The Systematics of Yeasts*. Berlin: Akademie Verlag, 1960 [in German].
31. Boidin J, Pignal MC, Besson M. The genus *Pichia sensu lato*. *Bull Soc Mycol France*. 1965; 81: 566–606 [in French].
32. Von Arx JA, Rodrigues de Miranda L, Smith M, Yarrow D. The genera of yeasts and yeast-like fungi. *Stud Mycol*. 1977; 14: 1–42.
33. Kurtzman CP, Robnett CJ. Identification and phylogeny of ascomycetous yeasts from analysis of nuclear large subunit (26S) ribosomal DNA partial sequences. *Antonie Leeuwenhoek*. 1998; 73: 331–371.
34. Kurtzman CP, Robnett CJ, Basehoar-Powers E. Phylogenetic relationships among species of *Pichia*, *Issatchenkia* and *Williopsis* determined from multigene sequence analysis, and the proposal of *Barnettozyma* gen. nov., *Lindnera* gen. nov. and *Wickerhamomyces* gen. nov. *FEMS Yeast Res*. 2008; 8: 939–954.
35. Kurtzman CP, Smiley MJ, Johnson CJ. Emendation of the genus *Issatchenkia* Kudriavzev and comparison of species by deoxyribonucleic acid reassociation, mating reaction, and ascospore ultrastructure. *Int J Syst Bacteriol*. 1980; 30: 503–513.
36. Douglass AP, Offei B, Braun-Galleani S et al. Population genomics shows no distinction between pathogenic *Candida krusei* and environmental *Pichia kudriavzevii*: one species, four names. *PLoS Pathog*. 2018; 14: e1007138.
37. Kurtzman CP, Smiley MJ. Heterothallism in *Pichia kudriavzevii* and *Pichia terricola*. *Antonie Leeuwenhoek*. 1976; 42: 355–363.
38. Samaranayake YH, Wu PC, Samaranayake LP, Ho PL. The relative pathogenicity of *Candida krusei* and *C. albicans* in the rat oral mucosa. *J Med Microbiol*. 1998; 47: 1047–1057.
39. Tuntiwongwanich S, Leenanon B. Morphology and identification of yeasts isolated from Toddy palm in Thailand. *J Microsc Soc Thail*. 2009; 23: 34–37.
40. Al Mosaid A, Sullivan DJ, Coleman DC. Differentiation of *Candida dubliniensis* from *Candida albicans* on Pal's agar. *J Clin Microbiol*. 2003; 41: 4787–4789.
41. Sahand IH, Moragues MD, Eraso E, Villar-Vidal M, Quindós G, Pontón J. Supplementation of CHROMagar Candida medium with Pal's medium for rapid identification of *Candida dubliniensis*. *J Clin Microbiol*. 2005; 43: 5768–5770.
42. Horvath LL, Hospenthal DR, Murray CK, Dooley DP. Direct isolation of *Candida* spp. from blood cultures on the chromogenic medium CHROMagar *Candida*. *J Clin Microbiol*. 2003; 41: 2629–2632.
43. Rao SD, Wavare S, Patil S. Onycholysis caused by *Candida krusei*. *Indian J Med Microbiol*. 2004; 22: 258–259.
44. Bourdichon F, Casaregola S, Farrokh C et al. Food fermentations: Microorganisms with technological beneficial use. *Int J Food Microbiol*. 2012; 154: 87–97.
45. Jolly NP, Augustyn OPH, Pretorius IS. The role and use of non-*Saccharomyces* yeasts in wine production. *S Afr J Eno Vitic*. 2006; 27: 15–39.
46. Hayford AE, Jakobsen M. Characterization of *Candida krusei* strains from spontaneously fermented maize dough by profiles of assimilation, chromosome profile, polymerase chain reaction and restriction endonuclease analysis. *J Appl Microbiol*. 1999; 87: 29–40.
47. Nakayama S, Morita T, Negishi H, Ikegami T, Sakaki K, Kitamoto D. *Candida krusei* produces ethanol without production of succinic acid; a potential advantage for ethanol recovery by pervaporation membrane separation. *FEMS Yeast Res*. 2008; 8: 706–714.
48. Lategan PM, Erasmus SC, Du Preez JC. Characterisation of pathogenic species of *Candida* by gas chromatography: preliminary findings. *J Med Microbiol*. 1981; 14: 219–222.
49. Quan C-S, Fan S-D, Zhang L-H, Wang YJ, Ohta Y. Purification and properties of a phytase from *Candida krusei* WZ-001. *J Biosci Bioeng*. 2002; 94: 419–425.
50. Wang X, Yao X, Zhu Z et al. Effect of berberine on *Staphylococcus epidermidis* biofilm formation. *Int J Antimicrob Agents*. 2009; 34: 60–66.
51. Elder MJ, Matheson M, Stapleton F, Dart JKG. Biofilm formation in infectious crystalline keratopathy due to *Candida albicans*. *Cornea*. 1996; 15: 301–304.
52. Costerton JW. Cystic fibrosis pathogenesis and the role of biofilms in persistent infection. *Trends Microbiol*. 2001; 9: 50–52.
53. Baillie GS, Douglas LJ. Matrix polymers of *Candida* biofilms and their possible role in biofilm resistance to antifungal agents. *J Antimicrob Chemother*. 2000; 46: 397–403.
54. Samaranayake L, Fidel P, Naglik JR et al. Fungal infections associated with HIV infection. *Oral Dis*. 2002; 8: 151–160.
55. Douglas LJ. *Candida* biofilms and their role in infection. *Trends Microbiol*. 2003; 11: 30–36.
56. Park SJ, Han K-H, Park JY, Choi SJ, Lee K-H. Influence of bacterial presence on biofilm formation of *Candida albicans*. *Yonsei Med J*. 2014; 55: 449.
57. Bandara H, Yau JYY, Watt RM, Jin LJ, Samaranayake LP. *Pseudomonas aeruginosa* inhibits in-vitro *Candida* biofilm development. *BMC Microbiol*. 2010; 10: 125.
58. Thein ZM, Samaranayake YH, Samaranayake LP. Characteristics of dual species *Candida* biofilms on denture acrylic surfaces. *Arch Oral Biol*. 2007; 52: 1200–1208.
59. Santos JD, Piva E, Vilela SFG, Jorge AO, Junqueira JC. Mixed biofilms formed by *C. albicans* and non-*albicans* species: a study of microbial interactions. *Braz Oral Res*. 2016; 30: e23.
60. Rossoni RD, Barbosa JO, Vilela SFG et al. Competitive interactions between *C. albicans*, *C. glabrata* and *C. krusei* during biofilm formation and development of experimental candidiasis. *PLoS One*. 2015; 10: e0131700.
61. Barros PP, Ribeiro FC, Rossoni RD, Junqueira JC, Jorge AO. Influence of *Candida krusei* and *Candida glabrata* on *Candida albicans* gene expression in *in vitro* biofilms. *Arch Oral Biol*. 2016; 64: 92–101.
62. Barros PP, Freire F, Rossoni RD, Junqueira JC, Jorge AO. *Candida krusei* and *Candida glabrata* reduce the filamentation of *Candida albicans* by downregulating expression of HWP1 gene. *Folia Microbiol*. 2017; 62: 317–323.
63. Rossoni RD, de Barros PP, Freire F, Jorge AO, Junqueira JC. Study of microbial interaction formed by *Candida krusei* and *Candida glabrata*: *in vitro* and *in vivo* studies. *Braz Dent J*. 2017; 28: 669–674.
64. Korres AMN, Buss DS, Ventura JA, Fernandes PMB. *Candida krusei* and *Kloeckera apis* inhibit the causal agent of pineapple fusariosis, *Fusarium guttiforme*. *Fungal Biol*. 2011; 115: 1251–1258.
65. Fleischmann J, Broeckling CD, Lyons S. *Candida krusei* form mycelia along agar surfaces towards each other and other *Candida* species. *BMC Microbiol*. 2017; 17: 60.
66. Lamping E, Zhu J, Niimi M, Cannon RD. Role of ectopic gene conversion in the evolution of a *Candida krusei* pleiotropic drug resistance transporter family. *Genetics*. 2017; 205: 1619–1639.

67. Cuomo CA, Shea T, Yang B, Rao R, Forche A. Whole genome sequence of the heterozygous clinical isolate *Candida krusei* 81-B-5. *G3*. 2017; 7: 2883–2889.
68. Katiyar SK, Edlind TD. Identification and expression of multidrug resistance related ABC transporter genes in *Candida krusei*. *Med Mycol*. 2001; 39: 109–116.
69. Chan GF, Gan HM, Ling HL, Rashid NAA. Genome sequence of *Pichia kudriavzevii* M12, a potential producer of bioethanol and phytase. *Eukaryot Cell*. 2012; 11: 1300–1301.
70. van Rijswijck IMH, Derks MFL, Abee T, de Ridder D, Smid EJ. Genome sequences of *Cyberlindnera fabianii* 65, *Pichia kudriavzevii* 129, and *Saccharomyces cerevisiae* 131 isolated from fermented masau fruits in Zimbabwe. *Genome Announc*. 2017; 5: e00064–17.
71. Park HJ, Ko H-J, Jeong H et al. Draft genome sequence of a multistress-tolerant yeast, *Pichia kudriavzevii* NG7. *Genome Announc*. 2018; 6: e01515–17.
72. Hong S-M, Kwon H-J, Park S-J et al. Genomic and probiotic characterization of SJP-SNU strain of *Pichia kudriavzevii*. *AMB Express*. 2018; 8: 80.
73. EFSA BIOHAZ Panel. The 2019 updated list of QPS status recommended biological agents in support of EFSA risk assessments. *EFSA J*. 2020; 18: 5966.
74. Tornadijo ME, Fresno JM, Martin Sarmiento R, Carballo J. Study of the yeasts during the ripening process of Armada cheeses from raw goat's milk. *Le Lait*. 1998; 78: 647–659.
75. Bockelmann W, Willems KP, Neve H, Heller KH. Cultures for the ripening of smear cheeses. *Int Dairy J*. 2005; 15: 719–732.
76. Lore TA, Mbugua SK, Wangoh J. Enumeration and identification of microflora in suusac, a Kenyan traditional fermented camel milk product. *LWT-Food Sci Technol*. 2005; 38: 125–130.
77. Jespersen L, Nielsen D, Honholt S, Jakobsen M. Occurrence and diversity of yeasts involved in fermentation of West African cocoa beans. *FEMS Yeast Res*. 2005; 5: 441–453.
78. Gálvez SL, Loiseau G, Paredes JL, Barel M, Guiraud J-P. Study on the microflora and biochemistry of cocoa fermentation in the Dominican Republic. *Int J Food Microbiol*. 2007; 114: 124–130.
79. Oyewole OB. Characteristics and significance of yeasts' involvement in cassava fermentation for 'fufu' production. *Int J Food Microbiol*. 2001; 65: 213–218.
80. Oguntoyinbo FA. Evaluation of diversity of *Candida* species isolated from fermented cassava during traditional small scale gari production in Nigeria. *Food Control*. 2008; 19: 465–469.
81. Omemu AM, Andeosun OF. Evaluation of hazards and critical control points of ogi in small scale processing centres in Abeokuta, Nigeria. *J Appl Biosci*. 2010; 29: 1766–1773.
82. Ellis WO, Dziedzoave NT, Boakye K, Simpson BK, Smith JP. Effect of cassava variety and processing methods on the performance of 'kudeme' in agbelima production. *Food Control*. 1997; 8: 199–204.
83. Achi OK, Akubor PI. Microbial characterization of yam fermentation for 'elubo' (yam flour) production. *World J Microbiol Biotechnol*. 2000; 16: 3–7.
84. Liu Y, Liu D, Xie D. Improvement of glycerol production by *Candida krusei* in batch and continuous cultures using corn steep liquor. *Biotechnol Lett*. 2002; 24: 1539–1542.
85. Chen G, Yao S, Guan Y. Influence of osmoregulators on osmotolerant yeast *Candida krusei* for the production of glycerol. *Chin J Chem Eng*. 2006; 14: 371–376.
86. Gallardo JCM, Souza CS, Cicarelli RMB, Oliveira KF, Morais KF, Laluce C. Enrichment of a continuous culture of *Saccharomyces cerevisiae* with the yeast *Issatchenkia orientalis* in the production of ethanol at increasing temperatures. *J Ind Microbiol Biotechnol*. 2011; 38: 405–414.
87. Ikegami T, Morita T, Nakayama S et al. Processing of ethanol fermentation broth by *Candida krusei* to separate bioethanol by pervaporation using silicone rubber-coated silicate membranes. *J Chem Technol Biotechnol*. 2009; 84: 1172–1177.
88. Yu Z, Wen X. Screening and identification of yeasts for decolorizing synthetic dyes in industrial wastewater. *Int Biodeterior Biodegradation*. 2005; 56: 109–114.
89. Deivasigamani C, Das N. Biodegradation of basic violet 3 by *Candida krusei* isolated from textile wastewater. *Biodegradation*. 2011; 22: 1169–1180.
90. Dorko E, Zibrin M, Jenča A, Pilipčinec E, Danko J, Tkáčiková L. The histopathological characterization of oral *Candida* leukoplakias. *Folia Microbiol*. 2001; 46: 447–451.
91. Jain N, Hasan F, Fries BC. Phenotypic switching in fungi. *Curr Fungal Infect Rep*. 2008; 2: 180–188.
92. Vargas KG, Srikantha R, Holke A, Sifiri T, Morris R, Joly S. *Candida albicans* switch phenotypes display differential levels of fitness. *Med Sci Monit*. 2004; 10: 198–206.
93. Arzmi MH, Abdul Razak F, Yusoff Musa M, Wan Harun WHA. Effect of phenotypic switching on the biological properties and susceptibility to chlorhexidine in *Candida krusei* ATCC 14243. *FEMS Yeast Res*. 2012; 12: 351–358.
94. Ibrahim AS, Mirbod F, Filler SG et al. Evidence implicating phospholipase as a virulence factor of *Candida albicans*. *Infect Immun*. 1995; 63: 1993–1998.
95. Hube B. Possible role of secreted proteinases in *Candida albicans* infections. *Rev Iberoam Micol*. 1998; 15: 65–68.
96. Yang Y. Virulence factors of *Candida* species. *J Microbiol Immunol Infect*. 2003; 36: 223–228.
97. Kawecki D, Swoboda-Kopec E, Dabkowska M et al. Enzymatic variability of *Candida krusei* isolates in a course of fungal infection in a liver transplant recipient. *Transplant Proc*. 2006; 38: 250–252.
98. Costa CR, Passos XS, Souza LKH, PdeA Lucena. Fernandes OdeFL, Silva MdoR. Differences in exoenzyme production and adherence ability of *Candida* spp. isolates from catheter, blood and oral cavity. *Rev Inst Med Trop S Paulo*. 2010; 52: 139–143.
99. Trick WE, Fridkin SK, Edwards JR et al. Secular trend of hospital-acquired candidemia among intensive care unit patients in the United States during 1989–1999. *Clin Infect Dis*. 2002; 35: 627–630.
100. Poikonen E, Lyytikäinen O, Anttila V-J et al. Secular trend in candidemia and the use of fluconazole in Finland, 2004–2007. *BMC Infect Dis*. 2010; 10: 312.
101. Chi H-W, Yang Y-S, Shang S-T et al. *Candida albicans* versus non-*albicans* bloodstream infections: the comparison of risk factors and outcome. *J Microbiol Immunol Infect*. 2011; 44: 369–375.
102. Quindós G, Marcos-Arias C, San-Millán R, Mateo E, Eraso E. The continuous changes in the aetiology and epidemiology of invasive candidiasis: from familiar *Candida albicans* to multiresistant *Candida auris*. *Int Microbiol*. 2018; 21: 107–119.
103. Pfaller MA, Diekema DJ, Turnidge JD, Castabheira M, Jones RN. Twenty years of the SENTRY antifungal surveillance program: results for *Candida* species from 1997–2016. *Open Forum Infect Dis*. 2019; 6: S79–S94.
104. McCarty TP, McCarty TP. Invasive candidiasis. *Infect Dis Clin North Am*. 2016; 30: 103–124.
105 Pappas PG, Lionakis MS, Arendrup MC, Ostrosky-Zeicher L, Krullberg BJ. Invasive candidiasis. *Nat Rev Dis Primers*. 2018; 4: 18026.
106. Pfaller M, Neofytos D, Diekema D et al. Epidemiology and outcomes of candidemia in 3648 patients: data from the Prospective Antifungal Therapy (PATH Alliance®) registry, 2004–2008. *Diagn Microbiol Infect Dis*. 2012; 74: 323–331.
107. Castanheira M, Messer SA, Rhomberg PR, Pfaller MA. Antifungal susceptibility patterns of a global collection of fungal isolates: results of the SENTRY antifungal surveillance program (2013). *Diagn Microbiol Infect Dis*. 2016; 85: 200–204.
108. Pfaller M, Diekema DI, Gibbs DL et al. Results from the ARTEMIS DISK global antifungal surveillance study. 1997 to 2007: a 10.5-year analysis of susceptibilities of *Candida* species to fluconazole and voriconazole as determined by CLSI standardized disk diffusion. *J Clin Microbiol*. 2010; 48: 1366–1377.
109. Van Schalkwyk E, Iyaloo S, Naicker SD et al. Large outbreaks of fungal and bacterial bloodstream infections in a neonatal unit, South Africa, 2012–2016. *Emerg Infect Dis*. 2018; 24: 1204–1212.
110. Hachem R, Hanna H, Kontoyiannis D, Jiang Y, Raad I. The changing epidemiology of invasive candidiasis. *Cancer*. 2008; 112: 2493–2499.
111. Wingard JR, Merz WG, Rinaldi MG, Johnson TR, Karp JE, Saral R. Increase in *Candida krusei* infection among patients with bone marrow transplantation and neutropenia treated prophylactically with fluconazole. *N Engl J Med*. 1991; 325: 1274–1277.
112. Muñoz P, Sánchez-Somolinos M, Alcalá L, Rodríguez-Créixems M, Peláez T, Bouza E. *Candida krusei* fungaemia: antifungal susceptibility and clinical presentation of an uncommon entity during 15 years in a single general hospital. *J Antimicrob Chemother*. 2005; 55: 188–193.
113. Krcmery V, Barnes AJ. Non-*albicans Candida* spp. causing fungaemia: pathogenicity and antifungal resistance. *J Hosp Infect*. 2002; 50: 243–260.

114. Abi Said D, Anaissie E. Epidemiology of non-*albicans Candida* spp. *Clin Infect Dis*. 1998; 7: 1131–1133.
115. Goodman JL, Winston DJ, Greenfield RA et al. A controlled trial of fluconazole to prevent fungal infections in patients undergoing bone marrow transplantation. *N Engl J Med*. 1992; 326: 845—851.
116. Berrouane YF, Hollis RJ, Pfaller MA. Strain variation among and antifungal susceptibilities of isolates of *Candida krusei*. *J Clin Microbiol*. 1996; 34: 1856–1858.
117 Majoros L, Szegedi I, Kardos G et al. Slow response of invasive *Candida krusei* infection to amphotericin B in a clinical time-kill study. *Europ J Clin Microbiol Infect Dis*. 2006; 25: 803–806.
118. Olver WJ, Scott F, Shankland S. Successful treatment of *Candida krusei* fungemia with amphotericin B and caspofungin. *Med Mycol*. 2006; 44: 655–657.
119. Pfaller MA, Diekema DJ, Gibbs DL et al. *Candida krusei*, a multidrug-resistant opportunistic fungal pathogen: geographic and temporal trends from the ARTEMIS DISK antifungal surveillance program, 2001 to 2005. *J Clin Microbiol*. 2008; 46: 515–521
120. Lee JK, Peters D, Obias AA, Noskin GA, Peterson LR. Activity of voriconazole against *Candida albicans* and *Candida krusei* isolated since 1984. *Int J Antimicrob Agents*. 2000; 16: 205–209.
121. Fukuoka T, Johnston DA, Winslow CA et al. Genetic basis for differential activities of fluconazole and voriconazole against *Candida krusei*. *Antimicrob Agents Chemother*. 2003; 47: 1213–1219.
122. Rybak JM, Marx KR, Nishimoto AT, Rogers PD. Isavuconazole: pharmacology, pharmacodynamics, and current clinical experience with a new triazole antifungal agent. *Pharmacotherapy*. 2015; 35: 1037–1051.
123. Espinel-Ingroff A, Pfaller MA, Bustamante B et al. Multilaboratory study of epidemiological cutoff values for detection of resistance in eight *Candida* species to fluconazole, posaconazole, and voriconazole. *Antimicrob Agents Chemother*. 2014; 58: 2006–2012.
124. Pfaller MA, Rhomberg PR, Messer SA, Jones RN, Castanheira M. Isavuconazole, micafungin, and 8 comparator antifungal agents' susceptibility profiles for common and uncommon opportunistic fungi collected in 2013: temporal analysis of antifungal drug resistance using CLSI species-specific clinical breakpoints and proposed epidemiological cutoff values. *Diagn Microbiol Infect Dis*. 2015; 82: 303–313.
125. Arendrup MC, Sulim S, Holm A et al. Diagnostic issues, clinical characteristics, and outcomes for patients with fungemia. *J Clin Microbiol*. 2011; 49: 3300–3308.
126. Hakki M, Staab JF, Marr KA. Emergence of a *Candida krusei* isolate with reduced susceptibility to caspofungin during therapy. *Antimicrob Agents Chemother*. 2006; 50: 2522–2524.
127. Pfaller M, Boyken L, Hollis R et al. Use of epidemiological cutoff values to examine 9-year trends in susceptibility of *Candida* species to anidulafungin, caspofungin, and micafungin. *J Clin Microbiol*. 2011; 49: 624–629.
128. Canturk Z. Evaluation of synergistic anticandidal and apoptotic effects of ferulic acid and caspofungin against *Candida albicans*. *J Food Drug Anal*. 2018; 26: 439–443.
129. Rex JH, Pfaller MA, Galgiani JN et al. Development of interpretive breakpoints for antifungal susceptibility testing: conceptual framework and analysis of in vitro-in vivo correlation data for fluconazole, itraconazole, and *Candida* infections. *Clin Infect Dis*. 1997; 24: 235–247.
130. Anderson JB. Evolution of antifungal-drug resistance: mechanisms and pathogen fitness. *Nature Rev Microbiol*. 2005; 3: 547–556.
131. Marichal P, Koymans L, Willemsens S et al. Contribution of mutations in the cytochrome P450 14α-demethylase (Erg11p, Cyp51p) to azole resistance in *Candida albicans*. *Microbiology*. 1999; 145: 2701–2713.
132. Jiang C, Dong D, Yu B et al. Mechanisms of azole resistance in 52 clinical isolates of *Candida tropicalis* in China. *J Antimicrob Chemother*. 2013; 68: 778–785.
133. Xiang M-J, Liu J-Y, Ni P-H et al. *Erg11 mutations associated with azole resistance in clinical isolates of Candida albicans*. *FEMS Yeast Res*. 2013; 13: 386–393.
134. You L, Qian W, Yang Q et al. ERG11 gene mutations and MDR1 upregulation confer pan-azole resistance in *Candida tropicalis* causing disseminated candidiasis in an acute lymphoblastic leukemia patient on posaconazole prophylaxis. *Antimicrob Agents Chemother*. 2017; 61: e02496–16.
135. Orozco AS, Higginbotham LM, Hitchcock CA, Peláez T, Bouza E. Mechanism of fluconazole resistance in *Candida krusei*. *Antimicrob Agents Chemother*. 1998; 42: 2645–2649.
136. Venkateswarlu K, Denning DW, Kelly SL. Inhibition and interaction of cytochrome P450 of *Candida krusei* with azole antifungal drugs. *Med Mycol*. 1997; 35: 19–25.
137. Lamping E, Ranchod A, Nakamura K et al. Abc1p is a multidrug efflux transporter that tips the balance in favor of innate azole resistance in *Candida krusei*. *Antimicrob Agents Chemother*. 2009; 53: 354–369.
138. MacPherson S, Akache B, Weber S, De Deken X, Raymond M, Turcotte B. *Candida albicans* zinc cluster protein Upc2p confers resistance to antifungal drugs and is an activator of ergosterol biosynthetic genes. *Antimicrob Agents Chemother*. 2005; 49: 1745–1752.
139. Tavakoli M, Zaini F, Kordbacheh M, Safra M, Raoofian R, Heidari M. Up-regulation of the ERG11 gene in *Candida krusei* by azoles. *Daru*. 2010; 18: 276–280.
140. He X, Zhao M, Chen J et al. Overexpression of both ERG11 and ABC2 genes might be responsible for itraconazole resistance in clinical isolates of *Candida krusei*. *PLoS One*. 2015; 10: e0136185.
141. Pao SS, Paulsen IT, Saier MH. Major facilitator superfamily. *Microbiol Mol Biol Rev*. 1998; 62: 1–34
142. Rees DC, Johnson E, Lewinson O. ABC transporters: the power to change. *Nat Rev Mol Cell Biol*. 2009; 10: 218–27.
143. Falagas ME, Roussos N, Vardakas KZ. Relative frequency of *albicans* and the various non-*albicans Candida* spp. among candidemia isolates from inpatients in various parts of the world: a systematic review. *Int J Infect Dis*. 2010; 14: e954–e966.
144. Rogers T. Antifungal drug resistance: limited data, dramatic impact? *Int J Antimicrob Agents*. 2006; 27: 7–11.
145. Ricardo E, Miranda IM, Faria-Ramos I, Silva RM, Rodrigues AG, Pina-Vaz C. In vivo and in vitro acquisition of resistance to voriconazole by *Candida krusei*. *Antimicrob Agents Chemother*. 2014; 58: 4604–4611.
146. Vincent BM, Lancaster AK, Scherz-Shouval R, Whitesell L, Lindquist S. Fitness trade-offs restrict the evolution of resistance to amphotericin B. *PLoS Biol*. 2013; 11: e1001692.
147. Young LY, Hull CM, Heitman J. Disruption of ergosterol biosynthesis confers resistance to amphotericin B in *Candida lusitaniae*. *Antimicrob Agents Chemother*. 2003; 47: 2717–2724.
148. Sheikh N, Jahagirdar V, Kothadia S, Nagoba B. Antifungal drug resistance in *Candida* species. *Eur J Gen Med*. 2013; 10: 254–258.
149. Sanglard D. Emerging threats in antifungal-resistant fungal pathogens. *Front Med*. 2016; 3: 11.
150. Vandeputte P, Tronchin G, Larcher G et al. A nonsense mutation in the ERG6 gene leads to reduced susceptibility to polyenes in a clinical isolate of *Candida glabrata*. *Antimicrob Agents Chemother*. 2008; 52: 3701–3709.
151. Martel CM, Parker JE, Bader O et al. A clinical isolate of *Candida albicans* with mutations in ERG11 (encoding Sterol 14α-demethylase) and ERG5 (encoding C22 desaturase) is cross resistant to azoles and amphotericin B. *Antimicrob Agents Chemother*. 2010; 54: 3578–3583.
152. Hull CM, Bader O, Parker JE et al. Two clinical isolates of *Candida glabrata* exhibiting reduced sensitivity to amphotericin B both harbor mutations in ERG2. *Antimicrob Agents Chemother*. 2012; 56: 6417–6421.
153. Jensen RH, Astvad KMT, Silva LV et al. Stepwise emergence of azole, echinocandin and amphotericin B multidrug resistance in vivo in *Candida albicans* orchestrated by multiple genetic alterations. *J Antimicrob Chemother*. 2015; 70: 2551–2555.
154. Pfaller MA, Messer SA, Boyken L et al. Caspofungin activity against clinical isolates of fluconazole-resistant *Candida*. *J Clin Microbiol*. 2003; 41: 5729–5731.
155. Arendrup MC, Perlin DS. Echinocandin resistance. *Curr Opin Infect Dis*. 2014; 27: 484–492.
156. Vandeputte P, Ferrari S, Coste AT. Antifungal resistance and new strategies to control fungal infections. *Int J Microbiol*. 2012; 2012: Art 713687.
157. Park S, Kelly R, Kahn JN et al. Specific substitutions in the echinocandin target Fks1p account for reduced susceptibility of rare laboratory and clinical *Candida* sp. isolates. *Antimicrob Agents Chemother*. 2005; 49: 3264–3273.

158. Ksiezopolska E, Gabaldón T. Evolutionary emergence of drug resistance in *Candida* opportunistic pathogens. *Genes*. 2018; 9: 461.
159. Garcia-Effron G, Katiyar SK, Park S, Edlin TD, Perlin DS. A naturally occurring proline-to-alanine amino acid change in Fks1p in *Candida parapsilosis*, *Candida orthopsilosis*, and *Candida metapsilosis* accounts for reduced echinocandin susceptibility. *Antimicrob Agents Chemother*. 2008; 52: 2305–2312.
160. Jensen RH. Resistance in human pathogenic yeasts and filamentous fungi: prevalence, underlying molecular mechanisms and link to the use of antifungals in humans and the environment. *Dan Med J*. 2016; 63: 1–34.
161. Jensen RH, Justesen US, Rewes A, Perlin DS, Arendrup MC. Echinocandin failure case due to a previously unreported FKS1 mutation in *Candida krusei*. *Antimicrob Agents Chemother*. 2014; 58: 3550–3552.
162. Cowen LE, Sanglard D, Howard SJ, Rogers PD, Perlin DS. Mechanisms of antifungal drug resistance. *Cold Spring Harb Perspect Med*. 2015; 5: a019752.
163. Ben-Ami R, Garcia-Effron G, Lewis RE et al. Fitness and virulence costs of *Candida albicans* FKS1 hot spot mutations associated with echinocandin resistance. *J Infect Dis*. 2011; 204: 626–635.
164. Munro CA, Selvaggini S, de Bruijn I et al. The PKC, HOG and $Ca^{2+}$ signalling pathways co-ordinately regulate chitin synthesis in *Candida albicans*. *Mol Microbiol*. 2007; 63: 1399–1413.
165. Walker LA, Munro CA, de Bruijn I, Lenardon MD, McKinnon A, Gow NA. Stimulation of chitin synthesis rescues *Candida albicans* from echinocandins. *PLoS Pathog*. 2008; 4: e1000040.
166. Ramage G, Rajendran R, Sherry L, Williams C Fungal biofilm resistance. *Int J Microbiol*. 2012; 2012: 528521.
167. Desai JV, Mitchell AP, Andes DR. Fungal biofilms, drug resistance, and recurrent infection. *Cold Spring Harb Perspect Med*. 2014; 4: a019729–a019729.
168. Finkel JS, Mitchell AP. Genetic control of *Candida albicans* biofilm development. *Nat Rev Microbiol*. 2011; 9: 109–118.
169. Rustchenko E. Chromosome instability in *Candida albicans*. *FEMS Yeast Res*. 2007; 7: 2–11.
170. Selmecki A, Forche A, Berman J. Genomic plasticity of the human fungal pathogen *Candida albicans*. *Eukaryot Cell*. 2010; 9: 991–1008.
171. Rodrigues ME, Silva S, Azeredo J, Henriques M. Novel strategies to fight *Candida* species infection. *Crit Rev Microbiol*. 2016; 42: 594–606.
172. Van Deale R, Spriet I, Wauters J et al. Antifungal drugs: what brings the future? *Med Mycol*. 2019; 57: S328–S343.
173. Ong V, Hough G, Schlosser M et al. Preclinical evaluation of the stability, safety, and efficacy of CD101, a novel echinocandin. *Antimicrob Agents Chemother*. 2016; 60: 6872–6879.
174. Sandison T, Ong V, Lee J, Thye D. Safety and pharmacokinetics of CD101 IV, a novel echinocandin, in healthy adults. *Antimicrob Agents Chemother*. 2017; 61: e01627–16.
175. Zhao Y, Prideaux B, Nagasaki Y et al. Unraveling drug penetration of echinocandin antifungals at the site of infection in an intra-abdominal abscess model. *Antimicrob Agents Chemother*. 2017; 61: e01009–17.
176. Tóth Z, Forgács L, Locke JB et al. In vitro activity of rezafungin against common andrare *Candida* species and Saccharomyces cerevisiae. *J Antimicrob Chemother*. 2019; 74: 3505–3510.
177. Wring SA, Randolph R, Park S et al. Preclinical pharmacokinetics and pharmacodynamics target of SCY-078, a first-in-class orally active antifungal glucan synthesis inhibitor, in murine models of disseminated candidiasis. *Antimicrob Agents Chemother*. 2017; 61: e02068–16.
178. Scorneaux B, Angulo D, Borroto-Esoda K, Ghannoum M, Peel M, Wring S. SCY-078 is fungicidal against *Candida* species in time-kill studies. *Antimicrob Agents Chemother*. 2017; 61: e01961–16.
179. Wiederhold NP, Patterson TF, Srinivasan A et al. Repurposing auranofin as an antifungal: in vitro activity against a variety of medically important fungi. *Virulence*. 2017; 8: 138–142.
180. Wall G, Chaturvedi AK, Wormley FL, Wiederhold NP, Patterson HP, Patterson TF, Lopez-Ribot JL. Screening a repurposing library for inhibitors of multidrug-resistant *Candida auris* identifies ebselen as a repositionable candidate for antifungal drug development. *Antimicrob Agents Chemother*. 2018; 61: e01084–18.
181. May HC, Yu J- J, Guentzel MN, Chambers JP, Cap AP, Arulanandam BP. Repurposing auranofin, ebselen, and PX-12 as antimicrobial agents targeting the thioredoxin system. *Front Microbiol*. 2018; 9: 336.
182. Azad GK, Singh V, Mandal P, Singh P, Golla U, Baranwal S, Chauhan S, Tomar RS. Ebselen induces reactive oxygen species (ROS)-mediated cytotoxicity in *Saccharomyces cerevisiae* with inhibition of glutamate dehydrogenase being a target. *FEBS Open Bio*. 2014; 4: 77–89.
183. Thangamani S, Eldesouky HE, Mohammad H, Pascuzzi PE, Avramova L, Hazbun TR, Seleem MN. Ebselen exerts antifungal activity by regulating glutathione (GSH) and reactive oxygen species (ROS) production in fungal cells. *Biochim Biophys Acta Gen Subj*. 2017; 1861: 3002–3010.
184. Kang K, Wong K-S, Jayampath Seneviratne C, Samaranayake LP, Fong WP, Tsang PW-K. In vitro synergistic effects of metergoline and antifungal agents against *Candida krusei*. *Mycoses*. 2009; 53: 495–499.
185. Chang Y-L, Yu S-J, Heitman J, Wellington M, Chen YL. New facets of antifungal therapy. *Virulence*. 2017; 8: 222–236.
186. Prasad R, Banerjee A, Shah AH. Resistance to antifungal therapies. *Essays Biochem*. 2017; 61: 157–166.
187. Schilling A, Seibold M, Mansmann V, Gleissner B. Successfully treated *Candida krusei* infection of the lumbar spine with combined caspofungin/posaconazole therapy. *Med Mycol*. 2008; 46: 79–83.
188. Katragkou A, McCarthy M, Meletiadis J et al. In vitro combination therapy with isavuconazole against *Candida* spp. *Med Mycol*. 2017; 55: 859–868.
189. Cruz MC, Goldstein AL, Blankenship JR et al. Calcineurin is essential for survival during membrane stress in *Candida albicans*. *EMBO J*. 2002; 21: 546–559.
190. Onyewu C, Blankenship JR, Del Poeta M, Heitman J. Ergosterol biosynthesis inhibitors become fungicidal when combined with calcineurin Inhibitors against *Candida albicans*, *Candida glabrata*, and *Candida krusei*. *Antimicrob Agents Chemother*. 2003; 47: 956–964.
191. Shanmughapriya A, Somakumari H, Lency A, Kavitha S, Natarajaseenivasan K. Synergistic effect of amphotericin B and tyrosol on biofilm formed by *Candida krusei* and *Candida tropicalis* from intrauterine device users. *Med Mycol*. 2014; 52: 853–861.
192. Sharifzadeh A, Khosravi AR, Shokri H, Tari PS. Synergistic anticandidal activity of menthol in combination with itraconazole and nystatin against clinical *Candida glabrata* and *Candida krusei* isolates. *Microb Pathog*. 2017; 107: 390–396.
193. Moraes RC, Carvalho AR, Lana AJD et al. In vitro synergism of a water insoluble fraction of *Uncaria tomentosa* combined with fluconazole and terbinafine against resistant non-*Candida albicans* isolates. *Pharm Biol*. 2017; 55: 406–415.
194. Scorzoni L, Benaducci T, Almeida AMF, Silva DHS, Bolzani VS, Mendes-Giannini MJS. Comparative study of disk diffusion and microdilution methods for evaluation of antifungal activity of natural compounds against medical yeasts *Candida* spp. and *Cryptococcus* sp. *J Appl Pharm Sci*. 2007; 28: 25–34.
195. Marcos-Arias C, Eraso E, Madariaga L, Quindos G. In vitro activities of natural products against oral *Candida* isolates from denture wearers. *BMC Complement Altern Med*. 2011; 11: 119.
196. Faria NCG, Kim JH, Goncalves LAP, Martins MdeL, Chan KL, Campbell BC. Enhanced activity of antifungal drugs using natural phenolics against yeast strains of *Candida* and *Cryptococcus*. *Lett Appl Microbiol*. 2011; 52, 506–513.
197. Kang K, Fong W-P, Tsang PW-K. Novel antifungal activity of purpurin against *Candida* species in vitro. *Med Mycol*. 2010; 48: 904–911.
198. Bliss JM, Bigelow CE, Foster TH, Haidaris CG. Susceptibility of *Candida* species to photodynamic effects of photofrin. *Antimicrob Agents Chemother*. 2004; 48: 2000–2006.
199. Dovigo LN, Pavarina AC, Garcia Ribeiro D Adriano CS, Bagnato VS. Photodynamic inactivation of four *Candida* species induced by Photogem®. *Braz J Microbiol*. 2010; 41: 42–49.
200. De Souza SC, Campos Junqueira J, Balducci I, Koga-Ito CY, Munin E, Jorge AO. Photosensitization of different *Candida* species by low power laser light. *J Photochem Photobiol B*. 2006; 83: 34–38.
201. Rezusta A, López-Chincón P, Paz-Cristobal MP et al. In vitro fungicidal photodynamic effect of hypericin on *Candida* species. *Photochem Photobiol*. 2012; 88: 613–619.
202. Inglis DO, Arnaud MB, Binkley J et al. The *Candida* genome database incorporates multiple *Candida* species: multispecies search and analysis tools with curated gene and protein information for *Candida albicans* and *Candida glabrata*. *Nucleic Acids Res*. 2011; 40: D667–D674.
203. ten Cate JM, Klis FM, Pereira-Cenci T, Crielaard W, de Groot PW. Molecular and cellular mechanisms that lead to *Candida* bofilm formation. *J Dent Res*. 2009; 88: 105–115.

204. Abbas J, Bodey GP, Hanna HA et al. *Candida krusei* fungemia: an escalating serious infection in immunocompromised patients. *Arch Intern Med*. 2000; 160: 2659.
205. Jiang K, Jones P, Shekar R. Severe soft tissue abscess caused by *Candida krusei*. *Infect Dis Clin Pract*. 2006; 14: 166–167.
206. McQuillen DP, Zingman BS, Meunier F, Levitz SM. Invasive infections due to *Candida krusei*: report of ten cases of fungemia that include three cases of endophthalmitis. *Clin Infect Dis*. 1992; 14: 472–478.
207. Peman J, Jarque I, Bosch M et al. Spondylodiscitis caused by *Candida krusei*: case report and susceptibility patterns. *J Clin Microbiol*. 2006; 44: 1912–1914.
208. Petrocheilou-Paschou V, Georgilis K, Kontoyannis D et al. Pneumonia due to *Candida krusei*. *Clin Microbiol Infect*. 2002; 8: 806–809.
209. Reichart PA, Samaranayake LP, Samaranayake YH, Grote M, Pow E, Cheung B. High oral prevalence of *Candida krusei* in leprosy patients in northern Thailand. *J Clin Microbiol*. 2002; 40: 4479–4485.
210. Safdar A, van Rhee F, Henslee-Downey J, Singhal S, Mehta J. *Candida glabrata* and *Candida krusei* fungemia after high-risk allogeneic marrow transplantation: no adverse effect of low-dose fluconazole prophylaxis on incidence and outcome. *Bone Marrow Transplant*. 2001; 28: 873–878.
211. Singh S, Sobel JD, Bhargava P, Boikov D, Vazquez JA. Vaginitis due to *Candida krusei*: epidemiology, clinical aspects, and therapy. *Clin Infect Dis*. 2002; 35: 1066–1070.
212. Thomalla N, Steidle CP, Leapman SB, Filo RS. Ureteral obstruction of a renal allograft secondary to *Candida krusei*. *Transplant Proc*. 1998; 20: 551–554.

**The published article described in *SECTION B* and this section form the complete literature review for this dissertation. This section is followed by general conclusions of chapter 1, and the aim and objectives of this dissertation**

## 1.1 Introduction

Undoubtedly, antimicrobial resistance is an enormous public health crisis responsible for escalated therapeutic failures, increased hospitalisation, high morbidity and mortality, and amplified economic burden (Prestinaci et al. 2015; Shrestha et al. 2018; Dadgostar 2019). By extension, antifungal resistance amongst several pathogenic fungal species, especially *Candida* species, poses a considerable threat to human and veterinary medicine (Moran et al. 2010; Arastehfar et al. 2020; Bhattacharya et al. 2020). Additionally, the number of antifungal drugs available is limited compared to antibacterial counterparts. This is partially due to the eukaryotic nature of both fungi and humans, which in turn makes the development of safe, less toxic and broad-spectrum antifungal agents a more challenging endeavour (Campoy and Adrio 2017). As a result, other therapeutic approaches are being explored. One such strategy is combination therapy which has been harnessed against pathogens in various forms, including combination of conventional antifungal drugs with appropriate non-antimicrobial compounds (e.g. fatty acids, calcineurin inhibitors, phytochemicals) (Ells et al. 2009; Shrestha et al. 2015; Sharifzadeh et al. 2018; Jia et al. 2019).

The use of fatty acids (FAs) as antifungal compounds, especially as adjuvants that potentiate the activity of known antifungals, is of interest in the current study. Certain FAs have been reported to exhibit antiviral, antibacterial, and antifungal activity (Chanda et al. 2018). Such antimicrobial properties are usually dependent on various factors, including the length of carbon chain and degree of unsaturation. Interestingly, FAs can also be used as adjuncts to enhance the efficacy of antimicrobial agents. Polyunsaturated fatty acids (PUFAs), such as AA and stearidonic acid (SDA), have been found to increase the susceptibility of biofilms of *Candida* spp. to antifungal drugs, including amphotericin B, clotrimazole and FLC (Ells et al. 2009; Thibane et al. 2012b; Mishra et al. 2014; Kuloyo et al. 2020). Although the precise mechanisms of action of these adjunct FAs remain unclear, they have been implicated to induce membrane disorganisation, increase oxidative stress and interfere with ATP synthesis (Ells et al. 2009; Thibane et al. 2012b; Kuloyo et al. 2020).

## 1.2 Antifungal drugs and their mechanistic profiles

Among the available classes of antifungals, only three classes are effective for the treatment of obstinate invasive candidal infections, and these include the azoles, polyenes, and

echinocandins. Nucleoside analogues, allylamines, and morpholines are usually used for topical treatment or adjuvants with other antifungal drugs (Zhanel et al. 1997; Finch and Warshaw 2007). The descriptions and mechanisms of action of these drugs are discussed herein.

### 1.2.1 Azoles

Azoles are heterocyclic compounds with at least one nitrogen atom in their (five-membered) rings. The azoles are excellent inhibitors of the cytochrome P450 enzyme, Erg11p encoded by *ERG11* in *Candida* and *Cryptococcus* spp., and *CYP51* in *Aspergillus* spp., a key enzyme involved in the conversion of lanosterol to ergosterol during the biosynthesis of ergosterol (Kathiravan et al. 2012). More specifically, the iron atom within the heme group of the active site of the enzyme is bound by the free nitrogen atom of the azole ring, thus preventing the activation of oxygen and as a result inhibits the synthesis of ergosterol from lanosterol (Hitchcock, 1991). Like cholesterol in animals, ergosterol is an essential component of fungal cell membranes, playing an important role in maintaining membrane fluidity and stability, inhibition of its biosynthesis by azoles results in the depletion of ergosterol and accumulation of toxic methylated sterol, 14α-methyl-3,6-diol, and this results in the disruption of cell membrane fluidity and stability, increased membrane permeability and arrest of cell growth (**Fig. 1**) (Sheehan et al. 1999; Weete et al. 1999). Furthermore, azoles have also been reported to exert antifungal effects via the inhibition of hyphal development, inactivation of vacuolar ATPases, as well as through the induction of oxidative and nitrosative stress (Odds et al. 1986; Zhang et al. 2010; Arana et al. 2010; Kabir and Ahmad 2013; Peng et al. 2018; Dbouk et al. 2019).

Azoles are classified as imidazole or triazole based on the number and arrangement of their nitrogen atoms. Whilst imidazole has two non-adjacent nitrogen atoms; triazole has three adjacent nitrogen atoms in its five-membered rings (Arnold et al. 2010; Campestre et al. 2017). The imidazoles (bifonazole, clotrimazole, econazole, ketoconazole) are limited to topical treatment of fungal infections, due to their poor water solubility and severe side effects when used orally and/or systemically. Ketoconazole can be used systemically; however, it is less preferred to the triazoles due to severe associated toxicity (Maertens 2004). The limitations of the imidazoles led to the development of the first generation (FLC, itraconazole) and second-generation (voriconazole, posaconazole, isavuconazole) triazoles that generally exhibit a broader spectrum of activity due to the presence of triazole structure instead of the imidazole ring. Additionally, in comparison to the imidazoles, they have improved safety profiles due to their increased affinities for the target enzyme (Girmenia 2009; Mast et al. 2013). Among azoles, FLC is the most widely used azole for the treatment of candidiasis because of its affordability, broad-spectrum activity, high water-solubility, high bioavailability, and good tolerance with few side effects (Grant and Clissold 1990; Andriole 2000; Falci and Pasqualotto

2013). However, its fungistatic nature, widespread, misuse, and extended use, have led to increased resistance among yeasts (Shukla et al. 2016). At present, the azole with the broadest activity is posaconazole, which has high effectiveness against invasive candidiasis (Campoy and Adrio 2017).

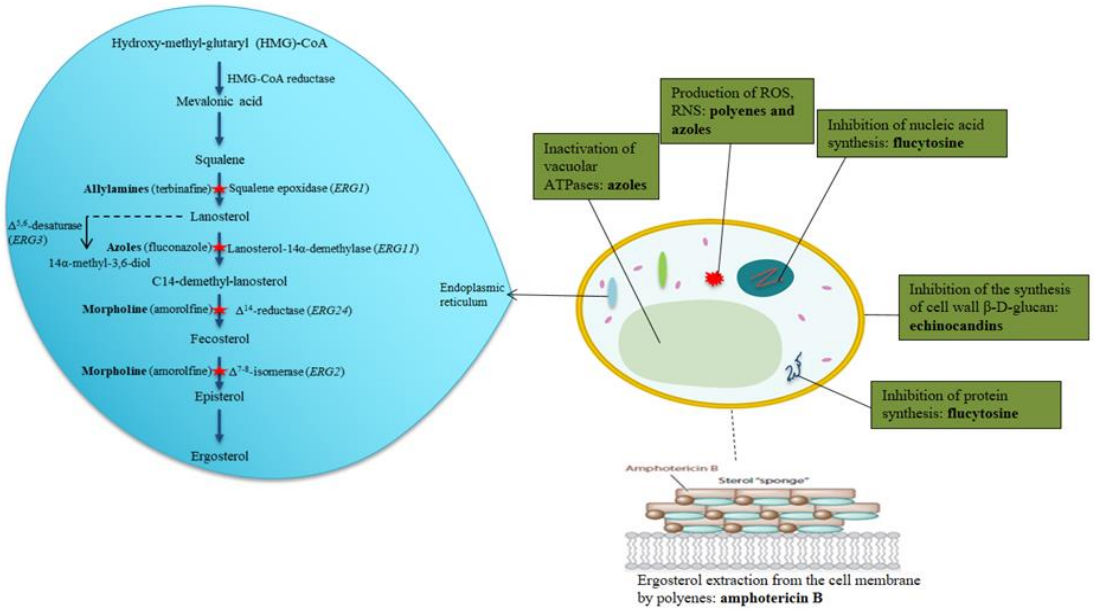


**Fig. 1** Schematic representation of targets of representative various antifungal classes (Adapted from Lupetti et al. 2002; Robbins et al. 2017).

### 1.2.2 Polyenes

The polyenes are amphiphilic macrolides consisting of a 20 to 40 carbons macrolactone ring, conjugated with a d-mycosimine group (Mayers 2009). They are fungicidal and are produced by *Streptomyces* species (Moen et al. 2009; Kabir and Ahmad 2013). Like azoles, polyenes, such as amphotericin B, nystatin, and natamycin, affect the fungal cell membrane; they exert antifungal effect by binding and forming complexes with ergosterol. This results in the formation of transmembrane channels, plasma membrane disruption, leakage of monovalent ions, as well as other intracellular cell contents, and ultimately, fungal cell death (Hossain and Ghannoum 2001; Andes 2003; Yadav et al. 2012). More recently, a detailed structural and biophysical study has highlighted polyenes' mode of action to be beyond complex formation with ergosterol. The study emphasized that polyenes bind and directly extract ergosterol from the fungal cell membrane (**Fig. 1**). This consequently hinders the essential cellular functions of ergosterol, resulting in increased membrane permeability, membrane leakage and consequently, cell death (Anderson et al. 2014). Furthermore, polyenes also exert anti-mycotic action via the production of reactive oxygen species, which results in oxidative damage and impairment of fungal membranes (Mesa-Arango et al. 2012; Mesa-Arango et al. 2014;

Scorzoni et al. 2017). Polyenes were the first antifungal drugs for clinical use and they possess the broadest spectrum of activity against fungal pathogens. However, their clinical use is hindered due to their poor distribution in the body and associated high (renal) toxicity. Such toxicity is due to their slight affinities for the ergosterol homologues, cholesterol in mammalian cells (Paterson et al. 2003; Lemke et al. 2005). Despite this, polyene resistance is very uncommon, and they (especially amphotericin B) remain good therapeutic options when an infection resists treatment with azoles and echinocandins (Mora-Duarte et al. 2002). Furthermore, over the years, concerted efforts have been made to alleviate polyene-associated toxicities. An example is amphotericin B's lipid formulations in liposomes or disc-like or ribbon-like lipid complexes to reduce its toxicity (Dupont 2002; Chandrasekar 2011). Moreover, new semisynthetic polyenes with lower toxicity and better water solubility than amphotericin B, and better activity against amphotericin B-resistant *C. albicans* have also been developed (Kakeya et al. 2008; Santo 2010).

### 1.2.3 Echinocandins

The echinocandins are semisynthetic amphiphilic lipopeptides derived from fungi, such as *Glarea lozoyensis* (caspofungin), *Aspergillus nidulans* var. *echinulatus* (micafungin), and *Coleophoma empetri* (anidulafungin) (Vazquez and Sobel 2006; Eschenauer et al. 2007; Campoy and Adrio 2017; Ksiezopolska and Gabaldon 2018). The echinocandins exert antifungal effects by inhibiting the biosynthesis of β-1,3-D-glucan, a vital component of the fungal cell wall via the non-competitive inhibition of β-1,3-D-glucan synthase (encoded by *FKS* genes). The inhibition of this enzyme leads to the formation of a defective fungal cell wall, disruption of cell wall integrity, cell lysis, and consequent cell death (Sanguinetti et al. 2015). Despite their expensive costs and absence of oral forms, the three echinocandins remain the best therapeutic options for treating candidaemia and invasive candidiasis because they: (i) have fungicidal activities against all *Candida* spp. (including azole and polyene-resistant strains); (ii) show no interaction with other drugs; and (iii) do not cause severe side effects due to the absence of their target, β-1,3-D-glucan synthase in mammalian cells (Pfaller et al. 2003; Theuretzbacher 2004). Interestingly, however, azole therapy is preferred for certain medical conditions, such as urinary tract candidiasis, meningitis, and ophthalmitis because the echinocandins are not excreted into the urine, do not effectively cross the blood-brain barrier, and do not effectively penetrate the ocular system, respectively (Pappas et al. 2018).

### 1.2.4 Nucleoside/pyrimidine analogues

Flucytosine or 5-fluorocytosine (5-FC), a derivative of cytosine, is the only antifungal drug that inhibits the syntheses of nucleic acid and protein (Onishi et al. 2000). It is a prodrug, and it only exerts antifungal effects after its conversion to 5-fluorouracil (5-FU). This prodrug (5-FC) is transported into fungal cells via cytosine permease (Fcy2p) and converted to 5-fluorouracil

(5-FU) in fungal cells by cytosine deaminase (Fcy1p), an enzyme not found in mammalian cells. The fluorouracil is converted into 5-fluorouridine monophosphate (FUMP) by uracil phosphoribosyltransferase (Fur1p). The FUMP produced can be incorporated directly into RNA (ribonucleic acid), in place of the normal uridine triphosphate, and this results in the inhibition of fungal protein synthesis (Vermes et al. 2000; Kabir and Ahmad 2013). Alternatively, 5-FU can be converted into 5-fluorodeoxyuridine monophosphate (5-FdUMP), which inhibits DNA (deoxyribonucleic acid) synthesis via the inhibition of thymidylate synthase, an important enzyme for DNA synthesis. The inhibition of DNA synthesis results in the blockage of cell division and ultimately, fungal cell death (**Fig. 2**) (Waldorf and Polak 1983; Morio et al. 2017). Flucytosine is effective against *Candida* and *Cryptococcus* spp.; however, it is less ideal for primary therapy due to rapid resistance development amongst yeasts. Notably, it is more appropriate as an adjunct than a primary therapy, and when combined with amphotericin B, it is effective for the treatment of cryptococcosis (Zhanel et al. 1997).

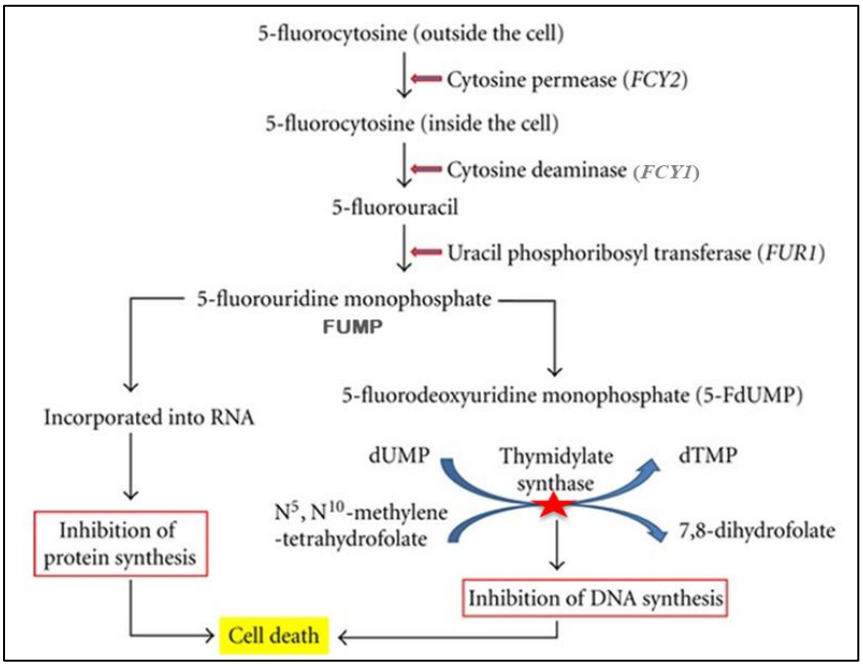


**Fig. 2** Description of the mechanism of action of flucytosine (Obtained from Kabir and Ahmad 2013).

### 1.2.5 Allylamines and Morpholines

In addition to the azoles and polyenes, other classes of antifungal that affect the fungal cell membrane are the allylamines and morpholines. The allylamines (e.g. naftifine, terbinafine) exert fungicidal effects by non-competitively inhibiting the squalene epoxidase enzyme encoded by *ERG1* gene (**Fig. 1**). This enzyme catalyses the conversion of squalene to 2,3-squalene epoxide, which is converted to lanosterol, and then to ergosterol after a series of enzymatic steps. Thus, the inhibition of this enzyme leads to the blockage of ergosterol biosynthesis, depletion of ergosterol, and accumulation of squalene (Andriole 2000; Denning

and Hope 2010). The accumulation of squalene rather than the depletion of ergosterol results in increased membrane permeability, altered cell membrane, and ultimate cell death (Ryder 1988; Campoy and Adrio 2017; Abdel-Kader and Muharram 2017).

Morpholines (e.g. amorolfine) also exert antifungal and fungistatic effects by blocking the ergosterol biosynthetic pathway. This is done via the inhibition of two enzymes, $\Delta^{7-8}$-isomerase (Erg2p) and $\Delta^{14}$-reductase (Erg24p), this results in the depletion of cell membrane ergosterol and accumulation of toxic sterols (**Fig. 1**) (Polak 1992). Amorolfine is usually used for topical treatment of mycoses, and it is effective against yeasts, some moulds and even some bacteria (e.g. *Actinomyces* spp.) (Gupta et al. 2003; Finch and Warshaw 2007).

## 1.3 Combination therapy with fatty acids

As a result of the increase in antifungal resistance, complicated by the paucity of available antifungals and host toxicity, the exploitation of alternative treatment approaches is imperative. One such approach is through combination therapy and this has been harnessed in various forms, including the combination of two antifungal drugs (Graybill et al. 1995; Olver et al. 2006; Schilling et al. 2008; DiDone et al. 2011; Chen et al. 2013); the combination of an antifungal drug and a non-antimicrobial compound (Ells et al. 2009; Gamarra et al. 2010; da Silva et al. 2013; Shrestha et al. 2015; Hacioglu et al. 2018; Sharifzadeh et al. 2018; Jia et al. 2019); and combination of appropriate non-antimicrobial compounds (Bae and Rhee 2019). Whilst antagonism is sometimes possible, combination therapy, if the compounds exhibit synergy, is usually more effective and provides greater benefits compared to monotherapy. Its benefits include increased efficacy, due to the complementary effects of both agents; reduced evolution of resistance; decreased drug(s) dosage, which translates to decreased host toxicity; and microbicidal activity, which may result from the combination of two fungistatic agents (Chang et al. 2017; Prasad et al. 2017).

As previously discussed in **Section B**, a considerable number of studies have reported the synergistic effects of various combinations of antifungal drugs and that of antifungal drugs with non-antimicrobial agents. Here, we briefly review available reports on the synergistic activity of fatty acids with antifungal drugs against *Candida* spp. Fatty acids (FAs) are organic molecules characterised by a hydrophilic carboxyl group (-COOH) at one end and a hydrophobic methyl group ($-CH_3$) at the other end, thus they are amphipathic in nature. These molecules are important building blocks of cellular lipids and membranes, and they regulate various signalling pathways, are involved in the storage of energy (adipose tissues), are essential for the synthesis and functions of hormones (Calder 2015; Pohl et al. 2011). Fatty acids generally have chain lengths between 4 and 28 carbon atoms; those with <8 carbons, 8 to 12 carbons, and >12 carbons are classified as short-chain, medium-chain, and long-chain FAs, respectively. Additionally, FAs are also classified as either saturated or unsaturated,

depending on the presence or absence of a double bond. Unsaturated FAs are further classified as monounsaturated (MUFAs) or polyunsaturated FAs (PUFAs), the former possess just a single double bond, while the latter contains more than one double bond (Pohl et al. 2011; Yoon et al. 2018).

Interestingly, certain FAs exhibit antimicrobial activity against viruses, bacteria, and fungi (Chanda et al. 2018). This antimicrobial property is usually dependent on various factors such as carbon chain length, degree of unsaturation (including number, location, and spatial property of double bonds), and structure of the fatty acid (Desbois and Smith 2010). More specifically, the chief mechanistic action of antibacterial FAs is through the alteration of cellular lipids and membranes, and disruption of several cellular processes such as oxidative phosphorylation where FAs bind to electron carriers, disrupt electron transport, and consequently decrease membrane potential and proton gradient (Galbraith and Miller 1973; Yoon et al. 2018). The major target of antifungal FAs is the fungal membrane, where they are incorporated into the lipid bilayer, resulting in increased membrane fluidity and permeability, perturbation of membrane functions and structure, and ultimately, cell death (Avis and Belanger 2001; Pohl et al. 2011; Mishra et al. 2014). Additionally, increased oxidative stress, resulting from lipid peroxidation, has been attributed to the insertion of PUFAs into fungal membranes (Thibane et al. 2012a). Fatty acids may also directly inhibit membrane proteins, such as glucosyltransferase (Won et al. 2007; Zhou et al. 2018). Furthermore, antifungal FAs can also disrupt fatty acid metabolism, protein synthesis and topoisomerase activity (Pohl et al. 2011). Interestingly, some antifungal FAs have also been reported to influence virulence factors, such as biofilm formation, hyphal growth, secreted aspartyl proteinases, and lipases, without affecting fungal growth (Muthamil et al. 2020). Such anti-virulence effect, without the inhibition of microbial growth, will considerably reduce selective pressure and result in a reduced rate of antimicrobial resistance development. For this reason, FAs may also be used as adjuncts to complement conventional antimicrobial agents that are highly prone to pathogen resistance due to their influence on microbial growth (Pierce and Lopez-Ribot 2013; Vila et al. 2017; Wall and Lopez-Ribot 2020).

Unsurprisingly, the synergism of FAs and conventional antifungals has been demonstrated. Polyunsaturated fatty acids such as AA and SDA, have been reported to increase the susceptibility of *C. albicans* and *C. dubliniensis* biofilms to antifungal drugs, such as amphotericin B. These fatty acids possibly exert additive effects via the disruption of membrane organisation and increased oxidative stress, leading to apoptosis (Ells et al. 2009; Thibane et al. 2012a). Similarly, Mishra and co-workers (2014) have demonstrated the synergism of AA with FLC and terbinafine. Additionally, Bae and Rhee (2019) reported the synergistic activity of caprylic acid (a medium-chain fatty acid found in palm oil and coconut oil) with carvacrol or thymol against *C. albicans*. The observed synergistic effect was attributed

to membrane disruption and inhibition of efflux pumps by these compounds (Bae and Rhee 2019). Further, a more recent study by Kuloyo and co-workers (2020) demonstrated that AA potentiates the susceptibility of FLC to *C. albicans* via interference with methionine and ATP synthesis pathways. **Table 1** depicts cases of combination therapy with fatty acids against some pathogenic fungi.

**Table 1** Selected examples of combination therapy with fatty acids against pathogenic fungi

| Type | Combination | Fungus | Suggested mechanism | Reference |
|---|---|---|---|---|
| **Fatty acids and antifungal** | Arachidonic acid and amphotericin B or clotrimazole | *C. albicans*<br>*C. dubliniensis* | Influences ergosterol and unsaturation content; Increases oxidative stress | Ells et al. 2009 |
| | Stearidonic acid and amphotericin B | *C. albicans*<br>*C. dubliniensis* | Not known | Thibane et al. 2012b |
| | Arachidonic acid and fluconazole or terbinafine | *C. glabrata*<br>*C. parapsilosis*<br>*C. tropicalis* | Influences prostaglandin production | Mishra et al. 2014 |
| | Arachidonic acid and fluconazole | *C. albicans* | Interferes with methionine ATP production and methionine synthesis | Kuloyo et al. 2020 |
| **Fatty acids and non-antimicrobials** | Caprylic acid and carvacrol or thymol | *C. albicans* | Influences membrane integrity and efflux pump activity | Bae and Rhee 2019 |

## 1.4 General conclusions for Chapter 1

The epidemiology of candidiasis has changed with a shift to non-*albicans Candida* (NAC) species, including *C. krusei*. This epidemiological shift is partly explained by the increasing resistance of NAC species to antifungal drugs. *Candida krusei* can cause life-threatening infections in immune-compromised patients, such as those with hematologic malignancies. Those using prolonged azole prophylaxis are also at higher risk. The teleomorph of *C. krusei*,

*Pichia kudriavzevii* has been given the Generally Regarded as Safe status by the United States Food and Drug Administration (FDA). It is used for the production of various food products, including chocolate. However, this needs to be revisited, given the pathogenic potential of *C. krusei*. The widespread use and misuse of the limited antifungal arsenal against an ever-increasing number of fungal infections (due to the rise in the number of immunocompromised and terminally ill individuals) have continued to create selective pressure for resistance development amongst fungal pathogens. Understanding the mechanisms of antifungal resistance of these pathogens is crucial for effective management of their infections, proper use of the limited antifungals, and insights into future drug development. For instance, drugs or adjuvants that are efflux pump inhibitors can be developed to tackle drug resistance due to overexpression of efflux pumps. The paucity of antifungal agents coupled with the problem of antifungal resistance, host toxicity, as well as difficulty in antifungal drug development partially due to the eukaryotic nature of both fungi and humans, have heightened fungal infections treatment failures which in turn prompt researchers to exploit alternative therapeutic options. One of these numerous alternatives is combination therapy, and if synergism is obtained, it exhibits better activity than monotherapy (Pierce and Lopez-Ribot 2013) (**Fig. 3**). This combination therapy has been explored and exploited in various forms, including the co-administration of an antifungal drug(s) with fatty acids. More so, anti-virulent fatty acids represent excellent adjuvant candidates, because, unlike conventional drugs, they do not influence cell viability, and thus have a lower ability to induce resistance due to low selective pressure (Wall and Lopez-Ribot 2020). This research area's full exploitation is envisaged as being worthwhile and could be used as an efficient tool to combat the menace of antifungal resistance.

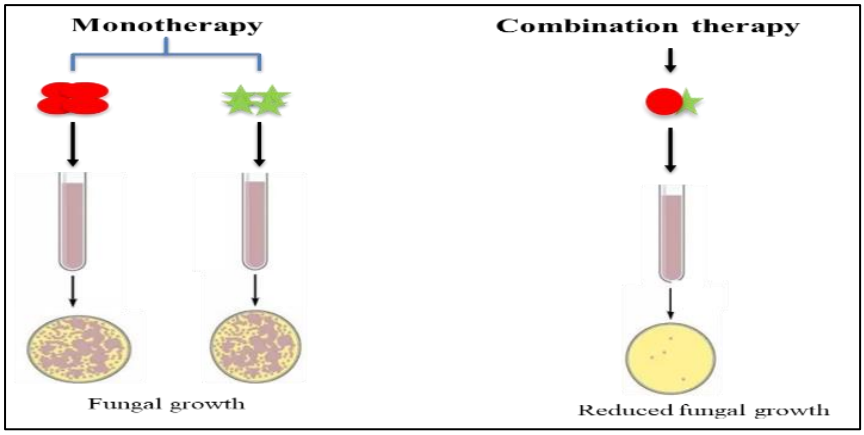


**Fig. 3** Simple illustration of the outcome of mono- and combination therapeutic approaches

## 1.5 Research Aim and Objectives

Based on this background and due to the apparent knowledge gaps, the aim of this dissertation is to investigate the influence of polyunsaturated fatty acids on fluconazole susceptibility and drug efflux in *Candida krusei*. The specific objectives to achieve this aim are listed below:

- **Objective 1:** Establish the susceptibility profiles of clinical and environmental isolates of *C. krusei* to fluconazole and unsaturated fatty acids with varying degrees of unsaturation [oleic acid (18:1), linoleic acid (18:2), gamma-linolenic acid (18:3), arachidonic acid (20:4), and eicosapentaenoic acid (20:5)] (**Chapter 2**).
- **Objective 2:** Determine the potentiating effect of fatty acids on fluconazole susceptibility in *C. krusei* and examine the underlying mechanisms of the observed effect (**Chapter 2**).
- **Objective 3:** Examine the potentiating effect of the combination of fatty acid and fluconazole against *C. krusei* in a *C. elegans* infection model (**Chapter 2**).
- **Objective 4:** Develop a CRISPR-Cas9 genome editing system for *C. krusei* (**Chapter 3**).
- **Objective 5:** Determine the influence of exogenous arachidonic acid and fluconazole on the expression, localisation, and activity of Abc1p efflux pump in *C. krusei* (**Chapter 4**).

## 1.6 References


Abdel-Kader MS, Muharram MM (2017) New microbial source of the antifungal allylamine "Terbinafine." Saudi Pharmaceutical Journal 25:440–442. https://doi.org/10.1016/j.jsps.2016.06.006

Anderson TM, Clay MC, Cioffi AG, et al (2014) Amphotericin forms an extramembranous and fungicidal sterol sponge. Nature Chemical Biology 10:400–406. https://doi.org/10.1038/nchembio.1496

Andes D (2003) *In vivo* pharmacodynamics of antifungal drugs in treatment of candidiasis. Antimicrobial Agents and Chemotherapy 47:1179–1186. https://doi.org/10.1128/aac.47.4.1179-1186.2003

Andriole VT (2000) Current and future antifungal therapy: new targets for antifungal therapy. International Journal of Antimicrobial Agents 16:317–321. https://doi.org/10.1016/s0924-8579(00)00258-2

Arana DM, Nombela C, Pla J (2010) Fluconazole at subinhibitory concentrations induces the oxidative- and nitrosative-responsive genes *TRR1*, *GRE2* and *YHB1*, and enhances the resistance of *Candida albicans* to phagocytes. Journal of Antimicrobial Chemotherapy 65:54–62. https://doi.org/10.1093/jac/dkp407

Arastehfar A, Lass-Flörl C, Garcia-Rubio R, et al (2020) The quiet and underappreciated rise of drug-resistant invasive fungal pathogens. Journal of Fungi 6:138. https://doi.org/10.3390/jof6030138

Arnold TM, Dotson E, Sarosi GA, Hage CA (2010) Traditional and emerging antifungal therapies. Proceedings of the American Thoracic Society 7:222–228. https://doi.org/10.1513/pats.200906-048al

Avis TJ, Belanger RR (2001) Specificity and mode of action of the antifungal fatty acid cis-9-heptadecenoic acid produced by *Pseudozyma flocculosa*. Applied and Environmental Microbiology 67:956–960. https://doi.org/10.1128/aem.67.2.956-960.2001

Bae YS, Rhee MS (2019) Short-term antifungal treatments of caprylic acid with carvacrol or thymol induce synergistic 6-log reduction of pathogenic *Candida albicans* by cell membrane disruption and efflux pump inhibition. Cellular Physiology and Biochemistry 53:285–300. https://doi.org/10.33594/000000139

Bhattacharya S, Sae-Tia S, Fries BC (2020) Candidiasis and mechanisms of antifungal

resistance. Antibiotics 9:312. https://doi.org/10.3390/antibiotics9060312

Bizerra FC, Nakamura CV, De Poersch C, et al (2008) Characteristics of biofilm formation by *Candida tropicalis* and antifungal resistance. FEMS Yeast Research 8:442–450. https://doi.org/10.1111/j.1567-1364.2007.00347.x

Calder PC (2015) Functional roles of fatty acids and their effects on human health. Journal of parenteral and enteral nutrition 39:18S-32S. https://doi.org/10.1177/0148607115595980

Campestre C, Locatelli M, Guglielmi P, et al (2017) Analysis of imidazoles and triazoles in biological samples after MicroExtraction by packed sorbent. Journal of Enzyme Inhibition and Medicinal Chemistry 32:1053–1063. https://doi.org/10.1080/14756366.2017.1354858

Campoy S, Adrio JL (2017) Antifungals. Biochemical Pharmacology 133:86–96. https://doi.org/10.1016/j.bcp.2016.11.019

Chanda W, Joseph TP, Guo X, et al (2018) Effectiveness of omega-3 polyunsaturated fatty acids against microbial pathogens. Journal of Zhejiang University-SCIENCE B 19:253–262. https://doi.org/10.1631/jzus.b1700063

Chandrasekar P (2011) Management of invasive fungal infections: A role for polyenes. Journal of Antimicrobial Chemotherapy 66:457–465. https://doi.org/10.1093/jac/dkq479

Chang YL, Yu SJ, Heitman J, et al (2017) New facets of antifungal therapy. Virulence 8:222–236. https://doi.org/10.1080/21505594.2016.1257457

Chen YL, Lehman VN, Averette AF, et al (2013) Posaconazole exhibits *in vitro* and *in vivo* synergistic antifungal activity with caspofungin or FK506 against *Candida albicans*. PLoS ONE 8:e57672. https://doi.org/10.1371/journal.pone.0057672

Chi HW, Yang YS, Shang ST, et al (2011) *Candida albicans* versus non-*albicans* bloodstream infections: The comparison of risk factors and outcome. Journal of Microbiology, Immunology and Infection 44:369–375. https://doi.org/10.1016/j.jmii.2010.08.010

da Silva CR, de Andrade Neto JB, Sidrim JJC, et al (2013) Synergistic effects of amiodarone and fluconazole on *Candida tropicalis* resistant to fluconazole. Antimicrobial Agents and Chemotherapy 57:1691–1700. https://doi.org/10.1128/aac.00966-12

Dadgostar P (2019) Antimicrobial resistance: Implications and costs. Infection and Drug

Resistance Volume 12:3903–3910. https://doi.org/10.2147/idr.s234610

Dbouk NH, Covington MB, Nguyen K, Chandrasekaran S (2019) Increase of reactive oxygen species contributes to growth inhibition by fluconazole in *Cryptococcus neoformans*. BMC Microbiology 19:243 https://doi.org/10.1186/s12866-019-1606-4

Denning DW, Hope WW (2010) Therapy for fungal diseases: opportunities and priorities. Trends in Microbiology 18:195–204. https://doi.org/10.1016/j.tim.2010.02.004

Desbois AP, Smith VJ (2010) Antibacterial free fatty acids: activities, mechanisms of action and biotechnological potential. Applied Microbiology and Biotechnology 85:1629–1642. https://doi.org/10.1007/s00253-009-2355-3

DiDone L, Oga D, Krysan DJ (2011) A novel assay of biofilm antifungal activity reveals that amphotericin B and caspofungin lyse *Candida albicans* cells in biofilms. Yeast 28:561–568. https://doi.org/10.1002/yea.1860

Dixon DM, McNeil MM, Cohen ML, et al (1996) Fungal infections: A growing threat. Public health reports (Washington, DC : 1974) 111:226–35

Dupont B (2002) Overview of the lipid formulations of amphotericin B. Journal of Antimicrobial Chemotherapy 49:31–36. https://doi.org/10.1093/jac/49.suppl_1.31

Ells R, Kock JLF, Van Wyk PWJ, et al (2009) Arachidonic acid increases antifungal susceptibility of *Candida albicans* and *Candida dubliniensis*. Journal of Antimicrobial Chemotherapy 63:124–128. https://doi.org/10.1093/jac/dkn446

Eschenauer G, DePestel DD, Carver PL (2007) Comparison of echinocandin antifungals. Therapeutics and Clinical Risk Management 3:71–97. https://doi.org/10.2147/tcrm.2007.3.1.71

Falci DR, Pasqualotto A (2013) Profile of isavuconazole and its potential in the treatment of severe invasive fungal infections. Infection and Drug Resistance 22:163–74. https://doi.org/10.2147/idr.s51340

Filler SG, Sheppard DC (2006) Fungal invasion of normally non-phagocytic host cells. PLoS Pathogens 2:e129. https://doi.org/10.1371/journal.ppat.0020129

Finch JJ, Warshaw EM (2007) Toenail onychomycosis: Current and future treatment options. Dermatologic Therapy 20:31–46. https://doi.org/10.1111/j.1529-8019.2007.00109.x

Finkel JS, Mitchell AP (2011) Genetic control of *Candida albicans* biofilm development. Nature Reviews Microbiology 9:109–118. https://doi.org/10.1038/nrmicro2475

Fukuoka T, Johnston DA, Winslow CA, et al (2003) Genetic basis for differential activities of fluconazole and voriconazole against *Candida krusei*. Antimicrobial Agents and Chemotherapy 47:1213–1219. https://doi.org/10.1128/aac.47.4.1213-1219.2003

Galbraith H, Miller TB (1973) Effect of long chain fatty acids on bacterial respiration and amino acid uptake. Journal of Applied Bacteriology 36:659–675. https://doi.org/10.1111/j.1365-2672.1973.tb04151.x

Gamarra S, Rocha EMF, Zhang YQ, et al (2010) Mechanism of the synergistic effect of amiodarone and fluconazole in *Candida albicans*. Antimicrobial Agents and Chemotherapy 54:1753–1761. https://doi.org/10.1128/aac.01728-09

Girmenia C (2009) New generation azole antifungals in clinical investigation. Expert Opinion on Investigational Drugs 18:1279–1295. https://doi.org/10.1517/13543780903176407

Grant SM, Clissold SP (1990) Fluconazole. Drugs 39:877–916. https://doi.org/10.2165/00003495-199039060-00006

Graybill JR, Najvar LK, Holmberg JD, Luther MF (1995) Fluconazole, D0870, and flucytosine treatment of disseminated *Candida tropicalis* infections in mice. Antimicrobial Agents and Chemotherapy 39:924–929

Gupta AK, Ryder JE, Baran R (2003) The use of topical therapies to treat onychomycosis. Dermatologic Clinics 21:481–489. https://doi.org/10.1016/s0733-8635(03)00025-1

Hacioglu M, Birteksoz Tan AS, Dosler S, et al (2018) *In vitro* activities of antifungals alone and in combination with tigecycline against *Candida albicans* biofilms. PeerJ 6:e5263. https://doi.org/10.7717/peerj.5263

Hitchcock CA (1991) Cytochrome P-450-dependent 14α-sterol demethylase of *Candida albicans* and its interaction with azole antifungals. Biochemical Society Transactions 19:782–787. https://doi.org/10.1042/bst0190782

Hossain MA, Ghannoum MA (2001) New developments in chemotherapy for non-invasive fungal infections. Expert Opinion on Investigational Drugs 10:1501–1511. https://doi.org/10.1517/13543784.10.8.1501

Jia C, Zhang J, Zhuge Y, et al (2019) Synergistic effects of geldanamycin with fluconazole are

associated with reactive oxygen species in *Candida tropicalis* resistant to azoles and amphotericin B. Free Radical Research 53:618–628. https://doi.org/10.1080/10715762.2019.1610563

Kabir MA, Ahmad Z (2013) *Candida* infections and their prevention. ISRN Preventive Medicine 2013:1–13. https://doi.org/10.5402/2013/763628

Kakeya H, Miyazaki Y, Senda H, et al (2008) Efficacy of SPK-843, a novel polyene antifungal, in comparison with amphotericin B, liposomal amphotericin B, and micafungin against murine pulmonary aspergillosis. Antimicrobial Agents and Chemotherapy 52:1868–1870. https://doi.org/10.1128/aac.01369-07

Kathiravan MK, Salake AB, Chothe AS, et al (2012) The biology and chemistry of antifungal agents: A review. Bioorganic & Medicinal Chemistry 20:5678–5698. https://doi.org/10.1016/j.bmc.2012.04.045

Kołaczkowska A, Kołaczkowski M (2016) Drug resistance mechanisms and their regulation in non-*albicans Candida* species. Journal of Antimicrobial Chemotherapy 71:1438–1450. https://doi.org/10.1093/jac/dkv445

Ksiezopolska E, Gabaldón T (2018) Evolutionary emergence of drug resistance in *Candida* opportunistic pathogens. Genes 9:461. https://doi.org/10.3390/genes9090461

Kuloyo O, Fourie R, Cason E, et al (2020) Transcriptome analyses of *Candida albicans* biofilms, exposed to arachidonic acid and fluconazole, indicates potential drug targets. G3 (Bethesda, Md) 10:3099–3108. https://doi.org/10.1534/g3.120.401340

Kuloyo OO (2020) Investigation into the mechanism of arachidonic acid increased fluconazole susceptibility in *Candida albicans* biofilms and application to drug repurposing. Ph.D. Thesis, University of the Free State, Bloemfontein, South Africa

Lemke A, Kiderlen AF, Kayser O (2005) Amphotericin B. Applied Microbiology and Biotechnology 68:151–62. https://doi.org/10.1007/s00253-005-1955-9

Lupetti A, Danesi R, Campa M, et al (2002) Molecular basis of resistance to azole antifungals. Trends in Molecular Medicine 8:76–81. https://doi.org/10.1016/s1471-4914(02)02280-3

Maertens JA (2004) History of the development of azole derivatives. Clinical Microbiology and Infection 10:1–10. https://doi.org/10.1111/j.1470-9465.2004.00841.x

Mast N, Zheng W, Stout CD, Pikuleva IA (2013) Antifungal azoles: Structural insights into undesired tight binding to cholesterol-metabolizing CYP46A1. Molecular Pharmacology 84:86–94. https://doi.org/10.1124/mol.113.085902

Mayers DL (2009) Antimicrobial Drug Resistance: Mechanism of drug resistance. Humana Press/Springer, Totowa/New York

Mesa-Arango AC, Scorzoni L, Zaragoza O (2012) It only takes one to do many jobs: amphotericin B as antifungal and immunomodulatory drug. Frontiers in Microbiology 3:286. https://doi.org/10.3389/fmicb.2012.00286

Mesa-Arango AC, Trevijano-Contador N, Román E, et al (2014) The production of reactive oxygen species is a universal action mechanism of amphotericin B against pathogenic yeasts and contributes to the fungicidal effect of this drug. Antimicrobial Agents and Chemotherapy 58:6627–6638. https://doi.org/10.1128/aac.03570-14

Mishra NN, Ali S, Shukla PK (2014) Arachidonic acid affects biofilm formation and $PGE_2$ level in *Candida albicans* and non-*albicans* species in presence of subinhibitory concentration of fluconazole and terbinafine. The Brazilian Journal of Infectious Diseases 18:287–293. https://doi.org/10.1016/j.bjid.2013.09.006

Moen MD, Lyseng-Williamson KA, Scott LJ (2009) Liposomal amphotericin B. Drugs 69:361–392. https://doi.org/10.2165/00003495-200969030-00010

Mora-Duarte J, Betts R, Rotstein C, et al (2002) Comparison of caspofungin and amphotericin B for invasive candidiasis. New England Journal of Medicine 347:2020–2029. https://doi.org/10.1056/nejmoa021585

Moran C, Grussemeyer CA, Spalding JR, et al (2010) Comparison of costs, length of stay, and mortality associated with *Candida glabrata* and *Candida albicans* bloodstream infections. American Journal of Infection Control 38:78–80. https://doi.org/10.1016/j.ajic.2009.06.014

Morio F, Jensen RH, Le Pape P, Arendrup MC (2017) Molecular basis of antifungal drug resistance in yeasts. International Journal of Antimicrobial Agents 50:599–606. https://doi.org/10.1016/j.ijantimicag.2017.05.012

Muthamil S, Prasath KG, Priya A, et al (2020) Global proteomic analysis deciphers the mechanism of action of plant derived oleic acid against *Candida albicans* virulence and biofilm formation. Scientific Reports 10:1–17. https://doi.org/10.1038/s41598-020-

61918-y

Odds FC, Cheesman SL, Abbott AB (1986) Antifungal effects of fluconazole (UK 49858), a new triazole antifungal, *in vitro*. The Journal of Antimicrobial Chemotherapy 18:473–478. https://doi.org/10.1093/jac/18.4.473

Olver WJ, Scott F, Shankland GS (2006) Successful treatment of *Candida krusei* fungemia with amphotericin B and caspofungin. Medical Mycology 44:655–657. https://doi.org/10.1080/13693780600686929

Onishi J, Meinz M, Thompson J, et al (2000) Discovery of novel antifungal (1,3)-beta-D-glucan synthase inhibitors. Antimicrobial Agents and Chemotherapy 44:368–377. https://doi.org/10.1128/aac.44.2.368-377.2000

Orozco AS, Higginbotham LM, Hitchcock CA, et al (1998) Mechanism of fluconazole resistance in *Candida krusei*. Antimicrobial Agents and Chemotherapy 42:2645–2649. https://doi.org/10.1128/aac.42.10.2645

Pappas PG, Lionakis MS, Arendrup MC, et al (2018) Invasive candidiasis. Nature Reviews Disease Primers 4:18026. https://doi.org/10.1038/nrdp.2018.26

Paterson PJ, Seaton S, Prentice HG, Kibbler CC (2003) Treatment failure in invasive aspergillosis: Susceptibility of deep tissue isolates following treatment with amphotericin B. Journal of Antimicrobial Chemotherapy 52:873–876. https://doi.org/10.1093/jac/dkg434

Peng CA, Gaertner AAE, Henriquez SA, et al (2018) Fluconazole induces ROS in *Cryptococcus neoformans* and contributes to DNA damage *in vitro*. PLoS ONE 13:e0208471. https://doi.org/10.1371/journal.pone.0208471

Pfaller MA, Diekema DJ (2007) Epidemiology of invasive candidiasis: A persistent public health problem. Clinical Microbiology Reviews 20:133–163. https://doi.org/10.1128/cmr.00029-06

Pfaller MA, Messer SA, Boyken L, et al (2003) Caspofungin activity against clinical isolates of fluconazole-resistant *Candida*. Journal of Clinical Microbiology 41:5729–5731. https://doi.org/10.1128/jcm.41.12.5729-5731.2003

Pierce CG, Lopez-Ribot JL (2013) Candidiasis drug discovery and development: new approaches targeting virulence for discovering and identifying new drugs. Expert

Opinion on Drug Discovery 8:1117–1126. https://doi.org/10.1517/17460441.2013.807245

Pohl CH, Kock JLF, Thibane VS (2011) Antifungal free fatty acids. In: Science Against Microbial Pathogens: Communicating Current Research and Technological Advances. Formatex Research Center, Spain

Poikonen E, Lyytikäinen O, Anttila VJ, et al (2010) Secular trend in candidemia and the use of fluconazole in Finland, 2004-2007. BMC Infectious Diseases 10:312 https://doi.org/10.1186/1471-2334-10-312

Polak AM (1992) Preclinical data and mode of action of amorolfine. Clinical and Experimental Dermatology 17:8–12. https://doi.org/10.1111/j.1365-2230.1992.tb00270.x

Prasad R, Banerjee A, Shah A (2017) Resistance to antifungal therapies. Essays in Biochemistry 61:157–166. https://doi.org/10.1042/ebc20160067

Prestinaci F, Pezzotti P, Pantosti A (2015) Antimicrobial resistance: a global multifaceted phenomenon. Pathogens and Global Health 109:309–318. https://doi.org/10.1179/2047773215y.0000000030

Ramage G, Martinez JP, Lopez-Ribot JL (2006) *Candida* biofilms on implanted biomaterials: a clinically significant problem. FEMS Yeast Research 6:979–986. https://doi.org/10.1111/j.1567-1364.2006.00117.x

Ramage G, Rajendran R, Sherry L, Williams C (2012) Fungal biofilm resistance. International Journal of Microbiology 2012:1–14. https://doi.org/10.1155/2012/528521

Robbins N, Caplan T, Cowen LE (2017) Molecular evolution of antifungal drug resistance. Annual Review of Microbiology 71:753–775. https://doi.org/10.1146/annurev-micro-030117-020345

Ryder NS (1988) Mechanism of action and biochemical selectivity of allylamine antimycotic agents. Annals of the New York Academy of Sciences 544:208–220. https://doi.org/10.1111/j.1749-6632.1988.tb40405.x

Sadeghi G, Ebrahimi-Rad M, Mousavi SF, et al (2018) Emergence of non-*Candida albicans* species: Epidemiology, phylogeny and fluconazole susceptibility profile. Journal de Mycologie Médicale 28:51–58. https://doi.org/10.1016/j.mycmed.2017.12.008

Samaranayake LP, MacFarlane TW (1990) Oral Candidosis. Wright-Butterworth, London

Sanguinetti M, Posteraro B, Lass-Flörl C (2015) Antifungal drug resistance among *Candida* species: mechanisms and clinical impact. Mycoses 58:2–13. https://doi.org/10.1111/myc.12330

Santo RD (2010) Natural products as antifungal agents against clinically relevant pathogens. Natural Product Reports 27:1084. https://doi.org/10.1039/b914961a

Schilling A, Seibold M, Mansmann V, Gleissner B (2008) Successfully treated *Candida krusei* infection of the lumbar spine with combined caspofungin/posaconazole therapy. Medical Mycology 46:79–83. https://doi.org/10.1080/13693780701552996

Scorzoni L, de Paula E Silva ACA, Marcos CM, et al (2017) Antifungal therapy: New advances in the understanding and treatment of mycosis. Frontiers in microbiology 8:36. https://doi.org/10.3389/fmicb.2017.00036

Sharifzadeh A, Khosravi AR, Shokri H, Shirzadi H (2018) Potential effect of 2-isopropyl-5-methylphenol (thymol) alone and in combination with fluconazole against clinical isolates of *Candida albicans*, *C. glabrata* and *C. krusei*. Journal de Mycologie Médicale 28:294–299. https://doi.org/10.1016/j.mycmed.2018.04.002

Sheehan DJ, Hitchcock CA, Sibley CM (1999) Current and emerging azole antifungal agents. Clinical Microbiology Reviews 12:40–79. https://doi.org/10.1128/cmr.12.1.40

Shrestha P, Cooper BS, Coast J, et al (2018) Enumerating the economic cost of antimicrobial resistance per antibiotic consumed to inform the evaluation of interventions affecting their use. Antimicrobial Resistance & Infection Control 7:98. https://doi.org/10.1186/s13756-018-0384-3

Shrestha SK, Fosso MY, Garneau-Tsodikova S (2015) A combination approach to treating fungal infections. Scientific Reports 5:17070. https://doi.org/10.1038/srep17070

Shukla PK, Singh P, Yadav RK, et al (2016) Past, present, and future of antifungal drug development. Topics in Medicinal Chemistry 125–167. https://doi.org/10.1007/7355_2016_4

Theuretzbacher U (2004) Pharmacokinetics/pharmacodynamics of echinocandins. European Journal of Clinical Microbiology & Infectious Diseases 23:805–812. https://doi.org/10.1007/s10096-004-1228-z

Thibane VS, Ells R, Hugo A, et al (2012a) Polyunsaturated fatty acids cause apoptosis in *C.*

*albicans* and *C. dubliniensis* biofilms. Biochimica et Biophysica Acta (BBA) - General Subjects 1820:1463–1468. https://doi.org/10.1016/j.bbagen.2012.05.004

Thibane VS, Kock JLF, Van Wyk PWJ, et al (2012b) Stearidonic acid acts in synergism with amphotericin B in inhibiting *Candida albicans* and *Candida dubliniensis* biofilms in vitro. International Journal of Antimicrobial Agents 40:284–285. https://doi.org/10.1016/j.ijantimicag.2012.05.021

Trick WE, Fridkin SK, Edwards JR, et al (2002) Secular trend of hospital-acquired candidemia among intensive care unit patients in the United States during 1989–1999. Clinical Infectious Diseases 35:627–630. https://doi.org/10.1086/342300

Vazquez JA, Sobel JD (2006) Anidulafungin: A novel echinocandin. Clinical Infectious Diseases 43:215–222. https://doi.org/10.1086/505204

Venkateswarlu K, Denning DW, Kelly SL (1997) Inhibition and interaction of cytochrome P450 of *Candida krusei* with azole antifungal drugs. Medical Mycology 35:19–25. https://doi.org/10.1080/02681219780000821

Vermes A (2000) Flucytosine: A review of its pharmacology, clinical indications, pharmacokinetics, toxicity and drug interactions. Journal of Antimicrobial Chemotherapy 46:171–179. https://doi.org/10.1093/jac/46.2.171

Vila T, Romo JA, Pierce CG, et al (2017) Targeting *Candida albicans* filamentation for antifungal drug development. Virulence 8:150–158. https://doi.org/10.1080/21505594.2016.1197444

Waldorf AR, Polak A (1983) Mechanisms of action of 5-fluorocytosine. Antimicrobial Agents and Chemotherapy 23:79–85. https://doi.org/10.1128/aac.23.1.79

Wall G, Lopez-Ribot JL (2020) Current antimycotics, new prospects, and future approaches to antifungal therapy. Antibiotics 9:445. https://doi.org/10.3390/antibiotics9080445

Weete JD, Abril M, Blackwell M (2010) Phylogenetic distribution of fungal sterols. PLoS ONE 5:e10899. https://doi.org/10.1371/journal.pone.0010899

Whaley SG, Berkow EL, Rybak JM, et al (2017) Azole antifungal resistance in *Candida albicans* and emerging non-*albicans Candida* species. Frontiers in Microbiology 7: https://doi.org/10.3389/fmicb.2016.02173

Won SR, Hong MJ, Kim YM, et al (2007) Oleic acid: An efficient inhibitor of

glucosyltransferase. FEBS Letters 581:4999–5002. https://doi.org/10.1016/j.febslet.2007.09.045

Yadav JSS, Bezawada J, Yan S, et al (2012) *Candida krusei*: Biotechnological potentials and concerns about its safety. Canadian Journal of Microbiology 58:937–952. https://doi.org/10.1139/w2012-077

Yoon B, Jackman J, Valle-González E, Cho NJ (2018) Antibacterial free fatty acids and monoglycerides: Biological activities, experimental testing, and therapeutic applications. International Journal of Molecular Sciences 19:1114. https://doi.org/10.3390/ijms19041114

Zhanel GG, Karlowsky JA, Harding GA, et al (1997) *In vitro* activity of a new semisynthetic echinocandin, LY-303366, against systemic isolates of *Candida* species, *Cryptococcus neoformans*, *Blastomyces dermatitidis*, and *Aspergillus* species. Antimicrobial Agents and Chemotherapy 41:863–865. https://doi.org/10.1128/aac.41.4.863

Zhang YQ, Gamarra S, Garcia-Effron G, et al (2010) Requirement for ergosterol in V-ATPase function underlies antifungal activity of azole drugs. PLoS Pathogens 6:e1000939. https://doi.org/10.1371/journal.ppat.100093

Zhou X, Stevens MJA, Neuenschwander S, et al (2018) The transcriptome response of the ruminal methanogen *Methanobrevibacter ruminantium* strain M1 to the inhibitor lauric acid. BMC Research Notes 11:135. https://doi.org/10.1186/s13104-018-3242-8

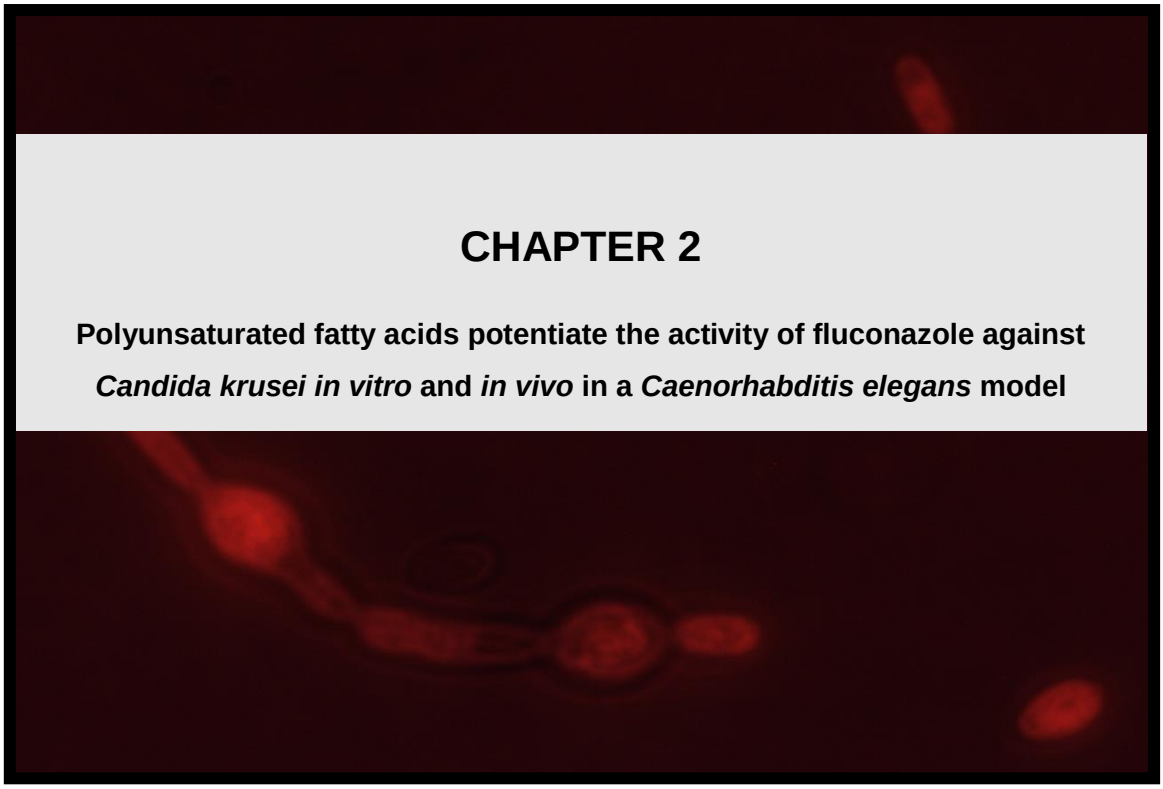

# CHAPTER 2

**Polyunsaturated fatty acids potentiate the activity of fluconazole against *Candida krusei in vitro* and *in vivo* in a *Caenorhabditis elegans* model**

# *RESEARCH OUTPUT*

**A manuscript from this chapter was submitted to *Antimicrobial Agents and Chemotherapy* for consideration for publication.**

## 2.1 Abstract

Although *Candida albicans* remains the major cause of invasive candidiasis, the incidence of infections caused by non-*albicans Candida* species, including *C*. *krusei*, is increasing and demands urgent public health attention. *Candida krusei* exhibits innate resistance to fluconazole (FLC) while also rapidly displaying adaptive resistance to other antifungal drugs. Moreover, this yeast has the propensity to form a recalcitrant biofilm with increased resistance. Hence, there is a need to develop novel therapeutic strategies to combat infections caused by this pathogen. One such approach is through combination therapy with natural compounds such as polyunsaturated fatty acids (PUFAs). This study was conceptualised to investigate the effect of PUFAs on FLC susceptibility of *C. krusei* biofilms and the conserved nature of this effect in the *Caenorhabditis elegans* infection model. This was carried out by exposing *C. krusei* biofilms to FLC in the presence and absence of linoleic acid (LA) or gamma-linolenic acid (GLA). The effect of these treatments on biofilm formation, cell ultrastructure, membrane integrity, oxidative stress, and efflux pump activity was evaluated. In addition, the ability of the PUFAs to prolong the survival and reduce the fungal burden of infected *C. elegans* was assessed. Our results showed that both PUFAs potentiate the susceptibility of *C. krusei* biofilms to FLC *in vitro* via cell membrane damage, induction of oxidative stress, and disruption of efflux pump activity. This potentiating effect was also observed *in vivo* in *C. elegans*. Taken together, PUFAs show potential as antifungal potentiating agents against intrinsically FLC-resistant *C. krusei*, both *in vitro* and *in vivo*. This may pave the way for future studies into novel therapeutic options for overcoming increasing antifungal resistance.

**Keywords:** *Candida krusei*, biofilm, antifungal resistance, polyunsaturated fatty acids, fluconazole, susceptibility, combination therapy, *Caenorhabditis elegans*

## 2.2 Introduction

Globally, *Candida* species remain the fourth causative agents of hospital-acquired systemic infections and the leading cause of nosocomial fungaemia, with more than 250,000 and 50,000 annual attributable cases of infections and deaths, respectively (Pfaller and Diekema 2007; Leroy et al. 2009; Kullberg and Arendrup 2015). Although *C. albicans* is the primary cause of invasive candidiasis, the epidemiology is evolving with an increasing number of infections being attributed to non-*albicans Candida* (NAC) species, including *C. krusei*. This epidemiological shift may be partly explained by the increasing resistance of NAC species to antifungal agents (Chi et al. 2011; da Silva et al. 2013; Sadeghi et al. 2018). Fluconazole, an ergosterol biosynthesis disruptor – via the inhibition of lanosterol-14α-demethylase, encoded by *ERG11*, is the most commonly used drug for the prevention and treatment of superficial and systemic candidiasis due to its affordability, broad-spectrum activity, high water-solubility, high bioavailability, and good tolerance with few side effects (Grant and Clissold 1990; Andriole 2000; Falci and Pasqualotto 2013). However, due to its fungistatic nature and extended use, its efficacy is challenged by rapid resistance development among many fungal species (Shukla et al. 2016). More alarmingly, *C. krusei* isolates display intrinsic resistance to FLC, with more than 97% isolates displaying resistance (Whaley et al. 2017), while also rapidly developing acquired resistance to other antifungal drugs, including the echinocandins (Forastiero et al. 2015). Hence, this yeast can be regarded as a potential multidrug-resistant pathogen (Arendrup and Perlin 2014). The resistance mechanisms of this yeast and other clinically significant *Candida* spp. include, but not limited to, the overexpression of antifungal targets (e.g. Erg11p), alteration of drug targets, and reduction in intracellular drug concentration (e.g. due to biofilm formation) (Pappas et al. 2016; Robbins et al. 2017).

A biofilm consists of surface-attached populations of sessile cells that are enclosed in a self-produced extracellular polymer matrix (Wang et al. 2009). Like bacterial biofilm, biofilm formation in *Candida* spp. contributes to antifungal resistance development by reducing effective drug penetration and concentration, and consequently increasing the non-susceptibility of fungal species to antifungal drugs, especially azoles, polyenes and nucleoside analogues (Ramage et al. 2012; Desai et al. 2014). Moreover, it has also been documented that *Candida* biofilms could be 1000-fold more resistant to antifungal drugs compared to planktonic counterparts (Hacioglu et al. 2018). This is unsurprising because unlike free-living planktonic cells, biofilms have reinforced functional and structural arsenal, such as enhanced efflux pump activity (e.g. Cdr1p, Cdr2p), which ultimately reduces the intracellular concentration of drugs; genetic changes of drug targets; extracellular polymer matrix (comprising of polysaccharides, glycoproteins, and signalling molecules), which decreases the penetration of drugs; dense population of cells within biofilms; modification of sterol

contents of fungal membranes; and presence of phenotypic variants, known as persister cells, that are tolerant to drugs (**Fig. 1**) (Finkel and Mitchell 2011; Ramage et al. 2012). Furthermore, biofilms also play important roles in the virulence, infection, and protection of microorganisms from host defences (Baillie and Douglas 2000; Samaranayake et al. 2002). Indeed, their presence on medical implants, such as catheters and dentures, increases the risk of invasive infections and represent a possible source of recurrent infections, mainly because of their resilience and refractory nature (Ramage et al. 2006). Moreover, detached cells from biofilms have been reported to be responsible for more significant mortality than planktonic yeast cells (Uppuluri et al. 2010; Ramage et al. 2012).

Consequently, there is an urgent need for the development of novel treatment approaches against fungal biofilms, and the combination of conventional antifungals with PUFAs might be a probable option since PUFAs have known antibacterial and antifungal properties (Huang and Ebersole 2010; Thibane et al. 2010; Chanda et al. 2018; Beavers et al. 2019; Kim et al. 2020; Muthamil et al. 2020). Additionally, in contrast to monotherapy, combination therapy may offer enhanced drug efficacy and bioavailability; alleviates host toxicity; decrease antimicrobial resistance development; and induce microbicidal activity, in the case of two fungistatic agents (Carradori et al. 2016; Chang et al. 2017; Prasad et al. 2017).

Furthermore, previous studies in our research group have found that PUFAs (e.g. arachidonic acid) increase the susceptibility of *C. albicans* and *C. dubliniensis* biofilms to FLC, clotrimazole, and amphotericin B (Ells et al. 2009; Thibane et al. 2012b). Other studies have also reported the antifungal activity of fatty acids-monotherapy and their additive effects with other antifungal and non-antifungal compounds against *Candida* spp. biofilms (Mishra et al. 2014; Bae and Rhee 2019). Although several mechanisms, such as increased oxidative stress and disruption of membrane organisation, have been implicated in this activity, there is a dearth of information on the ability of exogenous PUFAs to overcome intrinsic antifungal resistance, such as in the case of *C. krusei*. With this as background, this study was conceptualised to investigate the potentiating effects of fatty acids with FLC against *C. krusei* biofilms while also determining the underlying mechanisms of the observed effects. In addition, the ability of PUFAs to potentiate the activity of FLC *in vivo*, in a *Caenorhabditis elegans* infection model, is also investigated.

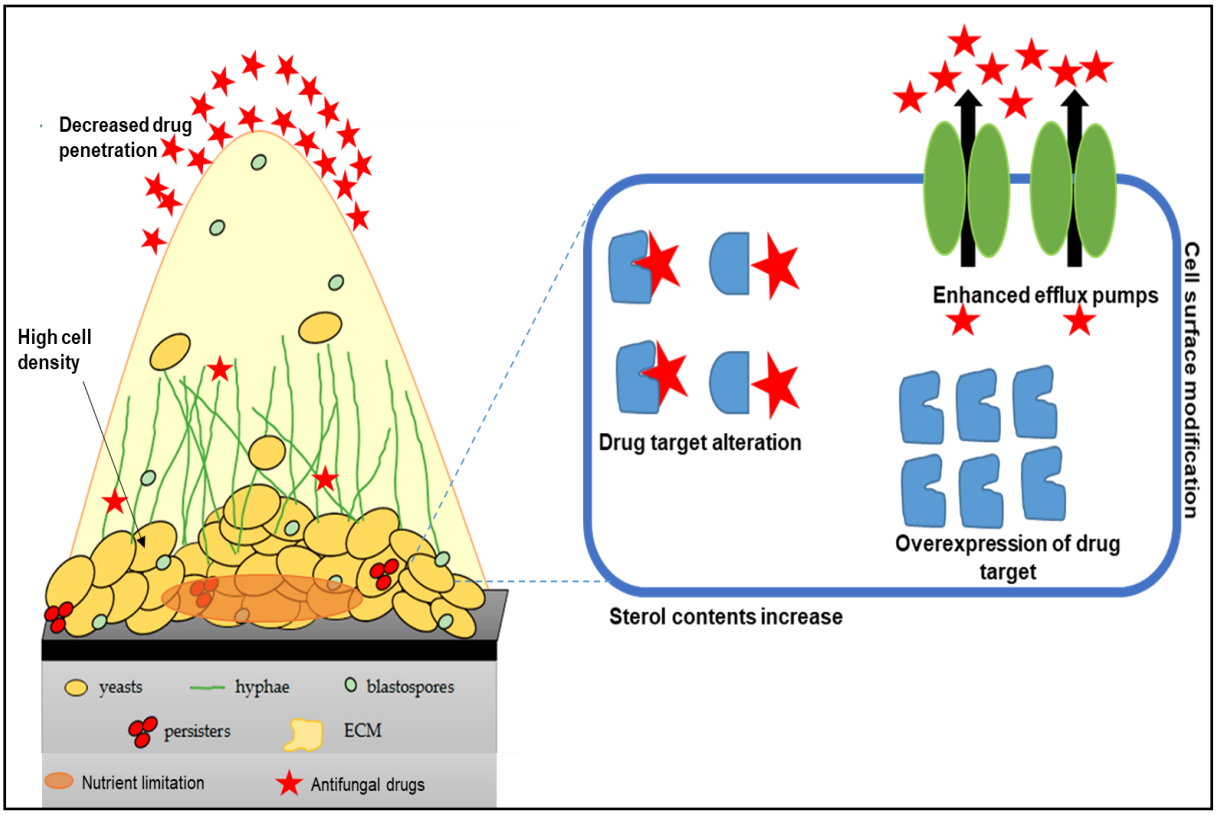


**Fig. 1** An illustration of the components and fundamental antifungal resistance mechanisms of fungal biofilm. A typical biofilm has reduced resistance to drugs due to inherent factors, such as increased cell density, presence of persister cells, modulated physiology, extracellular polymer matrix, overexpressed and modified drug targets, and enhanced efflux pump activity (Adapted from Costa-Orlandi et al. 2017).

## 2.3 Materials and Methods

### 2.3.1 Strains used

Four yeast strains, previously phenotypically-identified as either *Candida krusei* (UFS Y-0801, UFS Y-0217, UFS Y-0277) or *Pichia kudriavzevii* (UFS Y-0637) (test strains), as well as *Candida albicans* SC5314 (reference strain), were obtained from the Yeast Culture Collection of the University of the Free State, Bloemfontein, South Africa. The yeasts were revived on Yeast Malt extract (YM) agar plates (10 g/l glucose, 3 g/l yeast extract, 3 g/l malt extract, 5 g/l peptone, 16 g/l agar) at 30$^{o}$C for 24 h. The identities of these isolates were re-confirmed genotypically by D1/D2 sequencing. A glycerol stock (15%) was prepared for each strain and stocks were stored at -80$^{o}$C for future use.

### 2.3.2 Drug and fatty acids

Fluconazole (FLC) was obtained from Sigma-Aldrich (St. Louis, MO, USA), a stock of 5 mg/ml was prepared in dimethyl sulfoxide (DMSO) and stored at -20$^{o}$C. Unsaturated fatty acids,

including Oleic Acid (OA) (18:1), Linoleic Acid (LA) (18:2), Gamma-Linolenic Acid (GLA) (18:3), Arachidonic Acid (AA) (20:4), and Eicosapentaenoic Acid (EPA) (20:5) were also obtained from Sigma-Aldrich (St. Louis, MO, USA), a stock (10 mM) of each fatty acid was prepared in ethanol and stored at -20$^{o}$C.

### 2.3.3 Biofilm formation

Biofilms of test and reference strains were formed with slight modifications of previously described methods (Ramage et al. 2001; Mishra et al. 2014). Briefly, a loopful of cells of each yeast from YM agar plates was inoculated separately into 5 ml sterile Yeast Nitrogen Base (YNB) broth (10 g/l glucose, 6.7 g/l YNB), and was incubated at 30$^{o}$C for 24 h. After incubation, cells were harvested and washed twice with sterile Phosphate Buffered Saline [PBS; 10 mM phosphate buffer, 2.7 mM potassium chloride, 137 mM sodium chloride (pH 7.4) (Sigma-Aldrich, St. Louis, MO, USA)] by centrifugation (3000 *x g,* 5 min) (Eppendorf, Germany). Thereafter, cells were re-suspended in 5 ml sterile PBS, counted with a haemocytometer and standardised to a final concentration of 1.0 x $10^{7}$ cells/ml in 5 ml filter sterilised (0.20 µm cellulose acetate filter, GVS Life sciences ME, USA) YNB broth. A volume of 100 µl of standardised cell suspension was dispensed into a flat-bottom 96-well tissue culture-treated (polystyrene) microtiter plate (Corning Incorporated, Costar®, U.S.) and incubated for 90 min at 37$^{o}$C, to allow the cells to adhere to the well surface. Cell-free wells containing only sterile YNB broth without cells were included as blank. Following the adhesion phase, the media (containing non-adherent cells) was aspirated with a pipette, the wells re-filled with 200 µl of sterile YNB broth and the plates were incubated at 37$^{o}$C for 48 h to allow biofilm formation. After biofilm formation, biofilm metabolic activity and biomass were quantified by XTT reduction and crystal violet (CV) assays, respectively.

#### 2.3.3.1 XTT reduction assay

The XTT reduction assay used for the assessment of biofilm metabolic activity was a slight modification of previously described methods (Kuhn et al. 2003; Al-Fattani et al. 2006). Briefly, XTT (2,3-bis (2-methoxy-4-nitro-5-sulfophenyl)-5[(phenylamino) carbonyl]-2H tetrazolium hydroxide) (Sigma-Aldrich, St. Louis, MO, USA) was prepared (1 mg/ml in PBS), filter sterilised, and stored at -20$^{o}$C. One (1) mM of menadione (Sigma-Aldrich, St. Louis, MO, USA) solution in acetone was also prepared, filter sterilised, and kept at -20$^{o}$C. Prior to each assay, both XTT and menadione solution were thawed. After biofilm formation, spent medium was aspirated with a pipette from the biofilm-coated wells, and each well was washed once with 200 µl of sterile PBS. Subsequently, a mixture of XTT (46.30 µl) and 1 mM menadione (3.7 µl) was dispensed into each well and incubated at 37$^{o}$C in the dark for 3 h. Following incubation, the water-soluble formazan product of XTT was measured at 492 nm using an EZ Read 800 microplate reader (Biochrom, England). The average of the blank absorbance

values was deducted from experimental values to eliminate background interferences and normalise data.

#### 2.3.3.2 Crystal violet assay

The crystal violet (CV) assay used for the quantification of biofilm biomass was a modification of previously described methods (Jin et al. 2003; O'Toole 2011; Hacioglu et al. 2018). Briefly, spent medium was aspirated from the biofilm-coated wells, the wells were washed once with 200 µl of sterile PBS and air-dried for 45 minutes at room temperature. The washed wells were stained with 110 µl of aqueous CV (0.1% v/v) (Merck Chemicals Pty. Ltd, South Africa) solution for 45 minutes at room temperature. Afterwards, the CV reagent was aspirated from each well, and the wells were washed twice by carefully submerging the microtiter plate in water, without disturbing the formed biofilm. Following this washing step, the biofilm was immediately de-stained with 200 µl of 30% acetic acid for 45 minutes at room temperature. After the de-staining procedure, 100 µl of the solubilised CV was transferred to a new microtiter plate and measured at 595 nm using an EZ Read 800 microplate reader (Biochrom, England). The average of blank absorbance values was deducted from experimental absorbance values to eliminate background interference and normalise values. Additionally, biofilm specific activity (BSA) was implemented to compare the data obtained from XTT and CV assays. This index was calculated with the formula indicated below.

$$\text{BSA} = (XCR) \times \left\{\frac{(XTT+CV)}{2}\right\}$$

Where *XCR* indicates XTT:CV ratio

### 2.3.4 Determination of minimum biofilm inhibitory concentration of fluconazole

The minimum biofilm inhibitory concentration (MBIC) of FLC against test and reference strains was determined with slight modifications of previously described microtiter-based methods (Ramage et al. 2001; Mishra et al. 2014). Briefly, biofilms were prepared as described above. Following the adhesion phase, media (containing non-adherent cells) was aspirated. The wells were re-filled with 200 µl of serially two-fold diluted concentrations (128 to 16 µg/ml) of FLC in sterile YNB broth (prepared from 5 mg/ml stock) and incubated at 37$^{o}$C for 48 h to allow biofilm formation. Drug-free wells (containing appropriate DMSO concentration in sterile YNB broth) and biofilm-free wells (containing sterile YNB broth only without cells) were included as negative control and blank, respectively. Next, the wells were washed once with 200 µl sterile PBS, then XTT reduction assay was performed (Kuhn et al. 2003), as described above. The average of blank absorbance values was subtracted from experimental (*E*) and negative control (*N*) values to eliminate background interferences and normalise values. The % inhibition was calculated as indicated below.

$$\% \text{ inhibition} = \left(\frac{N-E}{N}\right) \times 100$$

Where *N* and *E* represent the negative control and experimental values, respectively.

The $MBIC_{50}$ was defined as the lowest concentration that resulted in at least 50% reduction in biofilm metabolic activity (compared to drug-free control), while the sub-inhibitory concentration ($SMBIC_{50}$) was regarded as any concentration below the $MBIC_{50}$.

### 2.3.5 Determination of minimum biofilm inhibitory concentration of fatty acids

The MBIC of fatty acids against test and reference strains was determined with slight modifications of previously described microtiter-based methods (Ramage et al. 2001; Mishra et al. 2014). Cells were prepared as described above. Following incubation at 37ºC for 90 min to allow cell adhesion, the media was aspirated. Afterwards, 200 µl of serially ten-fold diluted concentrations (1 to 0.01 mM) of unsaturated fatty acids [Oleic Acid (OA, 18:1), Linoleic Acid (LA, 18:2), Gamma-Linolenic Acid (GLA, 18:3), Arachidonic Acid (AA, 20:4), and Eicosapentaenoic Acid (EPA, 20:5)] (Sigma-Aldrich, St. Louis, MO, USA) in sterile YNB broth was dispensed into designated wells and incubated at 37ºC for 48 h to allow biofilm formation. Fatty acid-free wells (containing appropriate ethanol concentration in sterile YNB) and biofilm-free wells (containing only sterile YNB broth without cells) were included as negative control and blank, respectively. Subsequently, the wells were washed once with 200 µl sterile PBS and biofilm metabolic activity was examined with XTT reduction assay (Kuhn et al. 2003). The average of the blank absorbance values was deducted from the experimental and negative control values to eliminate background interferences and normalise data. The % inhibition, $MBIC_{50}$, and $SMBIC_{50}$ were determined as described above.

### 2.3.6 Determination of the potentiating effect of fatty acids on fluconazole susceptibility

The effects of FLC and fatty acids on biofilms of the least-susceptible *C. krusei* strain (UFS Y-0277) was determined. Cells of this strain were prepared as described above. Following incubation at 37ºC for 90 min to allow cell adhesion, media was aspirated, then 200 µl of YNB broth containing both FLC at 32 µg/ml and fatty acid (LA or GLA) at 0.1 mM was dispensed into designated wells and incubated at 37ºC for 48 h to allow biofilm formation. Negative control (DMSO and EtOH, DE) and blank (PBS) were included. Afterwards, the wells were washed once with 200 µl sterile PBS, and the biofilm metabolic activity was examined with XTT reduction assay (Kuhn et al. 2003). The average of the blank absorbance values was subtracted from the experimental and negative control values to eliminate background interferences and normalise values. The % inhibition was calculated as described above, and the potentiating effect of the combination was determined by comparing the % inhibition values of the combination treatment with that of individual treatments.

### 2.3.7 Morphological examination of treated biofilms

Biofilm of the least-susceptible strain, *C*. *krusei* UFS Y-0277, was formed in the presence of FLC (32 µg/ml), fatty acid (LA or GLA) at 0.1 mM, a combination of both [FLC (32 µg/ml) + fatty acid (0.1 mM)], or YNB broth (control) as described above, in a flat bottom 6 well culture plates (Corning Incorporated, USA). After biofilm formation, the biofilm was washed once with sterile PBS, and 5 $mm^2$ rectangular sections of the bottom of the wells were excised, placed in sterile PBS, and prepared for SEM analysis according to the protocol of Swart and co-workers (2010). Briefly, each sample was fixed with the primary fixative, 3% (v/v) glutardialdehyde (Merck, Darmstadt, Germany) buffered with 0.1 M sodium phosphate buffer (pH 7.0) for 3 h. Secondary fixation was done using a buffered solution of 1% osmium tetroxide (Merck, Darmstadt, Germany) for another 1 h. The samples were rinsed with sodium phosphate buffer after each of the fixation steps. Next, the samples were dehydrated with varying concentrations of ethanol (50%, 70% and 95%) for 20 min each and twice with 100% ethanol for 1 h. After dehydration, the samples were dried with a critical point dryer (Tousimis, Maryland, USA), that uses pressurised liquid $CO_2$, at 35 – 40$^oC$, for 1.5 hours. Following drying, samples were mounted on metal stubs and gold coated with a sputter coater (Bio-Rad, United Kingdom) to become electrically conductive. The specimens were then viewed and imaged with a JEOL JSM-7800F SEM (Tokyo, Japan).

### 2.3.8 Influence of fatty acids on membrane integrity of *C. krusei*

The effect of various treatments on the membrane integrity of cells within *C*. *krusei* UFS Y-0277 (least-susceptible strain) biofilm was analysed using propidium iodide assay with a few modifications of previous protocols (Ogundeji et al. 2016; Bae and Rhee 2019). Briefly, biofilms of the least-susceptible were formed in the presence of either FLC (32 µg/ml), fatty acid (LA or GLA) at 0.1 mM, a combination of both [FLC (32 µg/ml) + fatty acid (0.1 mM)], or DE (control), as described above, in a flat bottom 6 well culture plates. After biofilm formation, each biofilm was washed once, re-suspended in sterile PBS, and vortexed thoroughly to disrupt the biofilm (Gulati et al. 2018). The resulting suspension was standardised to a final concentration of 1.0 x $10^7$ cells/ml in filter sterilised PBS. Subsequently, 99 µl of the standardised suspension was transferred to a black 96-well microtiter plate (Thermo Scientific, Denmark) containing 1 µl propidium iodide stain (200 µg/ml). The plate was incubated at 37$^oC$ for 30 min, then the extent of cell membrane damage was quantified by measuring the red fluorescence of stained cells at an excitation wavelength of 485 nm and an emission wavelength of 635 nm using a Fluoroskan Ascent Fluorimeter (Thermo Scientific, China). Additionally, the fluorescence of the stained cells for all the treatment conditions was visualised using an inverted (fluorescence) CKX53 Microscope (Olympus, Japan) combined

with a 130 W high-pressure mercury lamp (Olympus, Japan). Red fluorescence was visualised using a blue filter.

### 2.3.9 Influence of antioxidants on the potentiating effect of the combination treatments

Cells were prepared as described above. Following incubation at 37ºC for 90 min to allow cell adhesion, media was aspirated, then 200 µl of YNB broth containing the combination of FLC at 32 µg/ml and 0.1 mM fatty acid (LA or GLA) with or without 2 mM α-tocopherol polyethylene glycol succinate (TPGS, vitamin E) or 2 mM butylated hydroxytoluene (BHT) (Sigma-Aldrich, St. Louis, MO, USA) was dispensed into designated wells (Ak and Gülçin 2008). The wells were incubated at 37ºC for 48 h to allow biofilm formation. Negative control and blank were included. Accordingly, the wells were washed once with 200 µl sterile PBS, the biofilm biomass was examined with CV assay (Jin et al. 2003; O'Toole 2011; Hacioglu et al. 2018). The percentage biofilm biomass relative to the untreated (negative) control was determined.

### 2.3.10 Influence of fatty acids on efflux pump activity of *C. krusei*

The influence of fatty acids on the efflux pump(s) activity of *C. krusei* biofilm was evaluated using Rhodamine 6G efflux assay with slight modifications of previous methods (Maesaki et al. 1999; Ells et al. 2013; Szczepaniak et al. 2017). Briefly, biofilms were formed as described above, in a black 96-well microtiter plate (Thermo Scientific, Denmark) for 6 h at 37ºC. After biofilm formation, spent medium was removed from the wells, 200 µl of sterile PBS was dispensed into each well, and the plate was incubated at 37 °C for 1 h to de-energise the biofilm cells. Following incubation, PBS was removed from the wells, and 200 µl of 10 µM Rhodamine 6G (Rh6G) (Sigma-Aldrich, St. Louis, MO, USA) in sterile PBS (prepared from 10 mM Rh6G stock in DMSO) was dispensed into each well. The plate was incubated at 37ºC, and the uptake of Rh6G was measured every 10 min for 1 h at an excitation wavelength of 530 nm and emission of 590 nm using Fluoroskan Ascent Fluorimeter (Thermo Scientific, China). Following the uptake step, leftover Rh6G was removed from the wells, and 200 µl of LA (0.1 or 1 mM), GLA (0.1 or 1 mM), AA (0.1 or 1 mM), FLC (32 µg/ml), FLC+LA, FLC+GLA, FLC+AA, or DE (control) in sterile PBS was subsequently dispensed into designated wells, and the plate was incubated at 37ºC for another 1 h (Fourie 2020). Subsequently, the supernatant was removed from the wells, and 200 µl of 2 mM glucose (in sterile PBS) was dispensed into each well to induce Rh6G efflux from the treated biofilm cells. The plate was incubated at 37ºC, and the efflux of Rh6G from the cells was measured extracellularly every 10 min for 1 h at an excitation wavelength of 530 nm and an emission wavelength of 590 nm using a Fluoroskan Ascent Fluorimeter (Thermo Scientific, China).

### 2.3.11 *In vivo* evaluation of the potentiating effect of fatty acids on fluconazole activity

#### 2.3.11.1 Nematode propagation and bacterial culture

*Caenorhabditis elegans* AU37 (*glp-4*(*bn2*) I; *sek-1*(*km4*) X) nematode and non-pathogenic *Escherichia coli* OP50 (a uracil auxotroph) were obtained from *Caenorhabditis* Genetics Centre (University of Minnesota, USA). Prior to each experiment, glycerol stock of *E. coli* OP50 kept at -80°C was thawed on Luria-Bertani (LB) agar (10 g/l tryptone powder, 10 g/l yeast extract, 5 g/l sodium chloride, 17 g/l agar) and incubated at 37°C for 24 h. A loopful of resulting colonies from the LB agar plates was inoculated into fresh LB broth and incubated (37°C, 24 h). Accordingly, *E. coli* OP50 lawn was spotted on nematode growth medium (NGM) agar plates [2.5 g/l peptone powder, 3 g/l sodium chloride, 17 g/l agar, 1 ml/l cholesterol (5 mg/ml), 1 ml/l $MgSO_4$ (1 M), 1 ml/l $CaCl_2$ (1 M), 25 ml/l potassium phosphate buffer (1 M)] and incubated overnight at 37°C. The nematodes were then propagated on the resulting *E. coli* OP50-seeded NGM agar plates at 15°C for 96 h to reach L4 larvae or young adult stage prior to the infection assay (Brenner 1974).

#### 2.3.11.2 Infection of *C. elegans*

For infection with the least-susceptible strain (*C. krusei* UFS Y-0277), cells of this strain were inoculated into a 5 ml YPD broth (5 g/l peptone, 3 g/l yeast extract, 10 g/l glucose) and incubated overnight at 30°C. The resulting culture was standardised to $OD_{600}$ of 0.8, and a 100 µl lawn was prepared on brain-heart infusion (BHI) agar (BHI 37g/l, Agar 17g/l) plates and incubated at 30°C for 24 h. Synchronized L4 or young adult nematodes were carefully harvested and washed twice with sterile M9 buffer (3 g/l $KH_2PO_4$, 6 g/l $Na_2PO_4$ and 1 mM $MgSO_4$) at 4000 *x g*, 2 min. Thereafter, approximately 400 to 500 washed nematodes were deposited onto *C. krusei* lawn on BHI agar plates and incubated at 25°C for 4 h (infection stage). Plates with uninfected nematodes on *E. coli* OP50 were included as a control.

#### 2.3.11.3 *C. elegans* treatment assay

The ability of the combination treatments to enhance the survival of infected nematodes was assessed with a few modifications of previously described methods (Breger et al. 2007; Eldesouky et al. 2020). Briefly, following infection, infected nematodes were carefully harvested off the BHI agar plates with sterile M9 buffer and washed thrice (5000 *x g*, 5 min) to remove undigested yeast cells. Subsequently, 40 nematodes were treated with either FLC (32 µg/ml), LA (0.1 mM), GLA (0.1 M), FLC+LA, FLC+GLA, or DE (control) in 2 ml liquid medium (80% M9 buffer, 20% BHI, kanamycin 90 µg/ml/) in 6-well plates (Corning Incorporated, USA) and incubated at 25ºC. The nematodes were monitored daily using a stereomicroscope (Olympus, Vietnam) and scored as either alive or dead. A nematode is considered dead if it shows no motility in response to mechanical stimulation with a sterile pipette tip. This assay

was done in triplicate, with a total of 120 nematodes per treatment. The survival metrics, including Kaplan-Meier statistics, median survival time and log-rank test, were performed with online application for survival analysis 2 (OASIS 2) (Han et al. 2016).

#### 2.3.11.4 Evaluation of fungal burden within *C. elegans*

The combination treatments' propensity to reduce the fungal burden of infected nematodes was assessed with a few modifications of previously described methods (Breger et al. 2007; Eldesouky et al. 2018). Briefly, nematodes were infected as described above. Following infection, nematodes were carefully harvested off the BHI agar plates with sterile M9 buffer and washed thrice with M9 buffer to get rid of all undigested yeast cells. Subsequently, 60 nematodes (20 nematodes per replicate) were treated with either FLC (32 µg/ml), LA (0.1 mM), GLA (0.1 M), FLC+LA, FLC+GLA, or DE (control) in 2 ml liquid medium (80% M9 buffer, 20% BHI, 90 µg/ml kanamycin) in 6-well plates (Corning Incorporated, USA) and incubated at 25$^{o}$C for 24 h. Following incubation, nematodes were washed twice with sterile M9 buffer and ingested *C. krusei* cells were released from the nematodes by a vigorous-vortex procedure with beads (150 mg in 3 ml M9 buffer) for 2 min (without affecting fungal viability). The resulting *C. elegans* homogenates were diluted hundred-fold, plated onto YPD agar (supplemented with ampicillin 100 µg/ml/ and kanamycin 90 µg/ml/ to preclude bacterial growth), and incubated at 30$^{o}$C for 24 to 48 h. Accordingly, the percentage fungal burden per nematode relative to the untreated control (DE) was determined (Eldesouky et al. 2020).

### 2.3.12 Statistical analysis

Unless stated otherwise, all experiments were conducted in triplicate. Averages and standard deviations were calculated using Excel 2013. Graphs were constructed with GraphPad Prism. The data of different groups, unless stated otherwise, were compared using one-way analysis of variance (ANOVA) complemented with Tukey's multiple comparisons test. Unless stated otherwise, a $p$-value ≤ 0.05 was considered significant and statistical difference was indicated by different letters on the bars.

## 2.4 Results and Discussions

### 2.4.1 Biofilm formation and quantification

Microbial biofilms have remarkable medical, veterinary, and environmental importance. Estimatedly, 65% of all hospital infections are associated with biofilm cells rather than planktonic cells, and this has redirected increased focus on biofilm communities when microbial pathogenicity and virulence are investigated (Mah and O'Toole 2001; Silva et al. 2010; Alnuaimi et al. 2013). Protection against host defences, virulence and increased antifungal resistance is afforded by biofilms (Baillie and Douglas 2000; Samaranayake et al. 2002). Many fungal species, including *Candida* spp., such as *C. albicans* and *C. krusei*, have

the capacity to form a biofilm. Biofilm formation in *Candida* spp. reduces the effective drug penetration, which consequently confers decreased susceptibility to antifungal drugs, especially the azoles, polyenes, and nucleoside analogues (Ramage et al. 2012; Desai et al. 2014). Furthermore, it has been documented that biofilm structures and physiology are not only species-dependent but could also be strain-specific (Silva et al. 2009). Here, we briefly evaluate and compare the biofilm physiology of four *C. krusei* strains and a reference strain (*C. albicans* SC5314).

The metabolic activity of biofilms of the strains was assessed using XTT reduction assay (**Fig. 2A**). This colorimetric assay depends on the reduction of XTT reagent to formazan by the dehydrogenases of metabolically active cells (Kuhn et al. 2002; Kuhn et al. 2003). While there was no significant difference in the metabolic activity of the four *C. krusei* strains ($p > 0.05$), their metabolic activity was in the hierarchy: **UFS Y-0217** > **UFS Y-0637** > **UFS Y-0801** > **UFS Y-0277**. Moreover, the reference strain biofilm displayed a very high metabolic activity compared to any of the *C. krusei* strains ($p < 0.05$) (**Fig. 2A**). However, caution must be taken when comparing biofilms of different strains and species with XTT reduction assay, since the reduction of XTT to formazan is usually species and strain-dependent (Kuhn et al. 2003). Furthermore, we also quantified the biofilm biomass of strains using CV assay (**Fig. 2B**). Amongst the *C. krusei* strains, strain UFS Y-0801 had the highest biomass quantity, however, this was not significantly different from that of strain UFS Y-0217 ($p > 0.05$). The lowest biomass quantity was recorded for strain UFS Y-0277 ($p < 0.05$), and this is concordant with the earlier observed lower metabolic activity of the strain (**Fig. 2A**). In addition, similar to the XTT results, the reference strain had the highest biofilm biomass ($p < 0.05$). Notably, with the exception of *C. krusei* strain UFS Y-0277, the biomass quantities of all strains, including the reference strain, were more pronounced than corresponding metabolic activities (**Fig. 2B**). A similar observation has been reported by previous studies (Peeters et al. 2008; Xu et al. 2016). This is unsurprising since XTT reduction assay only measures the viability of the biofilm cells, while CV assay represents a good indicator of the amount of biofilm (i.e. viable cells, non-viable cells, and extracellular matrix) (Pitts et al. 2003; Kuhn et al. 2003). Rather than considering XTT and CV assays as two identical descriptors (i.e. providing the same information), it is more practical to use them complementarily. Moreover, a complementary use of both assays by Muthamil and co-workers (2020) highlighted the biofilm-reducing potential, without the inhibition of metabolic viability, of a plant-derived OA against *Candida* spp.

As a result of these different types of information produced by XTT and CV assays, the use of XTT and CV ratio (XCR) has been attempted to compare the results produced by these two assays. However, this ratio (XCR) has poor performance and produces extremely high values when the CV value is relatively low. Thus, we resorted to using an index with a better

performance and without low CV value-related problems, known as biofilm specific activity (BSA) (Corte et al. 2019). As shown in **Figure 2C**, there was no significant difference in the BSA values obtained for the four *C. krusei* strains ($p > 0.05$). However, the reference strain had a high BSA value ($p < 0.05$) and this observation is seemingly comparable to the XTT assay results.

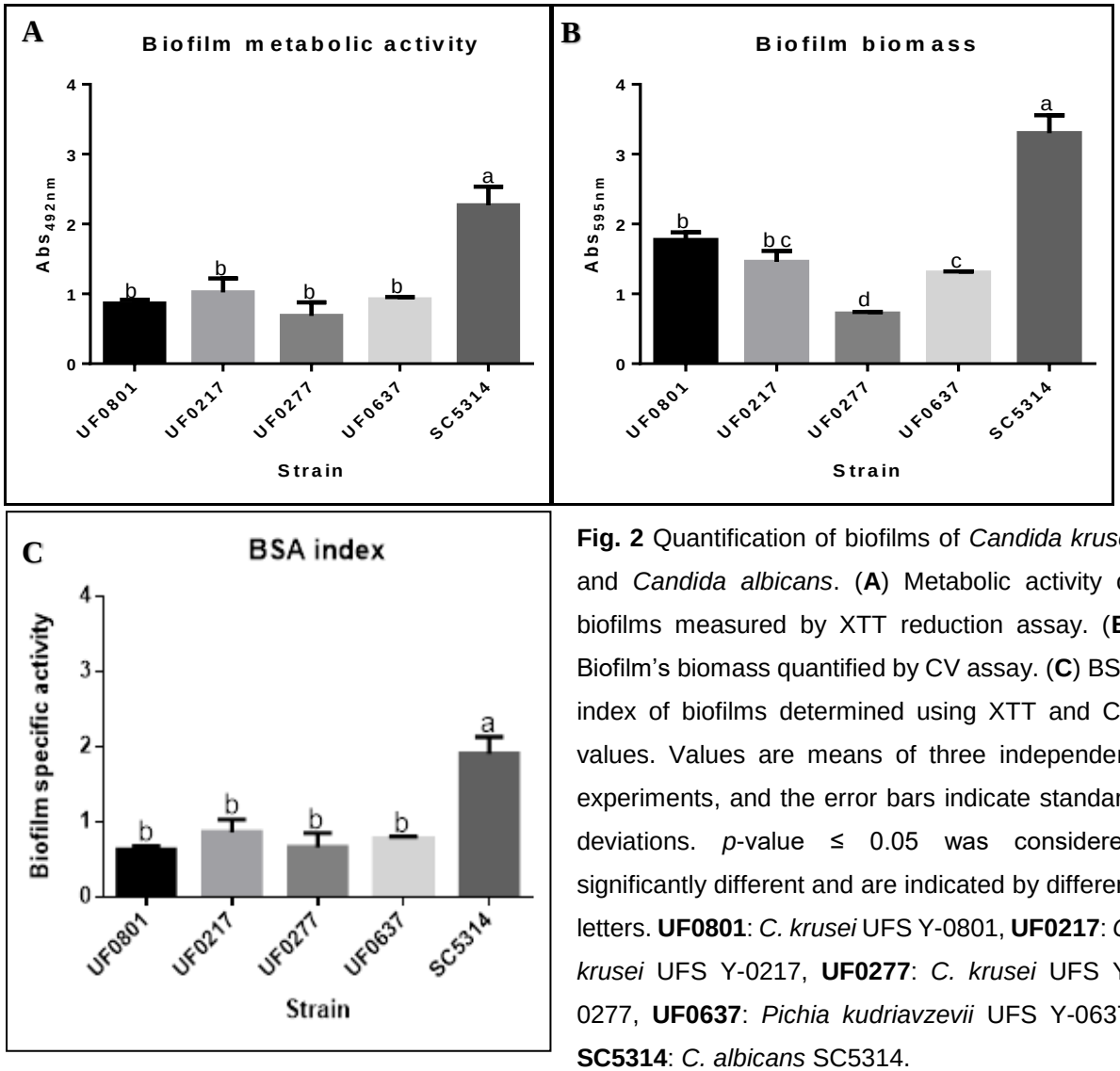


**Fig. 2** Quantification of biofilms of *Candida krusei* and *Candida albicans*. (**A**) Metabolic activity of biofilms measured by XTT reduction assay. (**B**) Biofilm's biomass quantified by CV assay. (**C**) BSA index of biofilms determined using XTT and CV values. Values are means of three independent experiments, and the error bars indicate standard deviations. *p*-value ≤ 0.05 was considered significantly different and are indicated by different letters. **UF0801**: *C. krusei* UFS Y-0801, **UF0217**: *C. krusei* UFS Y-0217, **UF0277**: *C. krusei* UFS Y-0277, **UF0637**: *Pichia kudriavzevii* UFS Y-0637, **SC5314**: *C. albicans* SC5314.

### 2.4.2 Determination of minimum biofilm inhibitory concentration of fluconazole

While the inhibitory effect of FLC on the metabolic activity of all *C. krusei* isolates was concentration-dependent, the most pronounced reduction for all strains, including *C. albicans* SC5314, was recorded at the highest drug concentration (128 µg/ml) (**Fig. 3**). Additionally, the reference strain, *C. albicans* SC5314, was susceptible to all FLC concentrations tested with inhibition of >85%.

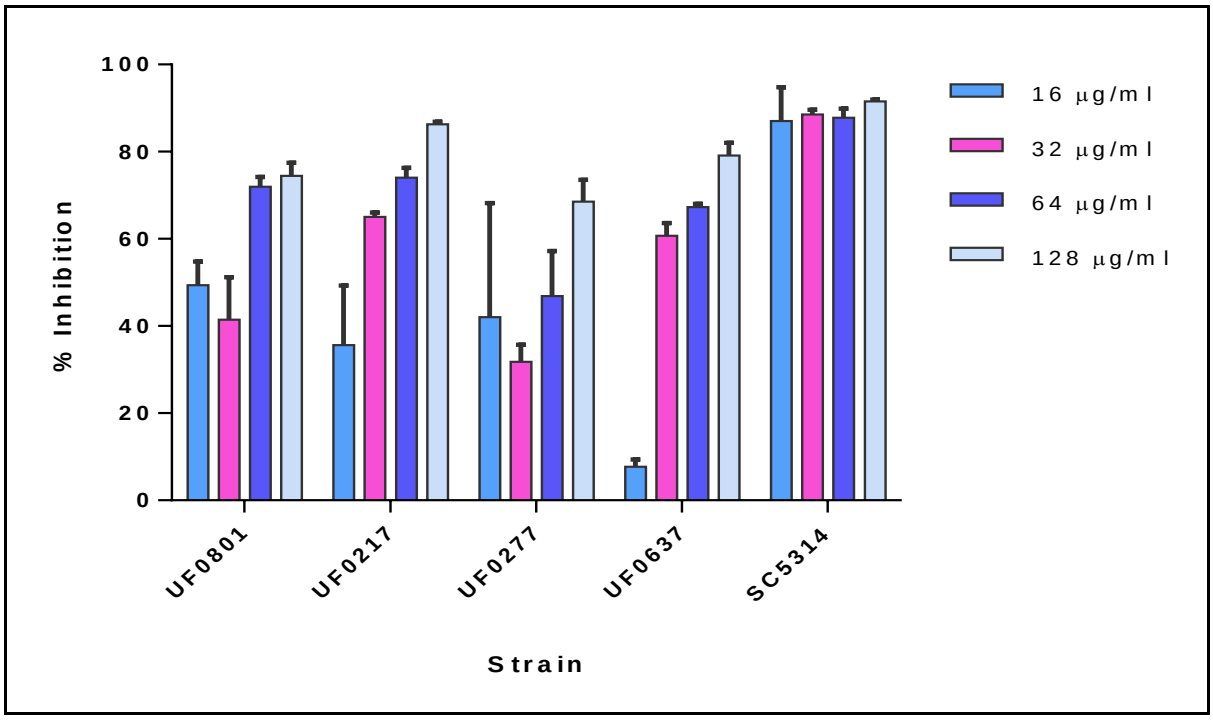


**Fig. 3** The effect of various concentrations of fluconazole on the metabolic activity of biofilms of *C. krusei* strains and *C. albicans* SC5314 after incubation at 37°C for 48 h, using XTT reduction assay. Values are means of three independent experiments and the error bars indicate standard deviations. **UF0801**: *C. krusei* UFS Y-0801, **UF0217**: *C. krusei* UFS Y-0217, **UF0277**: *C. krusei* UFS Y-0277, **UF0637**: *Pichia kudriavzevii* UFS Y-0637, **SC5314**: *C. albicans* SC5314.

The $MBIC_{50}$ and $SMBIC_{50}$ of FLC against the isolates were also determined (**Table 1**). The reference strain (*C. albicans* SC5314) biofilm was most susceptible to FLC with recorded $MBIC_{50}$ value of <16 µg/ml ($p < 0.05$). However, the $MBIC_{50}$ values of FLC ranged from 32 to 128 µg/ml for *C. krusei*, while their $SMBIC_{50}$ values were between 16 and 64 µg/ml. The lowest $MBIC_{50}$ value ($MBIC_{50}$ = 32 µg/ml) was recorded against strains UFS Y-0217 and UFS Y-0637, and this might suggest them as the most susceptible *C. krusei* strains in this study. Notably, strain UFS Y-0217 ($CBS573^T$) is the type strain of *C. krusei,* and a previous study has reported $MBIC_{50}$ for FLC against this strain as 32 µg/ml (Douglass et al. 2018). In addition, biofilms of

strain UFS Y-0801 was moderately resistant ($MBIC_{50}$ = 64 µg/ml), while that of strain UFS Y-0277 was the least susceptible ($MBIC_{50}$ = 128 µg/ml).

Overall, as expected, all tested *C. krusei* strains exhibited reduced sensitivity to FLC compared to the reference strain (*C. albicans* SC5314). Generally, about 97% of *C. krusei* isolates are considered inherently resistant to FLC (Whaley et al. 2017). The mechanism for this remains obscure; however, many studies have ascribed it to the unusually low affinity of Erg11p of *C. krusei* for FLC (Venkateswarlu et al. 1997; Orozco et al. 1998; Fukuoka et al. 2003). Moreover, a later study by Lamping and co-workers (2009) has attributed it to decreased susceptibility of Erg11p and constitutive expression of Abc1p (Cdr1p).

**Table 1** The $MIC_{50}$ and $SMIC_{50}$ of fluconazole against biofilms

| **Strain** | Fluconazole (µg/ml) | |
|---|---|---|
| | **$MBIC_{50}$** | **$SMBIC_{50}$** |
| **UF0801** | 64 | 32 |
| **UF0217** | 32 | 16 |
| **UF0277** | 128 | 64 |
| **UF0637** | 32 | 16 |
| **SC5314** | <16 | <16 |

The $MBIC_{50}$ denotes the concentration that resulted in at least 50% reduction in the biofilm metabolic activity (relative to the drug-free control), while the sub-inhibitory concentration ($SMBIC_{50}$) is the concentration below the $MBIC_{50}$. **UF0801**: *C. krusei* UFS Y-0801, **UF0217**: *C. krusei* UFS Y-0217, **UF0277**: *C. krusei* UFS Y-0277, **UF0637**: *Pichia kudriavzevii* UFS Y-0637, **SC5314**: *C. albicans* SC5314.

### 2.4.3 Determination of minimum biofilm inhibitory concentration of fatty acids

In order to determine the most effective fatty acids and their accompanying non-inhibitory concentrations suitable for the combination treatment assay, the antifungal activity of varying doses of fatty acids was determined against the biofilms of all strains. This assay was done by treating the biofilms with serially ten-fold diluted concentrations (0.01, 0.1 and 1 mM) of unsaturated fatty acids (OA, LA, GLA, AA, and EPA) for 48 h, at 37$^{o}$C and evaluating their metabolic activities. As shown in **Figure 4**, the unsaturated fatty acids tested exerted considerable anti-candidal activity. Notably, except for EPA – which exhibited an inverse dose-dependent effect against *C. krusei* UFS Y-0801, the inhibitory effect of all the tested fatty acids was dose-dependent, and the most pronounced effect was observed for GLA against the biofilms of all strains (**Fig. 4C**). This observation conforms with previous findings of Muthamil and co-workers (2020), which demonstrated a concentration-dependent biofilm inhibitory activity of OA against *Candida* spp. Similarly, a better anti-biofilm effect of some PUFAs [LA and alpha-linolenic acid (ALA)] against *C. albicans* and *Staphylococcus aureus* was observed

at 100 µg/ml compared to 20 µg/ml (Kim et al. 2020). Moreover, AA has also been shown to exhibit bactericidal activity against *Staphylococcus aureus* in a dose-dependent manner (Beavers et al. 2019). Additionally, the inhibitory activity of the unsaturated fatty acids against all strains was also fatty acid-specific and strain-dependent.

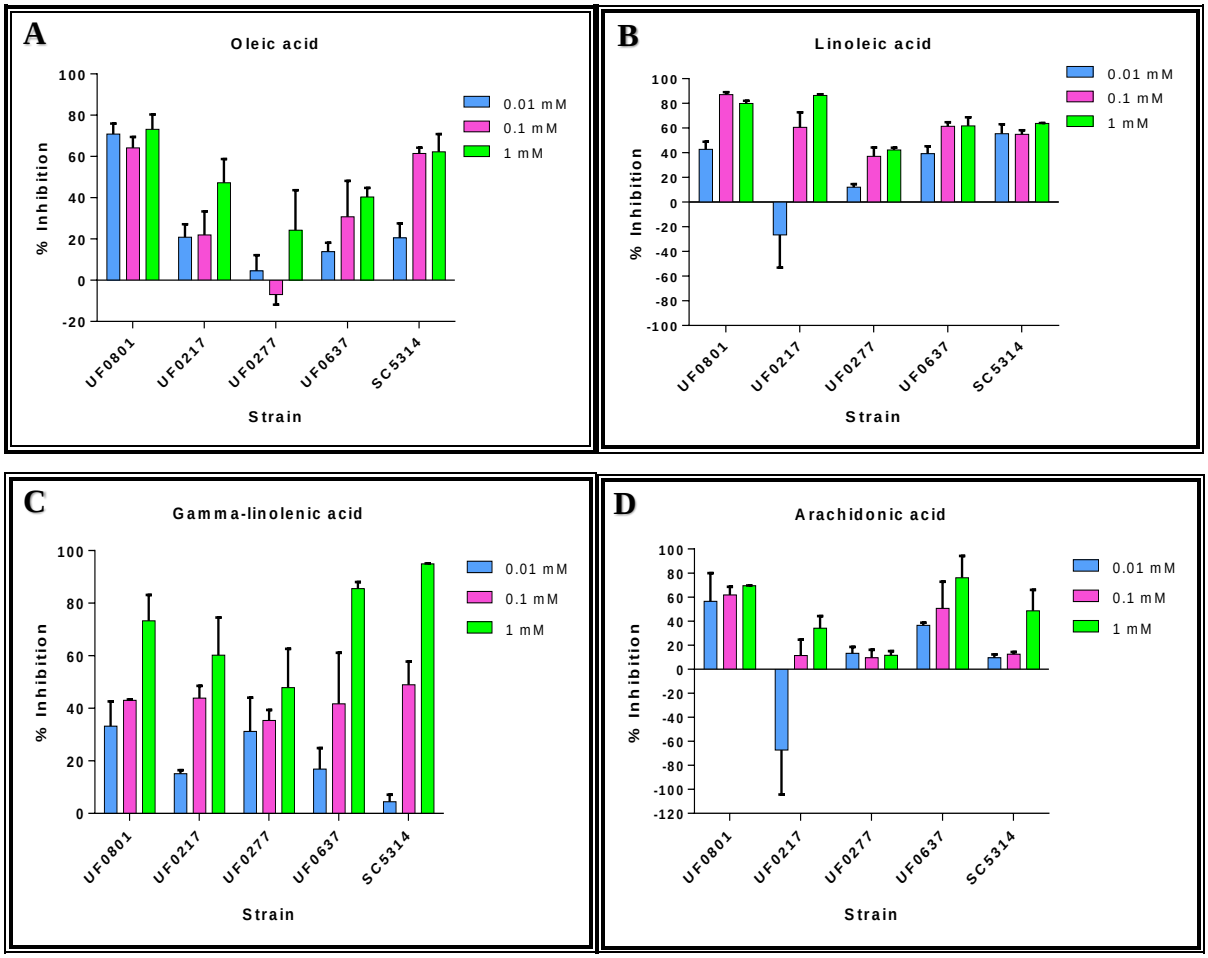


**Fig. 4** Effect of varying concentrations of various fatty acids (**A**- oleic acid, **B**- linoleic acid, **C**- gamma-linolenic acid, **D**- arachidonic acid, **E**- eicosapentaenoic) on the metabolic activity of *C. krusei* strains and *C. albicans* SC5314 biofilms after incubation at 37ºC for 48 h, using XTT reduction assay. Values are means of three independent experiments and the error bars indicate standard deviations. **UF0801**: *C. krusei* UFS Y-0801, **UF0217**: *C. krusei* UFS Y-0217, **UF0277**: *C. krusei* UFS Y-0277, **UF0637**: *Pichia kudriavzevii* UFS Y-0637, **SC5314**: *C. albicans* SC5314.

The $MBIC_{50}$ and $SMBIC_{50}$ of the fatty acids against the biofilms of all strains were also determined. As shown in **Table 2**, while the reference strain (*C. albicans* SC5314) was the most susceptible to LA ($MBIC_{50}$ <0.01 mM), it was the least sensitive to AA ($MBIC_{50}$ >1 mM). Amongst *C. krusei* strains, the lowest $MBIC_{50}$ (<0.01 mM) of OA was recorded against UFS Y-0801, and its highest $MBIC_{50}$ (>1.0 mM) was observed against the other three *C. krusei* strains (UFS Y-0217, UFS Y-0277, UFS Y-0637). Similarly, this high $MBIC_{50}$ was also seen for strain UFS Y-0277 in the cases of LA, GLA, and AA, while strain UFS Y-0801 also had the lowest $MBIC_{50}$ (<0.01 mM) against AA. Additionally, the $MBIC_{50}$ values of EPA against all *C. krusei* strains, except UFS Y-0801, were identical (1.0 mM).

**Table 2** $MIC_{50}$ and $SMIC_{50}$ of unsaturated fatty acids against *C. krusei* and *C. albicans* biofilms

| Strain | OA (mM) | | LA (mM) | | GLA (mM) | | AA (mM) | | EPA (mM) | |
|---|---|---|---|---|---|---|---|---|---|---|
| | $MBIC_{50}$ | $SMBIC_{50}$ | $MBIC_{50}$ | $SMBIC_{50}$ | $MBIC_{50}$ | $SMBIC_{50}$ | $MBIC_{50}$ | $SMBIC_{50}$ | $MBIC_{50}$ | $SMBIC_{50}$ |
| **UF0801** | <0.01 | <0.01 | 0.1 | 0.01 | 1.0 | 0.1 | <0.01 | <0.01 | * | * |
| **UF0217** | >1.0 | 1.0 | 0.1 | 0.01 | 1.0 | 0.1 | >1.0 | 1.0 | 1.0 | 0.1 |
| **UF0277** | >1.0 | 1.0 | >1.0 | 1.0 | >1.0 | 1.0 | >1.0 | 1.0 | 1.0 | 0.1 |
| **UF0637** | >1.0 | 1.0 | 0.1 | 0.01 | 1.0 | 0.1 | 0.1 | 0.01 | 1.0 | 0.1 |
| **SC5314** | 0.1 | 0.01 | <0.01 | <0.01 | 1.0 | 0.1 | >1.0 | 1.0 | 0.1 | 0.01 |

The $MBIC_{50}$ denotes the concentration that resulted in at least 50% reduction in the biofilm metabolic activity (compared to the drug-free control), while the sub-inhibitory concentration ($SMBIC_{50}$) is the concentration below the $MBIC_{50}$. OA: oleic acid, LA: linoleic acid, GLA: gamma-linolenic acid, AA: arachidonic acid, EPA: eicosapentaenoic acid. *: reverse dose-dependent activity observed. **UF0801**: *C. krusei* UFS Y-0801, **UF0217**: *C. krusei* UFS Y-0217, **UF0277**: *C. krusei* UFS Y-0277, **UF0637**: *Pichia kudriavzevii* UFS Y-0637, **SC5314**: *C. albicans* SC5314.

Overall, similar to what was observed for FLC, *C. krusei* UFS Y-UF0277 appears least susceptible to the inhibitory effect of all fatty acids, and this prompted further analysis of its data. With the exception of AA, the biofilm inhibitory effect of fatty acids against this strain at the highest concentration tested (1 mM) directly correlates with their chain length and degree of unsaturation [**EPA** (5: double bonds) > **GLA** (3) > **LA** (2) > **OA** (1)] (**Fig. 5A**, **5B**). This corresponds to an earlier observation that the cytotoxic effect of fatty acids on mammalian cell lines is not only dose-dependent but also relates to their chain length and level of unsaturation (Lima et al. 2002). In addition, the interaction of fatty acids with phospholipid membrane varies with their chain length and saturation level (Thibane et al. 2012a).

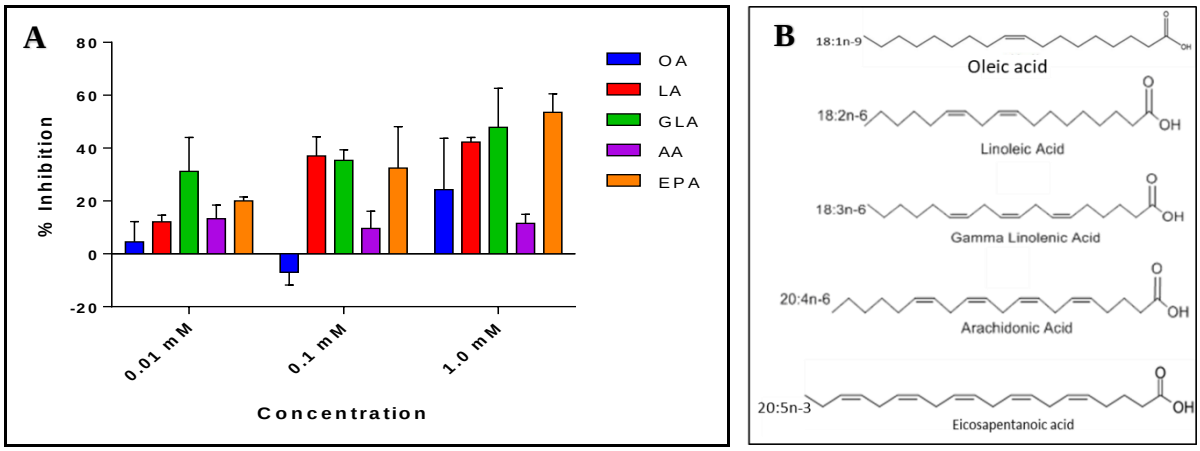


**Fig. 5** The biofilm inhibitory activity and structures of unsaturated fatty acids. (**A**) Effect of varying concentrations of unsaturated fatty acids on metabolic activity of *C. krusei* UFS Y-0277 biofilms after incubation at 37ºC for 48 h, using XTT reduction assay. Values are means of three independent experiments and the error bars indicate the standard deviation. (**B**) Structures of unsaturated fatty acids used in this study in ascending order of length and unsaturation. **OA**: oleic acid, **LA**: linoleic acid, **GLA**: gamma-linolenic acid, **AA**: arachidonic acid, **EPA**: eicosapentaenoic acid.

Consistent with our study, the antifungal property of long-chain unsaturated fatty acids has been reported by previous studies. A study by Thibane and co-workers (2010) reported significant inhibitory effect of PUFAs, such as stearidonic acid (SDA), docosapentaenoic acid, and EPA, against *C. albicans* and *C. dubliniensis* biofilms. A more recent study by Kim and co-workers (2020) also highlighted the remarkable anti-biofilm activity of LA and ALA from centipede oil against *C. albicans*. Another study by Muthamil and co-workers (2020) reported the biofilm-reducing potential of plant-derived OA against *C. albicans*, *C. glabrata*, and *C. tropicalis*. Although the mechanism of action of unsaturated fatty acids in our present study is unknown, their mode of action in previous studies was suggested to be mainly through their incorporation into fungal membranes - which increases unsaturation index, membrane fluidity and permeability, and ultimately elicits membrane disorganisation and disruption of membrane proteins (Avis and Belanger 2001; Pohl et al. 2011; Mishra et al. 2014). Increased oxidative stress and membrane disruption, resulting from lipid peroxidation, have also been attributed to the insertion of PUFAs into fungal membranes (Cipak et al. 2006; Thibane et al. 2012a). Moreover, antifungal fatty acids also inhibited hyphal morphogenesis and biofilm formation in certain *Candida* spp. (Shareck et al. 2011; Manoharan et al. 2017). Similarly, studies have reported the antibacterial activity of unsaturated fatty acids such as OA, LA, and AA (Kabara et al. 1972; Greenway and Dyke 1979; Lee et al. 2017; Beavers et al. 2019). The chief mechanism of action of antibacterial fatty acids is also via their incorporation into cellular lipids and membranes, which consequently induces alterations in the cell membrane and disruption of cellular processes, such as electron transport chain and oxidative phosphorylation

(Galbraith and Miller 1973; Yoon et al. 2018). Additionally, antibacterial fatty acids have also been reported to inhibit protein synthesis and influence virulence factors, such as biofilm formation (Yoon et al. 2018; Kim et al. 2019).

### 2.4.4 Polyunsaturated fatty acids potentiate the susceptibility of *C. krusei* biofilm to fluconazole

Because of our interest in the least-susceptible strain, the potentiating effect of unsaturated fatty acids (LA or GLA) on FLC activity was evaluated against the biofilm of *C. krusei* strain UFS Y-0277. While EPA was excluded from this assay, due to its reverse dose-dependent activity observed against strain UFS Y-0801, only LA and GLA were included due to their greater efficacy against UFS Y-0277 biofilm compared to other fatty acids tested. As shown in **Figure 6**, when combined with FLC, either of the fatty acids increased the susceptibility of the tested strain biofilm to FLC ($p < 0.05$). While GLA afforded 96% increased susceptibility, a 55% increase was observed for LA. Our observation coheres with the findings of Mishra and co-workers (2014), who reported that AA increases the susceptibility of *C. albicans*, *C. glabrata*, *C. parapsilosis* and *C. tropicalis* biofilms to FLC via influence on the lipid saturation level and fluidity of yeasts cell membranes. In addition, a similar study by Ells and co-workers (2009) demonstrated that AA increases the antifungal susceptibility of *C. albicans* and *C. dubliniensis* to amphotericin B and clotrimazole. Furthermore, the synergism of SDA and amphotericin B against *C. albicans* and *C. dubliniensis* biofilms has also been reported (Thibane et al. 2012b).

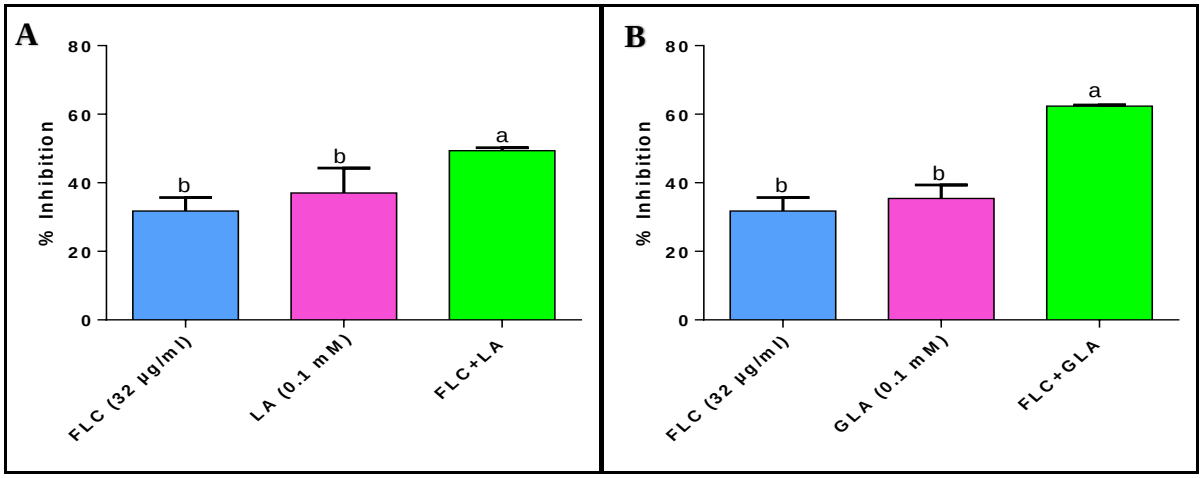


**Fig. 6** The effect of fluconazole in the presence or absence of LA (**A**) or GLA (**B**) on the metabolic activity of *C. krusei* UFS Y-0277 biofilm after incubation at 37°C for 48 h, using XTT reduction assay. Values are means of three independent experiments and the error bars indicate the standard deviation. *p*-value ≤ 0.05 was considered significantly different and indicated by different letters. **FLC**: fluconazole, **LA**: linoleic acid, **GLA**: Gamma-linolenic acid, **FLC+LA**: fluconazole and linoleic acid, **FLC+GLA**: fluconazole and gamma-linolenic acid.

In the present study, the underlying mechanism behind the observed increased susceptibility afforded by LA and GLA is obscure; however, it could be via the disruption of membrane organisation, due to increased membrane fluidity and permeability facilitated by the incorporation of unsaturation fatty acids into the fungal membrane, which allowed enhanced uptake of FLC (McDonough et al. 2002; Ells et al. 2009). Additionally, it is possibly due to increased oxidative stress, induced by the incorporation of PUFAs into cellular lipids and membranes, which makes the combination-treated cells more susceptible to FLC (Thibane et al. 2012a).

### 2.4.5 Morphological examination of treated biofilms

In order to delineate the underlying mechanism of the increased susceptibility observed following the combination treatments (**Fig. 6**), the morphology of *C*. *krusei* UFS Y-0277 biofilms treated with FLC in the presence or absence of a PUFA (LA or GLA) was examined using scanning electron microscopy (SEM). As shown in **Figure 7.1**, whilst LA-treated biofilm was the densest amongst the treated biofilms, all treated biofilms are sparser and have just one layer, compared to the untreated biofilm (**Fig. 7.1A**). Interestingly, hyphal or pseudohyphal cells were observed in all treatments with FLC, an observation that has not been previously reported for *C. krusei* grown in the presence of FLC. This was unexpected, as in addition to the inhibition of lanosterol 14α-demethylase (Erg11p), azoles exert antifungal activity in *C. albicans* via the inhibition of yeast-hyphae transition (Odds et al. 1985; Kabir and Ahmad 2013). However, in the presence of azoles, higher hyphal growth of azole-resistant *C. albicans* compared to the azole-susceptible isolates has been noted, presumably due to enough or increased ergosterol in the plasma membrane for hyphal production (Ha and White 1999; Costa et al. 2011; Sharma et al. 2019). Also, it is known that a defective azole target, Erg11p, responsible for ergosterol synthesis, limits hyphal growth (Lees et al. 1990). Hence, one possible explanation for the FLC-induced hyphal formation observed in this study is that it may be due to overproduction of ergosterol –which promotes hyphal formation since the upregulation of *ERG11* has been demonstrated in *Candida* spp. (including *C. krusei*) grown in the presence of azoles, including FLC (Henry et al. 2000).

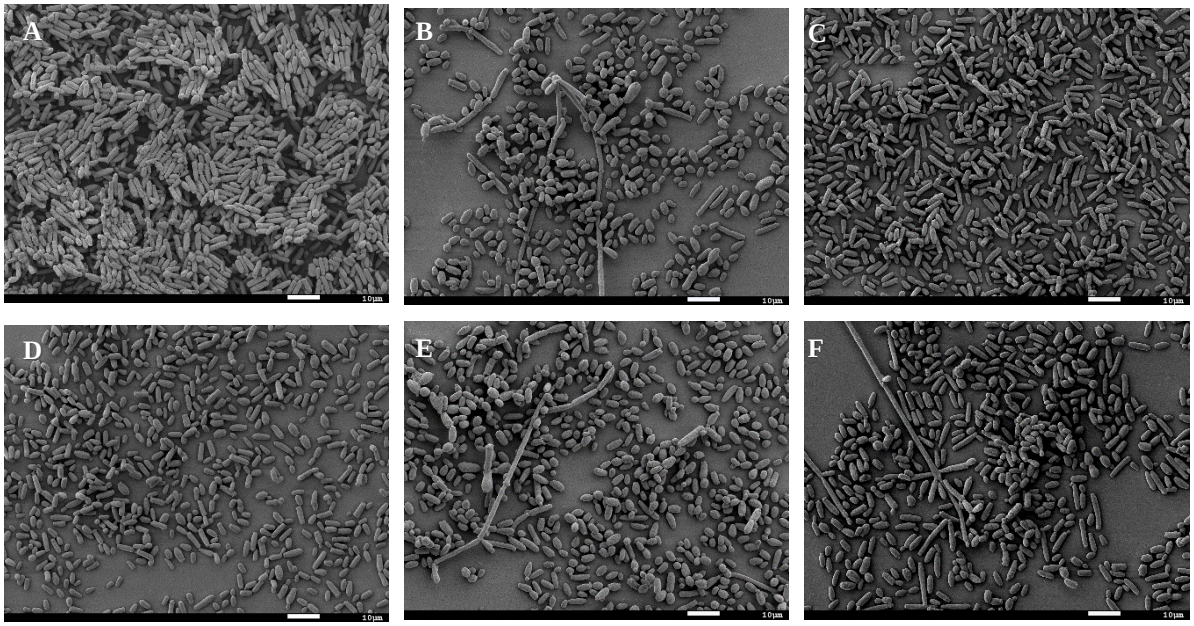


**Fig. 7.1** Scanning electron micrographs of *C. krusei* UFS Y-0277 biofilms under various treatment conditions after incubation at 37ºC for 48 h. No treatment (**A**), 32 µg/ml FLC (**B**), 0.1 mM LA (**C**), 0.1 mM GLA (**D**), FLC+LA (**E**), FLC+GLA (**F**). Scale bar represents 10 µm. **FLC**: fluconazole, **LA**: linoleic acid, **GLA**: gamma-linolenic acid, **FLC+LA**: fluconazole and linoleic acid, **FLC+GLA**: fluconazole and gamma-linolenic acid.

At higher magnifications (i.e. ×4000 and ×8000) the effect of these treatments on the ultrastructure of individual cells within the biofilm was observed. As shown in **Figure 7.2**, cells within both treated and untreated biofilms appear rough. However, extracellular vesicle (exosome or microvesicle)-like structures were visible on cells within biofilms exposed to the combination treatments. Extracellular vesicles (EVs), including exosomes, microvesicles, and apoptotic bodies, are membranous vesicles released by healthy and dying cells across the three domains of life (Gill et al. 2019; Zhao et al. 2019; Battistelli and Falcieri 2020). Extracellular vesicles are thought to play critical roles in pathogenesis, virulence, antifungal resistance, intercellular communication, host-pathogen interaction, and extracellular transport of macromolecules, such as lipids, polysaccharide, and proteins (Oliveira et al. 2010; Samuel et al. 2015; Joffe et al. 2016). More specifically, in *C. albicans*, biofilm-associated EVs secretions critical for antifungal resistance have been identified (Zarnowski et al. 2018). Additionally, Zhao and co-workers (2019) have demonstrated that EVs could protect *Saccharomyces cerevisiae* cells from the cytotoxic effect of caspofungin through cell wall remodelling or acting as decoys to antifungal molecules. Studies have reported the release of EV-like structures after exposure of yeast cells to oxidative stress inducers, such as miconazole (Nollin and Borgers 1975), allyl alcohol (Lemar et al. 2005), and oxidised lipids (Leeuw 2010). Furthermore, similar structures, *albeit* identified as protuberances and fibrillar

structures, were identified on cells within *C. albicans* and *C. dubliniensis* biofilms grown with marine PUFAs at 1 mM concentration (Thibane et al. 2010). Moreover, a follow-up study by the same authors concluded that these PUFAs exerted their antifungal effects via increased reactive oxygen species (ROS) production and induction of apoptosis (Thibane et al. 2012a). All this evidence suggests that the EVs-like vesicles observed in this study may be a response to increased oxidative stress induced by the combination treatments. Since FLC is a known inducer of oxidative stress (Arana et al. 2010; Peng et al. 2018; Dbouk et al. 2019), one would expect to see similar structures, presumably induced by increased oxidative stress, on cells treated with FLC only, however, this was not case. The possible explanation for this is that FLC alone had little or no effect on *C. krusei* biofilm, due to the yeast's intrinsic resistance to FLC.

Furthermore, as depicted below (**Fig. 7.2E**, **F**), it appeared that the combination treatments induced cell wall and plasma membrane stress, which ultimately caused cell rupture. However, this was not the case for cells treated with either of the fatty acids or FLC alone. Additionally, since unsaturated fatty acids are known inducers of oxidative stress, and are capable of promoting membrane permeability and disorganisation (Avis and Belanger 2001; Cipak et al. 2006; Thibane et al. 2010; Pohl et al. 2011). We speculated that the cell rupture observed with the combination treatments might be caused by a two-step process: an initial plasma membrane disorganisation and/or oxidative stress induced by the insertion of unsaturated fatty acid into the yeast membranes, followed by a further distortion of the plasma membrane and increased oxidative stress in the already vulnerable cells elicited by FLC.

Furthermore, although yeast cell death can be via apoptosis or necrosis, the death of subpopulation of cells within the combination-treated biofilms is more likely due to necrosis than apoptosis, this is because of the observed cell rupture and loss of intracellular components. In contrast to apoptosis, necrosis is characterised by cell swelling, disruption of membrane integrity, cell rupture, and loss of intracellular contents (Červinka and Půža 1995; Lima et al. 2002; Eisenberg et al. 2010). Moreover, studies have shown that unsaturated fatty acids can induce cell death via either of the two processes – apoptosis at low doses, and necrosis at higher concentrations (Finstad et al. 1998; Mainou-Fowler et al. 2001). Other agents, such as acriflavine (Keyhani et al. 2009), acetic acid (Ludovico et al. 2001), $H_2O_2$ (Madeo et al. 1999), and antifungal agent, amphotericin B (Phillips et al. 2003), can also trigger yeast cell death via both apoptosis and necrosis.

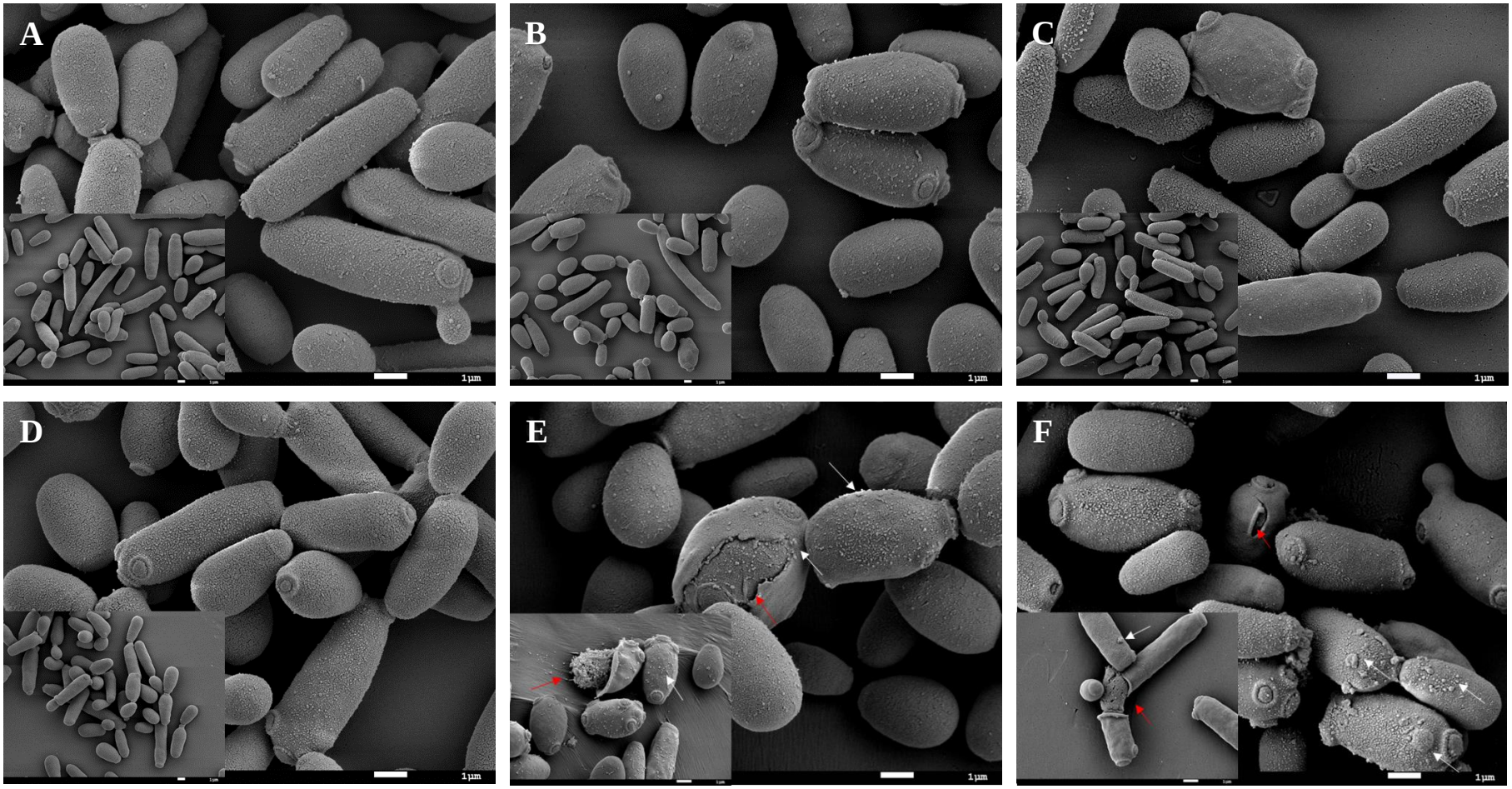


**Fig. 7.2** Scanning electron micrographs of *C. krusei* UFS Y-0277 biofilms under various treatment conditions after incubation at 37°C for 48 h (×8000). No treatment (**A**), 32 µg/ml FLC (**B**), 0.1 mM LA (**C**), 0.1 mM GLA (**D**), FLC+LA (**E**), FLC+GLA (**F**). Small panel on bottom-left corner indicates micrograph with a lower magnification (x4000). White arrows depict extracellular vesicles, while red arrows indicate damaged cell wall and membrane and/or cell rupture. Scale bar represents 1 µm. **FLC**: fluconazole, **LA**: linoleic acid, **GLA**: Gamma-linolenic acid, **FLC+LA**: fluconazole and linoleic acid, **FLC+GLA**: fluconazole and gamma-linolenic acid.

### 2.4.6 Influence of fatty acids on membrane integrity of *C. krusei*

To investigate the extent of cell membrane damage induced by various treatment groups and to further substantiate our SEM results, propidium iodide assay was performed. Propidium iodide is a membrane-impermeant nucleic acid-binding fluorescent dye, which only penetrates cells with compromised plasma membranes and emits red fluorescence upon interaction with nucleic acids (Boulos et al. 1999; Rosenberg et al. 2019). This assay was done by incubating cells, harvested from *C*. *krusei* UFS Y-0277 biofilms exposed to varying treatment conditions, with propidium iodide stain and measuring the resultant fluorescence of stained cells at excitation and emission wavelengths of 485 nm and 635 nm, respectively. As expected, a significant increase ($p < 0.05$) in fluorescence was observed with cells treated with FLC+LA in comparison to cells treated with LA only. Unexpectedly, however, there was no significant difference ($p > 0.05$) between the fluorescence of cells exposed to FLC (32 µg/ml) monotherapy and FLC+LA combination treatment (**Fig. 8A**). Similarly, as anticipated, GLA-treated cells had a significantly lower fluorescence ($p < 0.05$) compared to cells exposed to the combination of FLC and GLA. In addition, no significant difference ($p > 0.05$) was observed in the fluorescence of FLC-treated and FLC+GLA-treated cells (**Fig. 8B**). The reason for this statistically similar fluorescence ($p > 0.05$) observed for cells treated with FLC monotherapy and those treated with the combinations is unclear. However, future studies will benefit from implementing other cell membrane integrity assays, such as 7-Aminoactinomycin D (7-AAD), Trypan Blue, and ToxiLight (Ogundeji et al. 2016), to further corroborate these findings.

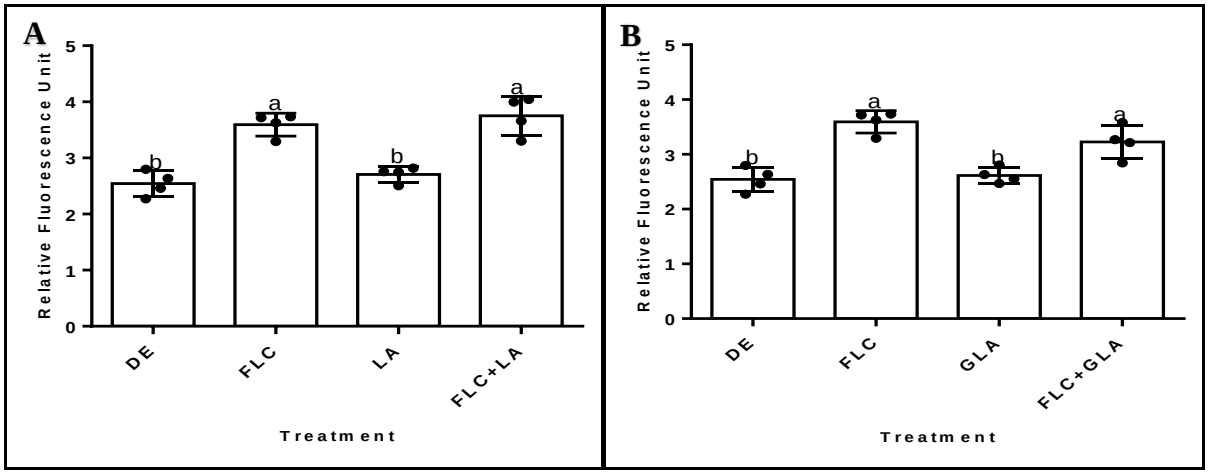


**Fig. 8** Fluorescence of *C. krusei* UFS Y-0277 cells stained with propidium iodide dye after exposure to various treatment conditions. Fluorescence of cells exposed to fluconazole in the presence or absence of LA (**A**) or GLA (**B**). The fluorescence corresponds to the quantity of dead cells and cells with damaged membranes. Values are means of four independent experiments, and error bars indicate standard deviation. *p*-value ≤ 0.05 was considered significantly different and are indicated by different letters. **DE**: DMSO+Ethanol (control), **FLC**: fluconazole, **LA**: linoleic acid, **GLA**: Gamma-linolenic acid.

The fluorescence of *C. krusei* UFS Y-0277 cells stained with propidium iodide dye after exposure to various treatment conditions was also observed with fluorescence microscopy. As depicted in **Figure 9**, cells exposed to either of the combinations accumulated more propidium iodide stain than any of the corresponding mono-treatments (i.e. fatty acid or FLC alone).

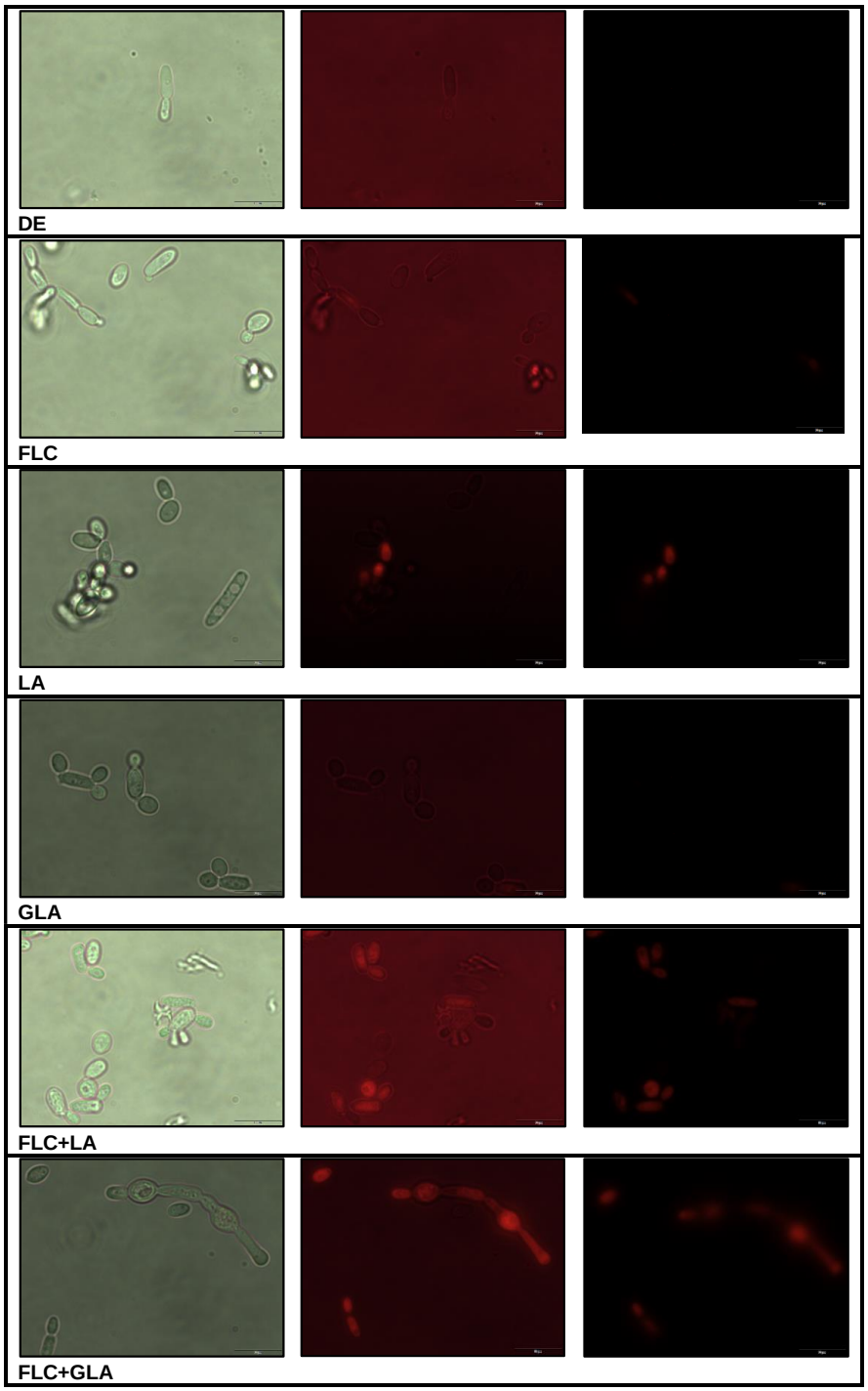


**Fig. 9** Fluorescence micrographs of *C. krusei* UFS Y-0277 cells stained with propidium iodide dye after exposure to various treatment conditions [**DE**: DMSO+Ethanol (control), **FLC**: fluconazole only, **LA**: linoleic acid only, **GLA**: gamma linolenic acid only, **FLC+LA**: combination of fluconazole and linoleic acid, **FLC+GLA**: combination of fluconazole and gamma-linolenic acid]. Left panel represents white light micrographs, Middle panel represents superimposed white light and fluorescent light micrographs, Right panel represents fluorescent light micrographs. Scale bar represents 10 µm.

### 2.4.7 Antioxidants rescue biofilm from the toxicity of combination treatments

Since we speculated induction of oxidative stress as a contributing factor responsible for the potentiating effect displayed by the combination treatments, it was important to examine the oxidative stress-inducing potential of the combination treatments in the presence and absence of known antioxidants. Our hypothesis was that if the increased susceptibility of the combination-treated biofilms was, in part, mediated by oxidative stress, the addition of antioxidants such as TPGS or BHT would offer biofilms some protective benefits. This was performed by exposing biofilms of the least-susceptible strain (*C. krusei* UFS Y-0277) to either of the combination treatments (FLC+LA or FLC+GLA) in the presence and absence of TPGS or BHT after which the biomass of the biofilms was quantified with CV assay. Notably, CV assay was used for this experiment instead of XTT assay since there is evidence that α-tocopherol (the active ingredient of TPGS) interferes with tetrazolium salt assays, such as XTT assay (Lim et al. 2015). As shown in **Figure 10A**, the addition of TPGS, but not BHT, was able to increase the biofilm biomass and rescue the biofilms from the oxidative stress effect induced by the combination of FLC and LA ($p < 0.05$). However, both TPGS and BHT rescued the biofilms from the toxic effect of the combination of FLC and GLA ($p < 0.05$) (**Fig. 10B**).

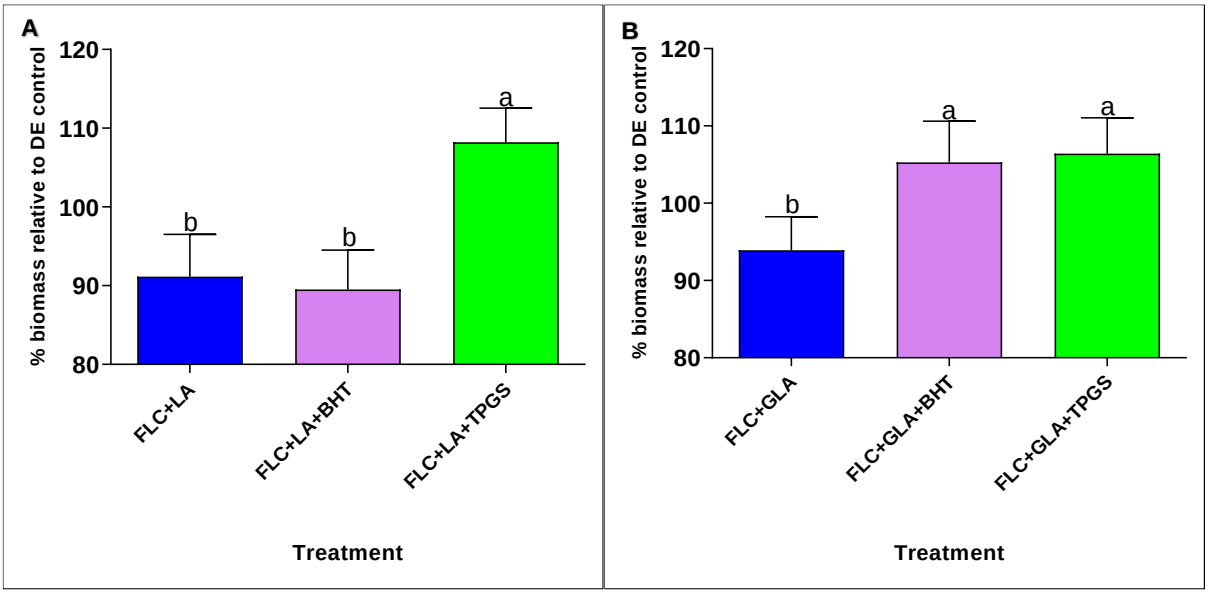


**Fig. 10** Biomass of *C. krusei* UFS Y-0277 biofilms after exposure to the combination of FLC and LA (**A**) and FLC+GLA (**B**) with or without antioxidants (BHT or TPGS). Values are means of three independent experiments and error bars indicate standard deviation. *p*-value ≤ 0.05 was considered significantly different and are indicated by different letters. **FLC+LA**: fluconazole and linoleic acid, **FLC+GLA**: fluconazole and gamma-linolenic acid, **BHT**: butylated hydroxytoluene, **TPGS**: α-tocopherol polyethylene glycol succinate.

The overall superior protection observed for TPGS compared to BHT may indicate that the combination treatments promote lipid peroxidation in the cell membrane since, unlike BHT (which is a general inhibitor of free radical-chain reactions), TPGS localises to the plasma membrane (Yin et al. 2011; Li et al. 2015; Yehye et al. 2015; Fourie 2020). Hence, this observation may suggest that the cell membrane damage observed earlier in this study is partly due to lipid peroxidation in the cell membrane. Taken together, these findings suggest oxidative stress as a contributing factor responsible for the potentiating effects of the combination treatments.

### 2.4.8 Influence of fatty acids on efflux pump activity of *C. krusei*

Drug efflux pumps belong to either ATP-Binding Cassette (ABC) family (Lubelski et al. 2007), Major Facilitator Superfamily (MFS) (Pao et al. 1998), Multidrug resistance And Toxic compound Extrusion (MATE) family (Kuroda and Tsuchiya 2009), Small Multidrug Resistance (SMR) family (Jack et al. 2001), Resistance Nodulation Division (RND) superfamily (Nikaido and Takatsuka 2009), or Drug Metabolite Transporter (DMT) superfamily (Piddock 2006; Soto 2013) of transporters. Each of these proteins functions to pump out toxic compounds, including antimicrobial agents, and their overexpression results in multidrug-resistant phenotype in pathogenic microbes (Lamping et al. 2009). In *Candida* spp., only the ABC and MFS transporters have been characterised (Wirsching et al. 2001; White et al. 2002; Cannon et al. 2009). While the MFS transporters are secondary transporters, which are powered by electrochemical proton-motive force, ABC family members are primary transporters and rely on the hydrolysis of ATP for energy (Pao et al. 1998; Cannon et al. 2009; Rees et al. 2009; Redhu et al. 2016). Additionally, although *C. krusei* possesses ABC transporters, such as Abc1p, Abc2p, Abc11p, and Abc12p (Katiyar and Edlind 2001; Lamping et al. 2009; Lamping et al. 2017; Douglass et al. 2018), no MFS transporter has been characterised in this yeast. Evidently, efflux pumps play a role in *C. krusei* resistance to FLC (Lamping et al. 2009; Lamping et al. 2017). We, therefore, hypothesised that the increased susceptibility of combination-treated biofilms might be due to the disruption of efflux pump activity. To test this hypothesis, the influence of either of the unsaturated fatty acids (LA or GLA) alone or in combination with FLC on efflux pump activity of *C. krusei* UFS Y-0277 biofilm was evaluated using Rh6G efflux assay. The fluorescent dye, Rh6G, is a substrate of efflux pump (ABC) transporters (Nakamura et al. 2001; Mukherjee et al. 2003; Tsao et al. 2009).

As depicted in **Figure 11A**, at a concentration of 0.1 mM, LA alone had a slight inhibitory influence on efflux pump activity, which was further enhanced by the combination. Interestingly, GLA (0.1 mM) alone could not inhibit the efflux of Rh6G; however, its combination with FLC significantly inhibited the activity of the efflux pumps ($p < 0.05$) (**Fig. 11C**). An unexpected, slightly reduced efflux of Rh6G was observed for treatment with FLC

only (**Fig. 11C**). This might be a result of competitive inhibition since both compounds (i.e. FLC and Rh6G) are substrates for efflux pumps (Maesaki et al. 1999; Lamping et al. 2009; Prasad et al. 2015). Strikingly, a more pronounced inhibition of efflux pump activity was observed after treatment with a higher concentration (1 mM) of the fatty acids alone or in combination with FLC (**Fig. 8B**, **D**).

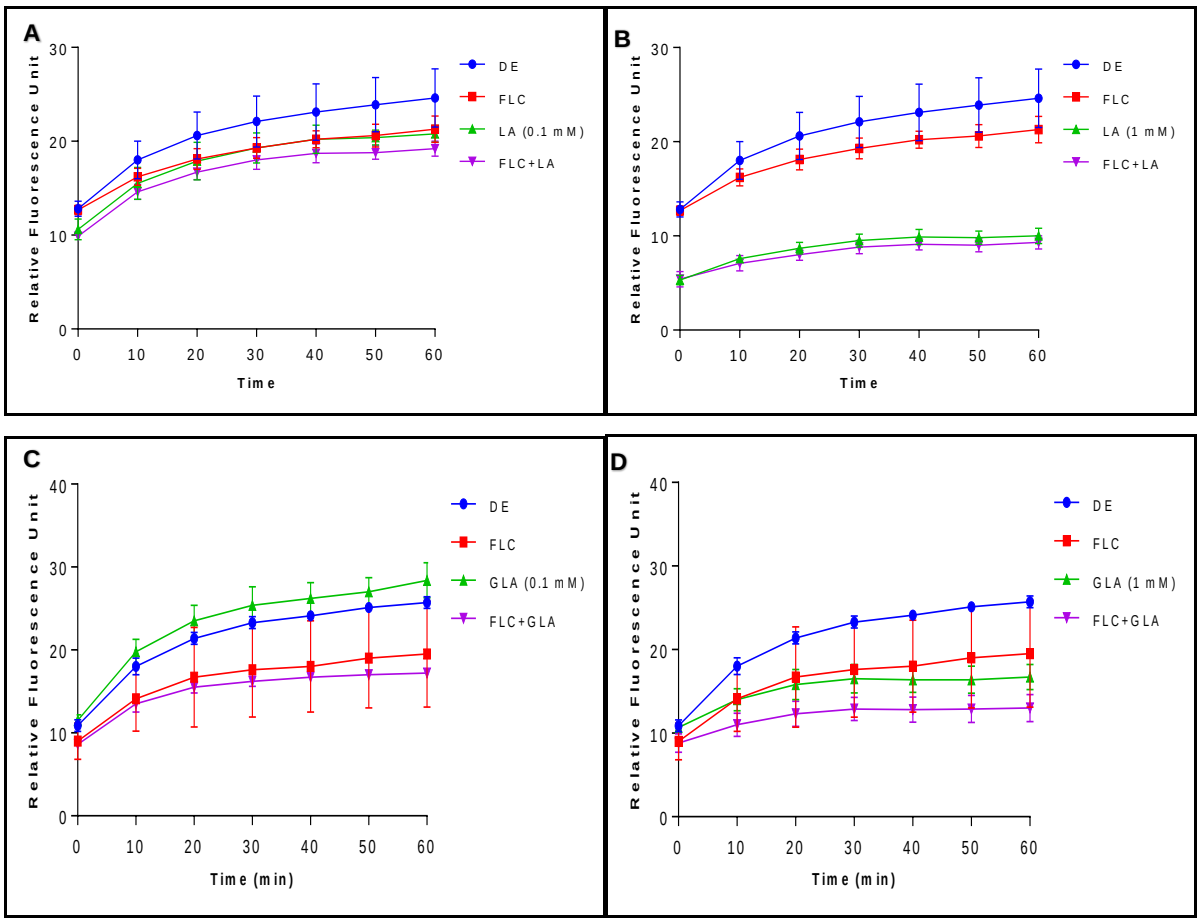


**Fig. 11** Rhodamine 6G efflux in *C. krusei* UFS Y-0277 biofilms after treatment with fluconazole in the presence or absence of 0.1 mM LA (**A**), 1 mM LA (**B**), 0.1 mM GLA (**C**) or 1 mM GLA (**D**). Values are means of three independent experiments and error bars indicate standard deviation. **DE**: DMSO+Ethanol (control), **FLC**: fluconazole, **LA**: linoleic acid, **GLA**: Gamma-linolenic acid.

Since drug efflux pumps are localised to the cell membrane, and it is known that unsaturated fatty acids could elicit cell membrane disruption (Avis and Belanger 2001; Pohl et al. 2011; Mishra et al. 2014), the observed inhibition of efflux pump activity may be due to the mislocalisation of efflux pumps, following the disruption of membrane fluidity and membrane disorganisation. Additionally, since all the presently characterised efflux pumps in *C. krusei* are ABC transporters, which hydrolyse ATP for their efflux activities (Lamping et al. 2017; Douglass et al. 2018), another factor that might have contributed to the loss of activities of the efflux pumps could be ATP deficit. This may be because antimicrobial fatty acids have been

reported to disrupt cellular processes, such as oxidative phosphorylation, which synthesise ATP essential for efflux pump activity (Galbraith and Miller 1973; Yoon et al. 2018). Similarly, a recent study of Kuloyo and co-workers (2020) has demonstrated that AA potentiates C. albicans biofilm's sensitivity to FLC via interference with ATP biosynthetic pathways.

### 2.4.9 Combination treatments prolong the lifespan of infected nematodes

Undoubtedly, *in vitro* experimental findings do not always correlate with that of *in vivo* assays. Because of this, animal models are employed not to only assess the correlation between observations generated by *in vitro* and *in vivo* assays, but to also gain insights into the mechanisms of microbial pathogenesis in humans since some virulence traits and immune reactions are only induced *in vivo* (Brenner 1974; Marsh and May 2012). Hence, to further corroborate our *in vitro* findings, we evaluated the protective effect of the combination treatments in a *C. elegans* infection model. *Caenorhabditis elegans* has been described as a powerful system for many studies, including drug discovery because unlike mammalian models, it has simple growth conditions, great ease of cultivation, a rapid life cycle, it is tractable, and its use requires no ethical clearance (Brenner 1974; Pukkila-Worley et al. 2009; Corsi et al. 2015; Madende et al. 2020). Moreover, this model also has innate immunity which overlaps with that found in humans (Pukkila-Worley et al. 2011). The use of this nematode in this study instead of a mammalian model also ensures compliance with the Russell's and Burch's 3Rs (Replacement, Reduction, and Refinement) principles which recommend the replacement of "conscious" vertebrates with "non-sentient" or "less sentient" invertebrates such as *C. elegans* and *Drosophila melanogaster* (Russell and Burch 1959; Kretlow et al. 2010; Cheluvappa et al. 2017).

For this study, *Caenorhabditis elegans* AU37 (*glp-4*(*bn2*) I; *sek-1*(*km4*) X) strain was selected because of its enhanced immune-deficiency which facilitates microbial infections due to mutation in *SEK-1* which encodes a conserved mitogen-activated protein kinase (Kim et al. 2002). Moreover, this strain cannot propagate at a temperature of 25$^{o}$C due to *GLP-4* mutation (Miyata et al. 2008). Additionally, the ability of *C. krusei* to infect and kill this *C. elegans* strain has been previously demonstrated (Scorzoni et al. 2013). Thus, the *in vivo* treatment assay was done by infecting nematodes with the least-susceptible strain of *C. krusei* (*C. krusei* UFS Y-0277). Thereafter, the infected nematodes were exposed to various treatments, including the combination treatments, and were monitored daily for survival. The survival statistical analysis and differences (log-rank test) were determined using OASIS 2 (Han et al. 2016). As depicted in **Figure 12**, in contrast to uninfected nematodes fed with *E. coli* OP50 with a median lifespan of 8.37 ± 0.14 days, infection with *C. krusei* significantly shortened the median lifespan of infected nematodes (2.83 ± 0.11 days) and resulted in a 100% mortality within five days post-infection. Although both FLC and LA singly could slightly extend the median lifespan of

infected nematodes for 3.56 days, superior protection and elongation of the lifespan of the infected nematode were observed upon treatment with FLC and LA (5.08 ± 0.19 days) (**Fig. 12A**). A previous study by Breger and co-workers (2007) has demonstrated that FLC (at 32 µg/ml) could prolong the survival of *C. albicans* and *C. parapsilosis*. However, in their study, it could not extend the survival of and had a toxic effect on nematodes exposed to a FLC-resistant strain of *C. krusei*. This is not the case in the present study, and a possible explanation for this is that its antifungal efficacy against the *C. krusei* strain used in this study outweighs its toxicity on *C. elegans*. Importantly, although GLA alone was also able to prolong the median lifespan of infected nematodes (4.06 ± 0.16 days), a more pronounced lifespan extension (median lifespan of 5.32 ± 0.20 days) was observed when *C. elegans* was exposed to the combination of FLC and GLA (**Fig. 12B**). The overall enhanced activity displayed by the combination treatments may be due to a direct antifungal effect on *C. krusei*, as observed *in vitro*. Additionally, it might be due to improved immunity and ultimate enhanced clearance of fungal infection afforded by the fatty acids, since there is evidence that endogenous and exogenous PUFAs, such as GLA and SDA, are required for *C. elegans* immunity (Nandakumar and Tan 2008). Although LA does not have a direct impact on *C. elegans* immunity, it might have been converted to GLA or SDA (following its conversion to ALA by *fat-1*) by Δ6-desaturase *fat-3* to facilitate the observed antifungal and immunoprotective effect (Watts and Browse 2002). Other studies have also reported possible links between fatty acid metabolism and immunity in this model (Lee et al. 2010; Ward et al. 2014; Anderson et al. 2019). Furthermore, a recent study by Lee and co-workers (2020) has demonstrated the ability of a medium-chain fatty acid, nonanoic acid, to prolong the survival of *C. elegans* infected with *C. albicans*.

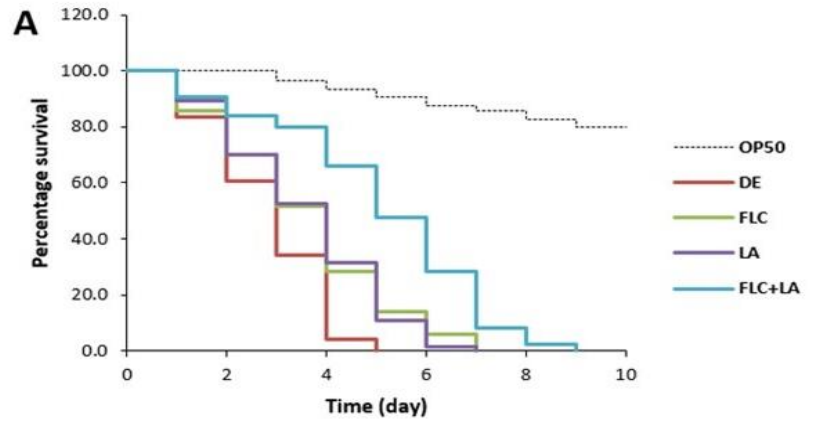


| Condition | Median lifespan (day) | S.E. | Days of 50% mortality | Days of 100% mortality | Log-rank test *P*-value (Bonferroni corrected) |
|---|---|---|---|---|---|
| **OP50** | 8.37 | 0.14 | | | <0.00001* |
| **DE** | 2.83 | 0.11 | 3 | 5 | 1.00000 |
| **FLC** | 3.56 | 0.16 | 4 | 7 | 0.00003* |
| **LA** | 3.56 | 0.14 | 4 | 7 | 0.00001* |
| **FLC+LA** | 5.08 | 0.19 | 5 | 9 | <0.00001*# |

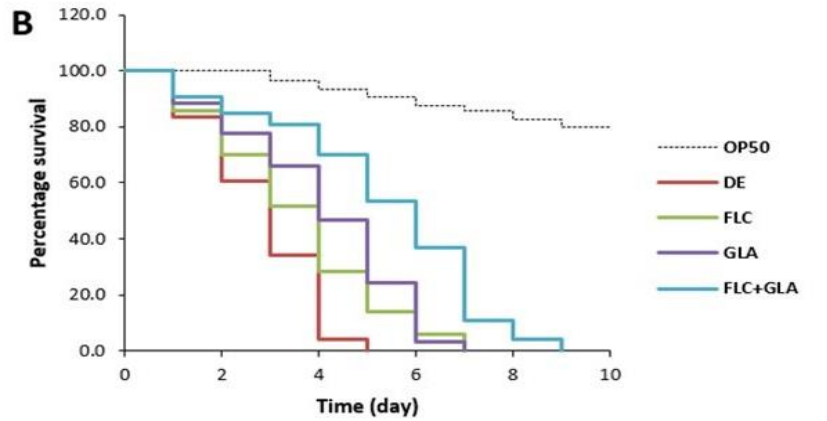


| Condition | Median lifespan (day) | S.E. | Days of 50% mortality | Days of 100% mortality | Log-rank test P-value (Bonferroni corrected) |
|---|---|---|---|---|---|
| **OP50** | 8.37 | 0.14 | | | <0.00001* |
| **DE** | 2.83 | 0.11 | 3 | 5 | 1.00000 |
| **FLC** | 3.56 | 0.16 | 4 | 7 | 0.00003* |
| **GLA** | 4.06 | 0.16 | 4 | 7 | <0.00001* |
| **FLC+GLA** | 5.32 | 0.20 | 6 | 9 | <0.00001*# |

**Fig. 12** Survival of infected *Caenorhabditis elegans* after treatment with linoleic acid (**A**) or gamma-linolenic acid (**B**) in the presence or absence of fluconazole. **OP50** represents uninfected nematodes fed with *Escherichia coli* OP50 (uninfected group). **DE** represents infected nematodes treated with DMSO and ethanol (untreated group), **FLC** represents infected nematodes exposed to fluconazole (32 µg/ml), **LA** represents infected nematodes treated with linoleic acid (0.1 mM), **GLA** represents infected nematodes exposed to gamma-linolenic acid (0.1 mM), **FLC+LA** represents infected nematodes treated with fluconazole and linoleic acid, while **FLC+GLA** represents infected nematodes exposed to the combination of fluconazole and gamma-linolenic acid. The tables depict the median lifespan along with the standard error (S.E.) as well as the post-infection days to reach 50% and 100% mortality. Log-rank test was used to assess significant differences in survival. *Significantly different from the untreated control (DE). # indicates statistical difference between the combination treatments compared to either of the single treatments (FLC, LA, or GLA). **FLC**: fluconazole, **LA**: linoleic acid, **GLA**: Gamma-linolenic acid.

### 2.4.10 Combination treatments reduce the fungal burden of infected nematodes

To further strengthen our *in vitro* findings, the yeast burden within the intestine of infected *C. elegans* after exposure to the combination treatments was assessed. This was experimentally demonstrated by exposing nematodes infected with the least-susceptible strain of *C. krusei* (*C. krusei* UFS Y-0277) to various treatments, including the combination treatments, for 24 h after which the fungal burden of each nematode was determined. Consistent with the *C. elegans* treatment assay results, FLC, GLA, and LA were able to reduce the fungal burden of infected *C. elegans* by *circa* 32%, 13%, and 11%, respectively (**Fig. 13**). However, treatments with the combination of FLC and LA or GLA profoundly reduced the yeast burden by *circa* 66% and 71%, respectively ($p < 0.05$).

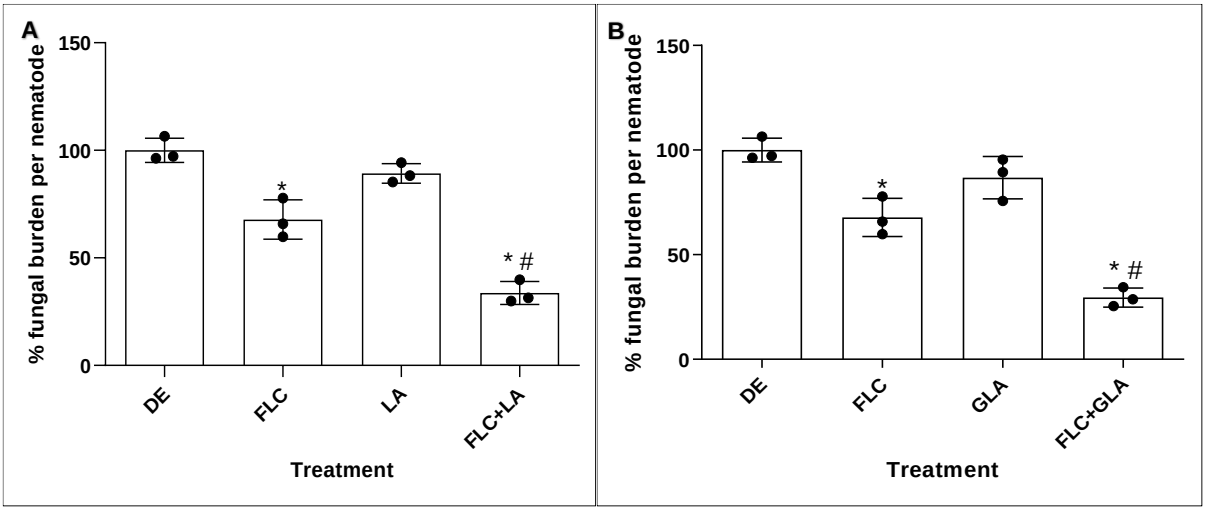


**Fig. 13** Fungal burden of infected *Caenorhabditis elegans* after treatment with linoleic acid (**A**) or gamma-linolenic acid (**B**) in the presence or absence of fluconazole. *Significantly different from the untreated group (DE). # indicates a statistical difference between the combination treatments compared to either of the monotherapies (FLC, LA, or GLA). **DE**: DMSO and ethanol (untreated group), **FLC**: fluconazole (32 µg/ml), **LA**: linoleic acid (0.1 mM), **GLA**: gamma-linolenic acid (0.1 mM), **FLC+LA** combination of fluconazole and linoleic acid, **FLC+GLA**: combination of fluconazole and gamma-linolenic acid.

Taken together, our *in vivo* findings correlate with the earlier observed *in vitro* susceptibility profiles of the combination treatments. However, one possible explanation for the overall increased antifungal efficacy displayed by all the treatments *in vivo* is that the innate immunity of infected *C. elegans* assisted with infection clearance, a phenomenon that cannot be assayed *in vitro* (Mylonakis et al. 2007; Pukkila-Worley et al. 2011).

## 2.5 Conclusions

Although *C. albicans* is the major cause of invasive candidiasis, the incidence of infections caused by NAC species, including *Candida krusei*, is on the rise. This epidemiological shift may be partly explained by the increasing resistance of NAC species to antifungal agents (Chi et al. 2011; da Silva et al. 2013; Sadeghi et al. 2018). For example, *C. krusei*, a potential multidrug-resistant NAC yeast, exhibits intrinsic resistance to FLC, with more than 97% isolates exhibiting resistance (Whaley et al. 2017), while also rapidly developing adaptive resistance to other antifungal drugs, including the echinocandins (Forastiero et al. 2015). The combination of antifungal agents with non-antimicrobial agents, including phytocompounds and fatty acids, has been receiving considerable attention as a potential infection control strategy, especially for drug-resistant fungal infections. Moreover, PUFAs, such as AA and SDA, have been shown to increase the sensitivity of *C. albicans* and *C. dubliniensis* biofilms to conventional antifungal drugs, including FLC, clotrimazole, and amphotericin B (Ells et al. 2009; Thibane et al. 2012b; Mishra et al. 2014). Several mechanisms, such as increased oxidative stress, disruption of membrane organisation, and inhibition of drug efflux pumps have been speculated to be involved in this phenomenon (McDonough et al. 2002; Ells et al. 2009; Thibane et al. 2012b).

The results of this present study demonstrate that either of two unsaturated fatty acid (LA or GLA) potentiates the susceptibility of the biofilm of the least-susceptible strain of *C. krusei* to FLC *in vitro* as observed by XTT and SEM assays. The *in vitro* underlying mechanisms of action of these combination treatments were demonstrated to be through damage to the cell wall and membrane. Additionally, the inhibition of efflux pump activity, following the disruption of membrane organisation, and induction of oxidative stress are suspected as complementary mechanisms responsible for this potentiating activity. Furthermore, due to the observed cell rupture and loss of intracellular contents, death following exposure of cells to the combination treatments might be due to necrosis. However, the occurrence of apoptosis following oxidative damage amongst subpopulation of cells within the combination-treated biofilms cannot be dismissed, since such insult could be inflicted by both unsaturated fatty acids (Finstad et al. 1998; Mainou-Fowler et al. 2001; Thibane et al. 2012a) and FLC (Peng et al. 2018; Dbouk et al. 2019). Further, our *in vivo* findings in a *C. elegans* model suggest that the combination treatments could prolong the overall survival and reduce the intestinal fungal burden of nematodes infected with *C. krusei*. This study demonstrates, for the first time, the potentiating activity of unsaturated fatty acids (LA or GLA) with FLC against intrinsically-resistant *C. krusei* *in vitro* and *in vivo* in a *C. elegans* infection model. However, future research would investigate if such activity is conserved amongst other notoriously recalcitrant fungal species, including

*C. auris* and *C. glabrata*, and should consider dissecting the specific mechanisms responsible for the antifungal effects of these combinations in the *C. elegans* infection model.

## 2.6 References


Ak T, Gülçin I (2008) Antioxidant and radical scavenging properties of curcumin. Chemico-biological interactions 174:27–37. https://doi.org/10.1016/j.cbi.2008.05.003

Al-Fattani MA, Douglas LJ (2006) Biofilm matrix of *Candida albicans* and *Candida tropicalis*: Chemical composition and role in drug resistance. Journal of Medical Microbiology 55:999–1008. https://doi.org/10.1099/jmm.0.46569-0

Alnuaimi AD, O'Brien-Simpson NM, Reynolds EC, McCullough MJ (2013) Clinical isolates and laboratory reference *Candida* species and strains have varying abilities to form biofilms. FEMS Yeast Research 13:689–699. https://doi.org/10.1111/1567-1364.12068

Anderson SM, Cheesman HK, Peterson ND, et al (2019) The fatty acid oleate is required for innate immune activation and pathogen defense in *Caenorhabditis elegans*. PLoS Pathogens 15:e1007893. https://doi.org/10.1371/journal.ppat.1007893

Andriole VT (2000) Current and future antifungal therapy: new targets for antifungal therapy. International Journal of Antimicrobial Agents 16:317–321. https://doi.org/10.1016/s0924-8579(00)00258-2

Arana DM, Nombela C, Pla J (2010) Fluconazole at subinhibitory concentrations induces the oxidative- and nitrosative-responsive genes *TRR1*, *GRE2* and *YHB1*, and enhances the resistance of *Candida albicans* to phagocytes. Journal of Antimicrobial Chemotherapy 65:54–62. https://doi.org/10.1093/jac/dkp407

Arendrup MC, Perlin DS (2014) Echinocandin resistance. Current Opinion in Infectious Diseases 27:484–492. https://doi.org/10.1097/qco.0000000000000111

Avis TJ, Belanger RR (2001) Specificity and mode of action of the antifungal fatty acid cis-9-heptadecenoic acid produced by *Pseudozyma flocculosa*. Applied and Environmental Microbiology 67:956–960. https://doi.org/10.1128/aem.67.2.956-960.2001

Bae YS, Rhee MS (2019) Short-term antifungal treatments of caprylic acid with carvacrol or thymol induce synergistic 6-log reduction of pathogenic *Candida albicans* by cell membrane disruption and efflux pump inhibition. Cellular Physiology and Biochemistry 53:285–300. https://doi.org/10.33594/000000139

Baillie GS, Douglas LJ (2000) Matrix polymers of *Candida* biofilms and their possible role in biofilm resistance to antifungal agents. Journal of Antimicrobial Chemotherapy 46:397–403. https://doi.org/10.1093/jac/46.3.397

Battistelli M, Falcieri E (2020) Apoptotic bodies: Particular extracellular vesicles involved in intercellular communication. Biology 9:21. https://doi.org/10.3390/biology9010021

Beavers WN, Monteith AJ, Amarnath V, et al (2019) Arachidonic acid kills *Staphylococcus aureus* through a lipid peroxidation mechanism. mBio 10: e01333-19 https://doi.org/10.1128/mbio.01333-19

Boulos L, Prévost M, Barbeau B, et al (1999) LIVE/DEAD® BacLight™: Application of a new rapid staining method for direct enumeration of viable and total bacteria in drinking water. Journal of Microbiological Methods 37:77–86. https://doi.org/10.1016/s0167-7012(99)00048-2

Breger J, Fuchs BB, Aperis G, et al (2007) Antifungal chemical compounds identified using a *C. elegans* pathogenicity assay. PLoS Pathogens 3:e18. https://doi.org/10.1371/journal.ppat.0030018

Brenner S (1974) The genetics of *Caenorhabditis elegans*. Genetics 77:71–94

Cannon RD, Lamping E, Holmes AR, et al (2009) Efflux-mediated antifungal drug resistance. Clinical Microbiology Reviews 22:291–321. https://doi.org/10.1128/cmr.00051-08

Carradori S, Chimenti P, Fazzari M, et al (2016) Antimicrobial activity, synergism and inhibition of germ tube formation by *Crocus sativus*-derived compounds against *Candida* spp. Journal of Enzyme Inhibition and Medicinal Chemistry 31:189–193. https://doi.org/10.1080/14756366.2016.1180596

Červinka M, Půža V (1995) Cellular and molecular stress regulation and apoptosis - apoptosis and necrosis: Dynamics of structural changes in cells cultivated *in vitro* after treatment with xenobiotics. Toxicology *in Vitro* 4:387–396

Chanda W, Joseph TP, Guo X, et al (2018) Effectiveness of omega-3 polyunsaturated fatty acids against microbial pathogens. Journal of Zhejiang University-SCIENCE B 19:253–262. https://doi.org/10.1631/jzus.b1700063

Chang YL, Yu SJ, Heitman J, et al (2017) New facets of antifungal therapy. Virulence 8:222–236. https://doi.org/10.1080/21505594.2016.1257457

Cheluvappa R, Scowen P, Eri R (2017) Ethics of animal research in human disease remediation, its institutional teaching; and alternatives to animal experimentation. Pharmacology Research & Perspectives 5:e00332. https://doi.org/10.1002/prp2.332

Chi HW, Yang YS, Shang ST, et al (2011) *Candida albicans* versus non-*albicans* bloodstream infections: The comparison of risk factors and outcome. Journal of Microbiology, Immunology and Infection 44:369–375. https://doi.org/10.1016/j.jmii.2010.08.010

Cipak A, Hasslacher M, Tehlivets O, et al (2006) *Saccharomyces cerevisiae* strain expressing a plant fatty acid desaturase produces polyunsaturated fatty acids and is susceptible to oxidative stress induced by lipid peroxidation. Free Radical Biology and Medicine 40:897–906. https://doi.org/10.1016/j.freeradbiomed.2005.10.039

Corsi AK, Wightman B, Chalfie M (2015) A transparent window into biology: A primer on *Caenorhabditis elegans*. Genetics 200:387–407. https://doi.org/10.1534/genetics.115.176099

Corte L, Casagrande Pierantoni D, Tascini C, et al (2019) Biofilm specific activity: A measure to quantify microbial biofilm. Microorganisms 7:73. https://doi.org/10.3390/microorganisms7030073

Costa CR, Souza LKH e, Ataídes FS, et al (2011) Molecular analysis and dimorphism of azole-susceptible and resistant *Candida albicans* isolates. Revista da Sociedade Brasileira de Medicina Tropical 44:740–744. https://doi.org/10.1590/s0037-86822011005000056

Costa-Orlandi C, Sardi J, Pitangui N, et al (2017) Fungal biofilms and polymicrobial diseases. Journal of Fungi 3:22. https://doi.org/10.3390/jof3020022

da Silva CR, de Andrade Neto JB, Sidrim JJC, et al (2013) Synergistic effects of amiodarone and fluconazole on *Candida tropicalis* resistant to fluconazole. Antimicrobial Agents and Chemotherapy 57:1691–1700. https://doi.org/10.1128/aac.00966-12

Dbouk NH, Covington MB, Nguyen K, Chandrasekaran S (2019) Increase of reactive oxygen species contributes to growth inhibition by fluconazole in *Cryptococcus neoformans*. BMC Microbiology 19:243 https://doi.org/10.1186/s12866-019-1606-4

Desai JV, Mitchell AP, Andes DR (2014) Fungal biofilms, drug resistance, and recurrent infection. Cold Spring Harbor Perspectives in Medicine 4:a019729–a019729. https://doi.org/10.1101/cshperspect.a019729

Douglass AP, Offei B, Braun-Galleani S, et al (2018) Population genomics shows no distinction between pathogenic *Candida krusei* and environmental *Pichia kudriavzevii*: One species, four names. PLoS Pathogens 14:e1007138. https://doi.org/10.1371/journal.ppat.1007138

Eisenberg T, Carmona-Gutierrez D, Büttner S, et al (2010) Necrosis in yeast. Apoptosis 15:257–268. https://doi.org/10.1007/s10495-009-0453-4

Eldesouky HE, Mayhoub A, Hazbun TR, Seleem MN (2018) Reversal of azole resistance in *Candida albicans* by sulfa antibacterial drugs. Antimicrobial Agents and Chemotherapy 62: e00701-17. https://doi.org/10.1128/AAC.00701-17

Eldesouky HE, Salama EA, Lanman NA, et al (2020) Potent synergistic interactions between lopinavir and azole antifungal drugs against emerging multidrug-resistant *Candida auris*. Antimicrobial Agents and Chemotherapy 65:e00684-20. https://doi.org/10.1128/aac.00684-20

Ells R, Kemp G, Albertyn J, et al (2013) Phenothiazine is a potent inhibitor of prostaglandin $E_2$ production by *Candida albicans* biofilms. FEMS Yeast Research 13:849–855. https://doi.org/10.1111/1567-1364.12093

Ells R, Kock JLF, Van Wyk PWJ, et al (2009) Arachidonic acid increases antifungal susceptibility of *Candida albicans* and *Candida dubliniensis*. Journal of Antimicrobial Chemotherapy 63:124–128. https://doi.org/10.1093/jac/dkn446

Falci DR, Pasqualotto A (2013) Profile of isavuconazole and its potential in the treatment of severe invasive fungal infections. Infection and Drug Resistance 22:163–74. https://doi.org/10.2147/idr.s51340

Finkel JS, Mitchell AP (2011) Genetic control of *Candida albicans* biofilm development. Nature Reviews Microbiology 9:109–118. https://doi.org/10.1038/nrmicro2475

Finstad H, Myhrstad MW, Heimli H, et al (1998) Multiplication and death-type of leukemia cell lines exposed to very long-chain polyunsaturated fatty acids. Leukemia 12:921–929. https://doi.org/10.1038/sj.leu.2401030

Forastiero A, Garcia-Gil V, Rivero-Menendez O, et al (2015) Rapid development of *Candida krusei* echinocandin resistance during caspofungin therapy. Antimicrobial Agents and Chemotherapy 59:6975–6982. https://doi.org/10.1128/aac.01005-15

Fourie R (2020) Investigating the influence of arachidonic acid on *Candida albicans* and its interaction with *Pseudomonas aeruginosa*. Ph.D. Thesis, University of the Free State, Bloemfontein, South Africa

Fukuoka T, Johnston DA, Winslow CA, et al (2003) Genetic basis for differential activities of fluconazole and voriconazole against *Candida krusei*. Antimicrobial Agents and Chemotherapy 47:1213–1219. https://doi.org/10.1128/aac.47.4.1213-1219.2003

Galbraith H, Miller TB (1973) Effect of long chain fatty acids on bacterial respiration and amino acid uptake. Journal of Applied Bacteriology 36:659–675. https://doi.org/10.1111/j.1365-2672.1973.tb04151.x

Gill S, Catchpole R, Forterre P (2019) Extracellular membrane vesicles in the three domains of life and beyond. FEMS Microbiology Reviews 43:273–303. https://doi.org/10.1093/femsre/fuy042

Grant SM, Clissold SP (1990) Fluconazole. Drugs 39:877–916. https://doi.org/10.2165/00003495-199039060-00006

Greenway DLA, Dyke KGH (1979) Mechanism of the inhibitory action of linoleic acid on the growth of *Staphylococcus aureus*. Journal of General Microbiology 115:233–245. https://doi.org/10.1099/00221287-115-1-233

Gulati M, Lohse MB, Ennis CL, et al (2018) *In vitro* culturing and screening of *Candida albicans* biofilms. Current Protocols in Microbiology 50:e60. https://doi.org/10.1002/cpmc.60

Ha KC, White TC (1999) Effects of azole antifungal drugs on the transition from yeast cells to hyphae in susceptible and resistant isolates of the pathogenic yeast *Candida albicans*. Antimicrobial Agents and Chemotherapy 43:763–768

Hacioglu M, Birteksoz Tan AS, Dosler S, et al (2018) *In vitro* activities of antifungals alone and in combination with tigecycline against *Candida albicans* biofilms. PeerJ 6:e5263. https://doi.org/10.7717/peerj.5263

Han SK, Lee D, Lee H, et al (2016) OASIS 2: Online application for survival analysis 2 with features for the analysis of maximal lifespan and healthspan in aging research. Oncotarget 7:56147–56152. https://doi.org/10.18632/oncotarget.11269

Henry KW, Nickels JT, Edlind TD (2000) Upregulation of *ERG* genes in *Candida* species by

azoles and other sterol biosynthesis inhibitors. Antimicrobial Agents and Chemotherapy 44:2693–2700. https://doi.org/10.1128/aac.44.10.2693-2700.2000

Huang CB, Ebersole JL (2010) A novel bioactivity of omega-3 polyunsaturated fatty acids and their ester derivatives. Molecular Oral Microbiology 25:75–80. https://doi.org/10.1111/j.2041-1014.2009.00553.x

Jack DL, Yang NM, H. Saier M (2001) The drug/metabolite transporter superfamily. European Journal of Biochemistry 268:3620–3639. https://doi.org/10.1046/j.1432-1327.2001.02265.x

Jin Y, Yip HK, Samaranayake YH, et al (2003) Biofilm-forming ability of *Candida albicans* is unlikely to contribute to high levels of oral yeast carriage in cases of human immunodeficiency virus infection. Journal of Clinical Microbiology 41:2961–2967. https://doi.org/10.1128/jcm.41.7.2961-2967.2003

Joffe LS, Nimrichter L, Rodrigues ML, Del Poeta M (2016) Potential roles of fungal extracellular vesicles during infection. mSphere 1:e00099-16 https://doi.org/10.1128/msphere.00099-16

Kabara JJ, Swieczkowski DM, Conley AJ, Truant JP (1972) Fatty acids and derivatives as antimicrobial agents. Antimicrobial Agents and Chemotherapy 2:23–28. https://doi.org/10.1128/aac.2.1.23

Kabir MA, Ahmad Z (2013) *Candida* infections and their prevention. ISRN Preventive Medicine 2013:1–13. https://doi.org/10.5402/2013/763628

Katiyar SK, Edlind TD (2001) Identification and expression of multidrug resistance related ABC transporter genes in *Candida krusei*. Medical Mycology 39:109–116. doi: 10.1080/mmy.39.1.109.116

Keyhani E, Khavari-Nejad S, Keyhani J, Attar F (2009) Acriflavine-mediated apoptosis and necrosis in yeast *Candida utilis*. Annals of the New York Academy of Sciences 1171:284–291. https://doi.org/10.1111/j.1749-6632.2009.04682.x

Kim DH, Feinbaum R, Alloing G, et al (2002) A conserved p38 MAP kinase pathway in *Caenorhabditis elegans* innate immunity. Science 297:623–626. https://doi.org/10.1126/science.1073759

Kim HS, Ham SY, Jang Y, et al (2019) Linoleic acid, a plant fatty acid, controls membrane

biofouling via inhibition of biofilm formation. Fuel 253:754–761. https://doi.org/10.1016/j.fuel.2019.05.064

Kim YG, Lee JH, Park JG, Lee J (2020) Inhibition of *Candida albicans* and *Staphylococcus aureus* biofilms by centipede oil and linoleic acid. Biofouling 36:126–137. https://doi.org/10.1080/08927014.2020.1730333

Kretlow A, Butzke D, Goetz ME, et al (2010) Implementation and enforcement of the 3Rs principle in the field of transgenic animals used for scientific purposes. Report and recommendations of the BfR expert workshop, May 18-20, 2009, Berlin, Germany. ALTEX 27:117–134

Kuhn DM, Balkis M, Chandra J, et al (2003) Uses and limitations of the XTT assay in studies of *Candida* growth and metabolism. Journal of Clinical Microbiology 41:506–508. https://doi.org/10.1128/jcm.41.1.506-508.2003

Kuhn DM, George T, Chandra J, et al (2002) Antifungal susceptibility of *Candida* biofilms: Unique efficacy of amphotericin B lipid formulations and echinocandins. Antimicrobial Agents and Chemotherapy 46:1773–1780. https://doi.org/10.1128/aac.46.6.1773-1780.2002

Kullberg BJ, Arendrup MC (2015) Invasive candidiasis. New England Journal of Medicine 373:1445–1456. https://doi.org/10.1056/nejmra1315399

Kuloyo O, Fourie R, Cason E, et al (2020) Transcriptome analyses of *Candida albicans* biofilms, exposed to arachidonic acid and fluconazole, indicates potential drug targets. G3 (Bethesda, Md) 10:3099–3108. https://doi.org/10.1534/g3.120.401340

Kuloyo OO (2020) Investigation into the mechanism of arachidonic acid increased fluconazole susceptibility in *Candida albicans* biofilms and application to drug repurposing. Ph.D. Thesis, University of the Free State, Bloemfontein, South Africa

Kuroda T, Tsuchiya T (2009) Multidrug efflux transporters in the MATE family. Biochimica et Biophysica Acta (BBA) - Proteins and Proteomics 1794:763–768. https://doi.org/10.1016/j.bbapap.2008.11.012

Lamping E, Ranchod A, Nakamura K, et al (2009) Abc1p is a multidrug efflux transporter that tips the balance in favor of innate azole resistance in *Candida krusei*. Antimicrobial Agents and Chemotherapy 53:354–369. https://doi.org/10.1128/aac.01095-08

Lamping E, Zhu J, Niimi M, Cannon RD (2017) Role of ectopic gene conversion in the evolution of a *Candida krusei* pleiotropic drug resistance transporter family. Genetics 205:1619–1639. https://doi.org/10.1534/genetics.116.194811

Lee JH, Kim YG, Khadke SK, Lee J (2020) Antibiofilm and antifungal activities of medium-chain fatty acids against *Candida albicans* via mimicking of the quorum-sensing molecule farnesol. Microbial Biotechnology. https://doi.org/10.1111/1751-7915.13710

Lee JH, Kim YG, Park JG, Lee J (2017) Supercritical fluid extracts of *Moringa oleifera* and their unsaturated fatty acid components inhibit biofilm formation by *Staphylococcus aureus*. Food Control 80:74–82. https://doi.org/10.1016/j.foodcont.2017.04.035

Lee KZ, Kniazeva M, Han M, et al (2010) The fatty acid synthase *fasn-1* acts upstream of WNK and Ste20/GCK-VI kinases to modulate antimicrobial peptide expression in *C. elegans* epidermis. Virulence 1:113–122. https://doi.org/10.4161/viru.1.3.10974

Lees ND, Broughton MC, Sanglard D, Bard M (1990) Azole susceptibility and hyphal formation in a cytochrome P-450-deficient mutant of *Candida albicans*. Antimicrobial Agents and Chemotherapy 34:831–836. https://doi.org/10.1128/aac.34.5.831

Leeuw NJ (2010) The influence of oxidized oils on fungal growth and lipid utilization. Ph.D. Thesis, University of the Free State, Bloemfontein, South Africa

Lemar KM, Passa O, Aon M, et al (2005) Allyl alcohol and garlic (*Allium sativum*) extract produce oxidative stress in *Candida albicans*. Microbiology 151:3257–3265. https://doi.org/10.1099/mic.0.28095-0

Leroy O, Gangneux JP, Montravers P, et al (2009) Epidemiology, management, and risk factors for death of invasive *Candida* infections in critical care: A multicenter, prospective, observational study in France (2005–2006). Critical Care Medicine 37:1612–1618. https://doi.org/10.1097/ccm.0b013e31819efac0

Li L, Naseem S, Sharma S, Konopka JB (2015) Flavodoxin-like proteins protect *Candida albicans* from oxidative stress and promote virulence. PLoS Pathogens 11:e1005147. https://doi.org/10.1371/journal.ppat.1005147

Lim SW, Loh HS, Ting KN, et al (2015) Reduction of MTT to purple formazan by vitamin E isomers in the absence of cells. Tropical Life Sciences Research 26:111–20

Lima TM, Kanunfre CC, Pompéia C, et al (2002) Ranking the toxicity of fatty acids on Jurkat

and Raji cells by flow cytometric analysis. Toxicology *in Vitro* 16:741–747. https://doi.org/10.1016/s0887-2333(02)00095-4

Lubelski J, Konings WN, Driessen AJM (2007) Distribution and physiology of ABC-type transporters contributing to multidrug resistance in bacteria. Microbiology and Molecular Biology Reviews 71:463–476. https://doi.org/10.1128/mmbr.00001-07

Ludovico P, Leão C, Sousa MJ, et al (2001) *Saccharomyces cerevisiae* commits to a programmed cell death process in response to acetic acid. Microbiology 147:2409–2415. https://doi.org/10.1099/00221287-147-9-2409

Madende M, Albertyn J, Sebolai O, Pohl CH (2020) *Caenorhabditis elegans* as a model animal for investigating fungal pathogenesis. Medical Microbiology and Immunology 209:1–13. https://doi.org/10.1007/s00430-019-00635-4

Madeo F, Fröhlich E, Ligr M, et al (1999) Oxygen stress: A regulator of apoptosis in yeast. Journal of Cell Biology 145:757–767. https://doi.org/10.1083/jcb.145.4.757

Maesaki S, Marichal P, Bossche HV, et al (1999) Rhodamine 6G efflux for the detection of *CDR1*-overexpressing azole-resistant *Candida albicans* strains. Journal of Antimicrobial Chemotherapy 44:27–31. https://doi.org/10.1093/jac/44.1.27

Mah TFC, O'Toole GA (2001) Mechanisms of biofilm resistance to antimicrobial agents. Trends in Microbiology 9:34–39. https://doi.org/10.1016/s0966-842x(00)01913-2

Mainou-fowler T, Proctor SJ, Dickinson AM (2001) γ-linolenic acid induces apoptosis in B-chronic lymphocytic leukaemia Cells *in vitro*. Leukemia & Lymphoma 40:393–403. https://doi.org/10.3109/10428190109057939

Manoharan RK, Lee JH, Kim YG, et al (2017) Inhibitory effects of the essential oils α-longipinene and linalool on biofilm formation and hyphal growth of *Candida albicans*. Biofouling 33:143–155. https://doi.org/10.1080/08927014.2017.1280731

Marsh EK, May RC (2012) *Caenorhabditis elegans*, a model organism for investigating immunity. Applied and Environmental Microbiology 78:2075–2081. https://doi.org/10.1128/aem.07486-11

McDonough V, Stukey J, Cavanagh T (2002) Mutations in erg4 affect the sensitivity of *Saccharomyces cerevisiae* to medium-chain fatty acids. Biochimica et Biophysica Acta (BBA) - Molecular and Cell Biology of Lipids 1581:109–118.

https://doi.org/10.1016/s1388-1981(02)00127-0

Mishra NN, Ali S, Shukla PK (2014) Arachidonic acid affects biofilm formation and $PGE_2$ level in *Candida albicans* and non-*albicans* species in presence of subinhibitory concentration of fluconazole and terbinafine. The Brazilian Journal of Infectious Diseases 18:287–293. https://doi.org/10.1016/j.bjid.2013.09.006

Miyata S, Begun J, Troemel ER, Ausubel FM (2008) DAF-16-dependent suppression of immunity during reproduction in *Caenorhabditis elegans*. Genetics 178:903–918. https://doi.org/10.1534/genetics.107.083923

Mukherjee PK, Chandra J, Kuhn DM, Ghannoum MA (2003) Mechanism of fluconazole resistance in *Candida albicans* biofilms: Phase-specific role of efflux pumps and membrane sterols. Infection and Immunity 71:4333–4340. https://doi.org/10.1128/iai.71.8.4333-4340.2003

Muthamil S, Prasath KG, Priya A, et al (2020) Global proteomic analysis deciphers the mechanism of action of plant derived oleic acid against *Candida albicans* virulence and biofilm formation. Scientific Reports 10:1–17. https://doi.org/10.1038/s41598-020-61918-y

Mylonakis E, Casadevall A, Ausubel FM (2007) Exploiting amoeboid and non-vertebrate animal model systems to study the virulence of human pathogenic fungi. PLoS Pathogens 3:e101. https://doi.org/10.1371/journal.ppat.0030101

Nakamura K, Niimi M, Niimi K, et al (2001) Functional expression of *Candida albicans* drug efflux pump Cdr1p in a *Saccharomyces cerevisiae* strain deficient in membrane transporters. Antimicrobial Agents and Chemotherapy 45:3366–3374. https://doi.org/10.1128/aac.45.12.3366-3374.2001

Nandakumar M, Tan MW (2008) Gamma-linolenic and stearidonic acids are required for basal immunity in *Caenorhabditis elegans* through their effects on p38 MAP kinase activity. PLoS Genetics 4:e1000273. https://doi.org/10.1371/journal.pgen.1000273

Nikaido H, Takatsuka Y (2009) Mechanisms of RND multidrug efflux pumps. Biochimica et Biophysica Acta (BBA) - Proteins and Proteomics 1794:769–781. https://doi.org/10.1016/j.bbapap.2008.10.004

Nollin SD, Borgers M (1975) Scanning electron microscopy of *Candida albicans* after *in vitro* treatment with miconazole. Antimicrobial Agents and Chemotherapy 7:704–711.

https://doi.org/10.1128/AAC.7.5.704

O'Toole GA (2011) Microtiter dish biofilm formation assay. Journal of Visualized Experiments. https://doi.org/10.3791/2437

Odds FC, Cockayne A, Hayward J, Abbott AB (1985) Effects of imidazole- and triazole-derivative antifungal compounds on the growth and morphological development of *Candida albicans* hyphae. Microbiology 131:2581–2589. https://doi.org/10.1099/00221287-131-10-2581

Ogundeji AO, Pohl CH, Sebolai OM (2016) Repurposing of aspirin and ibuprofen as candidate anti-*Cryptococcus* drugs. Antimicrobial Agents and Chemotherapy 60:4799–4808. https://doi.org/10.1128/AAC.02810-15

Oliveira DL, Nakayasu ES, Joffe LS, et al (2010) Characterization of yeast extracellular vesicles: Evidence for the participation of different pathways of cellular traffic in vesicle biogenesis. PLoS ONE 5:e11113. https://doi.org/10.1371/journal.pone.0011113

Orozco AS, Higginbotham LM, Hitchcock CA, et al (1998) Mechanism of fluconazole resistance in *Candida krusei*. Antimicrobial Agents and Chemotherapy 42:2645–2649. https://doi.org/10.1128/aac.42.10.2645

Pao SS, Paulsen IT, Saier MH (1998) Major facilitator superfamily. Microbiology and molecular biology reviews: MMBR 62:1–34

Pappas PG, Kauffman CA, Andes DR, et al (2016) Executive summary: Clinical practice guideline for the management of candidiasis: 2016 update by the Infectious Diseases Society of America. Clinical Infectious Diseases 62:409–417. https://doi.org/10.1093/cid/civ1194

Peeters E, Nelis HJ, Coenye T (2008) Comparison of multiple methods for quantification of microbial biofilms grown in microtiter plates. Journal of Microbiological Methods 72:157–165. https://doi.org/10.1016/j.mimet.2007.11.010

Peng CA, Gaertner AAE, Henriquez SA, et al (2018) Fluconazole induces ROS in *Cryptococcus neoformans* and contributes to DNA damage *in vitro*. PLoS ONE 13:e0208471. https://doi.org/10.1371/journal.pone.0208471

Pfaller MA, Diekema DJ (2007) Epidemiology of invasive candidiasis: A persistent public health problem. Clinical Microbiology Reviews 20:133–163.

https://doi.org/10.1128/cmr.00029-06

Phillips AJ, Sudbery I, Ramsdale M (2003) Apoptosis induced by environmental stresses and amphotericin B in *Candida albicans*. Proceedings of the National Academy of Sciences of the United States of America 100:14327–14332. https://doi.org/10.1073/pnas.2332326100

Piddock LJV (2006) Clinically relevant chromosomally encoded multidrug resistance efflux pumps in bacteria. Clinical Microbiology Reviews 19:382–402. https://doi.org/10.1128/cmr.19.2.382-402.2006

Pitts B, Hamilton MA, Zelver N, Stewart PS (2003) A microtiter-plate screening method for biofilm disinfection and removal. Journal of Microbiological Methods 54:269–276. https://doi.org/10.1016/s0167-7012(03)00034-4

Pohl CH, Kock JLF, Thibane VS (2011) Antifungal free fatty acids. In: Science Against Microbial Pathogens: Communicating Current Research and Technological Advances. Formatex Research Center, Spain

Prasad R, Banerjee A, Khandelwal NK, Dhamgaye S (2015) The ABCs of *Candida albicans* multidrug transporter Cdr1. Eukaryotic Cell 14:1154–1164. https://doi.org/10.1128/ec.00137-15

Prasad R, Banerjee A, Shah AH (2017) Resistance to antifungal therapies. Essays in Biochemistry 61:157–166. https://doi.org/10.1042/ebc20160067

Pukkila-Worley R, Ausubel FM, Mylonakis E (2011) *Candida albicans* infection of *Caenorhabditis elegans* induces antifungal immune defenses. PLoS Pathogens 7:e1002074. https://doi.org/10.1371/journal.ppat.1002074

Pukkila-Worley R, Holson E, Wagner F, Mylonakis E (2009) Antifungal drug discovery through the study of invertebrate model hosts. Current Medicinal Chemistry 16:1588–1595. https://doi.org/10.2174/092986709788186237

Ramage G, Martinez JP, Lopez-Ribot JL (2006) *Candida* biofilms on implanted biomaterials: a clinically significant problem. FEMS Yeast Research 6:979–986. https://doi.org/10.1111/j.1567-1364.2006.00117.x

Ramage G, Rajendran R, Sherry L, Williams C (2012) Fungal biofilm resistance. International Journal of Microbiology 2012:1–14. https://doi.org/10.1155/2012/528521

Ramage G, Walle KV, Wickes BL, López-Ribot JL (2001) Standardized method for *in vitro* antifungal susceptibility testing of *Candida albicans* biofilms. Antimicrobial Agents and Chemotherapy 45:2475–2479. https://doi.org/10.1128/AAC.45.9.2475-2479.2001

Redhu AK, Shah AH, Prasad R (2016) MFS transporters of *Candida* species and their role in clinical drug resistance. FEMS Yeast Research 16:fow043. https://doi.org/10.1093/femsyr/fow043

Rees DC, Johnson E, Lewinson O (2009) ABC transporters: The power to change. Nature reviews Molecular cell biology 10:218–27. https://doi.org/10.1038/nrm2646

Robbins N, Caplan T, Cowen LE (2017) Molecular evolution of antifungal drug resistance. Annual Review of Microbiology 71:753–775. https://doi.org/10.1146/annurev-micro-030117-020345

Rosenberg M, Azevedo NF, Ivask A (2019) Propidium iodide staining underestimates viability of adherent bacterial cells. Scientific Reports 9:6483 https://doi.org/10.1038/s41598-019-42906-3

Russell W, Burch R (1959) The Principles of humane experimental technique. Universities Federation for Animal Welfare. (Originally: Methuen & Co. Ltd), London

Sadeghi G, Ebrahimi-Rad M, Mousavi SF, et al (2018) Emergence of non-*Candida albicans* species: Epidemiology, phylogeny and fluconazole susceptibility profile. Journal de Mycologie Médicale 28:51–58. https://doi.org/10.1016/j.mycmed.2017.12.008

Samaranayake LP, Fidel PL, Naglik JR, et al (2002) Fungal infections associated with HIV infection. Oral Diseases 8:151–160. https://doi.org/10.1034/j.1601-0825.8.s2.6.x

Samuel M, Bleackley M, Anderson M, Mathivanan S (2015) Extracellular vesicles including exosomes in cross kingdom regulation: a viewpoint from plant-fungal interactions. Frontiers in Plant Science 6:766. https://doi.org/10.3389/fpls.2015.00766

Scorzoni L, de Lucas MP, Mesa-Arango AC, et al (2013) Antifungal efficacy during *Candida krusei* infection in non-conventional models correlates with the yeast *in vitro* susceptibility profile. PLoS ONE 8:e60047. https://doi.org/10.1371/journal.pone.0060047

Shareck J, Nantel A, Belhumeur P (2011) Conjugated linoleic acid inhibits hyphal growth in *Candida albicans* by modulating Ras1p cellular levels and downregulating *TEC1*

expression. Eukaryotic Cell 10:565–577. https://doi.org/10.1128/ec.00305-10

Sharma J, Rosiana S, Razzaq I, Shapiro R (2019) Linking cellular morphogenesis with antifungal treatment and susceptibility in *Candida* pathogens. Journal of Fungi 5:17. https://doi.org/10.3390/jof5010017

Shukla PK, Singh P, Yadav RK, et al (2016) Past, present, and future of antifungal drug development. Topics in Medicinal Chemistry 125–167. https://doi.org/10.1007/7355_2016_4

Silva S, Henriques M, Martins A, et al (2009) Biofilms of non-*Candida albicans Candida* species: quantification, structure and matrix composition. Medical Mycology 47:681–689. https://doi.org/10.3109/13693780802549594

Silva S, Henriques M, Oliveira R, et al (2010) *In vitro* biofilm activity of non-*Candida albicans Candida* species. Current Microbiology 61:534–540. https://doi.org/10.1007/s00284-010-9649-7

Soto SM (2013) Role of efflux pumps in the antibiotic resistance of bacteria embedded in a biofilm. Virulence 4:223–229. https://doi.org/10.4161/viru.23724

Swart CW, Swart HC, Coetsee E, et al (2010) 3-D architecture and elemental composition of fluconazole treated yeast asci. Scientific Research and Essays 5:3411–3417. https://doi.org/10.5897/SRE.9000064

Szczepaniak J, Cieślik W, Romanowicz A, et al (2017) Blocking and dislocation of *Candida albicans* Cdr1p transporter by styrylquinolines. International Journal of Antimicrobial Agents 50:171–176. https://doi.org/10.1016/j.ijantimicag.2017.01.044

Thibane VS, Ells R, Hugo A, et al (2012a) Polyunsaturated fatty acids cause apoptosis in *C. albicans* and *C. dubliniensis* biofilms. Biochimica et Biophysica Acta (BBA) - General Subjects 1820:1463–1468. https://doi.org/10.1016/j.bbagen.2012.05.004

Thibane VS, Kock JLF, Ells R, et al (2010) Effect of marine polyunsaturated fatty acids on biofilm formation of *Candida albicans* and *Candida dubliniensis*. Marine Drugs 8:2597–2604. https://doi.org/10.3390/md8102597

Thibane VS, Kock JLF, Van Wyk PWJ, et al (2012b) Stearidonic acid acts in synergism with amphotericin B in inhibiting *Candida albicans* and *Candida dubliniensis* biofilms *in vitro*. International Journal of Antimicrobial Agents 40:284–285.

https://doi.org/10.1016/j.ijantimicag.2012.05.021

Tsao S, Rahkhoodaee F, Raymond M (2009) Relative contributions of the *Candida albicans* ABC transporters Cdr1p and Cdr2p to clinical azole resistance. Antimicrobial Agents and Chemotherapy 53:1344–1352. https://doi.org/10.1128/aac.00926-08

Uppuluri P, Chaturvedi AK, Srinivasan A, et al (2010) Dispersion as an important step in the *Candida albicans* biofilm developmental cycle. PLoS Pathogens 6:e1000828. https://doi.org/10.1371/journal.ppat.1000828

Venkateswarlu K, Denning DW, Kelly SL (1997) Inhibition and interaction of cytochrome P450 of *Candida krusei* with azole antifungal drugs. Medical Mycology 35:19–25. https://doi.org/10.1080/02681219780000821

Wang X, Yao X, Zhu Z, et al (2009) Effect of berberine on *Staphylococcus epidermidis* biofilm formation. International Journal of Antimicrobial Agents 34:60–66. https://doi.org/10.1016/j.ijantimicag.2008.10.033

Ward JD, Mullaney B, Schiller BJ, et al (2014) Defects in the *C. elegans* acyl-CoA synthase, acs-3, and nuclear hormone receptor, nhr-25, cause sensitivity to distinct, but overlapping stresses. PLoS ONE 9:e92552. https://doi.org/10.1371/journal.pone.0092552

Watts JL, Browse J (2002) Genetic dissection of polyunsaturated fatty acid synthesis in *Caenorhabditis elegans*. Proceedings of the National Academy of Sciences of the United States of America 99:5854–5859. https://doi.org/10.1073/pnas.092064799

Whaley SG, Berkow EL, Rybak JM, et al (2017) Azole antifungal resistance in *Candida albicans* and emerging non-*albicans Candida* species. Frontiers in Microbiology 7:2173. https://doi.org/10.3389/fmicb.2016.02173

White TC, Holleman S, Dy F, et al (2002) Resistance mechanisms in clinical isolates of *Candida albicans*. Antimicrobial Agents and Chemotherapy 46:1704–1713. https://doi.org/10.1128/aac.46.6.1704-1713.2002

Wirsching S, Moran GP, Sullivan DJ, et al (2001) *MDR1*-mediated drug resistance in *Candida dubliniensis*. Antimicrobial Agents and Chemotherapy 45:3416–3421. https://doi.org/10.1128/aac.45.12.3416-3421.2001

Xu Z, Liang Y, Lin S, et al (2016) Crystal violet and XTT assays on *Staphylococcus aureus*

biofilm Quantification. Current Microbiology 73:474–482. https://doi.org/10.1007/s00284-016-1081-1

Yehye WA, Rahman NA, Ariffin A, et al (2015) Understanding the chemistry behind the antioxidant activities of butylated hydroxytoluene (BHT): A review. European Journal of Medicinal Chemistry 101:295–312. https://doi.org/10.1016/j.ejmech.2015.06.026

Yin H, Xu L, Porter NA (2011) Free radical lipid peroxidation: Mechanisms and analysis. Chemical Reviews 111:5944–5972. https://doi.org/10.1021/cr200084z

Yoon B, Jackman J, Valle-González E, Cho NJ (2018) Antibacterial free fatty acids and monoglycerides: Biological activities, experimental testing, and therapeutic applications. International Journal of Molecular Sciences 19:1114. https://doi.org/10.3390/ijms19041114

Zarnowski R, Sanchez H, Covelli AS, et al (2018) *Candida albicans* biofilm–induced vesicles confer drug resistance through matrix biogenesis. PLoS Biology 16:e2006872. https://doi.org/10.1371/journal.pbio.2006872

Zhao K, Bleackley M, Chisanga D, et al (2019) Extracellular vesicles secreted by *Saccharomyces cerevisiae* are involved in cell wall remodelling. Communications Biology 2:305 https://doi.org/10.1038/s42003-019-0538-8

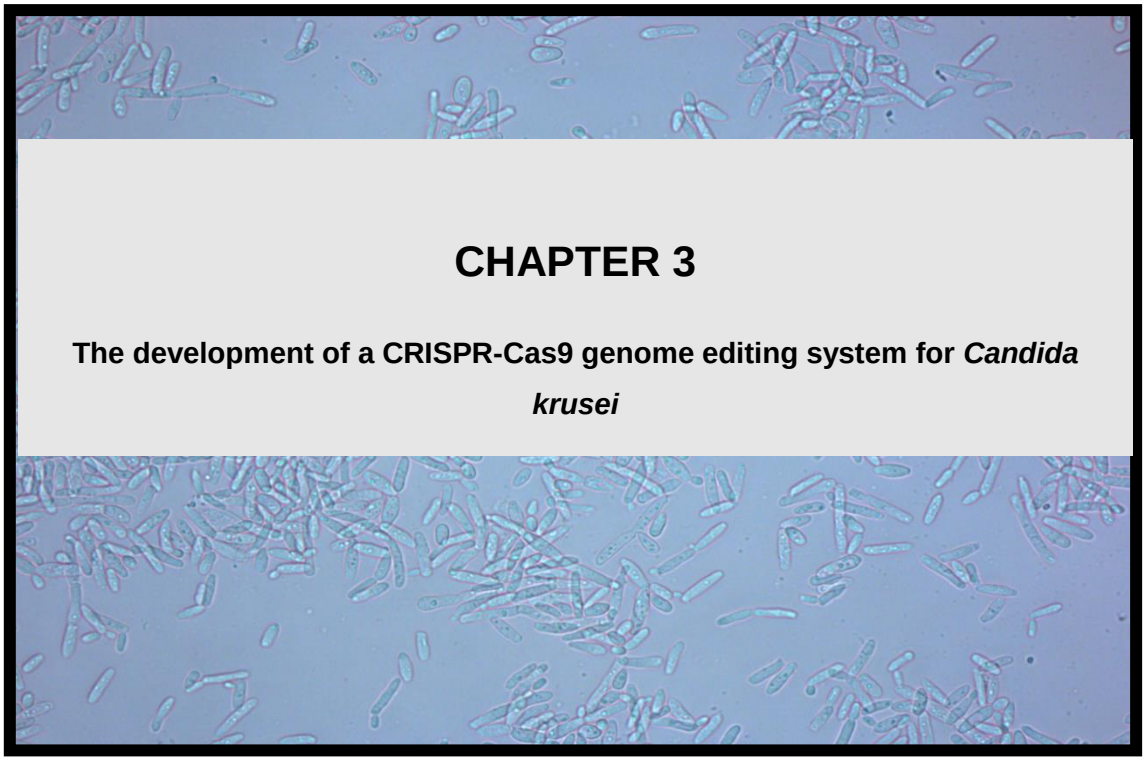

# CHAPTER 3

**The development of a CRISPR-Cas9 genome editing system for *Candida krusei***

## 3.1 Abstract

The 2020 Nobel Prize in Chemistry was co-awarded to Emmanuelle Charpentier and Jennifer Doudna for the discovery of Clustered Regularly Interspaced Short Palindromic Repeats- Cas associated protein 9 (CRISPR-Cas9) system – a precise editing tool that can be used for gene-editing in virtually all domains of life. This editing tool has revolutionised genetic engineering because it is facile, economical, rapid, and has a better efficiency compared to other genome editing systems. Although functional CRISPR-Cas9 editing systems have been designed and harnessed for gene engineering in many yeasts, including *Candida albicans* and other non-*albicans Candida* (NAC) species, such as *C. glabrata*, *C. parapsilosis*, and *C. auris*. No such system is available for *C. krusei.* The absence of such a simple and precise tool has dramatically hampered the full molecular delineation of this recalcitrant yeast's resistance mechanisms. This chapter involves developing a CRISPR-Cas9 mediated gene editing system for use in *C. krusei*. This was done by adapting a previously designed, *C. albicans*-specific, CRISPR-Cas9 system (HIS-FLP type). Our newly adapted system consists of a *CAS9* gene under the control of *C. krusei ENO1* promoter; and a gRNA, under the control of *SNR52* promoter, adaptable to target any locus within *C. krusei* genome. This system was designed to integrate at *HIS1* locus in the genome of *C. krusei,* and successful integration allows selection of transformants on nourseothricin-containing plates. As proof of concept, its efficacy was validated by the successful deletion of two auxotrophic marker genes, *URA3* and *ADE2*.

**Keywords:** CRISPR-Cas9, *Candida krusei*, Gene engineering, Resistance, Auxotrophic marker

## 3.2 Introduction

In modern biotechnology, the most important tools for gene modification are endonucleases, including zinc-finger nucleases, transcription activator-like effector nucleases, and engineered meganucleases (Richardson et al. 2016; Tang et al. 2019). However, these systems have various limitations and drawbacks, such as low specificity, single-site targeting, occurrence of non-specific mutations, low efficiency, huge complexity, high time-consumption and cost (Wang et al. 2013; Zhou et al. 2014; Abdallah et al. 2015; Adli 2018; Waryah et al. 2018).

An adaptive immune system known as CRISPR-Cas (Clustered Regularly Interspaced Short Palindromic Repeats-CRISPR associated protein) found in many bacteria and most archaea helps protect bacterial and archaeal genomes from invading phages and plasmids (Doudna and Charpentier 2014; Lander 2016; Hale et al. 2009; Khadempar et al. 2019). This system relies upon a dual RNA-Cas complex, formed by the association of a guide RNA (gRNA) [composed of CRISPR RNA (crRNA) and trans-activating crRNA (tracrRNA)] with Cas nuclease, to target and cleave foreign DNA with sites complementary to the protospacer sequence within the gRNA. A protospacer adjacent motif (PAM) site positioned next to the protospacer sequence is recognised by the Cas nuclease, and it is particularly important for this cleavage as it helps the Cas protein to discriminate between self-and invading DNA (Brouns et al. 2008; Deltcheva et al. 2011; Jinek et al. 2012; Nishimasu et al. 2014; Jiang et al. 2016). The discovery and subsequent elaborate study of this bacterial and archaeal adaptive immunity led to the development of a CRISPR-Cas9-mediated genome editing system. This editing tool has revolutionised genetic engineering because not only is it economical, versatile, and rapid, it is also simple to design and offers high-efficiency gene-editing compared to other genome editing systems (Khadempar et al. 2019; Saha et al. 2019). Moreover, the discovery of this revolutionary gene-editing tool has earned its discoverers, Emmanuelle Charpentier and Jennifer Doudna, the 2020 Nobel Prize in Chemistry (https://www.nobelprize.org/prizes/chemistry/2020/press-release/).

The CRISPR-Cas9 gene-editing tool uses a programmable Cas9 nuclease guided by a synthetic gRNA to introduce double-strand breaks (DSBs) at specific sites within the genome (Nguyen et al. 2017). These DSBs are usually lethal and require repair (Ranjha et al. 2018). Two repair mechanisms: non-homologous end-joining (NHEJ) and homology-directed repair (HDR) are involved in repairing these breaks. The NHEJ is the main repair pathway found in eukaryotes, and it repairs DSBs by ligating the broken ends of DNA without the need for a homologous DNA template (Lieber et al. 2003; Hefferin and Tomkinson 2005). Although this pathway has a high incidence rate (i.e. can occur and repair DSBs during all phases of the cell cycle), it has low fidelity (introduces indels), and could lead to frameshift mutations (Bernheim et al. 2017). Conversely, HDR has high fidelity and requires homologous DNA

sequences either from a sister chromosome (in case of a diploid cell) or a foreign donor DNA (dDNA) (Branzei and Foiani 2008; Arnoult et al. 2017; Saha et al. 2019). Notably, scientists have harnessed this pathway to generate precise gene-editing and modification by introducing desired exogenous dDNA fragments at target loci (Lin et al. 2014) (**Fig. 1**).

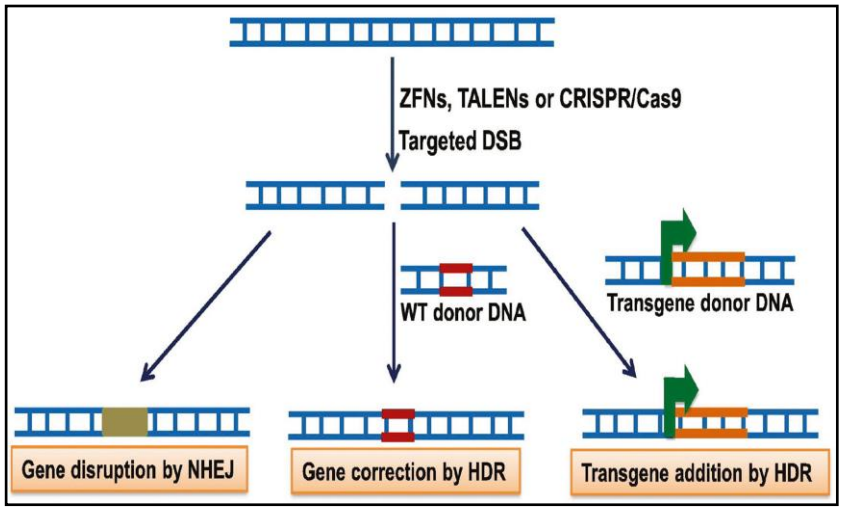


**Fig. 1** Mechanisms used to repair double-strand breaks (Obtained from Saha et al. 2019).

The first implementation of a CRISPR-Cas9 mediated gene-editing in a yeast was demonstrated by DiCarlo and co-workers (2013) in the model yeast, *Saccharomyces cerevisiae*. The system was constructed using a codon-optimised *CAS9* gene under the control of the *Gal-L* promoter and *CYC1* terminator; and a transient guide RNA, under the control of the *SNR52* promoter and *SUP4* terminator, designed to target *CAN1* gene, a cell membrane arginine permease, in *S. cerevisiae*. The gRNA cassette and dDNA fragment was co-transformed into *S. cerevisiae* cells constitutively expressing Cas9. The Cas9 guided by the gRNA induced DSBs at the *CAN1* locus. This was followed by homologous recombination with the supplied dDNA, and selection of transformed cells with disrupted *CAN1* on media containing canavanine, a toxic analogue of arginine transported only by a functional Can1p.

Several factors, such as diploidy, absence of plasmid systems, alternative codon usage, lack of selectable markers and a known meiotic phase, impede genetic engineering in many *Candida* species (Vyas et al. 2015; Nguyen et al. 2017; Román et al. 2019). Despite these hurdles, Vyas and co-workers (2015) successfully demonstrated the first use of a CRISPR-mediated genome editing system in *Candida albicans*. This system was constructed with a *C. albicans* codon-optimised version of *CAS9* (Ca*CAS9*) fused at the 3' end with SV40 nuclear localisation signal and FLAG-tag sequences. The CaCas9 cassette was integrated into *C. albicans* SC5314 at the *ENO1* locus and was expressed by the constitutive *ENO1* promoter. The gRNA cassette (containing a 20 bp protospacer specific to *ADE2* gene) under an *SNR52* promoter integrated at *RP10* locus (duet system) or at *ENO1* locus (solo system) directs CaCas9 to create DSBs at the *ADE2* locus. These breaks induce selective pressure for the

ultimate integration of an unmarked dDNA at the target locus via HDR. The system (duet system) was highly efficient and generated up to 80% *ade2Δ/Δ* transformants. Additionally, after successful transformation, the nourseothricin N-acetyltransferase (*NAT*) marker and gRNA fragment can be removed with the expression of flippase (*FLP*) recombinase. However, one allele of the *ENO1* gene is left permanently disrupted with this system because of the non-recyclable Cas9 fragment. This might affect the downstream use of the generated mutants since Eno1 protein plays essential roles in the morphogenesis, virulence, cell growth, and osmotic protection of *C. albicans* (Ko et al. 2013; Leu et al. 2020).

A similar system developed by Min and co-workers (2016) addressed this limitation by using transient Cas9 and gRNA cassettes that are not integrated into the *C. albicans* genome. Homozygous mutants generated using this system could be selected using marked dDNA fragments integrated at the target locus following the creation of site-specific DSBs by the RNA-guided Cas9. However, one limitation of this system is that it uses a non-recyclable marker – the dDNA does not get excised from the target locus. This roadblock was addressed with a revised system designed by Huang and Mitchell (2017), which allows the excision of the dDNA marker. However, this system does not fully represent a markerless genome editing tool since it relies upon two distinct selectable markers to achieve the CRISPR-Cas9-induced marker excision (Nguyen et al. 2017).

A new CRISPR system that supports markerless and rapid genome engineering was designed for gene-editing in *C. albicans*. This system not only eludes the need for lengthy gRNA cloning procedures, but also allows the removal of gRNA/Cas9 and dDNA cassettes, and enables homozygous restoration of complete wildtype open reading frame (ORF) at the native loci – i.e. allows the generation of complementary (addback) strains (Nguyen et al. 2017).

Furthermore, CRISPR-Cas9 systems have been developed for gene-editing in several common non-*albicans Candida* (NAC) species including *C. glabrata* (Enkler et al. 2016), *C. parapsilosis* (Lombardi et al. 2017), *C. tropicalis* (Zhang et al. 2019), *C. auris* (Grahl et al. 2017), and non-common NAC species, such as *C. lusitaniae* (Norton et al. 2017), *C. orthopsillosis* (Zoppo et al. 2019), and *C. aaseri* (Ibrahim et al. 2020). However, no such system is available for genetic engineering in *C. krusei*. The lack of such facile and precise tool for gene-editing in *C. krusei* has greatly impeded the molecular understanding of this yeast's resistance mechanisms.

Hence, this chapter aimed at developing a CRISPR-Cas9 system specific for genome engineering in *C. krusei* by adapting a previously designed, *C. albicans*-specific, HIS-FLP type CRISPR-Cas9 system of Nguyen and co-workers (2017).

## 3.3 Materials and Methods

### 3.3.1 Strains used

The type strain of *Candida krusei*, *C. krusei* UFS Y-0217 (CBS573$^T$), was used in this study. This strain is diploid (2n) and was specifically chosen for this study because of the availability of its annotated genome on the database of National Center for Biotechnology Information (Accession: PRJNA434433) (Douglass et al. 2018). This strain was obtained from the Yeast Culture Collection of the University of the Free State, Bloemfontein, South Africa, and was revived on Yeast Malt extract (YM) agar plates (10 g/l glucose, 3 g/l yeast extract, 3 g/l malt extract, 5 g/l peptone, 17 g/l agar) at 30$^o$C for 24 h. Glycerol stock (15%, v/v) was prepared and stored at -80$^o$C for future use. The XL-10 Gold competent *Escherichia coli* (Agilent Technologies) was used for bacterial transformation and cloning.

### 3.3.2 *In silico* analyses

Construction of primers, fragments and constructs, simulation of polymerase chain reaction, cloning, and restriction analyses, sequence alignments, and identification of CRISPR sites were done *in silico* with Geneious® 11.1.4 prior to all *in vitro* and *in vivo* assays.

### 3.3.3 Plasmids and primers used

This study involves constructing a CRISPR-Cas9 system for use in *C. krusei* by adapting a previously developed *C. albicans*-specific CRISPR-Cas9 (HIS-FLP) system. The CRISPR-Cas9 plasmids used for this purpose, previously designed by Prof. Aaron Hernday's research lab at the University of California Merced, Merced, California, USA (Nguyen et al. 2017), were obtained from Addgene and are shown in **Table 1**. All primers used in this study were purchased from Integrated DNA Technologies (IDT) and are listed in **Table 2**. Each primer was diluted to a concentration of 10 µM with Tris-EDTA (Ethylenediaminetetraacetic acid) (TE) buffer (10 mM Tris-HCl, 1 mM EDTA, pH 8.0) before use.

**Table 1** Description of HIS-FLP plasmids constructed by Nguyen and co-workers (2017)

| Plasmid | Addgene ID | Major component | Function |
|---|---|---|---|
| **pADH99** | #90979 | *Candida albicans* 5'-*HIS1* region + *C. albicans ENO1* promoter + *CAS9* gene + ½ *NAT* gene | Cas9 cassette |
| **pADH110** | #90982 | $^2/_2$ *NAT* gene + *C. albicans SNR52* promoter | ½ gRNA cassette |
| **pADH147** | #90991 | gRNA scaffold + *C. albicans* 3'-*HIS1* region | $^2/_2$ gRNA cassette |

**Table 2** Primers used in this study

| Primer | Sequence (5' to 3') | Tm (°C) | Reference |
|---|---|---|---|
| **pADH99-5' CK HIS1 overlap-F** | CGTTTAAACCGCCTCAAGCAGCACACAATTTCATGATTAATGGT | 65.6 | This study |
| **CK-5' HIS1-R** | CCGGATAATATCAAAACCCCTCT | 54.3 | This study |
| **pADH99::CK HIS1::FRT overlap** | TGTGAGAGGGGTTTTGATATTATCCGGGAAGTTCCTATACTTTCTAGAGAA | 64.9 | This study |
| **pADH99::CK FRT::ENO1 overlap** | GGGATGCCACGTGGTAATGAAACAGAAGTTCCTATTCTCTAGAAAGTAT | 65.1 | This study |
| **CK ENO1-F** | TGTTTCATTACCACGTGGCA | 54.9 | This study |
| **pADH99-3'-CK CAS9 overlap** | CAATACTATACTTTTTATCCATCCCTGTTTGGTTGGAGGGGGTTA | 64.0 | This study |
| **CK-3' HIS1-overlap-1F** | AGAGAATAGGAACTTCCCAATGTCACAAAACTCAAACAGGA | 63.6 | This study |
| **CK- 3' HIS1-overlap-1R** | CTGGGGTTTAAACACCGTAACTAGACAAGCGAGTTTGCA | 65.5 | This study |
| **pADH147-1F** | TACGGTGTTTAAACCCCAGC | 55.2 | This study |
| **pADH147-1R** | TGGGAAGTTCCTATTCTCTAGAAAGTA | 54.7 | This study |
| **CK-3' HIS1-F** | ATGTCACAAAACTCAAACAGGA | 52.7 | This study |
| **CK-3' HIS1-R** | ACTAGACAAGCGAGTTTGCA | 54.3 | This study |
| **AHO1096-ver2** | GACGGCACGGCCACGCGTTTAAAC | 65.1 | Modified from Nguyen et al. 2017 |
| **AHO1098-ver2** | CAAATTAAAAATAGTTTACGCAAGTCTCG | 53.8 | Modified from Nguyen et al. 2017 |
| **AHO1097** | CCCGCCAGGCGCTGGGGTTTAAACACCG | 70.2 | Nguyen et al. 2017 |
| **AHO1237** | AGGTGATGCTGAAGCTATTGAAG | 55.0 | Nguyen et al. 2017 |
| **URA3-CRISPR-1** | CGTAAACTATTTTTAATTTGATTGCGCAACACGATATGGGGTTTTAGAGCTAGAAATAGC | 65.2 | This study |
| **URA3-2F** | GCCTTTGTTAAACAACTTTTTCT | 50.6 | This study |
| **URA3-2R** | ATGGCGTCATGCTGGTTGGAATGCTTATTT | 62.5 | This study |
| **URA3-3F** | TCCAACCAGCATGACGCCATCCTTGACAAA | 65.1 | This study |
| **URA3-3R** | CGCCTTGAAATGAAAATGCTG | 53.3 | This study |
| **ADE2-CRISPR-2** | CGTAAACTATTTTTAATTTGTTAGGGTCTGATGTGCCAAAGTTTTAGAGCTAGAAATAGC | 64.4 | This study |
| **ADE2-2F** | TAGAAGGGCCAGAGTCAGAG | 55.5 | This study |
| **ADE2-2R** | TTCCATTTCAACCGATAGTTTTCGAGTCCA | 59.8 | This study |
| **ADE2-3F** | AACTATCGGTTGAAATGGAAACGTACATGAATT | 58.7 | This study |
| **ADE2-3R_new** | AGAACGCTATTTTAAACGCTAATA | 50.7 | This study |

NB: Target-specific CRISPR site is underlined

### 3.3.4 Polymerase chain reaction (PCR) amplification

In this study, PCR amplification of genes, fragments, and constructs was done using either KAPA Taq PCR kit (KAPA Biosystems), KAPA HiFi PCR kit (KAPA Biosystems), or KOD Hot Start DNA polymerase kit (Novagen®). The reaction components used for each kit are shown in **Tables 3, 4, and 5**. The concentration and volume of these components were scaled appropriately for each experiment. The PCR conditions (program) used for each kit are also depicted in **Tables 6, 7, and 8**. These conditions were modified as required to suit the purpose of each experiment. Additionally, the specific kit used for each amplification is indicated, where necessary.

**Table 3** Reaction mixture for KAPA Taq PCR kit (KAPA Biosystems)

| **Component** | **Reaction mixture** |
|---|---|
| Nuclease-free water | Up to 25 µl |
| 10X KAPA Taq Buffer | 2.5 µl |
| dNTP Mix (10 mM) | 0.5 µl |
| Forward primer (10 µM) | 1.0 µl |
| Reverse primer (10 µM) | 1.0 µl |
| KAPA Taq DNA polymerase (5 U/µl) | 0.1 µl |
| DNA template (less complex DNA)* | ≤25 ng |

*tenfold excess for genomic DNA

**Table 4** Reaction mixture for KAPA HiFi PCR kit (KAPA Biosystems)

| **Component** | **Reaction mixture** |
|---|---|
| Nuclease-free water | Up to 25 µl |
| 5X KAPA HiFi Buffer | 5.0 µl |
| KAPA dNTP Mix (10 mM) | 0.75 µl |
| Forward primer (10 µM) | 0.75 µl |
| Reverse primer (10 µM) | 0.75 µl |
| KAPA HiFi Hot Start DNA polymerase (1 U/µl) | 0.1 µl |
| Template DNA (less complex DNA)* | 1 ng |

*hundred-fold excess for genomic DNA

**Table 5** Reaction mixture for KOD Hot Start DNA polymerase kit (Novagen®)

| **Component** | **Reaction mixture** |
|---|---|
| Nuclease-free water | Up to 25 µl |
| 10X Buffer for KOD Hot Start DNA Polymerase | 2.5 µl |
| 25 mM $MgSO_4$ | 1.5 µl |
| dNTP Mix (2 mM) | 2.5 µl |
| Forward primer (10 µM) | 0.75 µl |
| Reverse primer (10 µM) | 0.75 µl |
| KAPA Taq DNA polymerase (5 U/µl) | 0.5 µl |
| Template DNA (less complex DNA)***** | ≤10 ng |

* tenfold excess for genomic DNA

**Table 6** PCR condition for KAPA Taq PCR kit (KAPA Biosystems)

| **Step** | **Temperature** | **Time** | **Cycle** |
|---|---|---|---|
| Initial denaturation | 94°C | 5 min | 1 |
| Denaturation | 94°C | 30 sec | 25 |
| Annealing | Lowest primer Tm - 5°C | 30 sec | |
| Extension | 72°C | 1 min | |
| Final extension | 72°C | 5 min | 1 |
| Hold | 4°C | ∞ | |

**Table 7** PCR condition for KAPA HiFi PCR kit (KAPA Biosystems)

| **Step** | **Temperature** | **Time** | **Cycle** |
|---|---|---|---|
| Initial denaturation | 95°C | 3 min | 1 |
| Denaturation | 98°C | 20 sec | 15 – 35 |
| Annealing | Lowest primer Tm - 1°C | 15 sec | |
| Extension | 72°C | 1 min /kb | |
| Final extension | 72°C | 1 min/kb | 1 |
| Hold | 4°C | ∞ | |

**Table 8** PCR condition for KOD Hot Start DNA polymerase kit (Novagen®)

| **Step** | **Target size** | | | | **Cycle** |
|---|---|---|---|---|---|
| | < 500 bp | 500 – 1000 bp | 1000 – 3000 bp | > 3000 bp | |
| Polymerase activation | 95°C, 2 min | 95°C, 2 min | 95°C, 2 min | 95°C, 2 min | 1 |
| Denaturation | 95°C, 20 sec | 95°C, 20 sec | 95°C, 20 sec | 95°C, 20 sec | 30 |
| Annealing | Lowest Primer Tm °C, 10 sec | | | | |
| Extension | 70°C, 10 sec/kb | 70°C, 15 sec/kb | 70°C, 20 sec/kb | 70°C, 25 sec/kb | 1 |

### 3.3.5 Genomic DNA extraction

In this study, extraction of genomic DNA from both wildtype and transformed yeast cells was done using either the Zymo Research Quick-DNA™ Fungal/Bacterial Miniprep kit or the manual method of Labuschagne and Albertyn (2007).

#### 3.3.5.1 DNA extraction with Zymo Research kit

Genomic DNA (gDNA) was extracted using the Zymo Research Quick-DNA™ Fungal/Bacterial Miniprep kit in accordance with the manufacturer's instructions. Briefly, pelleted cells of *C. krusei* was re-suspended in ZR Bashing Bead™ lysis tube containing 200 µl Phosphate Buffered Saline (PBS) [10 mM phosphate buffer, 2.7 mM potassium chloride, 137 mM sodium chloride (pH 7.4)]. A volume of 750 µl of the Bashing Bead™ buffer was dispensed into the lysis tube; the tube was secured in a bead beater [Lasec South Africa (Pty) Ltd] and processed at a maximum speed (400 *x g* for 3 min) to lyse the yeast cells. The tube was centrifuged (Eppendorf, Germany) at 10,000 *x g* for 1 min, after which 400 µl of the supernatant was transferred into a Zymo-Spin™ III-F filter (in a collection tube) and was centrifuged at 8,000 *x g* for 1 min. Subsequently, 1200 µl genomic lysis buffer was added to the filtrate obtained and 800 µl of the mixture (of the filtrate and genomic lysis buffer) was dispensed into a Zymo-Spin™ IIC column (in a new collection tube) and was centrifuged at 10,000 *x g* for 1 min. The flow-through was discarded, the remaining 800 µl volume of the previous mixture was dispensed into the Zymo-Spin™ IIC column (in the same collection tube) and was centrifuged again at 10,000 *x g* for 1 min. The Zymo-Spin™ IIC column was transferred into a new collection tube, 200 µl of DNA pre-wash buffer was added to the column, and centrifuged at 10,000 *x g* for 1 min. Following this step, the column was washed with 500 µl gDNA wash buffer at 10,000 *x g* for 1 min. The Zymo-Spin™ IIC column was subsequently transferred to a clean 1.5 ml microcentrifuge tube and the gDNA was eluted (10,000 *x g*, 30 sec) from the column with 100 µl DNA elution buffer (10 mM Tris-HCl, pH 8.5). The concentration of the eluted gDNA was determined with a Nanodrop (NanoDrop Technologies, USA) and the DNA was stored at -20°C prior to further use.

#### 3.3.5.2 DNA extraction with a manual method

A slightly modified protocol of Labuschagne and Albertyn (2007) was followed for the manual isolation of DNA from yeast cells. This manual method was utilised for the preliminary extraction of DNA from transformants. Briefly, pelleted cells of *C. krusei* was re-suspended in 500 µl lysis solution (10 mM Tris-HCl pH 8.0, 50 mM EDTA pH 8.0, 1% SDS) containing 200 µl glass beads. The mixture was vortexed for 5 min (with a 60-second incubation on ice after each minute vortexing), and 275 µl ammonium acetate (2.3 M, pH 7) was added. This was followed by incubating the mixture at 65°C for 5 min, on ice for another 5 min, and centrifugation (20,000 *x g*, 4°C, 2 min) after the addition of 500 µl chloroform. The resulting

supernatant was transferred to a new 1.5 ml Eppendorf tube, the DNA was precipitated at room temperature (5 min) with 1 volume isopropanol and centrifuged at 20,000 *x g* for 2 min at 4$^{o}$C. Subsequently, the supernatant was discarded, the pellet was washed with ice-cold 70% ethanol, dried with SpeedVac (Eppendorf, Germany), reconstituted in 100 µl TE buffer (10 mM Tris-HCl, 1 mM EDTA, pH 8.0) containing 5 µl of 0.5 mg/ml RNase, and stored at -20$^{o}$C prior to further use.

### 3.3.6 Agarose gel electrophoresis

Unless stated otherwise, successful extraction and amplification of DNA were confirmed using agarose gel [Whitehead Scientific (Pty) Ltd] at a concentration of 0.8% (w/v). The gel was prepared with 1X Tris Acetate EDTA (TAE) electrophoresis buffer (40 mM Tris base, 20 mM acetic acid, 1 mM EDTA) and stained with ethidium bromide (Science Lab) or SYBR® Safe DNA Gel Stain (Invitrogen) (in case of gel extraction) at 1:10,000 volume. DNA samples with loading dye were loaded into the wells of the solidified gel, and a 10 kb O'GeneRuler DNA ladder mix (Thermo Fisher Scientific) was used as a DNA marker for size comparison. The DNA samples were separated at 90 volts for 30 min, and the gel was visualised under UV light in a Gel Doc$^{TM}$ XR+ (Bio-Rad, Canada) (Lee et al. 2012).

### 3.3.7 Gel extraction

Following gel electrophoresis, DNA samples which needed to be purified prior to further downstream applications were purified using the Thermo Scientific GeneJET Gel Extraction kit according to the manufacturer's instructions. Briefly, agarose gel containing the desired DNA sample was excised from the gel and transferred to a 1.5 ml Eppendorf tube. The excised gel was incubated at 60$^{o}$C with a 1:1 volume of binding buffer until it completely dissolved. Subsequently, 1 volume isopropanol (100%) was added to the solubilised gel, and 800 µl of this mixture was transferred to a GeneJET purification column (in a collection tube). The column was centrifuged at 16,000 *x g* (Eppendorf, Germany) for 1 min, and the flow-through was discarded. Following this step, the column was washed (16,000 *x g*, 1 min) with 700 µl wash buffer and transferred to a new 1.5 ml Eppendorf tube. The ultrapure DNA was eluted (16,000 *x g*, 1 min) from the column with 50 µl DNA elution buffer (10 mM Tris-HCl, pH 8.5), its concentration was determined with a NanoDrop (NanoDrop Technologies, USA) and was stored at -20$^{o}$C until further use.

### 3.3.8 Restriction digest

Restriction digestion of DNA was done using the component depicted in **Table 9**. In the case of double digests, 1 µl of each restriction enzyme was included, and the reaction scaled appropriately. Following every digestion reaction, the enzyme(s) was inactivated at appropriate conditions.

**Table 9** Reaction mixture for digestion reaction

| Component | Reaction mixture |
|---|---|
| Nuclease-free water | Up to 25 µl |
| DNA | As required |
| Buffer (restriction-enzyme specific) | 2.0 µl |
| Restriction enzyme | 0.5 – 1.0 µl |

### 3.3.9 DNA assembly using NEBuilder®

All primers, including the overlapping primers, used for the amplification of fragments and/or plasmids expected to be assembled with the NEBuilder® HiFi DNA Assembly kit (New England Biolabs®Inc.) were designed as shown in **Figure 2**. Each overlapping primer was designed with an overlap sequence of about 15 – 25 nucleotides (with Tm >50°C). The reaction components used for assembly are indicated in **Table 10**. Following assembly reaction at 50°C (myBlock™ Mini Dry Bath, Benchmark Scientific) for 60 min, the assembled product was stored at -20°C until further use. An illustration of the assembly reaction is shown in **Figure 3**.

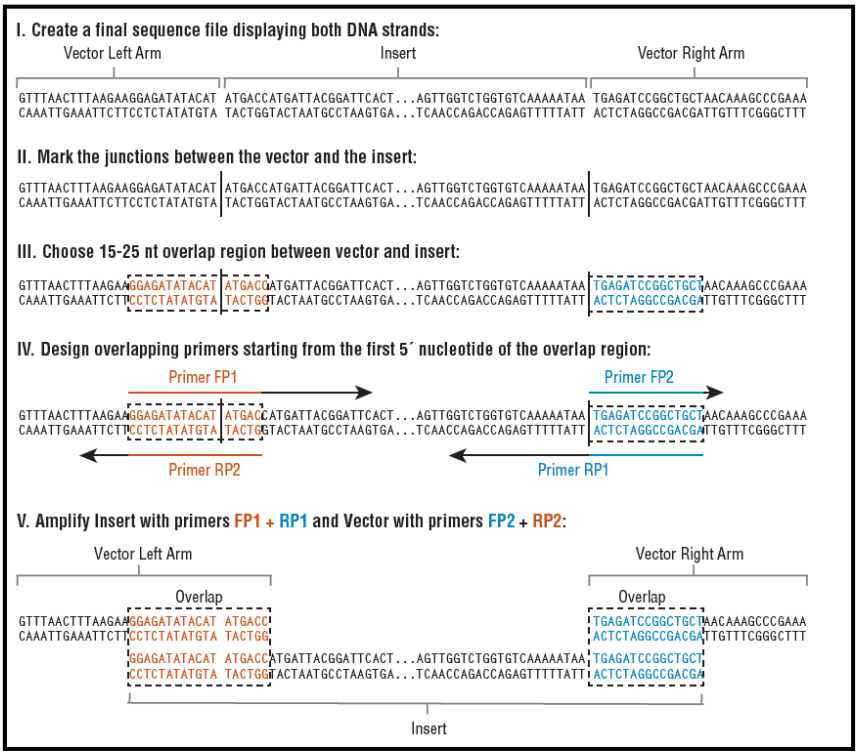


**Fig. 2** An illustration of the procedure followed for primer designs for the assembly of fragments with NEBuilder® HiFi DNA Assembly kit (https://international.neb.com/).

**Table 10** Reaction component for NEBuilder assembly

| Component | Reaction mixture |
|---|---|
| Nuclease-free water | Up to 20 µl |
| Fragments* | As required |
| NEBuilder HiFi DNA assembly master mix | 10.0 µl |

*Two-fold excess of insert(s) was used (i.e. when using 50 ng of vector mass, 100 ng of insert(s) was used).

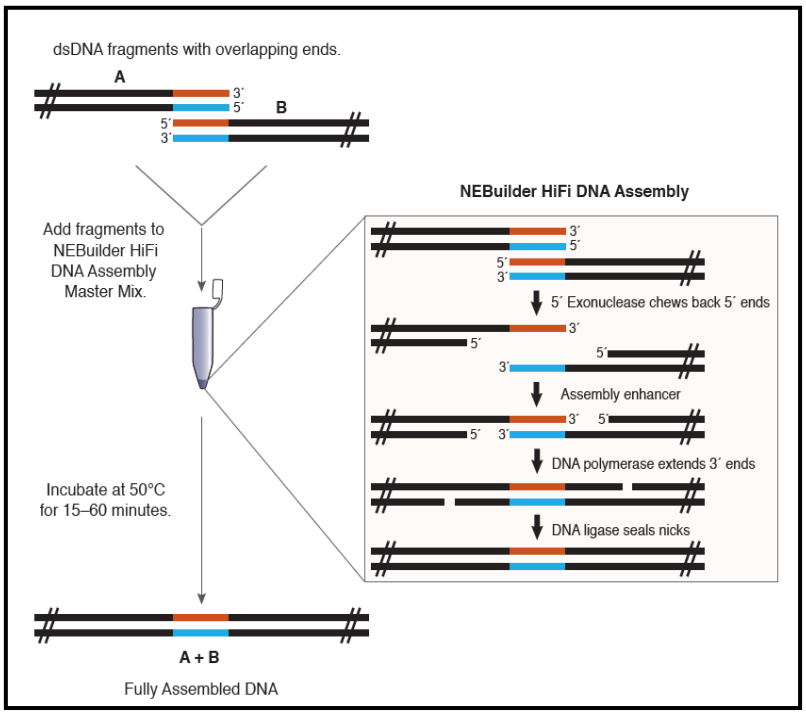


**Fig. 3** A schematic representation of the NEBuilder® HiFi DNA Assembly reaction (https://international.neb.com/).

### 3.3.10 Bacterial transformation

The bacterial transformation was done using a modified NEBuilder® HiFi DNA Assembly protocol. Briefly, competent *E. coli* cells removed from -80°C were thawed on ice. The cells were mixed with 2 µl DNA (e.g. assembled product), incubated on ice for 30 min, heat-shocked at 42°C (myBlock™ Mini Dry Bath, Benchmark Scientific) for 30 sec and returned on ice for 2 min. Subsequently, 1 ml Luria Bertani (LB) broth (10 g/l tryptone powder, 10 g/l yeast extract, 5 g/l sodium chloride) was added and cells were grown by gentle shaking at 37°C for 60 min. A 100 µl volume of the transformed cells was plated on LB agar plates (10 g/l tryptone powder, 10 g/l yeast extract, 5 g/l sodium chloride, 17 g/l agar) supplemented with 100 µg/ml ampicillin

(Roche®), and incubated overnight at 37ºC. Untransformed *E. coli* cells were used as a negative control.

### 3.3.11 Plasmid extraction and purification

#### 3.3.11.1 Miniprep – lysis by boiling method

After every bacterial transformation step, plasmid DNA was extracted using a modified lysis by boiling protocol of Holmes and Quigley (1981). Briefly, an overnight broth culture of transformed *E. coli* cells was centrifuged (10,000 × *g*, 2 min) (Eppendorf, Germany), the pelleted cells were re-suspended in 350 µl STET buffer [8% (w/v) sucrose, 5% (v/v) Triton X-100, 50 mM EDTA, 50 mM Tris-HCl, pH 8.0] in a 1.5 ml Eppendorf tube and was vortexed to allow complete mixing. A 5 µl volume of 50 mg/ml lysozyme was added, the mixture was mixed gently by inversion (7×, 35 sec) and was boiled in boiling water for 40 sec. Subsequently, the mixture was vortexed and allowed to precipitate at room temperature following the addition of 40 µl sodium acetate (2.5 M, pH 5.2) and 420 µl isopropanol. The resulting mixture was centrifuged (7800 × *g*, 4ºC, 5 min) and the supernatant was removed without disturbing the pellet. The pellet was washed with 1 ml of ethanol (70%) at 7800 × *g* for 2 min at 4ºC, and the remaining ethanol was removed. Following the washing step, the pellet was dried in a SpeedVac (Eppendorf, Germany) for 5 min and dissolved with 50 µl TE buffer (10 mM Tris-HCl, 1 mM EDTA, pH 8.0). After the extraction procedure, extracted plasmids were digested with an appropriate restriction enzyme(s), and their profiles were confirmed with gel electrophoresis. Plasmids confirmed to contain the inserted fragments in the correct orientation were subsequently purified using the Thermo Scientific GeneJET Plasmid Miniprep kit.

#### 3.3.11.2 Plasmid purification

The purification of plasmid DNA was done according to the protocol of Thermo Scientific GeneJET Plasmid Miniprep kit. Briefly, transformed *E. coli* cells (already verified to contain recombinant plasmids) were grown overnight at 37ºC in LB broth (supplemented with 100 µg/ml ampicillin). The overnight culture was centrifuged (10,000 *x g*, 2 min) (Eppendorf, Germany), and the resulting pelleted cells were re-suspended in 250 µl resuspension solution in a 1.5 ml Eppendorf tube. A 250 µl volume of lysis solution was added to the mixture and was thoroughly mixed by inversion until it became viscous. Following this step, a 350 µl neutralisation solution was added, and the mixture was again thoroughly mixed by inversion until it became cloudy. The resulting mixture was centrifuged (16,000 *x g*, 5 min) to pellet the chromosomal DNA and cell debris. The supernatant was pipetted into a GeneJET spin column (in a collection tube), the flow-through was discarded following centrifugation (16,000 *x g*, 1 min) and the column was returned to the collection tube. The column was washed twice with 500 µl wash solution at 16,000 *x g* for 60 sec, and this was followed by the elution of the

plasmid from the column into a new 1.5 ml Eppendorf tube with 50 µl pre-warmed elution buffer (pre-warmed at 70°C for better recovery) at 16,000 *x g* for 2 min. Expected profiles (i.e. insertion of inserts in the correct orientation) of the purified plasmids were again confirmed using gel electrophoresis after a digestion reaction.

### 3.3.12 Minimum fungicidal concentration (MFC) for nourseothricin

Since the CRISPR-Cas9 system used in this study utilises a dominant *NAT* marker, it was important to determine the concentration of nourseothricin (NTC) appropriate for the selection of transformed *C. krusei* cells. The MFC of NTC suitable for the selection of transformed cells of *C. krusei* was determined with a few modifications of a previous protocol (du Plooy 2019). Briefly, a loopful of *C. krusei* UFS Y-0217 cells from a YM agar plate was inoculated into 5 ml Yeast extract Peptone Dextrose (YPD) broth (10 g/l yeast extract, 20 g/l peptone, 20 g/l glucose) and was incubated overnight at 30°C in a shaking incubator. Following incubation, 100 µl of this culture was transferred onto YPD agar plates (10 g/l yeast extract, 20 g/l peptone, 20 g/l glucose, 17 g/l agar) supplemented with varying concentrations (600 µg/ml, 500 µg/ml, 400 µg/ml, 300 µg/ml, 200 µg/ml) of NTC (Jena Bioscience). These plates were subsequently incubated at 30°C for 2 to 3 days, after which the MFC of NTC for *C. krusei* UFS Y-0217 strain was determined. The MFC was defined as the lowest concentration of NTC that prevented any visible growth of the yeast. The yeast was unable to grow at a concentration of 400 µg/ml and higher; hence 400 µg/ml was used as a starting concentration for the selection of transformed cells.

### 3.3.13 Construction of a HIS-FLP type CRISPR-Cas9 system for *C. krusei*

In order to develop a working CRISPR-Cas9 system for use in *C. krusei*, a HIS-FLP type CRISPR-Cas9 system designed by Nguyen and co-workers (2017) for gene-editing in *C. albicans* was adapted. Plasmids required for this purpose were obtained from Addgene (**Table 1**), and were adapted for use in *C. krusei*.

#### 3.3.13.1 Adaptation of pADH99 plasmid

The pADH99 plasmid (#90979) was linearised by double digestion (Fig. 4) with *Nco*I and *Sma*I restriction enzymes (Thermo Scientific) (see section **3.3.8**), and subsequently gel purified. Next, the 5'-*HIS1* region was amplified from the genome of *C. krusei*, using the reaction mixture and PCR condition of KAPA HiFi PCR kit (**Tables 4, 7**), at an annealing temperature of 53°C, with primer pair pADH99-5' CK HIS1 overlap-F and CK-5' HIS1-R (**Table 2**). A flippase recognition target (FRT) fragment was amplified with overlapping oligonucleotides, pADH99::CK HIS1::FRT overlap and pADH99::CK FRT::ENO1 overlap, using the reaction mixture and program of KAPA Taq PCR kit (**Tables 3, 6**) at an annealing temperature of 50°C. The third round of PCR involved amplifying the *ENO1* promoter from the genome of *C. krusei*, with primer pair CK ENO1-F and pADH99-3'-CK CAS9 overlap, using the reaction mixture and

condition of KAPA HiFi PCR kit at an annealing temperature of 54°C. The oligonucleotides pADH99::CK HIS1::FRT overlap and pADH99::CK FRT::ENO1 overlap were designed to overlap with CK 5'-*HIS1* and CK *ENO1*p fragments, respectively, to aid the assembly of these fragments. Also, the primers pADH99-5' CK HIS1 overlap-F and pADH99-3'-CK CAS9 overlap contain sequences that are complementary to pADH99 backbone and *CAS9* gene, respectively, to aid cloning into the plasmid. The successful amplification of these fragments, except for the FRT fragment (which was visualised on a 2% agarose gel) was confirmed with a 0.8% agarose gel (see section **3.3.6**), the fragments were then gel extracted and purified using the Thermo Scientific GeneJET Gel Extraction kit (see section **3.3.7**) prior to assembly. Accordingly, the purified CK 5'-*HIS1*, FRT and CK *ENO1*p fragments were linked to the linearised pADH99 (**Fig. 4**) using the NEBuilder® HiFi DNA Assembly kit (see section **3.3.9**) and transformed into competent *E. coli* cells (see section **3.3.10**). Following transformation, plasmids were extracted from selected colonies using lysis by boiling method (see subsection **3.3.11.1**), and were screened for anticipated inserts by restriction digestion with *Xba*I (Thermo Scientific). Subsequently, plasmids were extracted and purified from selected colonies (suspected to be containing the anticipated plasmid based on the profile obtained after restriction digest with *Xba*I) but this time with the Thermo Scientific GeneJET Plasmid Miniprep kit (see section **3.3.11.1**). The newly purified plasmids' profiles were checked using gel electrophoresis following a digestion reaction with *Bam*HI to confirm the correct insertion and orientation of the inserted fragments. Following this, the concentration of the purified plasmid CK pADH99 was determined, and the plasmid was stored at -20°C prior to future use.

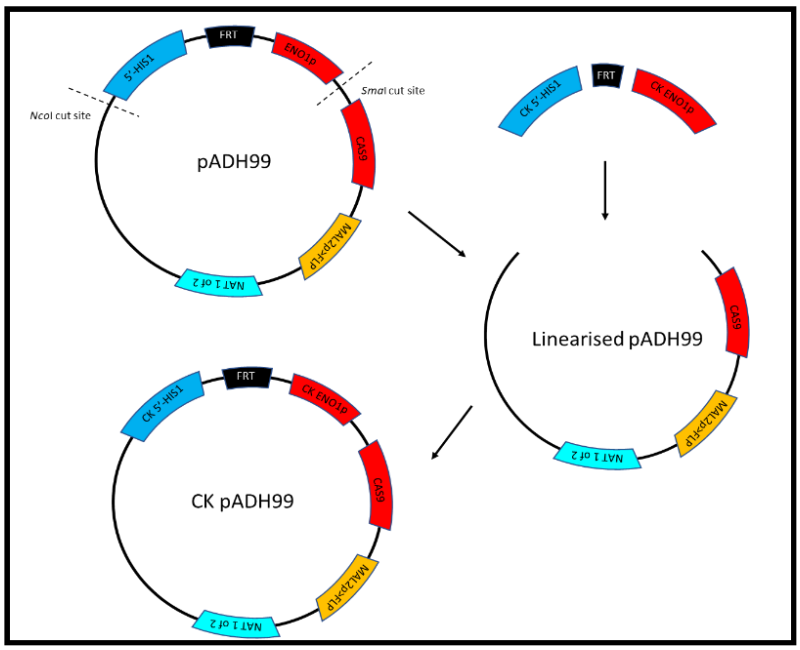


**Fig. 4** A schematic summary of the steps involved in the construction of CK pADH99 plasmid. First, pADH99 was double digested with *NcoI* and *SmaI* to linearise it and release the HIS1-ENO1p-FRT region. Next, an intact CK pADH99 plasmid is prepared by ligating amplified (overlapping) *C. krusei*-specific fragments into the linearised pADH99 plasmid. NB: Shapes not drawn to scale.

#### 3.3.13.2 Propagation of pADH110

More copies of pADH110 plasmid (#90982), containing an overlapping portion of *NAT* marker gene and a *C. albicans SNR52* promoter, were generated by transforming the plasmid into competent *E. coli* cells (see section **3.3.10**). Following transformation, the plasmid was purified using the Thermo Scientific GeneJET Plasmid Miniprep kit (see section **3.3.11.1**) and was stored at -20$^{o}$C until future use.

#### 3.3.13.3 Adaptation of pADH147

Plasmid pADH147 (#90991) was linearised with primer pair pADH147-1F and pADH147-1R (**Table 2**) using the reaction mixture and program of the KAPA HiFi PCR kit supplied in **Tables 4 and 7**, at an annealing temperature of 54$^{o}$C. Following confirmation of the successful amplification with agarose gel electrophoresis (see section **3.3.6**), the PCR product was digested with *Dpn*I (New England Biolabs$^{®}{}_{Inc.}$), and subsequently, gel purified using the Thermo Scientific GeneJET Gel Extraction kit (see section **3.3.7**). Next, the 3'-*HIS1* region was amplified from the genome of *C. krusei*, using the same kit as above, at an annealing temperature of 62.6$^{o}$C, with primer pair CK-3' HIS1-overlap-1F and CK-3' HIS1-overlap-1R. These two primers were designed to overlap with pADH147 plasmid to allow cloning of amplified 3'-*HIS1* region into the plasmid. The successful amplification of the CK 3'-*HIS1* fragment was confirmed using agarose gel electrophoresis; the amplicon was subsequently gel extracted and purified. The resulting purified amplicon was cloned into the linearised pADH147 fragment (**Fig. 5**) using the NEBuilder® HiFi DNA Assembly kit (see section **3.3.9**), and transformed into competent *E. coli* cells (see section **3.3.10**). Following transformation, plasmids were extracted from selected colonies using lysis by boiling protocol (see subsection **3.3.11.1**), and were screened for anticipated inserts by double digests with *Bgl*I and *Hind*III (Fermentas). Subsequently, anticipated plasmids were extracted, and purified from another group of selected colonies (suspected to be containing the anticipated plasmid based on the profile obtained after restriction digests with *Bgl*I and *Hind*III) but this time with the Thermo Scientific GeneJET Plasmid Miniprep kit (see section **3.3.11.1**). The purified plasmids were double-digested with *Bgl*I and *Hind*III (Fermentas), and their profiles reconfirmed using gel electrophoresis (A reaction with no plasmid and one with the original pADH147 plasmid were included as negative and positive controls, respectively). Following this, the concentration of the purified plasmid CK pADH147 was checked, and the plasmid was stored at -20$^{o}$C until future use.

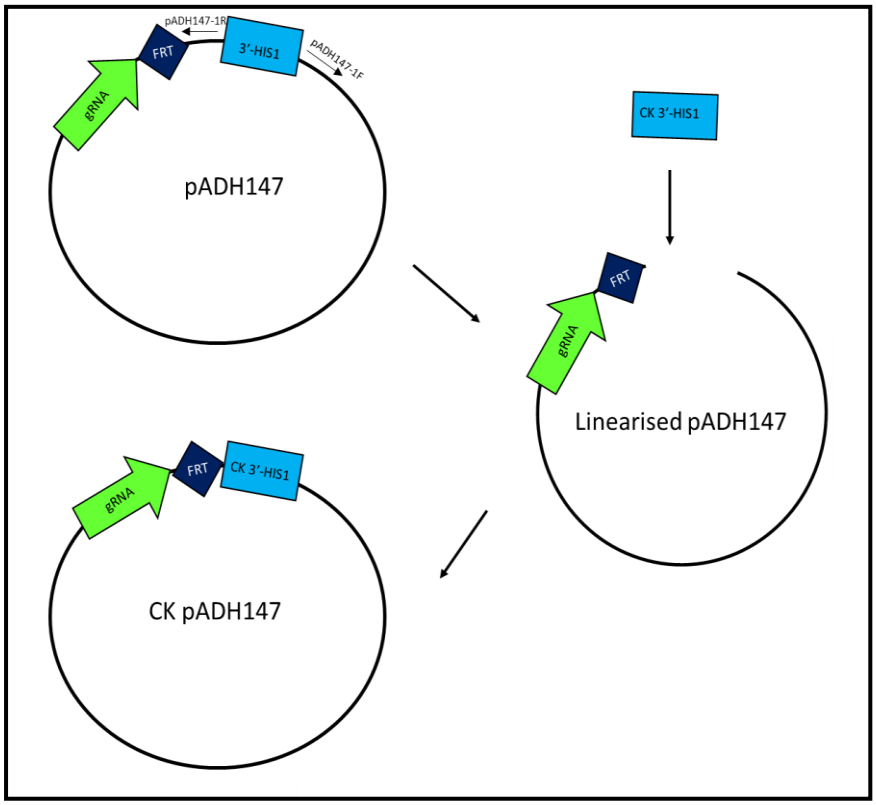


**Fig. 5** A workflow for the preparation of CK pADH147 plasmid. First, the plasmid was amplified with two primers to linearise it and release *C. albicans* 3'-*HIS1* region. Next, the linearised plasmid is cloned with amplified CK 5'-*HIS1* fragment to create an intact CK pADH147 plasmid. NB: Shapes not drawn to scale.

### 3.3.14 Validation of the system

Following the adaptation of the CRISPR-Cas9 plasmids for *C. krusei*, the efficacy of the system for gene-editing in this yeast was verified by targeting two auxotrophic marker genes, *URA3* and *ADE2*.

#### 3.3.14.1 Deletion of *URA3* gene

##### 3.3.14.1.1 Construction of CRISPR-Cas9 cassettes for the deletion of *URA3* gene

The Cas9 cassette (**Fig. 6A**) was liberated from CK pADH99 by digesting 2 µg concentration of the plasmid with restriction enzyme *Mss*I (Thermo Scientific) (see section **3.3.8**). Successful digestion was confirmed with agarose gel electrophoresis (see section **3.3.6**). The first component (Fragment A) of the gRNA cassette was amplified from pADH110, with primer pair AHO1096-ver2 and AHO1098-ver2 (**Table 2**), at an annealing temperature of 53.8ºC, using the reaction mixture and PCR program of KOD Hot Start DNA polymerase kit (Novagen®) (**Tables 5, 8**) (**Fig. 6B**). The second part (Fragment B, *URA3*-specific) of the gRNA cassette was amplified from CK pADH147 with oligonucleotide URA3-CRISPR-1 and primer AHO1097 with the same kit using touch down PCR (**Fig. 6B**). The URA3-CRISPR-1 oligo (alias URA3-specific gRNA oligo) contains a unique 20 bp CRISPR site or target sequence (5'-ATTGCGCAACACGATATGGG-3') complementary to a site present only within *URA3* gene in the entire genome of *C. krusei* UFS Y-0217 (Douglass et al. 2018). The CRISPR site was

identified with Geneious® 11.1.4, and was selected because it contains a protospacer adjacent motif (PAM) site, has high on-site activity score of 0.787 (Doench et al. 2014) and off-target activity score of 100% (Hsu et al. 2013). The 20 bp CRISPR site (without the PAM site) within the oligo is flanked by 5'-CGTAAACTATTTTTAATTTG-3' and 5'-GTTTTAGAGCTAGAAATAGC-3' complementary to 3' end of *SNR52* promoter (within pADH110) and 5' end of gRNA scaffold (within CK pADH147), respectively, to enable the generation of the full *URA3*-gRNA cassette. Using stitching PCR, Fragments A and B were fused with primer pair AHO1237 and CK-3' HIS1-R, at an annealing temperature of 54.3$^{o}$C to generate a complete gRNA cassette (Fragment C) (**Fig. 6C**). Successful amplification of these fragments was confirmed with agarose gel electrophoresis.

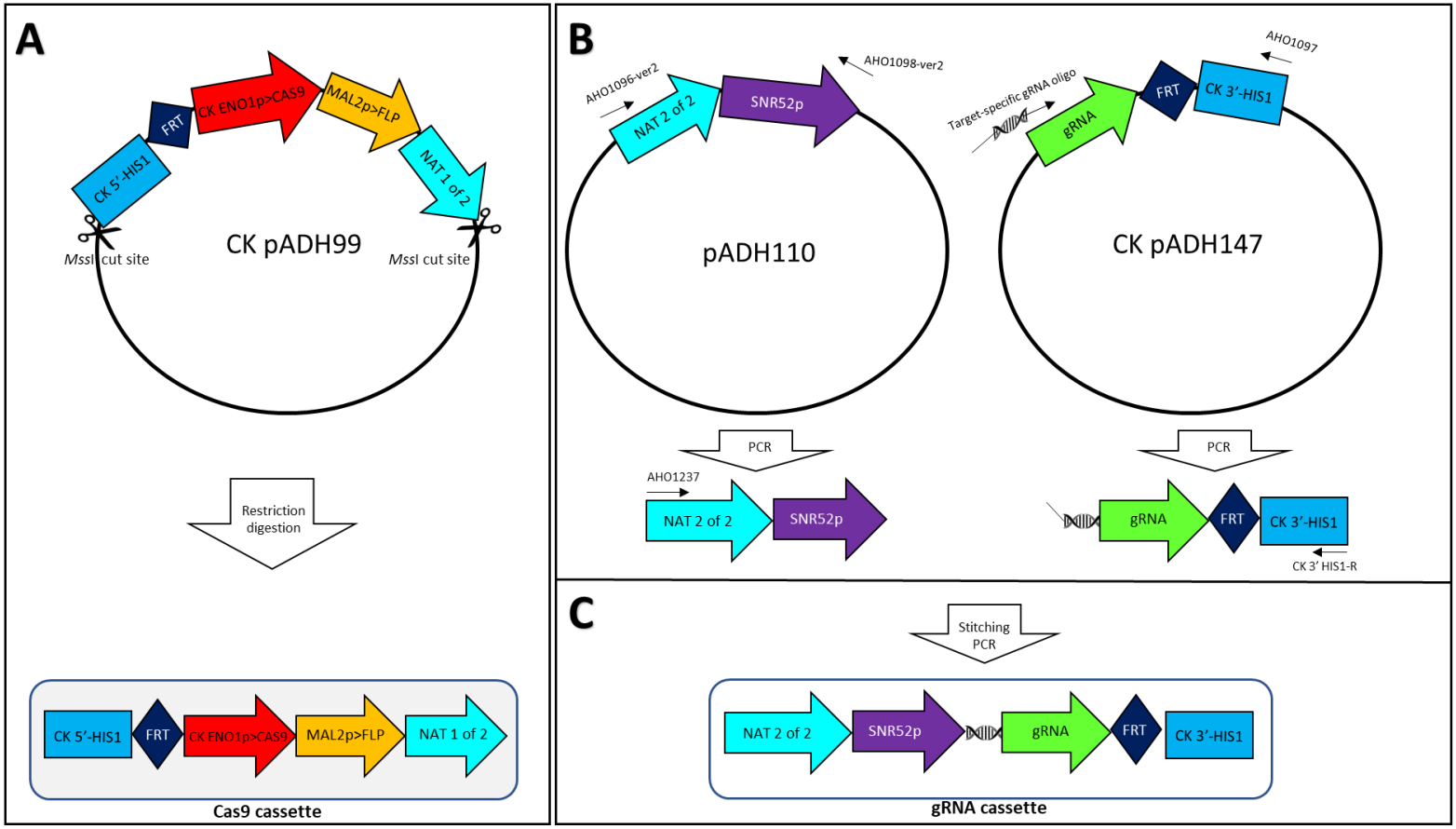


**Fig. 6** A flow chart of the steps followed to construct Cas9 and gRNA expression cassettes. (**A**) CK pADH99 plasmid is digested with restriction enzyme *Mss*I to generate an intact Cas9 cassette (**B**) The 5' (Fragment A) and 3' (Fragment B) regions of the gRNA cassette are prepared from pADH110 and CK pADH147, respectively, by PCR with appropriate primers and oligonucleotide. Note that the gRNA oligo is customised for each target. (**C**) The complete gRNA expression cassette is generated via ligation of Fragments A and B with stitching PCR.

### 3.3.14.1.2 Design and synthesis of *URA3* donor DNA

A full *URA3* dDNA was designed as described in **Figure 7**. The first part (Fragment 1) of *URA3* dDNA was amplified from the genome of *C. krusei* with primer pair URA3-2F and URA3-2R at an annealing temperature of 50.6$^{o}$C using the reaction mixture and PCR program of KOD Hot Start DNA polymerase kit supplied in **Tables 5 and 8**. The second fragment (Fragment 2) of the dDNA was amplified with primers URA3-3F and URA3-3R, at an annealing temperature of 53.3$^{o}$C with the same kit. Primers URA3-2R and URA3-3F share a 20 bp overlap sequence to aid ligation of the amplified fragments. Further, the full *URA3* dDNA was synthesised by fusing the two overlapping fragments in a stitching PCR with primer pair URA3-2F and URA3-3R, at an annealing temperature of 50.6$^{o}$C. Correct amplification of all amplicons was checked with agarose gel electrophoresis.

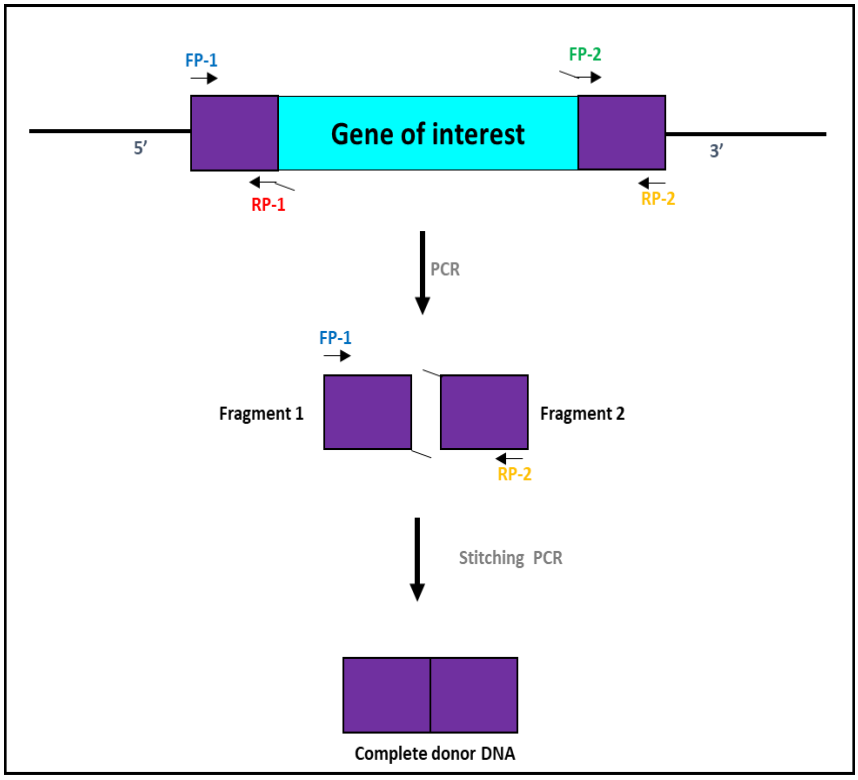


**Fig. 7** A schematic representation of the steps followed to design a donor DNA. First, fragment 1 of the dDNA is amplified from the genome of *Candida krusei* with FP-1 (forward primer-1) and RP-1 (reverse primer-1). Next, fragment 2 is synthesised with FP-2 (forward primer-2) and RP-2 (reverse primer-2). Finally, the two overlapping fragments are stitched with FP-1 and RP-2 to generate a full donor DNA.

### 3.3.14.1.3 Transformation of *URA3*-specific fragments into *C. krusei*

The co-transformation of *URA3* dDNA fragment, Cas9 cassette, and *URA3*-specific gRNA cassette into *C. krusei* was done following a modified protocol of Nguyen and co-workers (2017). Briefly, an overnight 5 ml YPD culture of *C. krusei* UFS Y-0217 was diluted in a fresh YPD broth at 1:50, incubated at 30$^{o}$C with shaking and allowed to reach $OD_{600}$ between 0.5 to 0.8. The cells were washed twice with milliQ water and re-suspended in 1/100 of the original volume. A 50 µl volume each of re-suspended cells, Cas9 cassette, full *URA3*-specific gRNA

cassette, and complete *URA3* dDNA fragment was mixed by gentle flicking with 1 ml plate mix [875 µl 50% PEG 3350 (Sigma-Aldrich), 100 µl 10X TE buffer, 25 µl 1 M Lithium acetate (adjusted to pH 7 with acetic acid; Sigma-Aldrich)] and incubated overnight at 30°C without shaking. In the following day, cells were heat-shocked (15 min, 44.6$^{o}$C), washed with sterile YPD, allowed to recover (5 h at 30$^{o}$C with shaking), plated onto YPD agar plate supplemented with 400 µg/ml NTC and incubated at 30$^{o}$C for 2 to 3 days for colonies formation.

#### 3.3.14.1.4 Selection and confirmation of *ura3*Δ/Δ mutant

Following transformation, visible colonies were selected, and replica plated on a new YPD plate (+ 600 µg/ml NTC) and a minimal medium lacking uracil plate [1.7 g/l YNB w/o amino acids and ammonium sulphate, glucose 20 g/l, 0.6 g/l Complete Supplement Mixture (CSM) w/o His-Leu-Trp-Ura, 5 g/l ammonium sulphate, 0.2 g/l histidine, 1 g/l leucine, 0.2 g/l tryptophan, 17 g/l agar], and incubated at 30$^{o}$C for 24 h (wildtype was included as control). Following incubation, colonies that showed no growth on the uracil-deficient medium upon comparison with the YPD plate were regarded as putative *ura3*Δ/Δ mutants. The genotype of these mutants was confirmed with PCR genotyping by amplifying the *URA3* dDNA. Genomic DNA of the mutants was extracted (see subsection **3.3.5.2**) and used as template. *URA3* dDNA was amplified with primer pair URA3-2F and URA3-3R, using the PCR program and reaction component of KAPA Taq PCR kit. Further, the morphological properties of the mutant and wildtype colonies were compared. The microscopic differences between the mutant and wildtype cells were also analysed with light microscopy.

### 3.3.14.2 Deletion of *ADE2* gene

#### 3.3.14.2.1 Construction of CRISPR-Cas9 cassettes for the deletion of *ADE2* gene

The Cas9 cassette (**Fig. 6A**) was removed from plasmid CK pADH99 as earlier described (see **3.3.14.1.1**). The first component (Fragment A) of the gRNA cassette was also prepared as previously described (**Fig. 6B**). However, this time, the second part (Fragment B) of the gRNA cassette was amplified from CK pADH147 with oligonucleotide ADE2-CRISPR-2 and primer AHO1097 (**Fig. 6B**). The ADE2-CRISPR-2 oligo (alias ADE2-specific gRNA oligo) contains a unique 20 bp target sequence (5'-TTAGGGTCTGATGTGCCAAA-3') complementary to a sequence within *ADE2* in the genome of this yeast (Douglass et al. 2018). This CRISPR site was identified as described earlier and had on-target activity and off-target scores of 0.864 and 100%, respectively. Further, an intact gRNA cassette (Fragment C) was generated by ligating Fragments A and B with primer pair AHO1237 and CK-3' HIS1-R using stitching PCR (**Fig. 6C**).

#### 3.3.14.2.2 Design and synthesis of *ADE2* donor DNA

A complete *ADE2* dDNA was designed as illustrated in **Figure 7**. Briefly, the first part (Fragment 1) of *ADE2* dDNA was amplified from the genome of *C. krusei* with primer pair

ADE2-2F and ADE2-2R at an annealing temperature of 55.5°C using the reaction mixture and PCR condition of KOD Hot Start DNA polymerase kit. Using the same kit, the second fragment (Fragment 2) of the dDNA was amplified with primers ADE2-3F and ADE2-3R_new at an annealing temperature of 50.7°C. Primer pair ADE2-2R and ADE2-3F share a 20 bp overlap to aid fusion of the amplified fragments. Subsequently, an intact *ADE2* dDNA was synthesised by ligating the two overlapping fragments in a stitching PCR with primer pair ADE2-2F and ADE2-3R_new at an annealing temperature of 50.7°C. Correct amplification of all amplicons was confirmed with agarose gel electrophoresis.

#### 3.3.14.2.3 Transformation of *ADE2*-specific fragments into *C. krusei*

The co-transformation of *C. krusei* with *ADE2*-specific gRNA cassette, *ADE2* dDNA fragment, and Cas9 cassette was done as described earlier. Briefly, an overnight culture of *C. krusei* UFS Y-0217 diluted at 1:50 was incubated at 30°C with shaking, allowed to reach $OD_{600}$ between 0.5 to 0.8, washed twice with milliQ water and re-suspended in 1/100 of the original volume. A 50 µl volume each of the re-suspended cells, Cas9 cassette, intact *ADE2*-specific gRNA cassette, and complete *ADE2* dDNA fragment was gently mixed with 1 ml plate mix and incubated overnight at 30°C without shaking. Following this, cells were heat-shocked at 44.6°C for 15 min, washed with sterile YPD, allowed to recover at 30°C for 5 h with shaking, plated onto YPD agar plate supplemented with 400 µg/ml NTC and incubated at 30°C for 2 to 3 days for colonies formation.

#### 3.3.14.2.4 Selection and confirmation of *ade2*Δ/Δ mutant

Following transformation, visible colonies were selected and replica plated on a new YPD plate (+ 600 µg/ml NTC) and a minimal medium lacking adenine plate [1.7 g/l YNB w/o amino acids and ammonium sulphate, glucose 20 g/l, 5 g/l ammonium sulphate, 0.3 g/l isoleucine, 1.5 g/l valine, 0.2 g/l arginine, 0.3 g/l lysine, 0.2 g/l methionine, 0.5 g/l phenylaIanine, 2 g/l threonine, 0.3 g/l tyrosine, 0.2 g/l uracil, 0.2 g/l histidine, 1 g/l leucine, 0.2 g/l tryptophan, 17 g/l agar] and incubated at 30°C for 24 h (wildtype was included as control). Following incubation, colony displaying reddish/pinkish phenotype on the adenine-deficient medium was considered *ade2*Δ/Δ mutant. PCR genotyping via the amplification of *ADE2* dDNA with primers ADE2-2F and ADE2-3R was implemented to confirm the genotype of the mutant. Further, the macroscopic and microscopic properties of the mutant and wildtype colonies were juxtaposed with unaided eyes and light microscopy, respectively.

### 3.3.15 Removal of CRISPR-Cas9 cassette

The CRISPR-Cas9 cassette was removed with growth in a maltose-supplemented media. Briefly, mutant cells were inoculated into a yeast extract peptone maltose (YPM) broth (10 g/l yeast extract, 20 g/l peptone, 20 g/l maltose) and were incubated at 30°C for 24 h with shaking. The resulting culture was diluted to $10^{-5}$ and plated onto YPD agar plates (30°C, 1 - 2 days).

Colonies obtained were re-streaked onto YPD plates (+ 600 µg/ml NTC) and incubated for 24 h at 30$^{o}$C to confirm the successful removal of the cassette.

## 3.4 Results and Discussions

### 3.4.1 Constructing a HIS-FLP type CRISPR-Cas9 system for *C. krusei*

Due to its high precision, low cost, simplicity, high efficiency, and great adaptability relative to other gene-engineering tools, the CRISPR-Cas9 system has been harnessed at an explosive rate for gene-editing in virtually all cell types, including many fungi since its evolution as a genome-editing tool (Adli 2018; Román et al. 2019). However, this system has not been customised for use in *C. krusei*. The absence of a simple, precise, and efficient tool like CRISPR technology for gene-editing in this recalcitrant yeast has greatly hampered the full molecular understanding of its resistance mechanisms, knowledge which is important for the preservation of the current antifungal arsenal and development of novel therapeutic interventions.

A functional CRISPR-Cas9 system was developed for *C. krusei* by adapting a system previously developed for use in *C. albicans*. In their study, Nguyen and co-workers (2017) designed two types of CRISPR systems, LEUpOUT and HIS-FLP. Both types utilise a recyclable CRISPR-Cas9 cassette and *NAT* marker and support homozygous genome editing in any strain of *C. albicans* that is NTC-sensitive. One bottleneck of the LEUpOUT system is that it can only be utilised in strains that are heterozygous for the *LEU2* gene (i.e. *LEU2*/*leu2Δ* mutant in case of a diploid strain). Due to this limitation, and because of our intention to perform gene-editing in a diploid *C. krusei* strain (2n), we resorted to using the HIS-FLP system, which is suitable for any strain. This system relies upon the FLP/FRT recombination system and was designed to integrate at the *HIS1* locus within the genome of *C. albicans*. The HIS-FLP system takes advantage of two cassettes; the Cas9 and gRNA cassettes. The Cas9 cassette is contained within the pADH99 plasmid and consists of the *ENO1* promoter linked to the Cas9 gene. The gRNA cassette is contained within pADH110 and pADH147. The co-transformation of the Cas9 and gRNA cassettes generates an intact CRISPR-Cas9 cassette with a full *NAT* marker gene that integrates at the *HIS1* locus of *C. albicans* by the 5'-*HIS1* and 3'-*HIS1* (integration) regions that flank the cassette. Following gene-editing by the RNA-guided Cas9 nuclease, the cassette is easily removed upon induction of the *FLP* recombinase with growth on a maltose-containing medium.

However, to optimise and utilise this system for genome editing in *C. krusei*, it was necessary to replace some of its components with homologous fragments from this yeast.

#### 3.4.1.1 Adapting pADH99 plasmid

The pADH99 plasmid contains a *C. albicans* 5'-*HIS1* integration region which, together with the 3'-*HIS1* region, is necessary for the integration of the CRISPR-Cas9 cassette at the *HIS1*

locus of *C. albicans*; a *Streptococcus pyogenes CAS9* gene under the control of a *C. albicans ENO1* promoter; a part of the *NAT* marker gene, necessary for NTC-resistance (NTC$^R$) together with an overlapping portion on pADH110; and an FRT sequence required for the removal of the cassette at a later stage (**Fig. 8**).

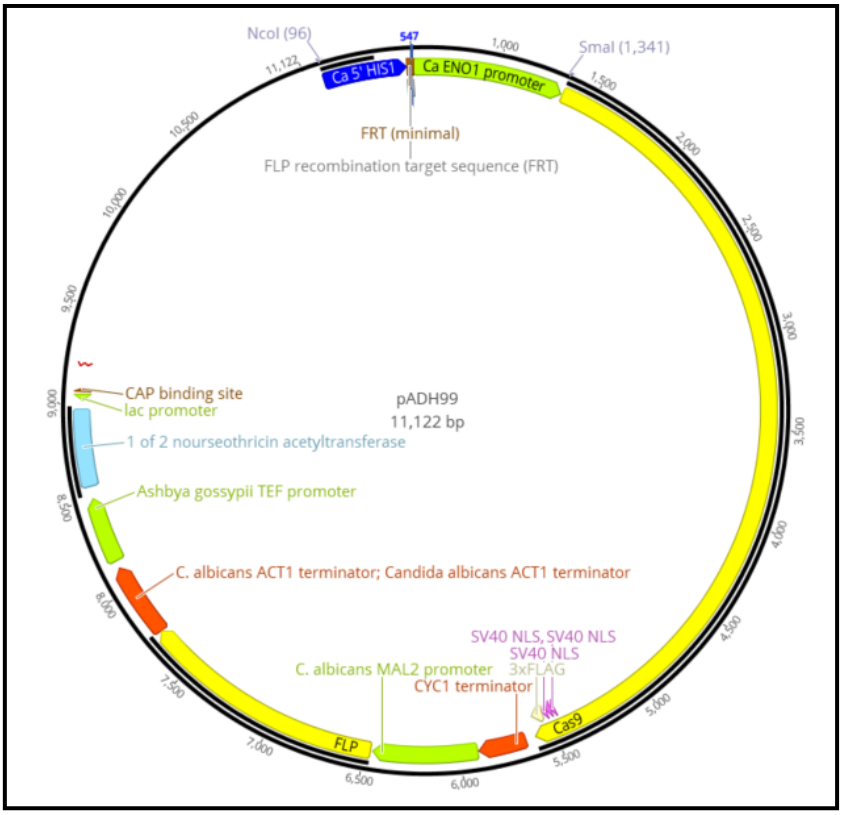


**Fig. 8** A plasmid map of pADH99 showing components such as *C. albicans* 5'-*HIS1* region, flippase recognition target (FRT) region, *CAS9* gene under the control of *C. albicans ENO1* promoter, and an overlapping portion of the nourseothricin N-acetyltransferase (*NAT*) marker gene. The plasmid map also indicates the *Nco*I and *Sma*I restriction sites used to remove the *C. albicans* HIS1-FRT-ENO1 region.

The customisation of the plasmid for use in *C. krusei* entailed replacing the *C. albicans* 5'-*HIS1* and *ENO1* promoter regions with 5'-*HIS1* and *ENO1* promoter regions from *C. krusei*. Substitution with *C. krusei* 5'-*HIS1* region was necessary to allow the integration of the CRISPR system into the genome of *C. krusei*. Further, the *ENO1* promoter of *C. krusei* was used to express the *CAS9* gene since species-specific promoters have been demonstrated to optimise the activity of the Cas9 nuclease (Lombardi et al. 2017; Norton et al. 2017).

The adaptation process started by double digesting the pADH99 with *Nco*I and *Sma*I restriction enzymes. This process linearised the plasmid (~9877 bp) and liberated the *C. albicans* HIS1-FRT-ENO1p region (~1245 bp) within it (**Fig. 9**).

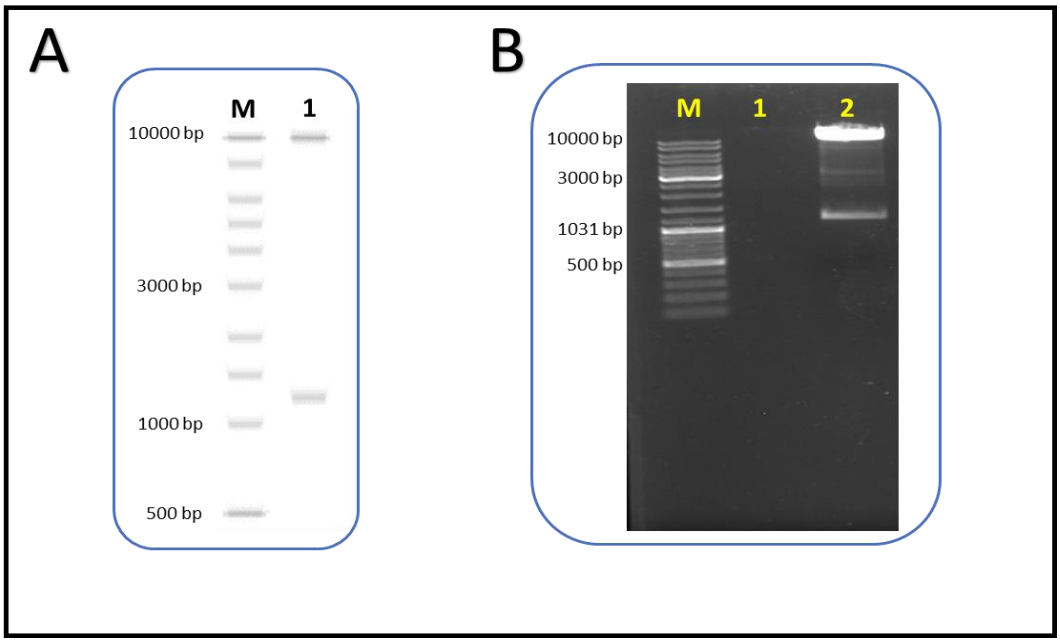


**Fig. 9** Profile of pADH99 plasmid digested with *Nco*I and *Sma*I restriction enzymes. (**A**) Profile obtained after an *in silico* digestion analysis of the plasmid (Lane 1). (**B**) Profile obtained after digesting the plasmid *in vitro* (Lane 2). Expected band sizes of 9877 bp and 1245 bp that represent plasmid backbone and removed HIS1-FRT-ENO1 region, respectively, were obtained. M represents the DNA ladder. Lane 1 in the *in vitro* gel is empty.

In order to replace the removed HIS1-FRT-ENO1p region, the 5'-*HIS1* region was first amplified from the genome of *C. krusei* with primers pADH99-5' CK HIS1 overlap-F and CK-5' HIS1-R. As depicted in **Figure 10**, the expected band size of ~522 bp was obtained. Moreover, the amplified product shares about 19 bp overlap sequence with pADH99 to aid its ligation into the plasmid. Next, the *ENO1* promoter was amplified from the yeast's genome with primer pair CK ENO1-F and pADH99-3'-CK CAS9 overlap. The expected band size of ~806 bp was obtained, as shown in **Figure 11**. Additionally, the amplicon generated shares a 25 bp overlap sequence with *CAS9* gene to streamline cloning into the linearised pADH99 plasmid.

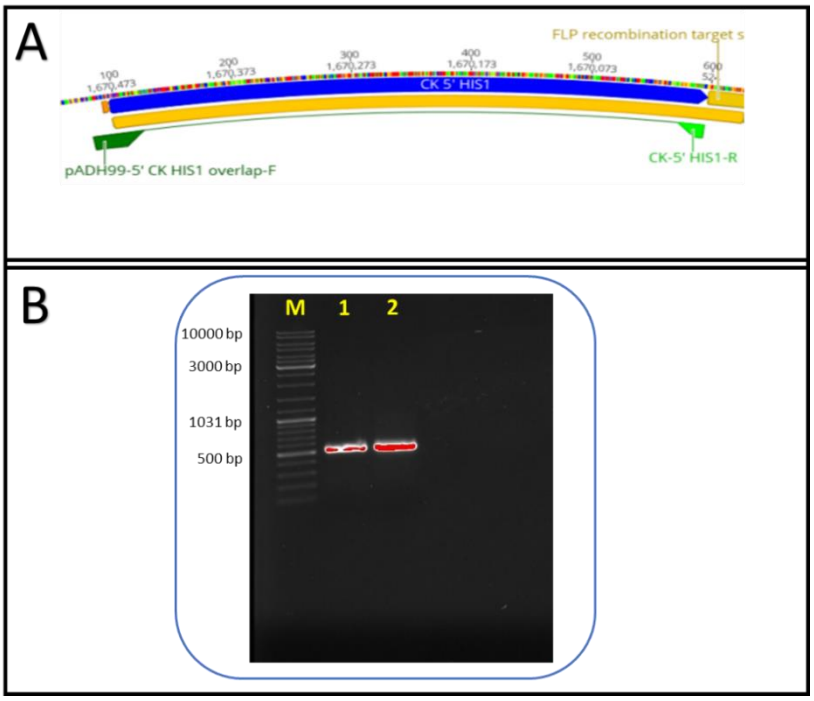


**Fig. 10** Amplification of 5'-*HIS1* region of *Candida krusei*. (**A**) A map depicting the 5'-*HIS1* region and primers used for its amplification. (**B**) A gel profile indicating successful amplification of the 5'-*HIS1* region (~522 bp; Lanes 1 and 2).

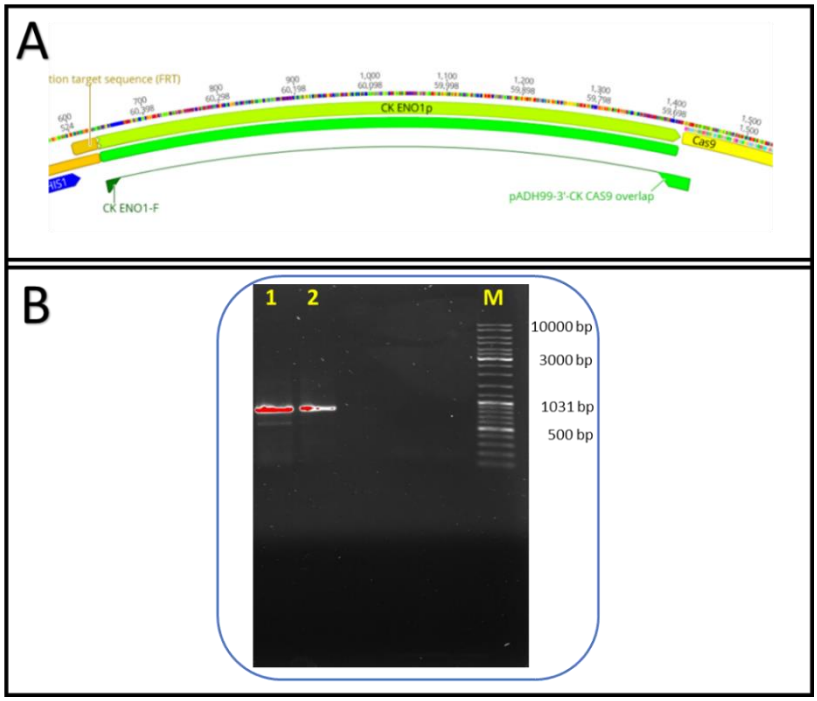


**Fig. 11** Amplification of *ENO1* promoter region of *Candida krusei*. (**A**) A map depicting the *ENO1* promoter region and primers used for its amplification. (**B**) A gel profile showing successful amplification of the *ENO1* promoter region (~806 bp; Lanes 1 and 2).

Further, two overlapping oligonucleotides, pADH99::CK HIS1::FRT overlap and pADH99::CK FRT::ENO1 overlap were used to synthesise the FRT fragment of approximately 85 bp (**Fig. 12**). The synthesised fragment is flanked by regions homologous to the 3' region of CK 5'-*HIS1* and 5' region of CK *ENO1*p fragments, respectively, necessary to link these two fragments.

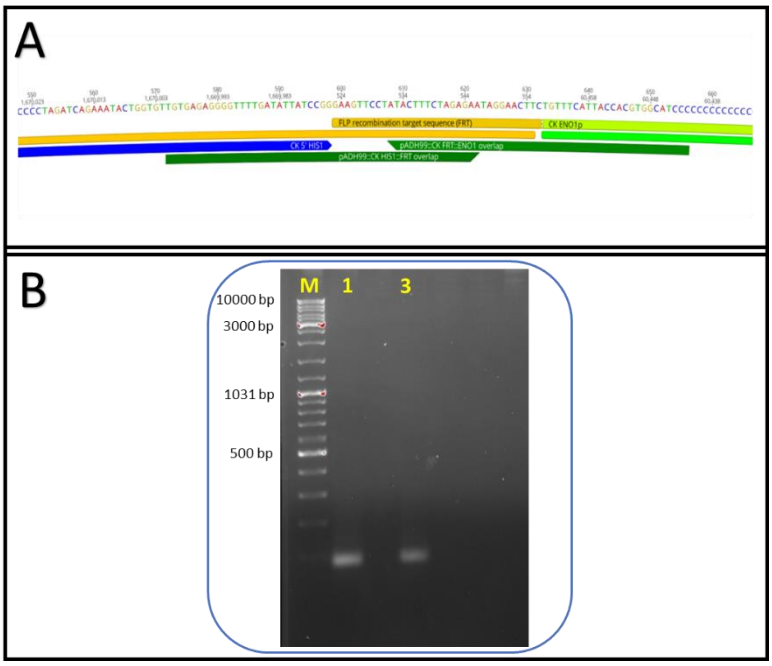


**Fig. 12** Synthesis of flippase recognition target (FRT) fragment. (**A**) Schematic depicting the FRT region and oligonucleotides used for its polymerisation. Oligonucleotides, pADH99::CK HIS1::FRT overlap and pADH99::CK FRT::ENO1 overlap, overlap with CK 5'-*HIS1* and CK *ENO1*p fragments, respectively (**B**) Gel profile indicating successful amplification of the FRT fragment (~85 bp; Lanes 1 and 3).

After confirming the successful amplification of these fragments with agarose gel electrophoresis, they were purified and integrated into the linearised pADH99 with NEBuilder® HiFi DNA Assembly kit in a single reaction. Gel purification prior to assembly was essential for improved assembly and transformation efficiency. The complete construct was transformed into competent *E. coli* cells. Transformed colonies were screened for anticipated plasmid with restriction digest using *Xba*I and *Bam*HI enzymes in two separate reactions. As depicted in **Figures 13 and 14**, plasmid profiles obtained after restriction digests revealed successful assembly and cloning, as well as the successful adaptation of pADH99 for use in *C. krusei*. The new construct was purified and denominated as CK pADH99.

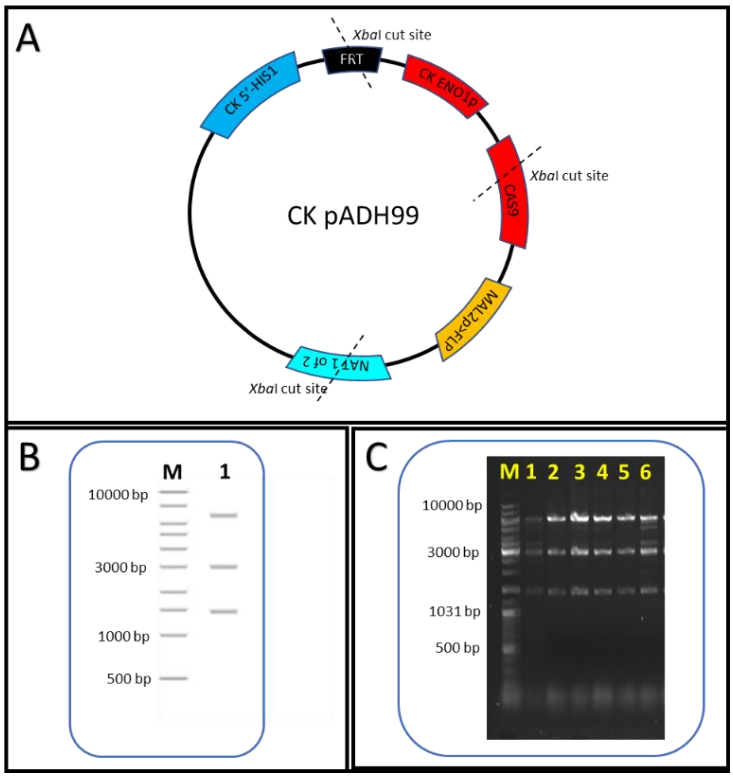


**Fig. 13** Screening of transformants for CK pADH99 plasmid with *XbaI* restriction enzyme (**A**) Physical map of CK pADH99 depicting cut sites of *Xba*I restriction enzyme (not drawn to scale). (**B**) Restriction digest profile obtained *in silico*. (**C**) Profile obtained after *in vitro* restriction digest assay. Expected band sizes of 6757 bp, 2981 bp, and 1457 bp were obtained. M represents the DNA ladder.

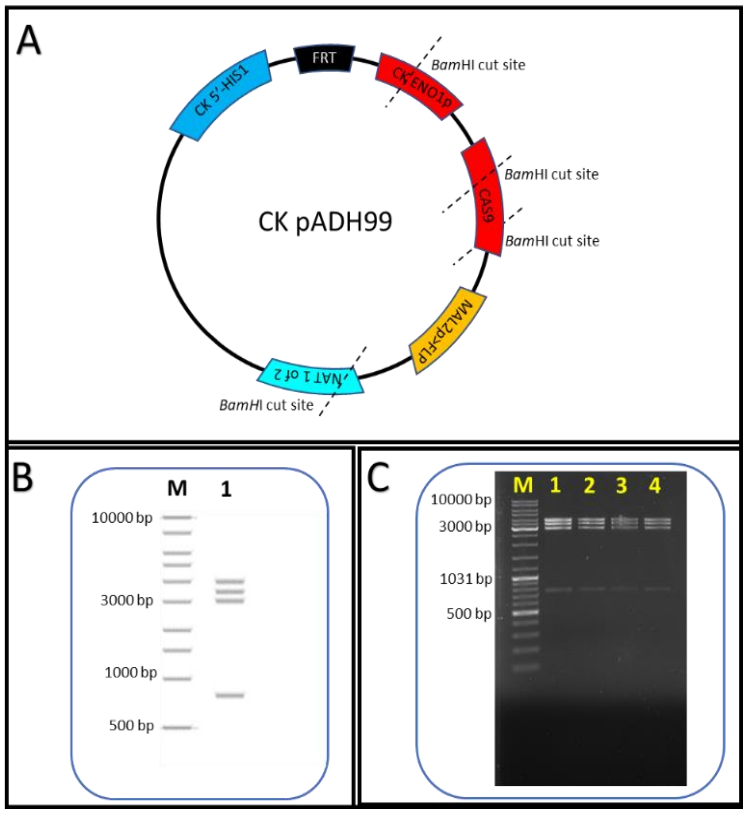


**Fig. 14** Screening of transformants for CK pADH99 plasmid with *BamHI* restriction enzyme (**A**) Physical map of CK pADH99 depicting the cut sites of *BamHI* restriction enzyme (not drawn to scale). (**B**) Restriction digest profile obtained *in silico*. (**C**) Profile obtained after *in vitro* restriction digest assay. Expected band sizes of 3976 bp, 3132 bp, 3004 bp, and 783 bp were obtained. M represents the DNA ladder.

### 3.4.1.2 Propagating pADH110

The pADH110 plasmid (**Fig. 15**) contains an overlapping portion of the *NAT* marker gene and a *C. albicans SNR52* promoter that regulates the expression of gRNA. Although the RNA pol III *SNR52* promoter of *C. albicans* is well characterised, identifying the uncharacterised *SNR52* promoter of any organism is difficult, especially because it does not get translated into protein. This process could be partly simplified with the availability of transcriptome data to guide the promoter's search (Morio et al. 2020); however, such data is currently unavailable for *C. krusei*. Further, there is evidence that supports the usage of slightly-related species promoter to drive the expression of gRNA (Fuller et al. 2015; Matsu-ura et al. 2015). Because of this, we reasoned that the CRISPR system should work in *C. krusei* with the *C. albicans SNR52* promoter; hence the promoter was not replaced. Instead, we propagated the pADH110 plasmid in competent *E. coli* cells to obtain enough concentration for further downstream experiments.

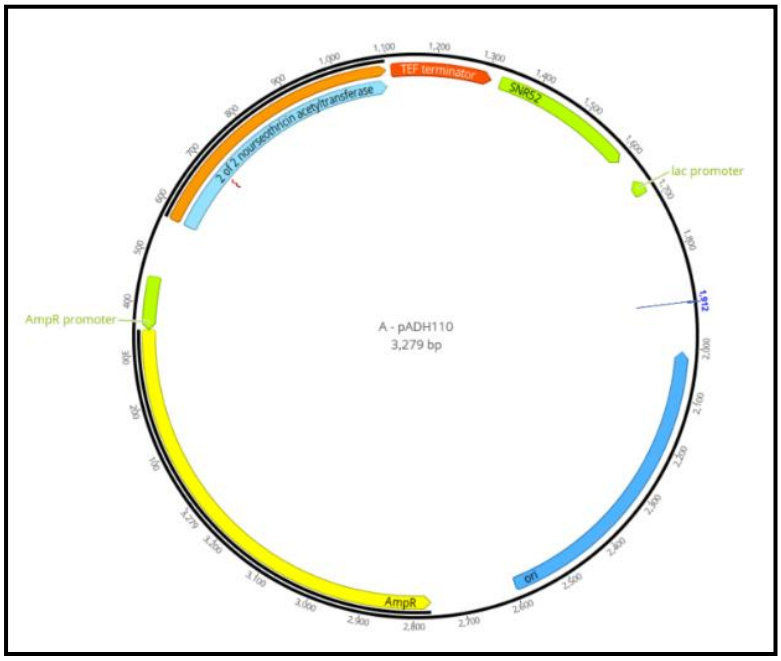


**Fig. 15** A map of pADH110 plasmid depicting an overlapping portion of the nourseothricin N-acetyltransferase (*NAT*) marker gene and *SNR52* promoter (of gRNA).

### 3.4.1.3 Adapting pADH147

The pADH147 (**Fig. 16**) contains the gRNA scaffold, FRT sequence, and *C. albicans* 3'-*HIS1* region which constitute the other half of a full gRNA cassette. As stated earlier, both the 5'-*HIS1* region located on pADH99 plasmid and the 3'-*HIS1* region are indispensable for the integration of the HIS-FLP system at the *HIS1* locus. Because of this, we adapted the plasmid for use in *C. krusei* by replacing the 3'-*HIS1* region of *C. albicans* with a homologous region from the *HIS1* locus of *C. krusei*.

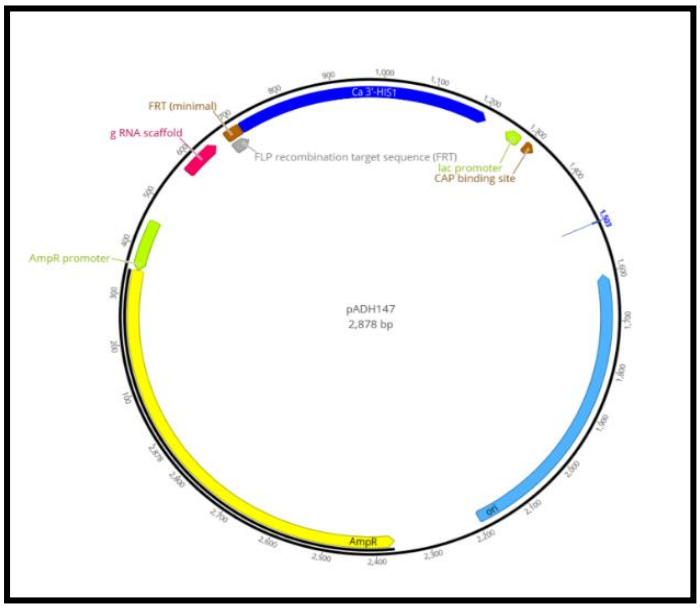


**Fig. 16** A map of pADH147 plasmid showing gRNA scaffold, flippase recognition target (FRT) region, and 3'-*HIS1* region of *C. albicans*.

Plasmid pADH147 was amplified with primer pair pADH147-1F and pADH147-1R, this linearised the plasmid, and also removed the *C. albicans* 3'-*HIS1* region. The gel profile depicted in **Figure 17B** showing a band of approximately 2383 bp (Lane 2) confirms the plasmid's successful linearisation. The generated amplicon was subsequently treated with *Dpn*I enzyme to remove plasmid template, and was gel purified for increased assembly and cloning efficiency. To replace the 3'-*HIS1* fragment, a 3'-*HIS1* region was amplified from the genome of *C. krusei* with primer pair CK-3' HIS1-overlap-1F and CK- 3' HIS1-overlap-1R. As shown in **Figure 18B**, an expected band size of approximately 551 bp was obtained. The generated amplicon shares overlaps with pADH147 to aid its cloning into the plasmid.

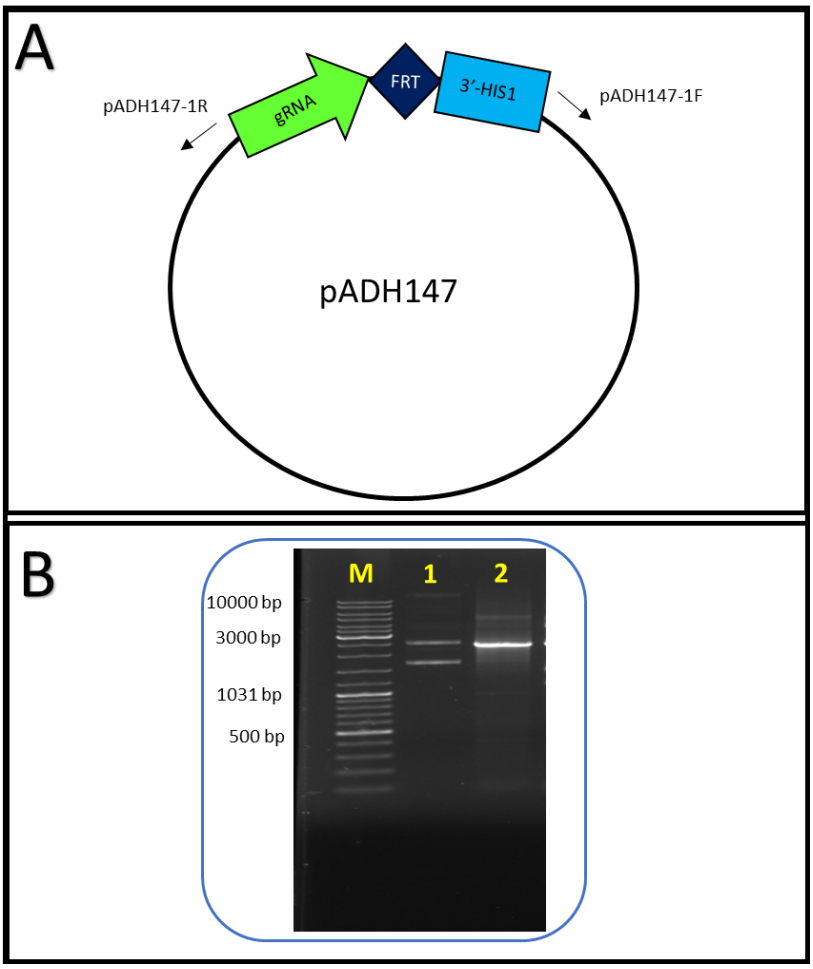


**Fig. 17** Linearisation of pADH147 (**A**) Physical map of pADH147 depicting the primers used for its linearisation (not drawn to scale). (**B**) Gel profile depicting successful linearisation of the plasmid (Lane 2; ~2383 bp). Lanes M and 1 represent the DNA ladder and negative control, respectively.

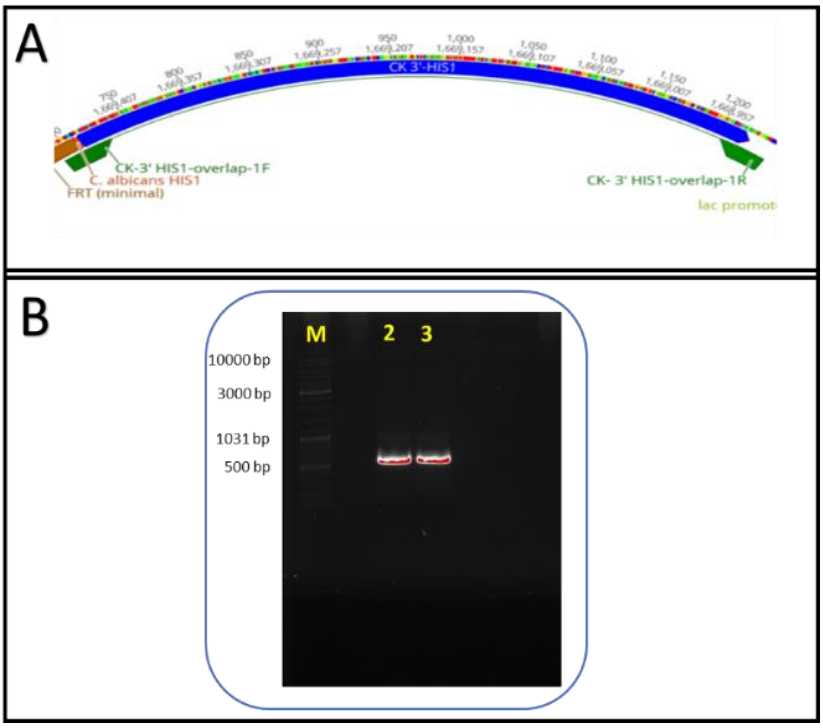


**Fig. 18** Amplification of 3'-*HIS1* region of *Candida krusei*. (**A**) A map depicting the 3'-*HIS1* region and primers used for its amplification. (**B**) A gel profile indicating successful amplification of the 3'-*HIS1* region (~551 bp; Lanes 2 and 3). M represents the DNA ladder.

The purified *C. krusei* 3'-*HIS1* region was thereafter cloned into the linearised pADH147 plasmid with NEBuilder® HiFi DNA Assembly kit and transformed into competent *E. coli* cells. Transformed colonies were screened for anticipated plasmid by double digestion with *Bgl*I and *Hind*III restriction enzymes. As depicted in **Figure 19**, band sizes of 1326 bp, 1081 bp, and 489 bp were obtained for lanes 3, 4, 5, and 6 which confirmed the success of the assembly and cloning procedures as well as the successful adaptation of the pADH147 for *C. krusei*. The new construct was purified and named as CK pADH147.

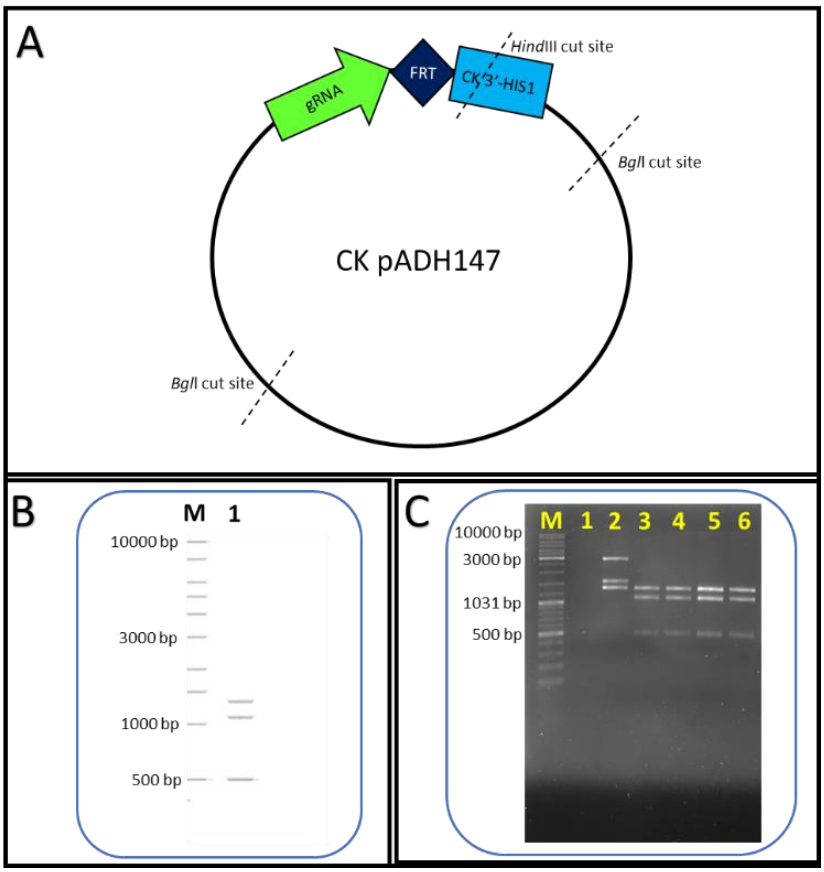


**Fig. 19** Screening of transformants for CK pADH147 plasmid with *Bgl*I and *Hind*III restriction enzymes (**A**) Physical map of CK pADH147 depicting the cut sites of *Bgl*I and *Hind*III restriction enzymes (not drawn to scale). (**B**) Restriction digest profile obtained *in silico*. (**C**) Profile obtained after *in vitro* restriction digest assay. Expected band sizes of 1326 bp, 1081 bp, and 489 bp were obtained (Lanes 3, 4, 5, and 6). M represents the DNA ladder. Lanes 1 and 2 represent negative and positive controls, respectively.

### 3.4.2 Validating the adapted system

After successfully adapting the HIS-FLP plasmids for *C. krusei*, it was important to validate the efficacy of the system for genetic engineering in this yeast. This was done by harnessing auxotrophy. Auxotrophy is a technique that has been widely used for recombinant DNA research in molecular genetics. By definition, an auxotrophic marker gene is essential for growth, and its disruption or deletion would result in the inability of an auxotrophic mutant to grow in a medium lacking an essential nutrient (Pronk 2002; Yuan 2011). This consequently allows easy identification of mutants upon replica plating (Lederberg and Lederberg 1952). The deletion of an auxotrophic marker, such as the *ADE2* gene, also produces a distinctive

phenotype in the absence of an essential nutrient. Hence, the system's efficacy was tested by targeting two auxotrophic marker genes, namely *URA3* and *ADE2*, for deletion.

The deletion of any gene using the CRISPR-Cas9 system requires two main components, the Cas9 and gRNA. In our case, the *CAS9* gene (encoding Cas9) is harboured within the Cas9 cassette located on the CK pADH99 plasmid, and the gRNA cassette is shared between pADH110 and CK pADH147. These two cassettes are co-transformed to generate a complete CRISPR-Cas9 cassette. Following the creation of double-strand breaks (DSBs) by the gRNA-guided *CAS9* nuclease, the breaks are repaired via NHEJ or HDR upon provision of a dDNA.

#### 3.4.2.1 Deleting *URA3* gene

A first approach to validate the efficacy of the adapted system involved targeting the *URA3* gene for deletion. The *URA3* gene encodes an enzyme known as orotidine 5'-monophosphate (OMP) decarboxylase, which plays a role in *de novo* pyrimidine ribonucleotide biosynthetic pathway – converts OMP to uridine monophosphate (UMP) (**Fig. 20**) (Losberger and Ernst 1989; Lay et al. 1998). The deletion or disruption of this gene consequently makes *ura3* mutants auxotrophic for uracil (uridine) biosynthesis (Lacroute 1968).

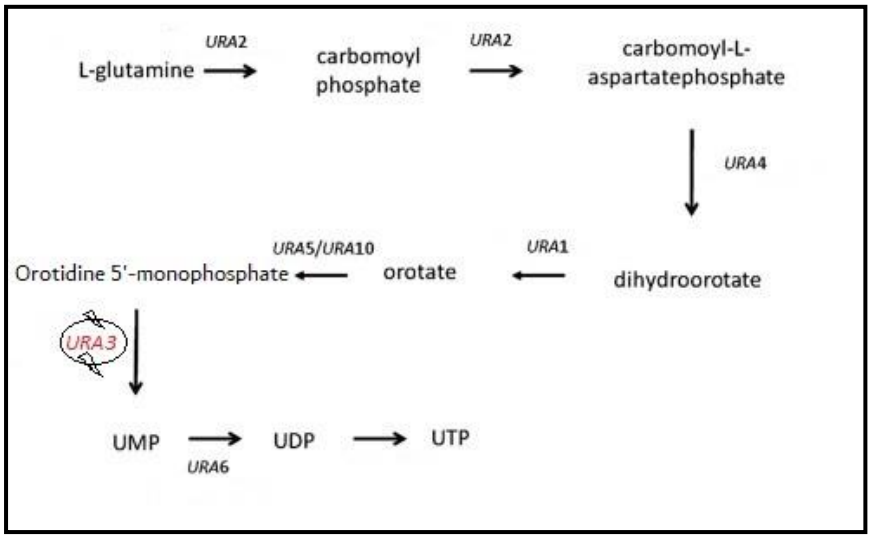


**Fig. 20** A representation of *de novo* pyrimidine ribonucleotide biosynthetic pathway. The deletion or mutation of *URA3* gene makes mutants become auxotrophic for uracil (uridine) biosynthesis (de Gontijo et al. 2014).

##### 3.4.2.1.1 Constructing CRISPR-Cas9 cassettes for deleting *URA3* gene

To delete the *URA3* gene, it was essential to first construct the CRISPR cassettes with respective plasmids. The Cas9 cassette (~8970 bp) was obtained from CK pADH99 by digesting the plasmid with *Mss*I restriction enzyme (**Fig. 21**). Using the pADH110 plasmid as a template, the first component (Fragment A) of the gRNA cassette, containing the *SNR52* promoter, was amplified with primer pair AHO1096-ver2 and AHO1098-ver2. As depicted in **Figure 22**, a band size of approximately 1066 bp obtained confirms this fragment's successful amplification.

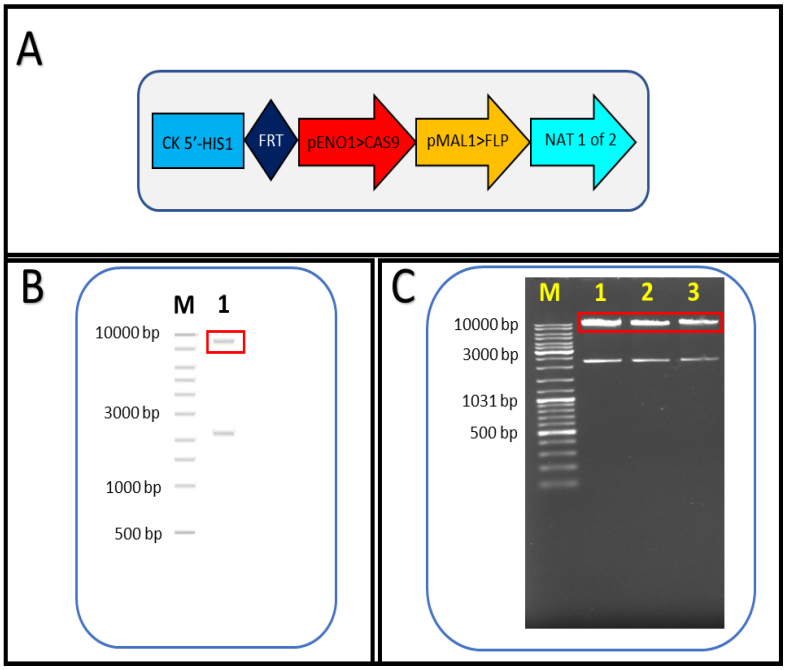


**Fig. 21** Construction of Cas9 cassette (**A**) A schematic of Cas9 cassette digested from CK pADH99 with *Mss*I restriction enzyme (**B**) Restriction digest profile obtained *in silico*. (**C**) Profile obtained after *in vitro* restriction digest assay. The expected band size of ~8970 bp (red box) represent the Cas9 cassette.

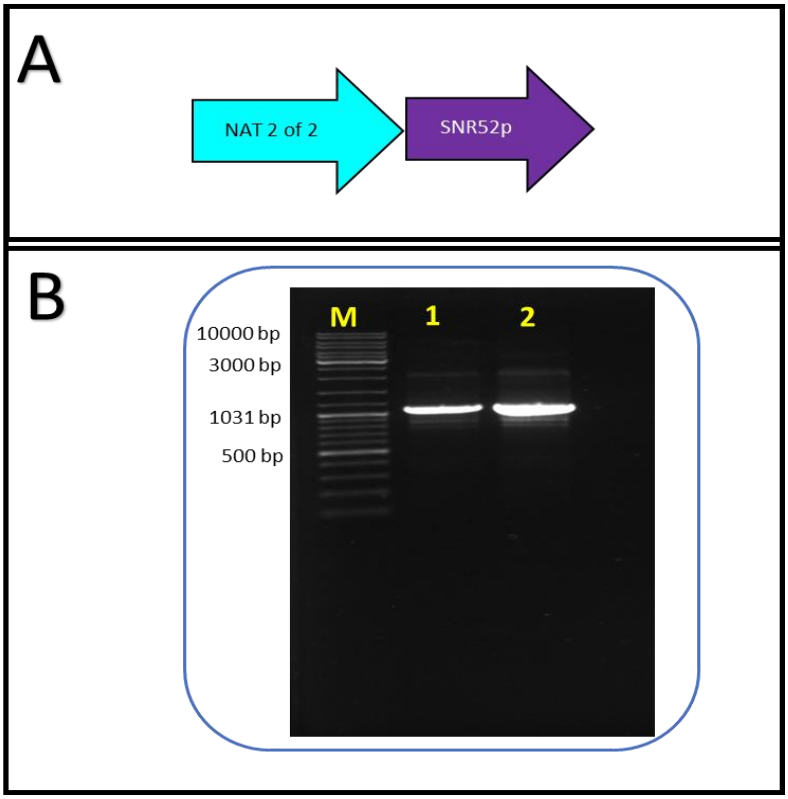


**Fig. 22** Construction of the first component (Fragment A) of gRNA cassette (**A**) A schematic of Fragment A amplified from pADH110 (**B**) Amplified product of Fragment A from pADH110. The expected band size of approximately 1066 bp was obtained.

Next, the second component (Fragment B, ~722 bp) of the gRNA cassette which contains the gRNA scaffold was amplified from CK pADH147 with a target-specific oligonucleotide URA3-CRISPR-1 and primer AHO1097. The URA3-CRISPR-1 oligo contains a 20 bp *URA3*-specific CRISPR sequence (5'-ATTGCGCAACACGATATGGG-3') which corresponds to a site within

the *URA3* gene, which is targeted and nicked by the Cas9 nuclease (**Fig. 23**). This CRISPR sequence within the oligo is flanked by regions complementary to the 3' end of *SNR52* promoter and 5' end of gRNA scaffold to enable ligation of Fragments A and B. Fragments A and B's successful ligation with stitching PCR generated an intact *URA3*-gRNA cassette (Fragment C) with a band size of approximately 1788 bp (**Fig. 24**).

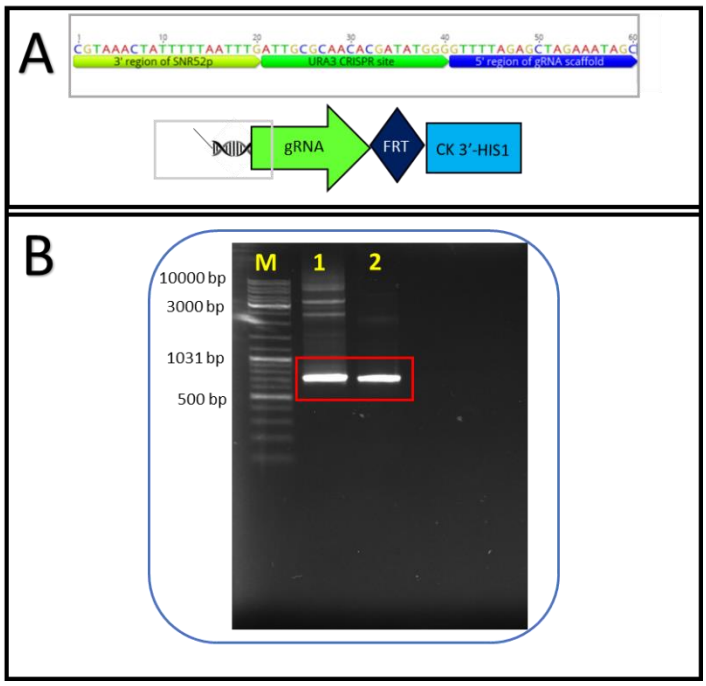


**Fig. 23** Construction of the second component (Fragment B) of gRNA cassette specific for *URA3* (**A**) A schematic of Fragment B amplified from CK pADH147. Grey box indicates CRISPR site specific for *URA3* and overlapping regions with *SNR52* promoter and gRNA (**B**) Amplified product of Fragment B from CK pADH147. Expected band size of approximately 722 bp was obtained (Red box).

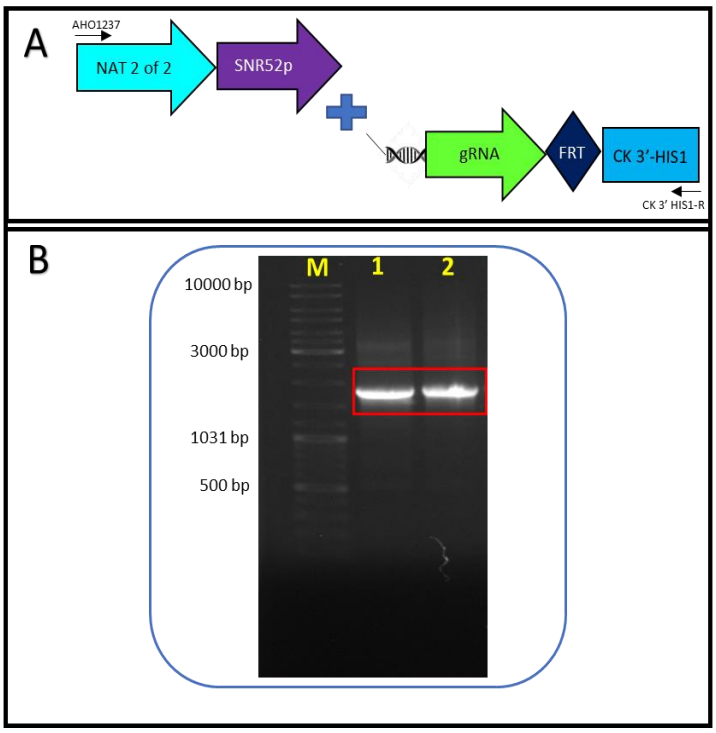


**Fig. 24** Construction of complete *URA3*-specific gRNA cassette (**A**) A schematic representing the stitching of Fragments A and B to generate full *URA3*-gRNA cassette (**B**) Gel profile depicting full *URA3*-gRNA cassette of approximately 1788 bp.

#### 3.4.2.1.2 Designing and synthesising *URA3* donor DNA

For the repair of DSBs with the HDR pathway, a dDNA is required to replace the targeted gene. The study by Vyas and co-workers (2015) with *C. albicans* demonstrated that the provision of a dDNA is important for genome engineering with CRISPR-Cas9 after obtaining targeting efficiencies of 0% and up to 80% in the absence and presence of a dDNA, respectively. A dDNA with homology arms of about 150 to 500 bp complementary to the targeted gene's flanking regions was used to replace nearly the entire ORF of the gene. The dDNA was constructed by amplifying two fragments (150 – 500 bp) that flank the gene of interest and fusing them to generate a full dDNA (**Fig. 7**). Specifically, the first part (Fragment 1) of *URA3* dDNA was amplified from the genome of *C. krusei* with primer pair URA3-2F and URA3-2R (overlap). An expected band size of approximately 209 bp was obtained (**Fig. 25A**). The second fragment (Fragment 2) of the dDNA was amplified with primer pair URA3-3F (overlap) and URA3-3R. An obtained band size of approximately 193 bp confirms this fragment's successful amplification (**Fig. 25A**). These two amplified fragments (Fragment 1 and 2) share an overlap sequence of 20 bp, when stitched with primers URA3-2F and URA3-3R a full *URA3* dDNA of approximately 382 bp was generated (**Fig. 25B**).

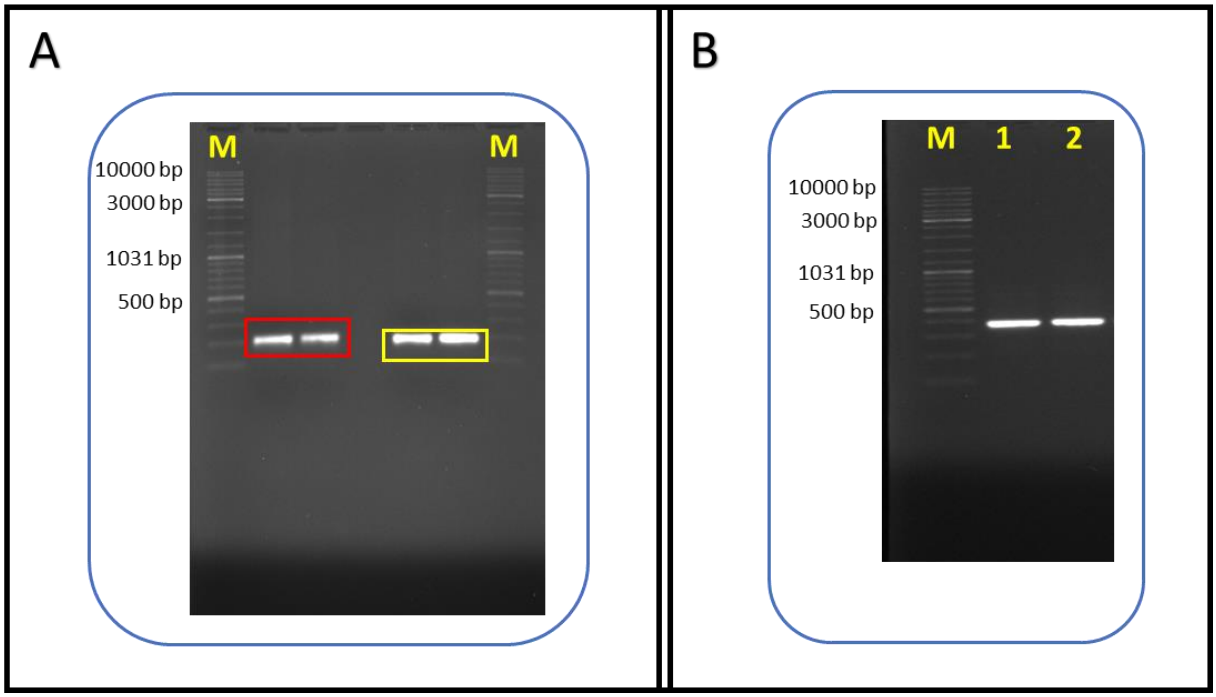


**Fig. 25** Synthesis of an intact *URA3* donor DNA (dDNA) (**A**) Gel profile showing expected band sizes of 209 bp (red box) and 193 bp (yellow box) for Fragment 1 and Fragment 2, respectively, of *URA3* dDNA (**B**) Gel profile depicting full *URA3* dDNA of an expected band size of ~382 bp (Lanes 1 and 2).

#### 3.4.2.1.3 Transforming, selecting, and confirming *ura3Δ/Δ* mutant

Upon co-transformation, into the yeast, the Cas9 cassette and the *URA3*-specific gRNA cassettes generate a complete CRISPR-Cas9 cassette which integrates at the *HIS1* locus. Successful transformants are NTC-resistant ($NTC^R$) accomplished by an intact *NAT* maker gene within the complete CRISPR-Cas9 cassette and were selected on YPD plates containing NTC. Out of 49 transformants obtained, eight were unable to grow on a minimal medium lacking uracil and were regarded as putative *ura3Δ/Δ* mutants (**Fig. 26**).

**Fig. 26** Uracil-deficient minimal medium plate with the transformed and wildtype colonies. Putative *ura3Δ/Δ* mutants showed no growth (black dotted boxes). Wildtype (green indication) and transformants with intact *URA3* gene grew on the plate.

PCR genotyping was performed, using the primers URA3-2F and URA3-3R, to confirm the genotype of the putative *ura3Δ/Δ* mutants obtained. As depicted in **Figure 27**, an expected band size of approximately 382 bp was obtained which confirms successful homozygous deletion of *URA3* gene and replacement of the gene with the supplied *URA3* dDNA in all the *ura3Δ/Δ* mutants. Homozygous *URA3* mutants demonstrated a $NTC^R$/$URA3^-$ phenotype as they were able to grow on plates containing NTC but unable on media lacking uracil.

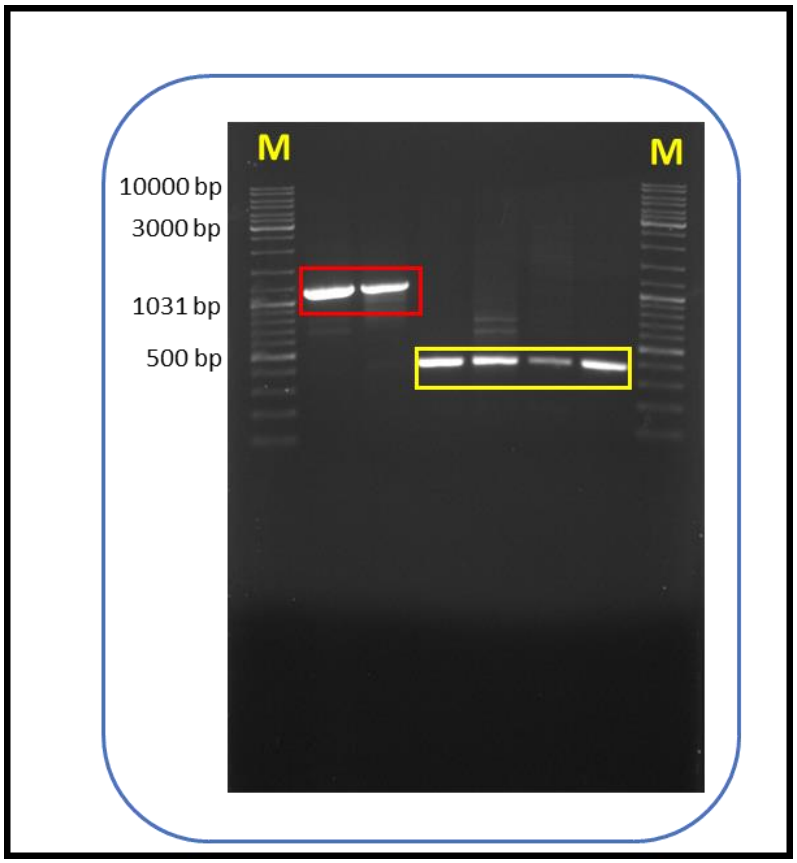


**Fig. 27** Gel profile of representative *ura3Δ/Δ* mutants. All putative mutants that were unable to grow on uracil-deficient media show expected band size of approximately 382 bp (corresponding to the size of *URA3* donor DNA, Yellow box). An expected band size of 1125 bp which correspond to the size of an intact *URA3* gene was obtained for the wildtype (red box).

Upon comparing the colonial morphology of the wildtype (*C. krusei* UFS Y-0217) and the mutant strains, we noticed that *ura3Δ/Δ* mutant appear smoother and less wrinkled compared to the wildtype strain (**Fig. 28**). This may suggest that the deletion or disruption of *URA3* may have a detrimental effect on filamentation in this yeast. This observation was supported by fewer pseudohyphae observed microscopically for the mutant strain (**Fig. 29**). Interestingly, literature has also attributed reduced virulence and adherence to *C. albicans* mutants with disrupted *URA3* gene (Kirsch and Whitney 1991; Bain et al. 2001; Staab and Sundstrom 2003). It is reasonable to suggest that the reduced virulence of *C. albicans ura3* mutants might be due to distorted filamentation since hyphal formation is a known virulence factor (Lo et al. 1997; Berman and Sudbery 2002; Pukkila-Worley et al. 2009). However, virulence studies are needed before such a conclusion could be made for *C. krusei ura3Δ/Δ* mutant.

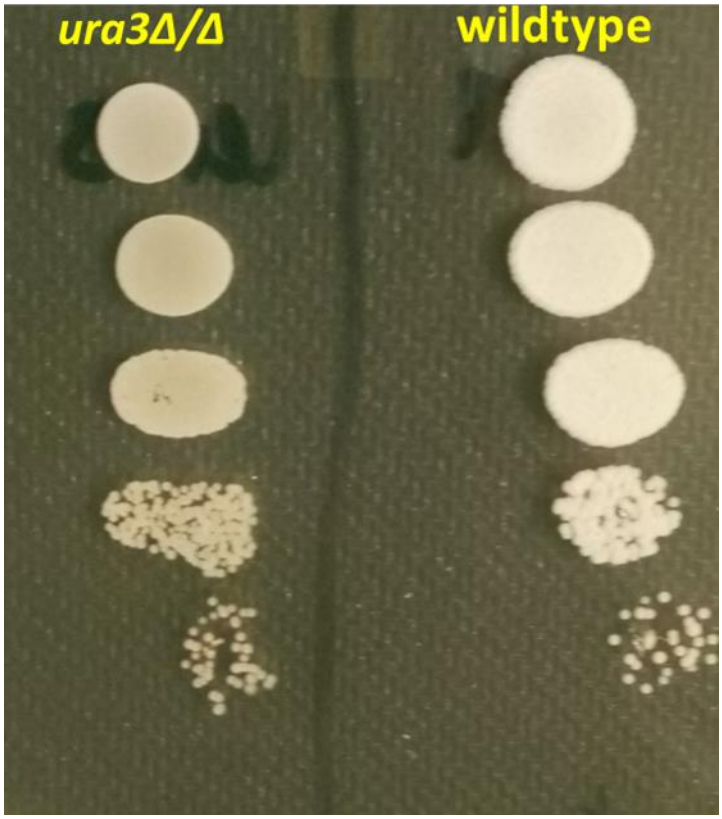


**Fig. 28** Comparison of the colonial morphology of *ura3Δ/Δ* mutant and wildtype strain. *ura3Δ/Δ* mutant appears smoother and less wrinkled compared to the wildtype strain. The yeast extract peptone dextrose (YPD) plate was inoculated with 10 µl of serially diluted culture of respective strain, $10^{-1}$ to $10^{-5}$ (top to bottom).

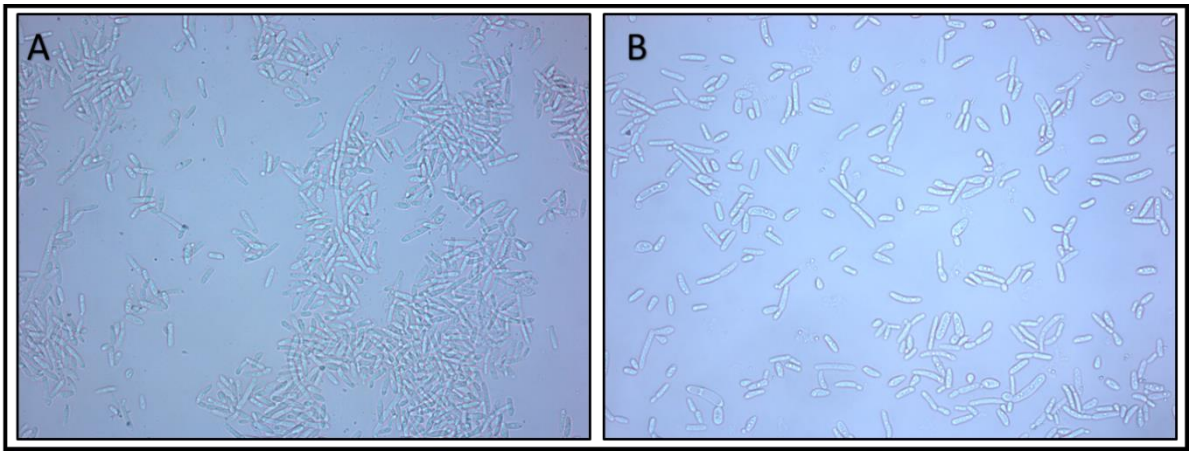


**Fig. 29** Microscopic comparison of the phenotype of *ura3Δ/Δ* mutant (**B**) and wildtype strain (**A**). A *ura3Δ/Δ* mutant appears more in yeast form compared to the wildtype strain, which displays more pseudohyphae. Light microscopy at 40X magnification.

### 3.4.2.2 Deleting *ADE2* gene

As a second approach to validate the efficacy of our adapted system, *ADE2* gene was targeted for deletion. This gene encodes P-ribosyl aminoimidazole carboxylase, which plays a role in *de novo* purine biosynthetic pathway. This enzyme converts P-ribosyl aminoimidazole (AIR) to P-ribosyl aminoimidazole carboxylate (CAIR) (**Fig. 30**) (Tsang et al. 1997). Mutation in the *ADE2* gene results in the accumulation of AIR which turns red/pink upon oxidation thus allowing distinctive reddish phenotype of *ADE2* mutants when grown in the absence of adenine (Poulter and Rikkerink 1983).

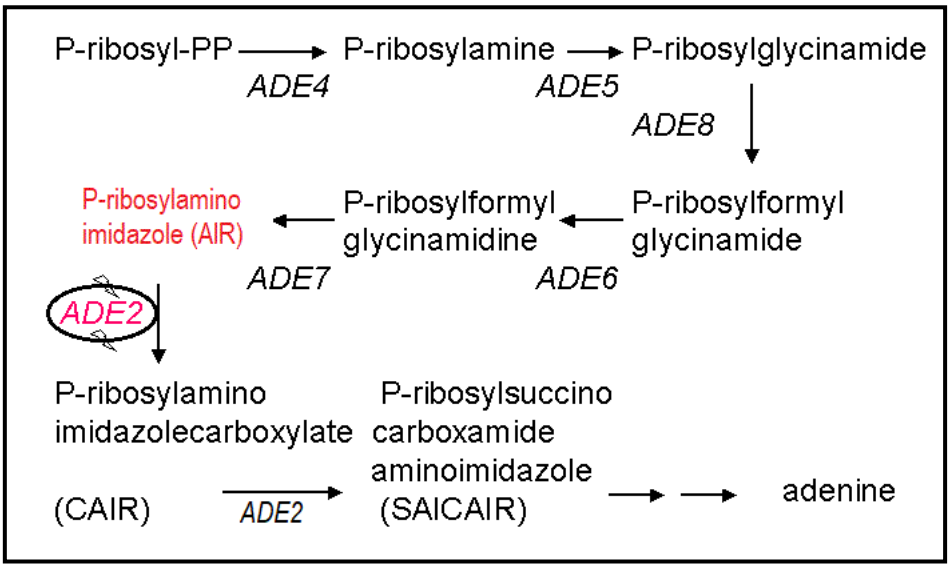


**Fig. 30** A representation of *de novo* purine biosynthetic pathway. The deletion or mutation of *ADE2* gene results in the accumulation of P-ribosyl aminoimidazole, which turns pink upon oxidation (https://www.phys.ksu.edu/gene/genefaq.html).

#### 3.4.2.2.1 Constructing CRISPR-Cas9 cassettes for deleting *ADE2* gene

The Cas9 cassette and the first component (Fragment A) of gRNA cassette are non-specific for the deletion of any gene using this system. However, the second part (Fragment B) of the gRNA cassette, which harbours the CRISPR site is specific for each gene and must be streamlined for each deletion. The Cas9 cassette was obtained by digesting CK pADH99 plasmid with *Mss*I restriction enzymes (**Fig. 21**). The first component (Fragment A) of the gRNA cassette (~1066 bp) was obtained upon amplifying pADH110 with primers AHO1096-ver2 and AHO1098-ver2 (**Fig. 22**). The target-specific part (Fragment B) of the gRNA was amplified from CK pADH147 with oligonucleotide ADE2-CRISPR-2 and primer AHO1097. The ADE2-CRISPR-2 oligo contains a 20 bp *ADE2*-specific target sequence (5'-TTAGGGTCTGATGTGCCAAA-3') (**Fig. 31**). This sequence is flanked by regions complementary to the 3' and 5' ends of *SNR52* promoter and gRNA scaffold, respectively, to

aid ligation of Fragments A and B. Upon ligation in a stitching PCR with primer pair AHO1237 and AHO1236, a full *ADE2*-gRNA cassette (Fragment C) with a band size of approximately 1788 bp was obtained (**Fig. 32**).

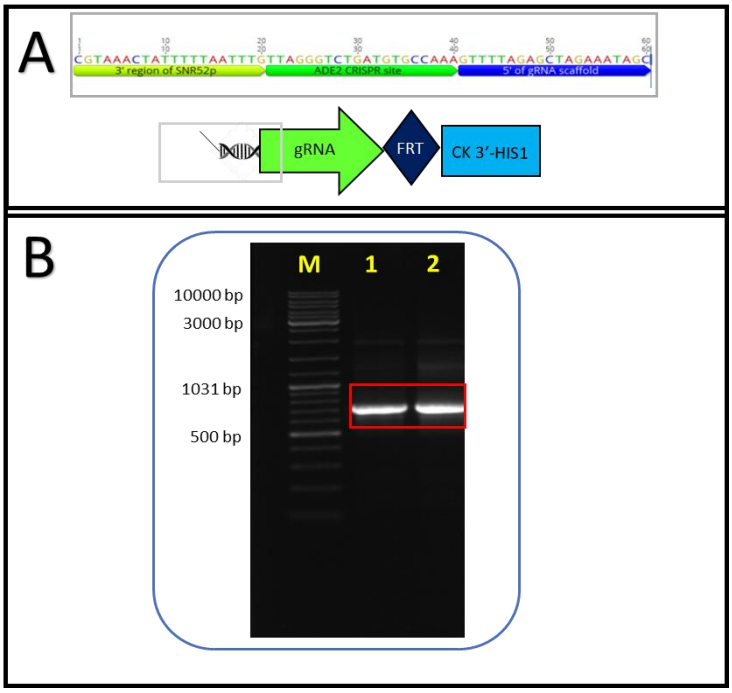


**Fig. 31** Construction of the second component (Fragment B) of gRNA cassette specific for *ADE2* gene (A) A representation of Fragment B amplified from CK pADH147. The grey box indicates *ADE2*-specific CRISPR site and overlapping regions with *SNR52* promoter and gRNA (B) Amplified product of Fragment B from CK pADH147. Expected band size of approximately 722 bp was obtained.

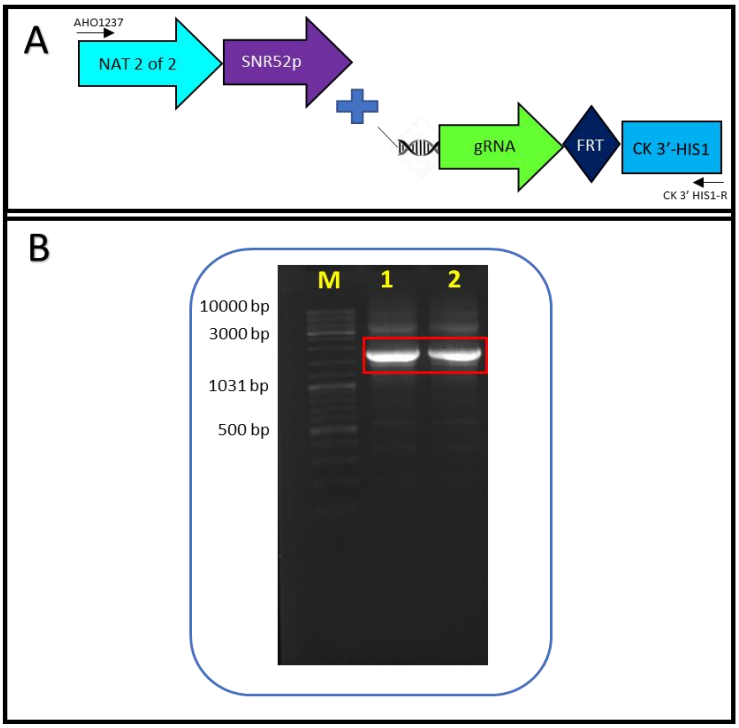


**Fig. 32** Construction of complete *ADE2*-specific gRNA cassette (A) A schematic depicting the stitching of Fragments A and B to generate a full *ADE2*-gRNA cassette (B) Gel profile depicting full *ADE2*-gRNA cassette of approximately 1788 bp.

#### 3.4.2.2.2 Designing and synthesising *ADE2* donor DNA

An intact *ADE2* dDNA was synthesised in a similar way to that of *URA3*, but with a different set of primers (**Fig. 7**). The first component (Fragment 1) of *ADE2* dDNA was amplified from the yeast's genome with primers ADE2-2F and ADE2-2R (overlap). As shown in **Figure 33A**, a band size of approximately 183 bp was obtained, which confirms the successful amplification of Fragment 1. Again, with the gDNA as a template, the second part (Fragment 2) of *ADE2* dDNA with a size of 214 bp was generated, with primer pair ADE2-3F (overlap) and ADE2-3R_new (**Fig. 33A**). The two generated overlapping fragments were stitched together with primers ADE2-2F and ADE2-3R_new, and an intact *ADE2* dDNA with an expected size of approximately 377 bp was obtained (**Fig. 33B**).

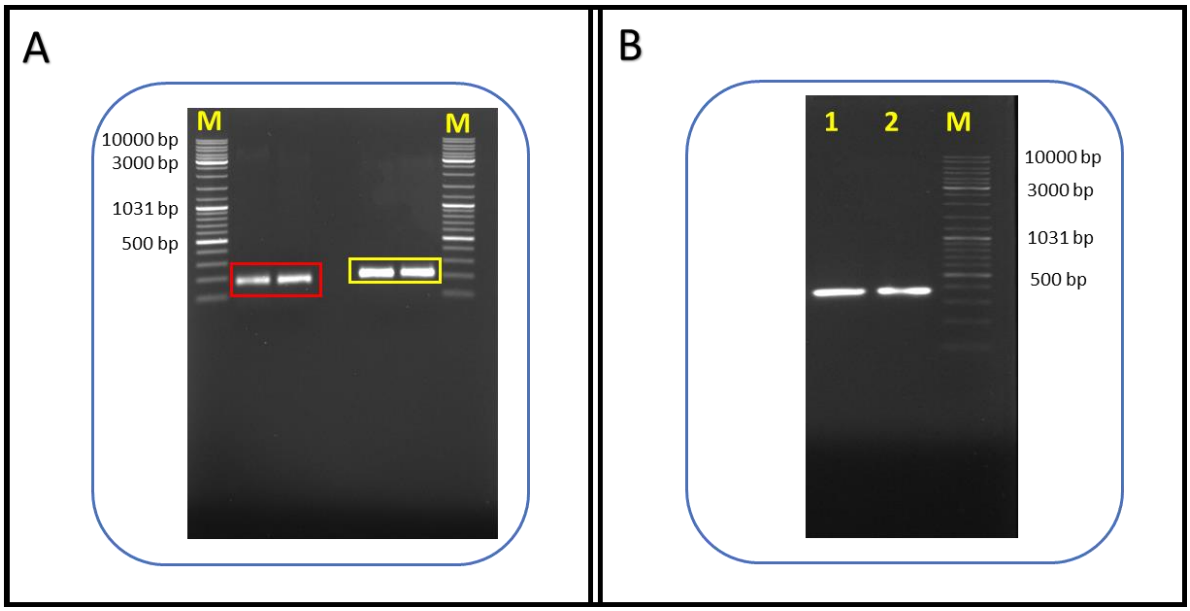


**Fig. 33** Synthesis of intact *ADE2* donor DNA (dDNA) (**A**) Gel profile showing expected band sizes of 183 bp (red box) and 214 bp (yellow box) for Fragment 1 and Fragment 2, respectively, of *ADE2* dDNA (**B**) Gel profile depicting complete *ADE2* dDNA of an expected band size of ~377 bp (Lanes 1 and 2).

#### 3.4.2.2.3 Transforming, selecting and confirming *ade2Δ/Δ* mutant

Upon co-transformation into *C. krusei*, the Cas9 cassette and the *ADE2*-specific gRNA cassettes generate a full CRISPR-Cas9 cassette – with an intact *NAT* marker gene, which integrates at the *HIS1* locus in this yeast's genome. Transformants were selected on YPD plates containing NTC. Out of 10 transformed colonies obtained, only one was an *ade2Δ/Δ* mutant evident of a distinctive red phenotype it displays on a minimal medium lacking adenine (**Fig. 34**). The homozygous *ADE2* mutant demonstrated a $NTC^{R}$/$ADE^{-}$ phenotype as it was able to grow on a plate supplemented with NTC and accumulated pink/reddish colour on plates lacking adenine.

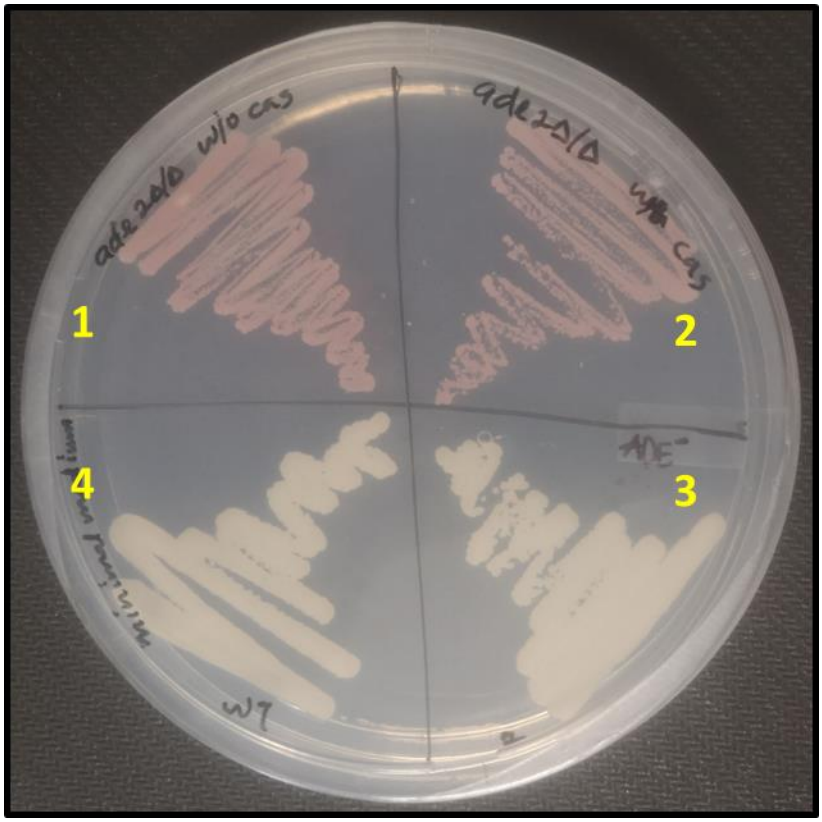


**Fig. 34** Adenine-deficient minimal medium plate showing growth of *ade2Δ/Δ* mutant. Mutant displays a distinctive reddish/pinkish colony. Labels 1 and 2 represent *ade2Δ/Δ* mutant without and with CRISPR-Cas9 cassette, respectively. Labels 3 and 4 represent transformant with intact *ADE2* gene and wildtype, respectively.

PCR genotyping was also performed, using the primers ADE2-2F and ADE2-3R_new, to confirm the genotype of the mutant. As shown in **Figure 35**, the band size obtained for the mutant strain is comparable to that of a white transformant and a wildtype. This observation indicates that, in the case of the *ADE2* gene, the DSBs created by the Cas9 nuclease were repaired via NHEJ instead of HDR. The reason why the organism chose NHEJ over HDR pathway to repair the nicked *ADE2* gene is unclear since a dDNA was co-transformed into the yeast alongside the CRISPR-Cas9 cassettes. This could be circumvented by inactivating genes, such as *KU70* and *LIG4*, which are essential for the NHEJ pathway (Norton et al. 2017; Weninger et al. 2017). However, care must be taken when performing pathogenesis and virulence studies since strains with defective NHEJ may exhibit reduced virulence (Wang et al. 2016).

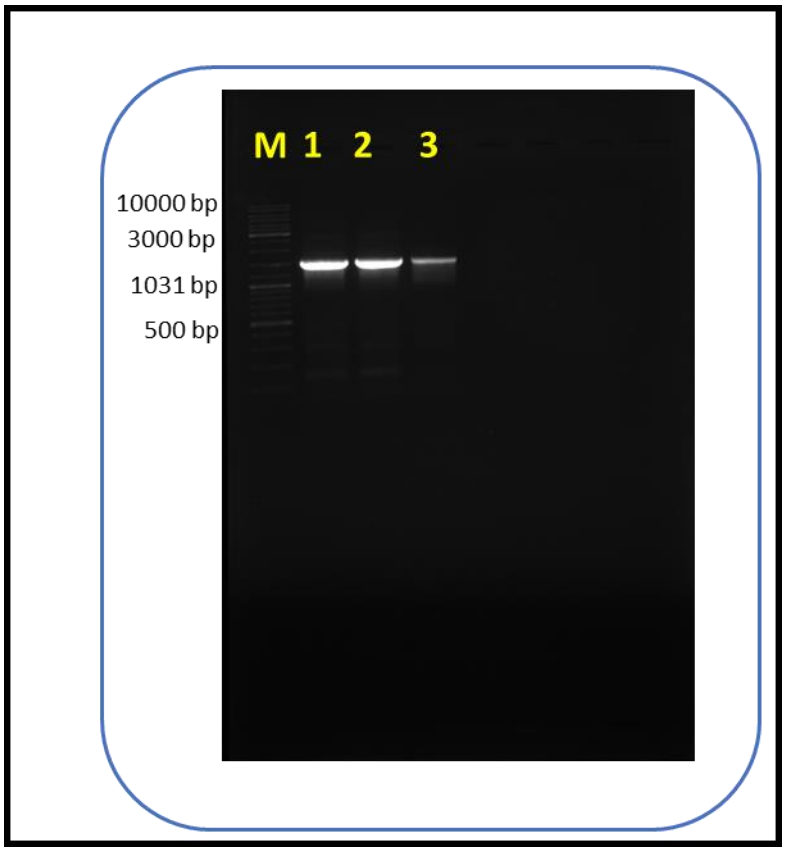


**Fig. 35** Gel profile of *ade2Δ/Δ* mutant (Lane 2), wildtype (Lane 1), and white transformant (Lane 3). An *ade2Δ/Δ* mutant display an unexpected band size of 1963 bp which corresponds to that of the wildtype and white transformant. This indicates that the double-strand break induced by Cas9 was repaired via non-homologous end joining (NHEJ) instead of homology-directed repair (HDR) pathway.

Furthermore, in addition to the red phenotype exhibited by the *ade2Δ/Δ* mutant, its colony morphology also appears smoother and shows less filamentation (**Fig. 36**), an observation which is similar to what was observed for *ura3Δ/Δ* mutant. Microscopic analysis also revealed that most cells of the *ade2Δ/Δ* mutant are in the yeast form (**Fig. 37**). Altogether, these observations suggest that the disruption of *ADE2* disruption may affect filamentation in this yeast. Additionally, previous studies with *C. albicans* have reported a reduced virulence of ade2*Δ/Δ* mutants (Kirsch and Whitney 1991; Donovan et al. 2001), which may possibly be attributed to diminished filamentation since hypha is an important virulence factor (Lo et al. 1997; Berman and Sudbery 2002; Pukkila-Worley et al. 2009).


**Fig. 36** Comparison of the colonial morphology of *ade2Δ/Δ* mutant and wildtype strain. *ade2Δ/Δ* mutant appears round, less wrinkled, and smoother compared to the wildtype strain. The yeast extract peptone dextrose (YPD) plate was inoculated with 10 µl of serially diluted culture of respective strain, $10^{-1}$ to $10^{-5}$ (top to bottom).

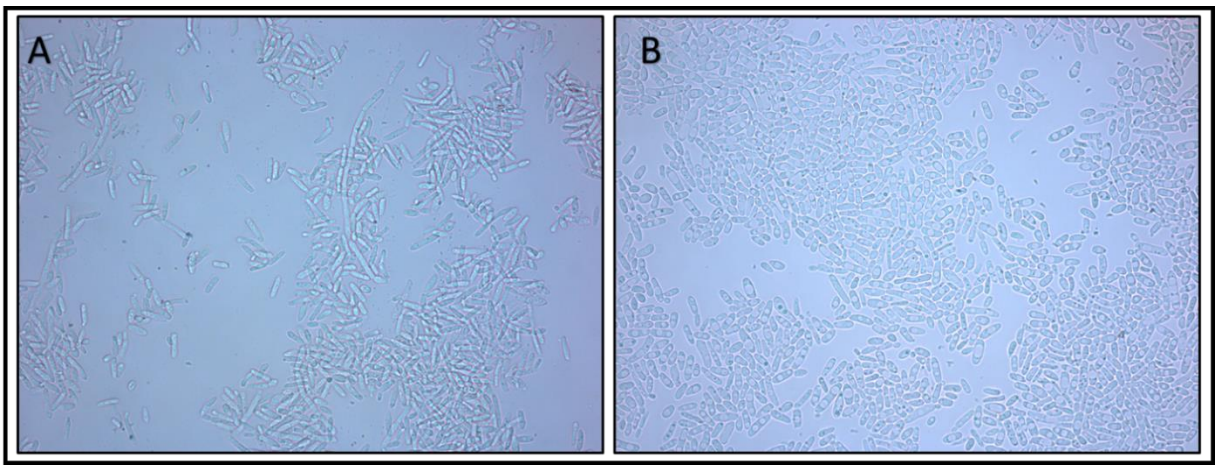


**Fig. 37** Microscopic comparison of the phenotype of *ade2Δ/Δ* mutant (**B**) and wildtype strain (**A**). *ade2Δ/Δ* mutant appear predominantly in yeast form. Light microscopy at 40X magnification.

### 3.4.3 Removing CRISPR-Cas9 cassette

Following confirmation of the genotypes of the mutants, the CRISPR-Cas9 cassette with the *NAT* marker was removed by inducing the *FLP* recombinase with growth in maltose-supplemented media. Mutants that have released the CRISPR-Cas9 cassette from their genomes consequently displayed a $NTC^S$ phenotype, and were unable to grow on NTC-supplemented media (**Fig. 38**).

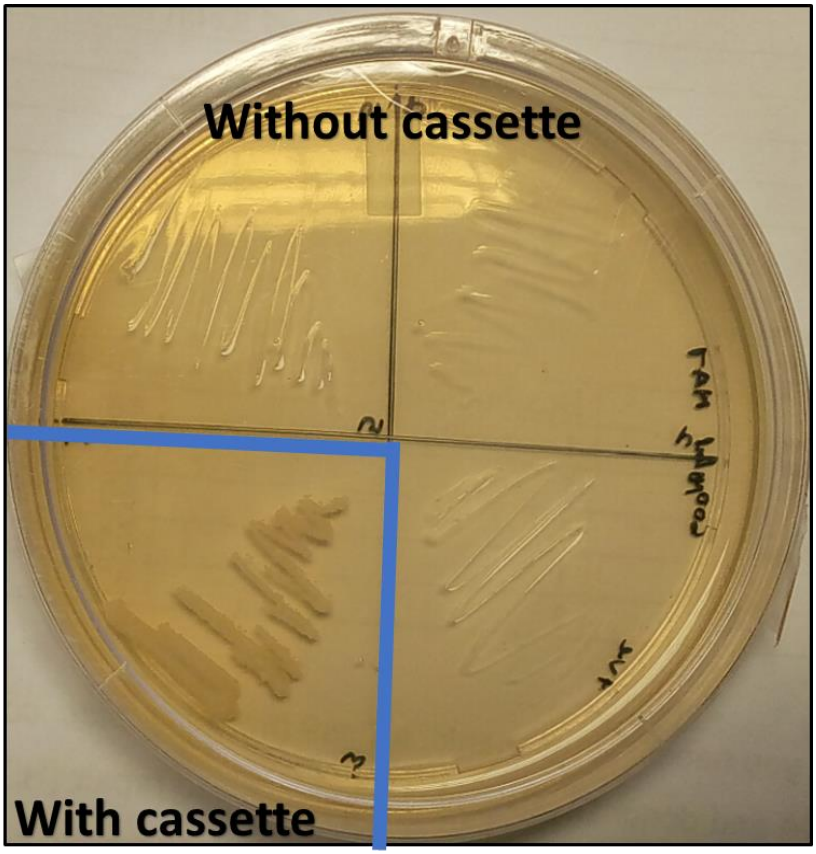


**Fig. 38** Successful excision of CRISPR-Cas9 cassette from the mutants' genome. After cassette removal, mutants displayed a nourseothricin-sensitive ($NTC^S$) phenotype and could not grow on media containing nourseothricin.

### 3.4.4 The complete system

This system consists of a *CAS9* gene (from *S. pyogenes*) – under the control of *C. krusei ENO1* promoter, which is carried on a Cas9 cassette; and a gRNA (under the control of *SNR52* promoter) – harboured within a gRNA cassette and adaptable to target any locus within *C. krusei* genome. Upon co-transformation, these two cassettes generate a complete CRISPR-Cas9 cassette, accomplished by homologous recombination between the overlapping *NAT* marker elements, integrated at the *HIS1* locus (**Fig. 39A**). Upon expression of the *CAS9* and gRNA, the Cas9 nuclease guided by the target-specific gRNA generates DSBs at the desired locus within the genome of *C. krusei*. The breaks are repaired via either NHEJ or HDR with a customised donor DNA (**Fig. 39B**). Successful transformants exhibit a $NTC^R$ phenotype fulfilled by the full *NAT* maker gene present on the intact CRISPR-Cas9 cassette. Following gene-editing, the CRISPR-Cas9 cassette (with *NAT* marker) is removed by growth on maltose-containing media, accomplished by the expression of flippase (*FLP*) recombinase gene and recombination between the *FLP* recognition target (FRT) sequences (**Fig. 39C**). As proof of principle, this system's efficacy for gene-editing in *C. krusei* was validated by the homozygous deletion of two auxotrophic marker genes, *URA3* and *ADE2*. One advantage of the adapted HIS-FLP system for *C. krusei* is that; in contrast to that of Nguyen and co-workers (2017) which integrates at, and replaces one allele of the *HIS1* ORF of *C. albicans* – which might consequently affect histidine biosynthesis, it was designed to integrate downstream of the *HIS1* ORF in the genome of *C. krusei* to avoid displacing the histidine biosynthetic gene.

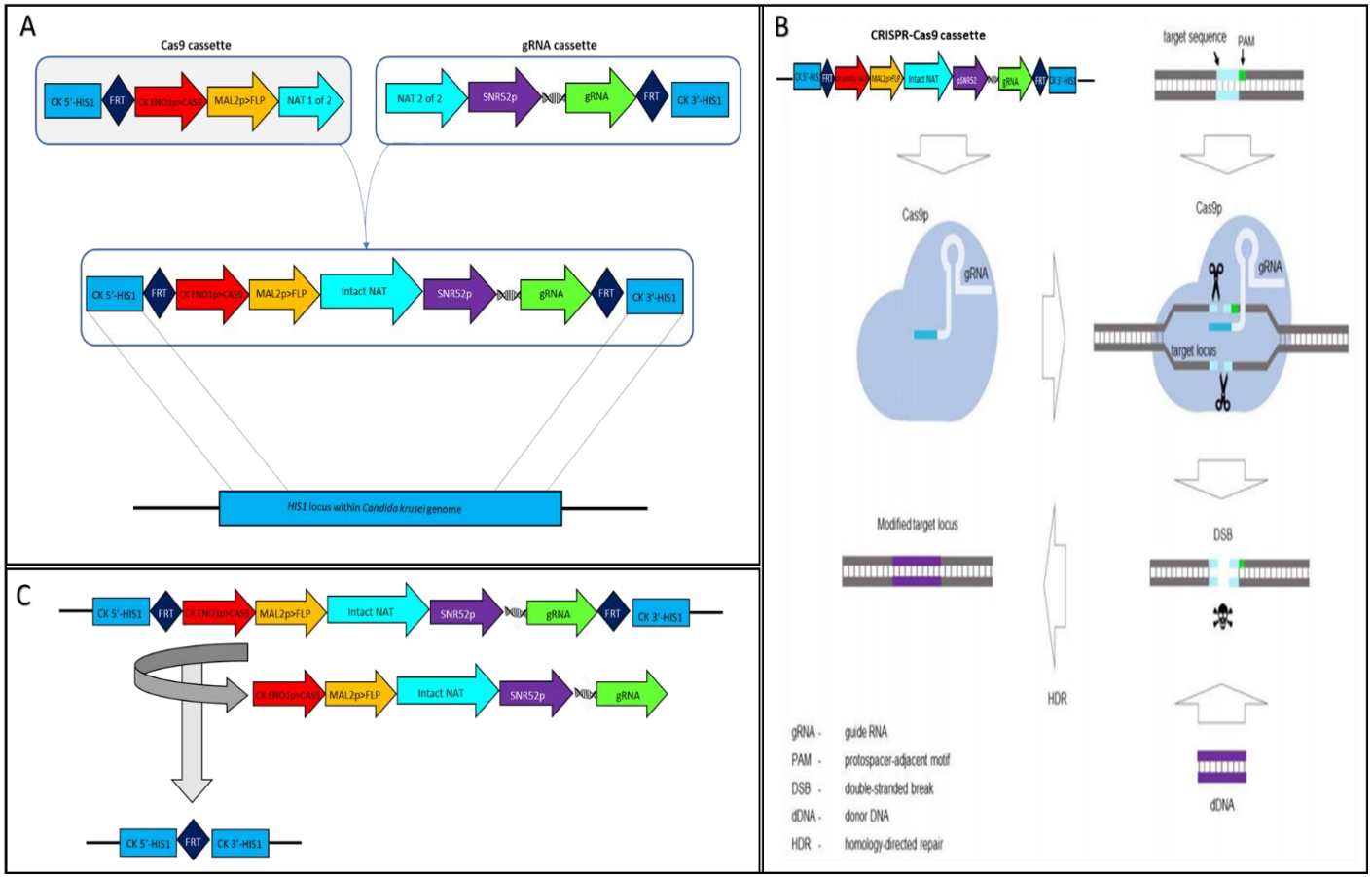


**Fig. 39** Schematic representation of the complete CRISPR-Cas9 system used for gene-editing in *Candida krusei*. (**A**) Upon co-transformation of the Cas9 and gRNA cassettes, an intact CRISPR-Cas9 cassette is obtained which integrate at the *HIS1* locus. (**B**) Upon expression of the gRNA and Cas9 protein, the gRNA-guided Cas9 generates a double-strand break at the target locus within the genome of *C. krusei* which is repaired via homology-directed repair with the supplied dDNA. (**C**) Following gene-editing, the CRISPR system is excised from the genome of the yeast via induction of the *FLP*-recombinase with growth in a maltose supplemented medium (Adapted from Fourie 2020).

## 3.5 Conclusions

With intrinsic resistance to FLC and increased non-susceptibility to other antifungal drugs, *C. krusei* represents a potential multidrug-resistant yeast (Whaley et al. 2017; Jamiu et al. 2020). However, the absence of an efficient, facile, fast, and precise tool like CRISPR technology for gene-editing in this yeast has greatly precluded full molecular insights into its mechanisms of resistance. Knowledge which is vital to preserve the current antifungal drugs and inspire the development of novel therapeutic strategies. In this chapter, we have demonstrated the development of a CRISPR-Cas9 system for genome engineering in *C. krusei* by adapting a *C. albicans*-specific system designed by Nguyen and co-workers (2017). As proof of concept, this system's efficacy was validated by successfully deleting *URA3* and *ADE2* auxotrophic marker genes. However, the system's engineering efficiency was not very high as expected – 16% and 10% for *URA3* and *ADE2* deletion, respectively. This might be because the *CAS9* gene was not codon-optimised for expression in *C. krusei* (Weninger et al. 2016; Raschmanová et al. 2018). Moreover, it might be because the gRNA was not placed under an *SNR52* promoter specific for *C. krusei* since there is evidence that species-specific gRNA promoters enable better gene-editing efficiency (Enkler et al. 2016; Morio et al. 2020). Hence, future research would consider harnessing a *C. krusei* codon-optimised *CAS9* gene and placing the gRNA under a *C. krusei*-specific RNA III promoter (*SNR52* promoter). Conclusively, to the best of our knowledge, this study represents the first development and usage of the CRISPR-Cas9 system for genome engineering in *C. krusei*. The mutants constructed during this study were submitted to the UFS Yeast Culture Collection for use within the broader scientific community (see ***Appendix B***)

## 3.6 References


Abdallah NA, Prakash CS, McHughen AG (2015) Genome editing for crop improvement: Challenges and opportunities. GM Crops & Food 6:183–205. https://doi.org/10.1080/21645698.2015.1129937

Adli M (2018) The CRISPR tool kit for genome editing and beyond. Nature Communications 9:1911. https://doi.org/10.1038/s41467-018-04252-2

Arnoult N, Correia A, Ma J, et al (2017) Regulation of DNA repair pathway choice in S and G2 phases by the NHEJ inhibitor CYREN. Nature 549:548–552. https://doi.org/10.1038/nature24023

Bain JM, Stubberfield C, Gow NAR (2001) Ura-status-dependent adhesion of *Candida albicans* mutants. FEMS Microbiology Letters 204:323–328.

https://doi.org/10.1016/S0378-1097(01)00420-7

Berman J, Sudbery PE (2002) *Candida albicans*: A molecular revolution built on lessons from budding yeast. Nature Reviews Genetics 3:918–931. https://doi.org/10.1038/nrg948

Bernheim A, Calvo-Villamañán A, Basier C, et al (2017) Inhibition of NHEJ repair by type II-A CRISPR-Cas systems in bacteria. Nature Communications 8:2094. https://doi.org/10.1038/s41467-017-02350-1

Branzei D, Foiani M (2008) Regulation of DNA repair throughout the cell cycle. Nature Reviews Molecular Cell Biology 9:297–308. https://doi.org/10.1038/nrm2351

Brouns SJJ, Jore MM, Lundgren M, et al (2008) Small CRISPR RNAs guide antiviral defense in prokaryotes. Science 321:960–964. https://doi.org/10.1126/science.1159689

de Gontijo FA, Pascon RC, Fernandes L, et al (2014) The role of the *de novo* pyrimidine biosynthetic pathway in *Cryptococcus neoformans* high temperature growth and virulence. Fungal Genetics and Biology 70:12–23. https://doi.org/10.1016/j.fgb.2014.06.003

Deltcheva E, Chylinski K, Sharma CM, et al (2011) CRISPR RNA maturation by trans-encoded small RNA and host factor RNase III. Nature 471:602–607. https://doi.org/10.1038/nature09886

DiCarlo JE, Norville JE, Mali P, et al (2013) Genome engineering in *Saccharomyces cerevisiae* using CRISPR-Cas systems. Nucleic Acids Research 41:4336–4343. https://doi.org/10.1093/nar/gkt135

Doench JG, Hartenian E, Graham DB, et al (2014) Rational design of highly active sgRNAs for CRISPR-Cas9–mediated gene inactivation. Nature Biotechnology 32:1262–1267. https://doi.org/10.1038/nbt.3026

Donovan M, Schumuke JJ, Fonzi WA, et al (2001) Virulence of a phosphoribosyl aminoimidazole carboxylase-deficient *Candida albicans* strain in an immunosuppressed murine model of systemic candidiasis. Infection and Immunity 69:2542–2548. https://doi.org/10.1128/iai.69.4.2542-2548.2001

Doudna JA, Charpentier E (2014) The new frontier of genome engineering with CRISPR-Cas9. Science 346:1258096–1258096. https://doi.org/10.1126/science.1258096

Douglass AP, Offei B, Braun-Galleani S, et al (2018) Population genomics shows no

distinction between pathogenic *Candida krusei* and environmental *Pichia kudriavzevii*: One species, four names. PLoS Pathogens 14:e1007138. https://doi.org/10.1371/journal.ppat.1007138

du Plooy LM (2019) The development of a CRISPR-Cas9 gene editing system for *Cryptococcus deneoformans*. M.Sc. Thesis, University of the Free State, Bloemfontein, South Africa

Enkler L, Richer D, Marchand AL, et al (2016) Genome engineering in the yeast pathogen *Candida glabrata* using the CRISPR-Cas9 system. Scientific Reports 6:1–12. https://doi.org/10.1038/srep35766

Fourie R (2020) Investigating the influence of arachidonic acid on *Candida albicans* and its interaction with *Pseudomonas aeruginosa*. Ph.D. Thesis, University of the Free State, Bloemfontein, South Africa

Frequently Asked Questions--Yeast Strains. https://www.phys.ksu.edu/gene/genefaq.html. Accessed 20 Dec 2020

Fuller KK, Chen S, Loros JJ, Dunlap JC (2015) Development of the CRISPR/Cas9 system for targeted gene disruption in *Aspergillus fumigatus*. Eukaryotic Cell 14:1073–1080. https://doi.org/10.1128/EC.00107-15

Grahl N, Demers EG, Crocker AW, Hogan DA (2017) Use of RNA-protein complexes for genome editing in non-*albicans Candida* species. mSphere 2:e00218-17 https://doi.org/10.1128/msphere.00218-17

Hale CR, Zhao P, Olson S, et al (2009) RNA-guided RNA cleavage by a CRISPR RNA-Cas protein complex. Cell 139:945–956. https://doi.org/10.1016/j.cell.2009.07.040

Hefferin ML, Tomkinson AE (2005) Mechanism of DNA double-strand break repair by non-homologous end joining. DNA Repair 4:639–648. https://doi.org/10.1016/j.dnarep.2004.12.005

Holmes DS, Quigley M (1981) A rapid boiling method for the preparation of bacterial plasmids. Analytical Biochemistry 114:193–197. https://doi.org/10.1016/0003-2697(81)90473-5

Hsu PD, Scott DA, Weinstein JA, et al (2013) DNA targeting specificity of RNA-guided Cas9 nucleases. Nature Biotechnology 31:827–832. https://doi.org/10.1038/nbt.2647

Huang MY, Mitchell AP (2017) Marker recycling in *Candida albicans* through CRISPR-Cas9-

induced marker excision. mSphere 2:e00050-17. https://doi.org/10.1128/msphere.00050-17

Ibrahim ZH, Bae JH, Lee SH, et al (2020) Genetic manipulation of a lipolytic yeast *Candida aaseri* SH14 using CRISPR-Cas9 system. Microorganisms 8:526. https://doi.org/10.3390/microorganisms8040526

Jamiu AT, Albertyn J, Sebolai OM, Pohl CH (2020) Update on *Candida krusei*, a potential multidrug-resistant pathogen. Medical Mycology 59:14-30. https://doi.org/10.1093/mmy/myaa031

Jiang F, Taylor DW, Chen JS, et al (2016) Structures of a CRISPR-Cas9 R-loop complex primed for DNA cleavage. Science 351:867–871. https://doi.org/10.1126/science.aad8282

Jinek M, Chylinski K, Fonfara I, et al (2012) A Programmable dual-RNA-guided DNA endonuclease in adaptive bacterial immunity. Science 337:816–821. https://doi.org/10.1126/science.1225829

Khadempar S, Familghadakchi S, Motlagh RA, et al (2019) CRISPR-Cas9 in genome editing: Its function and medical applications. Journal of Cellular Physiology 234:5751–5761. https://doi.org/10.1002/jcp.27476

Kirsch DR, Whitney RR (1991) Pathogenicity of *Candida albicans* auxotrophic mutants in experimental infections. Infection and Immunity 59:3297–3300

Ko HC, Hsiao TY, Chen CT, Yang YL (2013) *Candida albicans ENO1* null mutants exhibit altered drug susceptibility, hyphal formation, and virulence. Journal of Microbiology 51:345–351. https://doi.org/10.1007/s12275-013-2577-z

Labuschagne M, Albertyn J (2007) Cloning of an epoxide hydrolase-encoding gene from *Rhodotorula mucilaginosa* and functional expression in *Yarrowia lipolytica*. Yeast 24:69–78. https://doi.org/10.1002/yea.1437

Lacroute F (1968) Regulation of pyrimidine biosynthesis in *Saccharomyces cerevisiae*. Journal of Bacteriology 95:824–832

Lander ES (2016) The heroes of CRISPR. Cell 164:18–28. https://doi.org/10.1016/j.cell.2015.12.041

Lay J, Henry LK, Clifford J, et al (1998) Altered expression of selectable marker *URA3* in gene-

disrupted *Candida albicans* strains complicates interpretation of virulence studies. Infection and Immunity 66:5301–5306. https://doi.org/10.1128/IAI.66.11.5301-5306.1998

Lederberg J, Lederberg EM (1952) Replica plating and indirect selection of bacterial mutants. Journal of Bacteriology 63:399–406

Lee PY, Costumbrado J, Hsu CY, Kim YH (2012) Agarose gel electrophoresis for the separation of DNA fragments. Journal of Visualized Experiments. https://doi.org/10.3791/3923

Leu SJ, Lee YC, Lee CH, et al (2020) Generation and characterization of single chain variable fragment against alpha-enolase of *Candida albicans*. International Journal of Molecular Sciences 21:2903. https://doi.org/10.3390/ijms21082903

Lieber MR, Ma Y, Pannicke U, Schwarz K (2003) Mechanism and regulation of human non-homologous DNA end-joining. Nature Reviews Molecular Cell Biology 4:712–720. https://doi.org/10.1038/nrm1202

Lin S, Staahl BT, Alla RK, Doudna JA (2014) Enhanced homology-directed human genome engineering by controlled timing of CRISPR/Cas9 delivery. eLife 3:e04766. https://doi.org/10.7554/elife.04766

Lo HJ, Köhler JR, DiDomenico B, et al (1997) Non-filamentous *Candida albicans* mutants are avirulent. Cell 90:939–949. https://doi.org/10.1016/s0092-8674(00)80358-x

Lombardi L, Turner SA, Zhao F, Butler G (2017) Gene editing in clinical isolates of *Candida parapsilosis* using CRISPR/Cas9. Scientific Reports 7:1–11. https://doi.org/10.1038/s41598-017-08500-1

Losberger C, Ernst JF (1989) Sequence and transcript analysis of the *Candida albicans URA3* gene encoding orotidine-5'-phosphate decarboxylase. Current Genetics 16:153–158. https://doi.org/10.1007/BF00391471

Matsu-ura T, Baek M, Kwon J, Hong C (2015) Efficient gene editing in *Neurospora crassa* with CRISPR technology. Fungal Biology and Biotechnology 2:4. https://doi.org/10.1186/s40694-015-0015-1

Min K, Ichikawa Y, Woolford CA, Mitchell AP (2016) *Candida albicans* Gene Deletion with a Transient CRISPR-Cas9 System. mSphere 1:e00130-16.

https://doi.org/10.1128/msphere.00130-16

Morio F, Lombardi L, Butler G (2020) The CRISPR toolbox in medical mycology: State of the art and perspectives. PLoS Pathogens 16:e1008201. https://doi.org/10.1371/journal.ppat.1008201

Nguyen N, Quail MMF, Hernday AD (2017) An efficient, rapid, and recyclable system for CRISPR-mediated genome editing in *Candida albicans*. mSphere 2:e00149-17. https://doi.org/10.1128/mSphereDirect.00149-17

Nishimasu H, Ran FA, Hsu PD, et al (2014) Crystal structure of Cas9 in complex with guide RNA and target DNA. Cell 156:935–949. https://doi.org/10.1016/j.cell.2014.02.001

Norton EL, Sherwood RK, Bennett RJ (2017) Development of a CRISPR-Cas9 system for efficient genome editing of *Candida lusitaniae*. mSphere 2:e00217-17. https://doi.org/10.1128/mSphere.00217-17

Poulter RT, Rikkerink EH (1983) Genetic analysis of red, adenine-requiring mutants of *Candida albicans*. Journal of Bacteriology 156:1066–1077. https://doi.org/10.1128/jb.156.3.1066-1077.1983

Pronk JT (2002) Auxotrophic yeast strains in fundamental and applied research. Applied and Environmental Microbiology 68:2095–2100. https://doi.org/10.1128/aem.68.5.2095-2100.2002

Pukkila-Worley R, Peleg AY, Tampakakis E, Mylonakis E (2009) *Candida albicans* hyphal formation and virulence assessed using a *Caenorhabditis elegans* infection model. Eukaryotic Cell 8:1750–1758. https://doi.org/10.1128/EC.00163-09

Ranjha L, Howard SM, Cejka P (2018) Main steps in DNA double-strand break repair: an introduction to homologous recombination and related processes. Chromosoma 127:187–214. https://doi.org/10.1007/s00412-017-0658-1

Raschmanová H, Weninger A, Glieder A, et al (2018) Implementing CRISPR-Cas technologies in conventional and non-conventional yeasts: Current state and future prospects. Biotechnology Advances 36:641–665. https://doi.org/10.1016/j.biotechadv.2018.01.006

Richardson CD, Ray GJ, DeWitt MA, et al (2016) Enhancing homology-directed genome editing by catalytically active and inactive CRISPR-Cas9 using asymmetric donor

DNA. Nature Biotechnology 34:339–344. https://doi.org/10.1038/nbt.3481

Román E, Prieto D, Alonso-Monge R, Pla J (2019) New insights of CRISPR technology in human pathogenic fungi. Future Microbiology 14:1243–1255. https://doi.org/10.2217/fmb-2019-0183

Saha SK, Saikot FK, Rahman MS, et al (2019) Programmable molecular scissors: Applications of a new tool for genome editing in biotech. Molecular Therapy - Nucleic Acids 14:212–238. https://doi.org/10.1016/j.omtn.2018.11.016

Staab JF, Sundstrom P (2003) *URA3* as a selectable marker for disruption and virulence assessment of *Candida albicans* genes. Trends in Microbiology 11:69–73. https://doi.org/10.1016/s0966-842x(02)00029-x

Tang XD, Gao F, Liu MJ, et al (2019) Methods for enhancing clustered regularly interspaced short palindromic repeats/Cas9-mediated homology-directed repair efficiency. Frontiers in Genetics 10:551. https://doi.org/10.3389/fgene.2019.00551

The Nobel Prize in Chemistry 2020. https://www.nobelprize.org/prizes/chemistry/2020/press-release/. Accessed 25 Oct 2020

Tsang WK, Cao BY, Wang J (1997) Sequence analysis of *Candida albicans* phosphoribosyl-aminoimidazole carboxylase (*ADE2*) gene. Yeast 13:673–676. https://doi.org/10.1002/(SICI)1097-0061(19970615)13:73.0.CO;2-G

Vyas VK, Barrasa MI, Fink GR (2015) A *Candida albicans* CRISPR system permits genetic engineering of essential genes and gene families. Science Advances 1:e1500248. https://doi.org/10.1126/sciadv.1500248

Wang T, Wei JJ, Sabatini DM, Lander ES (2013) Genetic screens in human cells using the CRISPR-Cas9 System. Science 343:80–84. https://doi.org/10.1126/science.1246981

Wang Y, Wei D, Zhu X, et al (2016) A 'suicide' CRISPR-Cas9 system to promote gene deletion and restoration by electroporation in *Cryptococcus neoformans*. Scientific Reports 6:1–13. https://doi.org/10.1038/srep31145

Waryah CB, Moses C, Arooj M, Blancafort P (2018) Zinc fingers, TALEs, and CRISPR systems: A comparison of tools for epigenome editing. Methods in Molecular Biology 19–63. https://doi.org/10.1007/978-1-4939-7774-1_2

Weninger A, Fischer JE, Raschmanová H, et al (2017) Expanding the CRISPR/Cas9 toolkit

for *Pichia pastoris* with efficient donor integration and alternative resistance markers. Journal of Cellular Biochemistry 119:3183–3198. https://doi.org/10.1002/jcb.26474

Weninger A, Hatzl AM, Schmid C, et al (2016) Combinatorial optimization of CRISPR/Cas9 expression enables precision genome engineering in the methylotrophic yeast *Pichia pastoris*. Journal of Biotechnology 235:139–149. https://doi.org/10.1016/j.jbiotec.2016.03.027

Whaley SG, Berkow EL, Rybak JM, et al (2017) Azole antifungal resistance in *Candida albicans* and emerging non-*albicans Candida* species. Frontiers in Microbiology 7:2173. https://doi.org/10.3389/fmicb.2016.02173

Yuan DS (2011) Dithizone staining of intracellular zinc: An unexpected and versatile counter screen for auxotrophic marker genes in *Saccharomyces cerevisiae*. PLoS ONE 6:e25830. https://doi.org/10.1371/journal.pone.0025830

Zhang L, Zhang H, Liu Y, et al (2019) A CRISPR–Cas9 system for multiple genome editing and pathway assembly in *Candida tropicalis*. Biotechnology and Bioengineering 117:531–542. https://doi.org/10.1002/bit.27207

Zhou Y, Zhu S, Cai C, et al (2014) High-throughput screening of a CRISPR/Cas9 library for functional genomics in human cells. Nature 509:487–491. https://doi.org/10.1038/nature13166

Zoppo M, Luca MD, Villarreal SN, et al (2019) A CRISPR/Cas9-based strategy to simultaneously inactivate the entire *ALS* gene family in *Candida orthopsilosis*. Future Microbiology 14:1383–1396. https://doi.org/10.2217/fmb-2019-0168

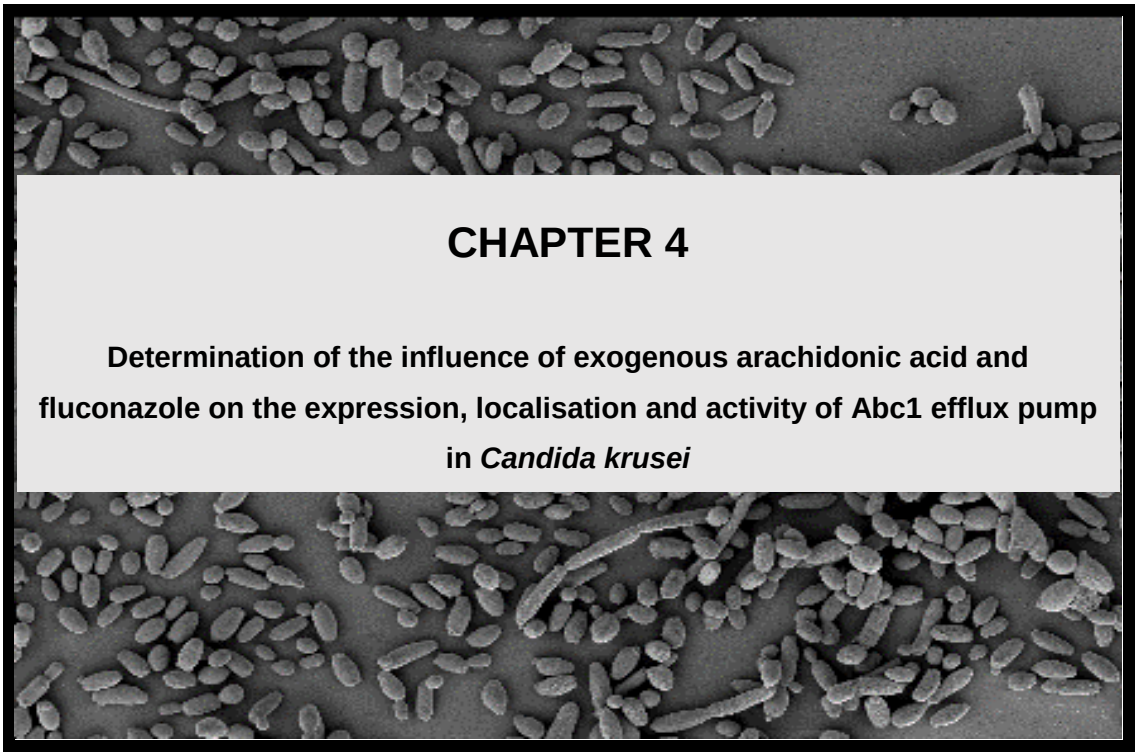

# CHAPTER 4

**Determination of the influence of exogenous arachidonic acid and fluconazole on the expression, localisation and activity of Abc1 efflux pump in *Candida krusei***

## *PLEASE NOTE*

---

**The CRISPR-Cas9 modification section of this chapter overlaps with *Chapter 3*.**

**Hence, duplication of some information could not be entirely avoided.**

## 4.1 Abstract

With innate resistance to fluconazole (FLC) and rapid acquired resistance to other antifungal drugs, *Candida krusei* represents a potential multidrug-resistant pathogen. The mechanism of intrinsic FLC resistance in this yeast has been chiefly attributed to decreased susceptibility of FLC target, lanosterol 14α-demethylase (Erg11p), however, the role of efflux pump transporters remains controversial, and requires further investigation. Furthermore, although the overexpression of these transporters, including Abc1p, results in a multidrug-resistance phenotype, their inhibitors are limited. There is currently no class of antifungal that specifically targets these transporters. Polyunsaturated fatty acids (PUFAs), including arachidonic acid (AA), which are known disruptors of the cellular membranes might function well as effective efflux pump inhibitors; however, this needs to be investigated. Hence, this study attempted to examine the influence of AA and FLC on the expression, localisation, and activity of a representative ABC transporter, Abc1p, in *C. krusei*. This was carried out by attempting to construct a Green Fluorescent Protein (GFP) fusion of Abc1 and exposing *C. krusei* biofilms to varying concentrations of AA and FLC alone or in combination; and determining Abc1p expression and function using western blot analysis and Rhodamine 6G efflux assay, respectively. Although the Abc1-GFP fusion construction was unsuccessful, our results demonstrate that Abc1p is overexpressed following exposure to FLC alone, but not in any treatments with AA. Further, Abc1p exhibited increased functionality in the presence of FLC; however, this was diminished upon exposure to 1 mM AA, either alone or in combination with FLC. These findings demonstrate AA as a potential inhibitor of Abc1p expression and subsequent activity and lent credence to the importance of this transporter in FLC resistance.

**Keywords:** *Candida krusei*, fluconazole, resistance, arachidonic acid, efflux pumps, Abc1 transporter

## 4.2 Introduction

The yeast *Candida krusei* is a potential multidrug-resistant pathogen with intrinsic resistance to FLC and rapid adaptive resistance to other antifungal drugs, including the echinocandins (Forastiero et al. 2015; Whaley et al. 2017; Jamiu et al. 2020). The key mechanisms of antifungal resistance in this yeast and other pathogenic *Candida* spp. include overexpression of target proteins (e.g. Erg11p); alteration of drug targets (e.g. Fks1p); and reduction in intracellular drug concentration, due to cell membrane modification, biofilm formation, or enhanced efflux pump activity (Mukhopadhyay et al. 2002; Sanglard and Odds 2002; Mansfield et al. 2010; Pappas et al. 2016; Robbins et al. 2017).

The mechanism of intrinsic resistance to FLC in *C. krusei* has been chiefly attributed to reduced sensitivity of Erg11p towards FLC (Venkateswarlu et al. 1997; Orozco et al. 1998; Fukuoka et al. 2003). However, the role of efflux pump transporters, including Abc1p (the homolog of Cdr1p in *C. albicans*), in this inherent resistance cannot be dismissed.

The Cdr (*Candida* drug resistance) transporters are members of the ABC transporter family and are capable of conferring resistance to all azole drugs (Prasad et al. 1995). Amongst these transporters, Cdr1 and Cdr2 are the most clinically relevant (Perea et al. 2001; Prasad et al. 2015). The homologs of these proteins in *C. krusei* are Abc1p and Abc2p, respectively, and their overexpression has been attributed to resistance to azole antifungals in this yeast. Specifically, the resistance mechanism of *C. krusei* to itraconazole and voriconazole has been partly attributed to the overexpression of Abc1 and Abc2 transporters (Tavakoli et al. 2010; Ricardo et al. 2014; He et al. 2015). However, these transporters' role, particularly Abc1, in the intrinsic mechanism of *C. krusei* remains unclear.

A study by Katiyar and Edlind (2001) demonstrated the upregulation of *ABC1* in the presence of other azoles, such as miconazole and clotrimazole, but not in the presence of FLC. Similarly, another report suggested that no ABC transporters are involved in the intrinsic resistance of *C. krusei* (Guinea et al. 2006). However, a later study by Lamping and co-workers (2009) demonstrated that the constitutive expression of Abc1p and low affinity of Erg11p are responsible for FLC resistance in *C. krusei*. Hence, these conflicting reports warrant further studies.

Furthermore, despite their crucial roles in antifungal resistance, there is currently no antifungal class available that specifically targets the efflux pumps. One approach to discovering novel efflux pump inhibitors is through the characterisation of efflux pump-inhibiting potential of natural compounds with known antimicrobial properties, including polyunsaturated fatty acids (PUFAs). Recent studies in our group have shown that a PUFA, arachidonic acid (AA), induces the upregulation of the *CDR1* gene and increases Cdr1 protein production in *C. albicans*. However, the activity of this transporter was severely diminished in the presence of

AA in the same yeast (Fourie 2020; Kuloyo 2020). The observed dissipated activity of Cdr1p was attributed to various factors, including possible mislocalisation of the Cdr1 transporter, reduced mitochondrial activity, and competitive inhibition. However, it is unknown if these phenomena are conserved amongst other *Candida* spp., including *C. krusei*. On this background, this study was conceptualised to determine the influence of AA and FLC on the localisation, expression, and activity of Abc1p in C. krusei to better understand the role of this efflux pump in antifungal resistance.

## 4.3 Materials and Methods

### 4.3.1 Strains used

Two strains of *Candida krusei*, *C. krusei* UFS Y-0217 (CBS573$^T$) and *C. krusei* UFS Y-0277 were used in this study. These strains were obtained from the Yeast Culture Collection of the University of the Free State, Bloemfontein, revived on Yeast Malt extract (YM) agar plates (10 g/l glucose, 3 g/l yeast extract, 3 g/l malt extract, 5 g/l peptone, 17 g/l agar) at 30$^o$C for 24 h, and their stocks were stored at -80$^o$C for future use.

### 4.3.2 Drug and fatty acids

Fluconazole (FLC) was obtained from Sigma-Aldrich (St. Louis, MO, USA), a stock of 5 mg/ml was prepared in dimethyl sulfoxide (DMSO) and stored at -20$^o$C. Arachidonic Acid (AA) (20:4) was also obtained from Sigma-Aldrich (St. Louis, MO, USA) and a 10 mM stock was prepared in ethanol and stored at -20$^o$C.

### 4.3.3 Construction of *ABC1*-GFP mutant with CRISPR-Cas9 system

The CRISPR-Cas9 system adapted for genome engineering in *C. krusei* in **Chapter 3** was used to attempt the insertion of Green Fluorescent Protein (GFP) sequence at the 3' end of *ABC1* gene to construct an *ABC1*-GFP mutant of *C. krusei*, in order to assess its fluorescence (localisation and expression) under various treatment conditions. The description of the adapted plasmids used for this purpose is depicted in **Table 1**. Design of primers and fragments, simulation of polymerase chain reaction (PCR), and identification of CRISPR sites were done *in silico* with Geneious® 11.1.5 (www.geneious.com) prior to all *in vitro* and *in vivo* assays. Unless stated otherwise, PCR was done with KOD Hot Start DNA polymerase kit (Novagen®) using the reaction mixture and PCR condition supplied in **Tables 2** and **3**, respectively. All primers used were purchased from Integrated DNA Technologies and are listed in **Table 4**.

**Table 1** Plasmids used in this study

| Plasmid | Major component | Function |
|---|---|---|
| **CK pADH99** | 5' CK *HIS1* locus + CK *ENO1* promoter + *CAS9* gene + ½ *NAT* gene | Cas9 cassette |
| **pADH110** | $^2/_2$ *NAT* gene + Ca *SNR52* promoter | ½ gRNA cassette |
| **CK pADH147** | gRNA scaffold + 3' CK *HIS1* locus | $^2/_2$ gRNA cassette |

**Table 2** Reaction mixture for KOD Hot Start DNA polymerase kit (Novagen®)

| Component | Reaction mixture |
|---|---|
| Nuclease-free water | Up to 25 µl |
| 10X Buffer for KOD Hot Start DNA Polymerase | 2.5 µl |
| 25 mM $MgSO_4$ | 1.5 µl |
| dNTP Mix (2 mM) | 2.5 µl |
| Forward primer (10 µM) | 0.75 µl |
| Reverse primer (10 µM) | 0.75 µl |
| KAPA Taq DNA polymerase (5 U/µl) | 0.5 µl |
| Template DNA (less complex DNA)***** | ≤10 ng |

* tenfold excess for genomic DNA

**Table 3** PCR condition for KOD Hot Start DNA polymerase kit (Novagen®)

| Step | Target size | | | | Cycle |
|---|---|---|---|---|---|
| | < 500 bp | 500 – 1000 bp | 1000 – 3000 bp | > 3000 bp | |
| Polymerase activation | 95°C, 2 min | 95°C, 2 min | 95°C, 2 min | 95°C, 2 min | 1 |
| Denaturation | 95°C, 20 sec | 95°C, 20 sec | 95°C, 20 sec | 95°C, 20 sec | 30 |
| Annealing | Lowest Primer Tm °C, 10 sec | | | | |
| Extension | 70°C, 10 sec/kb | 70°C, 15 sec/kb | 70°C, 20 sec/kb | 70°C, 25 sec/kb | 1 |

**Table 4** Primers used in this study

| Primer | Sequence (5' to 3') | Tm (ºC) | Description | Reference |
|---|---|---|---|---|
| **AHO1096-ver2** | GACGGCACGGCCACGCGTTTAAAC | 65.1 | Forward primer for the amplification of fragment A (5' region) of gRNA cassette | Modified from Nguyen et al. 2017 |
| **AHO1098-ver2** | CAAATTAAAAATAGTTTACGCAAGTCTCG | 53.8 | Reverse primer for the amplification of fragment A (5' region) of gRNA cassette | Modified from Nguyen et al. 2017 |
| **CK-ABC1-CRISPR-1** | CGTAAACTATTTTTAATTTGATATATCTGTGTTACCAAAAGTTTTAGAGCTAGAAATAGC | 61.8 | *ABC1* specific oligo and forward primer for the amplification of fragment B (3' region) of gRNA cassette | This study |
| **AHO1097** | CCCGCCAGGCGCTGGGGTTTAAACACCG | 70.2 | Reverse primer for the amplification of fragment B (3' region) of gRNA cassette | Nguyen et al. 2017 |
| **AHO1237** | AGGTGATGCTGAAGCTATTGAAG | 55.0 | Forward primer for stitching fragments A and B to obtain full gRNA cassette | Nguyen et al. 2017 |
| **CK-3' HIS1-R** | ACTAGACAAGCGAGTTTGCA | 54.3 | Reverse primer for stitching fragments A and B to obtain full gRNA cassette | This study |
| **CK-ABC1-1F** | GGAGAAAACTGCCAGACGTT | 55.4 | Forward primer for the amplification of fragment 1a of *ABC1*-GFP donor DNA (dDNA) | This study |
| **CK-ABC1-1R** | TGCTGGAGCACTCTTTTGGTAACACAGATA | 61.1 | Reverse primer for the amplification of fragment 1a of *ABC1*-GFP dDNA (Has overlap sequence with CK-ABC1-2F) | This study |
| **CK-ABC1-2F** | ACCAAAAGAGTGCTCCAGCAGTACTATCG | 61.4 | Forward primer for the amplification of fragment 1b of *ABC1*-GFP dDNA (Has overlap sequence with CK-ABC1-1R) | This study |

| | | | | |
|---|---|---|---|---|
| **CK-ABC1-2R** | TGCTTCAGAAGTAGTTTGTGG | 52.7 | Reverse primer for the amplification of fragment 1b of *ABC1*-GFP dDNA | This study |
| **GFP-1-F** | ATGTCTAAAGGTGAAGAATTATTCA | 50.4 | Forward primer for the amplification of fragment 2a of *ABC1*-GFP dDNA | Fourie 2020 |
| **CK-ABC1-GFP-overlap-R** | TTATTTGTACAATTCATCCATACC | 56.3 | Reverse primer for the amplification of fragment 2a of *ABC1*-GFP dDNA (Has overlap sequence with CK-GFP-ABC1-overlap-F) | This study |
| **CK-GFP-ABC1-overlap-F** | GTACAAATAAGAAGTTGCTTTTTTGACTAT | 53.2 | Forward primer for the amplification of fragment 2b of *ABC1*-GFP dDNA (Has overlap sequence with CK-ABC1-GFP-overlap-R) | This study |
| **CK-ABC1-3R** | CTGAACTCTTGGATCATTTCAAC | 51.9 | Reverse primer for the amplification of fragment 2b of *ABC1*-GFP dDNA | This study |
| **CK-ABC1::SPACER** | TCCACAAACTACTTCTGAAGCATCTGGTGCCGGTGCCGGTGCCGGTGCCGGTGCCATTTTG | 74.6 | Forward primer for the polymerisation of linker region (fragment 3) between ABC1 and GFP sequence (overlaps with CK-ABC1-2R) | This study |
| **SPACER-GFP-1R** | TGAATAATTCTTCACCTTTAGACATCAAAATGGCACCGGCACCGGCACCGGCACCGGCACCAGA | 73.4 | Reverse primer for the polymerisation of linker region (fragment 3) between ABC1 and GFP sequence (overlap with GFP-1-F) | Fourie 2020 |

NB: Target-specific CRISPR site is underlined

#### 4.3.3.1 CRISPR-Cas9 cassettes for *ABC1*-GFP fusion

The first component (Fragment A) of the gRNA cassette, containing the *SNR52* promoter, was amplified from pADH110 with primer pair AHO1096-ver2 and AHO1098-ver2 (**Table 4**), at an annealing temperature of 53.8$^{o}$C, using the reaction mixture and PCR program of KOD Hot Start DNA polymerase kit (Novagen®) (**Tables 2**, **3**). To introduce a CRISPR site specific for *ABC1* gene into the gRNA cassette, *ABC1* sequence with about 500 bp upstream and downstream were extracted from the genome of *C. krusei* UFS Y-0217 (CBS573$^{T}$) (Douglass et al. 2018). *ABC1* gene exists as an ABC11-ABC1 tandem with *ABC11* in this strain's genome and shares about 99% nucleotide identity with this gene. A CRISPR site specific for *ABC1* was only identified following the alignment of the nucleotide sequences of the two genes (**Fig. 1**). The CRISPR site (5'-ATATATCTGTGTTACCAAAAGGG-3') was retrieved with Geneious® 11.1.5, and was selected because it contains a protospacer adjacent motif (PAM) site, has high on-site activity score of 0.648 (Doench et al. 2014) and off-target activity score of 100% (Hsu et al. 2013). The flanking sequences 5'-CGTAAACTATTTTTAATTTG-3' and 5'-GTTTTAGAGCTAGAAATAGC-3', complementary to the 3' end of *SNR52* promoter (on pADH100) and 5' end of gRNA scaffold (on CK pADH147), respectively, were added to the 5' and 3' regions of the 20 bp CRISPR site without the PAM site (5'-ATATATCTGTGTTACCAAAA-3') to obtain CK-ABC1-CRISPR-1 oligonucleotide (**Table 4**). This oligo was used alongside primer AHO1097 to obtain the 3' region (Fragment B) of gRNA cassette by amplifying CK pADH147 (*Chapter 3*, **Fig. 6B**). Using stitching PCR, Fragments A and B were fused with primer pair AHO1237 and CK-3' HIS1-R, at an annealing temperature of 54.3$^{o}$C, to generate an intact gRNA cassette (Fragment C) (*Chapter 3*, **Fig. 6C**). Lastly, the Cas9 cassette was liberated from CK pADH99 by digesting 2 µg concentration of this plasmid with restriction enzyme *Mss*I (Thermo Scientific) (*Chapter 3*, **Fig. 6A**). Successful amplification and restriction digest of all fragments were confirmed with agarose gel electrophoresis.


**Fig. 1** Nucleotide sequence alignment of selected regions of *C. krusei ABC1* and *ABC11* genes. Using Clustal Omega tool (www.ebi.ac.uk) *ABC1* nucleotide sequence was aligned with that of *ABC11*. The two sequences share up to 99% identity. Highlighted sequence indicate *ABC1*-specific CRISPR site.

#### 4.3.3.2 Design of *ABC1*-GFP fusion donor DNA

The *ABC1*-GFP donor DNA (dDNA) was designed to consist of GFP sequence flanked by regions complementary to the *ABC1* gene (**Fig. 2**). This fragment (dDNA) was constructed with three components (fragments 1, 2, and 3). The first fragment (fragment 1) is a 1290 bp sequence from the 3' end of *ABC1* gene (without the stop codon); the 5' region (fragment 1a) of this fragment (representing the 5' end of the dDNA) was amplified from the genome of *C. krusei* with primers CK-ABC1-1F and CK-ABC1-1R, at an annealing temperature of 55.4$^{o}$C. The 3' region (fragment 1b) of this fragment modified to remove the CRISPR site was also amplified from this yeast's genome with primer pair CK-ABC1-2F and CK-ABC1-2R, at an annealing temperature of 52.7$^{o}$C. The two fragments (fragments 1a and 1b) were stitched together with primers CK-ABC1-1F and CK-ABC1-2R, at an annealing temperature of 52.7$^{o}$C, to obtain an intact fragment 1. The second component (fragment 2) of the dDNA is made up of GFP sequence (with stop codon) at its 5' end and a 231 bp sequence downstream the *ABC1* gene (representing the 3' end of the dDNA) at its 3' end. The GFP region of this fragment

(fragment 2a) was amplified from Clp10-*URA3-PMA1*-GFP construct (Fourie 2020) with primer pair GFP-1-F and CK-ABC1-GFP-overlap at an annealing temperature of 50.4ºC, while its 3' region (fragment 2b) was amplified from the genome of *C. krusei* with primers CK-GFP-ABC1-overlap-F and CK-ABC1-3R, at an annealing temperature of 51.9ºC. The primers CK-ABC1-GFP-overlap and CK-GFP-ABC1-overlap-F contain a 20 bp overlap sequence to aid stitching. The two fragments (fragments 2a and 2b) were subsequently stitched with primers GFP-1-F and CK-ABC1-3R at an annealing temperature of 50.4ºC to obtain an intact fragment 2. The last component of the dDNA, fragment 3, of approximately 86 bp was polymerised using two overlapping oligonucleotides, CK-ABC1::SPACER and SPACER-GFP-R. This fragment consists of a 39 bp sequence, for 13 amino acid linker (SGAGAGAGAGAIL) (Janke et al. 2004), flanked by regions complementary to the 3' and 5' ends of fragments 1 and 2, respectively, to enable the fusion of ABC1 and GFP, and facilitate proper folding of GFP (Janke et al. 2004). Lastly, fragments 1, 2, and 3 were ligated using the NEBuilder® HiFi DNA Assembly kit to generate the full *ABC1*-GFP dDNA. Following assembly reaction, primers CK-ABC1-1F and CK-ABC1-3R were used to confirm the correct ligation of these fragments.

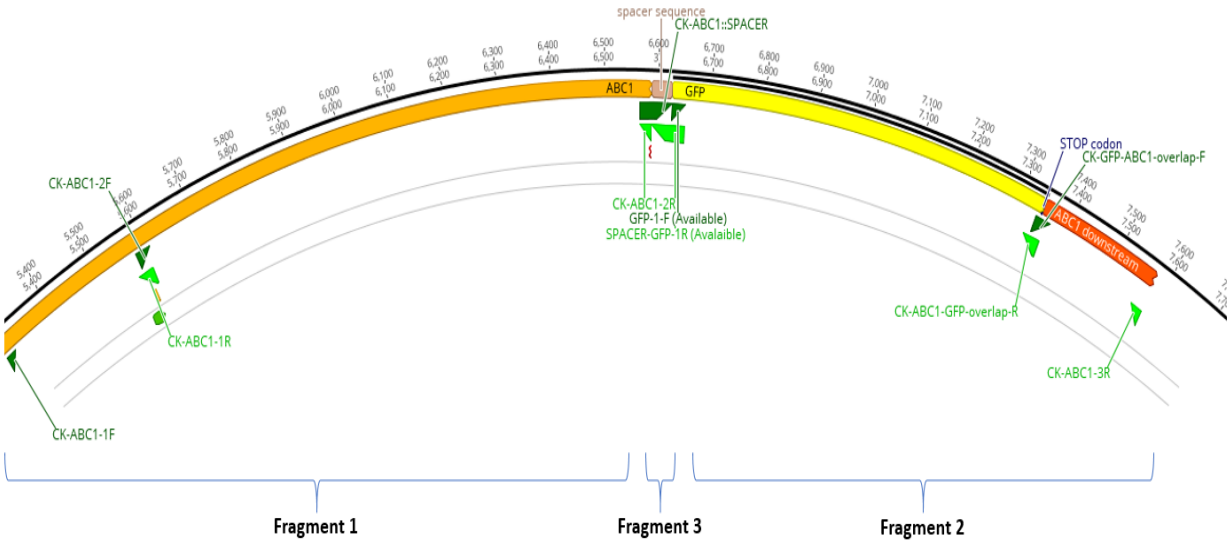


**Fig. 2** A section of a vector map depicting the components of *ABC1*-GFP donor DNA. The donor DNA is flanked by sites homologous to regions within the *ABC1* locus (Vector map generated using Geneious® 11.1.5).

#### 4.3.3.3 Transformation

This was done following a modified protocol of Nguyen and co-workers (2017). Briefly, an overnight 5 ml YPD culture of *C. krusei* UFS Y-0217 was diluted in a fresh YPD broth at 1:50, incubated at 30°C with shaking, allowed to reach $OD_{600}$ of 0.5 to 0.8, washed twice with milliQ water, and re-suspended in 1/100 of the original volume. A 50 µl volume of the re-suspended cells, Cas9 cassette, intact gRNA cassette, and complete dDNA fragment was mixed by gentle flicking with 1 ml plate mix [875 µl 50% PEG 3350 (Sigma-Aldrich), 100 µl 10X TE buffer, 25 µl 1 M Lithium acetate (adjusted to pH 7 with acetic acid; Sigma-Aldrich)], and incubated overnight at 30°C without shaking. In the following day, cells were heat-shocked (15 min, 44.6°C), washed with sterile YPD, allowed to recover (5 h at 30°C with shaking), plated onto YPD agar plate supplemented with 400 µg/ml nourseothricin (NTC), and incubated at 30°C for 2 to 3 days for colonies formation. Colony PCR was performed to confirm the integration of *ABC1*-GFP dDNA at the *ABC1* loci with primers CK-ABC1-1F and CK-ABC1-3R.

### 4.3.4 Influence of arachidonic acid and fluconazole on Abc1p expression

The influence of AA and FLC on the expression of Abc1 protein was assessed using SDS-PAGE and western blot analyses.

#### 4.3.4.1 Biofilm formation

Biofilm of *C. krusei* UFS Y-0277 strain exposed to various treatments was formed with a few modifications of previous methods (Ramage et al. 2001; Mishra et al. 2014). Briefly, a loopful of cells of this yeast was inoculated into a 5 ml sterile Yeast Nitrogen Base (YNB) broth (10 g/l glucose, 6.7 g/l YNB), and incubated for 24 h at 30°C. Cells were harvested and washed twice with sterile Phosphate Buffered Saline [PBS; 10 mM phosphate buffer, 2.7 mM potassium chloride, 137 mM sodium chloride (pH 7.4) (Sigma-Aldrich, St. Louis, MO, USA)] by centrifugation at 3000 *x g* for 5 min (Eppendorf, Germany). Accordingly, cells were re-suspended in a 5 ml sterile PBS, counted with a haemocytometer and standardised to a final concentration of $1.0 \times 10^7$ cells/ml in a 5 ml filter sterilised YNB broth. A volume of 2 ml of the standardised cell suspension was dispensed into the wells of 6-well plates (Thermo Scientific, Denmark), and incubated at 37°C for 90 min to facilitate cell adhesion. Following this step, the media (containing non-adherent cells) was aspirated, then 3 ml of YNB broth supplemented with AA (at 0.1 mM or 1 mM concentration) with and without FLC (32 µg/ml) was dispensed into designated wells, and incubated at 37°C for 6 h to allow biofilm formation. Each treatment group had three replicates.

#### 4.3.4.2 Protein extraction and visualisation of Abc1p on SDS-PAGE

Following biofilm formation, protein extraction from the biofilm cells was done following a previously described method (Szczepaniak et al. 2015). Briefly, biofilm was scrapped off and re-suspended in 1 ml ice cold milli-Q $H_2O$. Biofilm cells were lysed with a 150 µl volume of

1.85 M NaOH-7.5% mercaptoethanol solution and incubated for 10 min on ice. Next, a 150 µl volume of 50% trichloroacetic acid was added and incubated for 10 min on ice to precipitate proteins. Accordingly, the solution was centrifuged (10,000 *x g* for 5 min, 4$^{o}$C), washed twice with a 1 ml volume of Tris-HCl (1 M), resulting proteins were re-suspended in 50 µl sample buffer (40 mM Tris-HCl, 0.1 mM EDTA, 5% SDS, 8 M urea, 1% β-mercaptoethanol, 0.1 mg/ml bromophenol blue) and incubated at 37$^{o}$C for 30 min. A 10 µl volume of the protein sample was loaded onto a 7.5% acrylamide/bis-acrylamide SDS-PAGE, and proteins were allowed to separate for 60 min at 125 V. The gel was subsequently stained with Coomassie blue, de-stained with acetic acid (Fairbanks et al. 1971) and visualised under UV light in a Gel Doc™ XR+ (Bio-Rad, Canada) (Lee et al. 2012).

#### 4.3.4.3 Western blot analysis and Immunodetection of Abc1p

After the separation of proteins by SDS-PAGE analysis, proteins from the unstained SDS-PAGE gel were transferred onto a polyvinylidene fluoride (PVDF) membrane with a Trans-Blot Turbo Transfer System (Bio-Rad, USA). Accordingly, the immunodetection of Abc1p was performed with 1:2,500 anti-Cdr1p antibody (a generous gift from Prof. Dominique Sanglard, Lausanne, Switzerland) and horseradish peroxidase (HRP) conjugated secondary antibody (1:50,000) (Thermo Fischer Scientific, USA) following the manufacturers' specifications. Visualisation was achieved by viewing with a ChemiDocumentation™ MP imaging system (Bio-Rad).

### 4.3.5 Influence of arachidonic acid and fluconazole on the activity of Abc1p

The influence of AA on the function of Abc1p was evaluated using Rhodamine 6G efflux assay with slight modifications of previous methods (Maesaki et al. 1999; Ells et al. 2013; Szczepaniak et al. 2017). Briefly, biofilms were formed as described above in a black 96-well microtiter plate (Thermo Scientific, Denmark) for 6 h at 37$^{o}$C. After biofilm formation, the spent medium was removed, sterile PBS was dispensed into each well, and the plate was incubated at 37°C for 1 h to de-energise the biofilm cells. Following incubation, PBS was removed, and 200 µl of 10 µM Rhodamine 6G (Rh6G) (Sigma-Aldrich, St. Louis, MO, USA) in sterile PBS (prepared from 10 mM Rh6G stock in DMSO) was dispensed into each well. The plate was incubated at 37$^{o}$C, and the uptake of Rh6G was measured every 10 min for 1 h at an excitation wavelength of 530 nm and emission of 590 nm using Fluoroskan Ascent Fluorimeter (Thermo Scientific, China). Following the uptake step, leftover Rh6G was removed, and AA (0.1 or 1 mM), FLC (32 µg/ml), or DMSO and EtOH (DE, control) in sterile PBS was dispensed into designated wells, and the plate was incubated at 37$^{o}$C for another 1 h (Fourie 2020). Accordingly, the supernatant was removed from the wells, and 2 mM glucose (in sterile PBS) was dispensed into each well to induce efflux of Rh6G. The plate was incubated at 37$^{o}$C, and Rh6G efflux from the cells was measured extracellularly every 10 min for 1 h at an excitation

wavelength of 530 nm and emission wavelength of 590 nm using a Fluoroskan Ascent Fluorimeter (Thermo Scientific, China).

### 4.3.6 Statistical analysis

The data of different groups, unless stated otherwise, were compared using one-way analysis of variance (ANOVA) complemented with Tukey's multiple comparisons test and a *p*-value ≤ 0.05 was considered significant.

## 4.4 Results and Discussions

### 4.4.1 Constructing an *ABC1*-GFP mutant with CRISPR-Cas9 system

This chapter's main objective was to examine the influence of AA and FLC on the localisation, expression, and activity of Abc1p in *C. krusei*. To achieve this, we attempted to tag Abc1p with GFP using the adapted CRISPR-Cas9 system created in **Chapter 3**. This will then allow its fluorescence (localisation and expression) to be assessed under various treatments. This was done by first preparing relevant CRISPR cassettes and donor DNA, and then co-transforming these fragments into *C. krusei* to enable the creation of DSBs and knock-in of *ABC1*-GFP dDNA at the 3' end of *ABC1* gene.

#### 4.4.1.1 CRISPR-Cas9 cassettes for *ABC1*-GFP fusion

Firstly, the first component (fragment A) of the gRNA cassette was obtained from pADH110 with primer pair AHO1096-ver2 and AHO1098-ver2. A band size of approximately 1066 bp obtained confirms this fragment's successful amplification (**Fig. 3A**). Next, using CK pADH147 as a template, CK-ABC1-CRISPR-1 oligo and primer AHO1097 was used to amplify and introduce a CRISPR site (5'-ATATATCTGTGTTACCAAAA-3') specific for *ABC1* gene into the second component (fragment B) of the gRNA cassette. As depicted in **Figure 3A**, an expected band size of approximately 722 bp obtained confirms this fragment's successful amplification. As previously mentioned, the CK-ABC1-CRISPR-1 oligo is flanked by sequences complementary to the 3' end of *SNR52* promoter (on fragment A) and 5' end of gRNA scaffold (on fragment B), and this allowed the ligation of these two fragments to generate an intact gRNA cassette (fragment C) of approximately 1788 bp (**Fig. 3B**). Accordingly, the Cas9 cassette was liberated from CK pADH99 by digesting the plasmid with *Mss*I restriction enzyme. As depicted in **Figure 3B**, an expected size of approximately 8970 bp representing the Cas9 cassette was obtained.

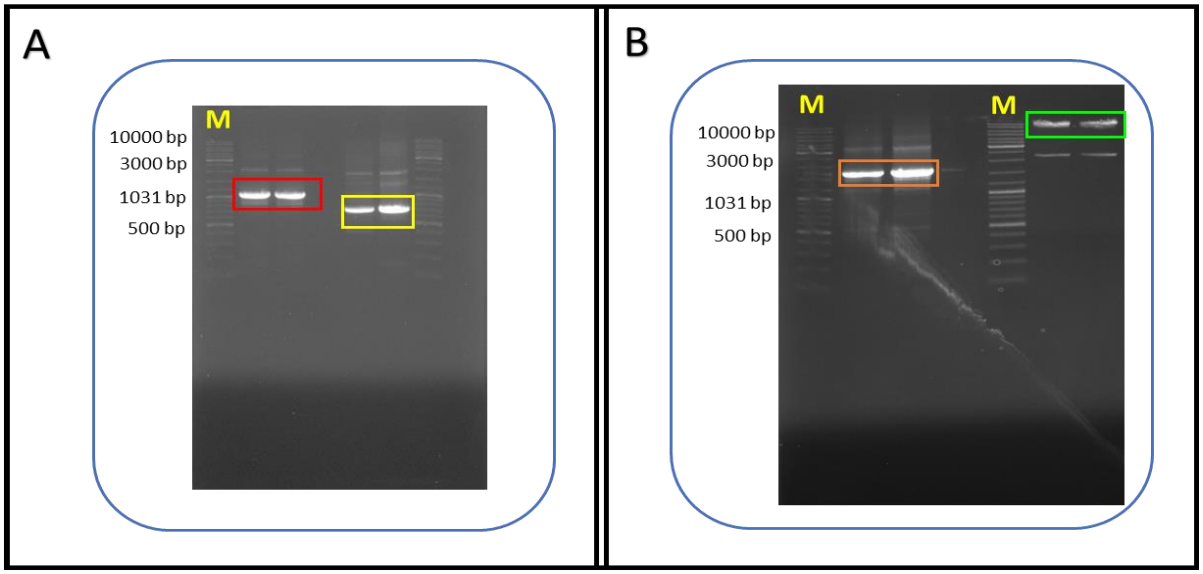


**Fig. 3** Construction of the components of CRISPR-Cas9 cassette. (**A**) An agarose gel profile depicting successful amplification of fragment A (red box) and fragment B (yellow box) of gRNA cassette. (**B**) A gel profile showing successful generation of an intact gRNA (orange box) following stitching of fragments A and B, and successful digestion of Cas9 cassette from CK pADH99 (green box). M represents 10 kb O'GeneRuler DNA ladder (Thermo Fisher Scientific).

#### 4.4.1.2 Designing *ABC1*-GFP fusion donor DNA

The *ABC1*-GFP donor DNA (dDNA) consists of a GFP sequence flanked by sequences homologous to regions within *ABC1* gene to enable its incorporation at the 3' region of this gene (via homology-directed repair) following the creation of DSBs by Cas9 protein (**Fig. 2**). Its successful incorporation at this region would result in the creation of *ABC1*-GFP mutant of *C. krusei*. This fragment (dDNA) was constructed with three components (fragments 1, 2, and 3). Specifically, the first fragment (fragment 1) consisting of a 1290 bp sequence from the 3' end of *ABC1* gene (without the stop codon) was obtained by stitching fragments 1a and 1b (**Fig. 4A**). The second fragment (fragment 2) of approximately 948 bp consisting of GFP sequence (with stop codon) and a 231 bp sequence downstream the *ABC1* gene was synthesised by stitching fragments 2a and 2b (**Fig. 4B**). These two fragments were ligated with a third fragment which consists of a 39 bp sequence (for 13 amino acid linker: SGAGAGAGAGAIL) (Janke et al. 2004), flanked by regions complementary to the 3' and 5' ends of fragments 1 and 2, respectively, to generate the full *ABC1*-GFP dDNA of approximately 2277 bp (**Fig. 5**). The intact dDNA also consists of homology arms of approximately 305 bp and 241 bp.

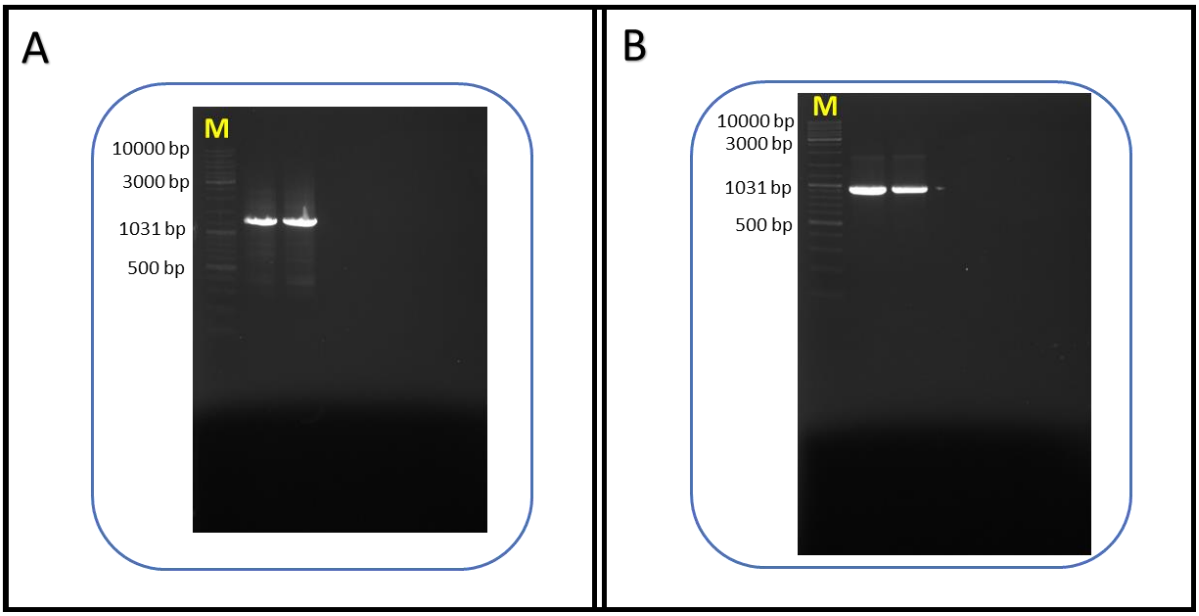


**Fig. 4** Synthesis of components of *ABC1*-GFP donor DNA (**A**) Gel profile showing expected band size of 1290 bp of fragment 1. (**B**) Gel profile depicting fragment 2 of an expected band size of ~948 bp. M represents DNA ladder.

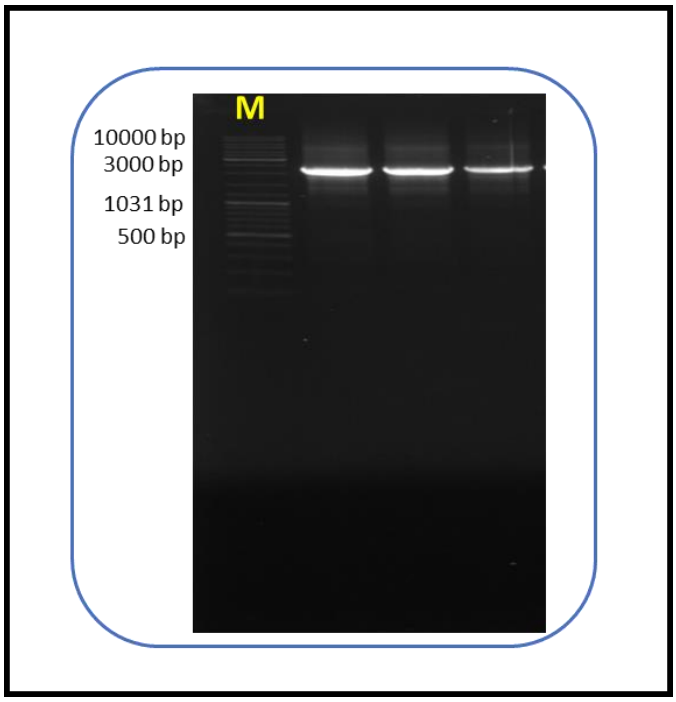


**Fig. 5** Gel profile showing successful synthesis and amplification of intact *ABC1*-GFP donor DNA (~2277 bp). M represents DNA ladder.

#### 4.4.1.3 Transformation

Following co-transformation, the Cas9 and gRNA cassettes generate a complete CRISPR-Cas9 cassette which integrates at the *HIS1* locus (*Chapter 3*, **Fig. 39**). Transformants are NTC-resistant (NTC$^{R}$) due to an intact *NAT* marker present within the complete CRISPR-Cas9 cassette and were selected on YPD plates containing NTC. However, none of the transformants incorporated the *ABC1*-GFP dDNA (**Fig. 6**), even after several attempts. The reason why the organism failed to incorporate the dDNA was unclear; however, future attempts would consider including longer homology arms into the dDNA (Wang et al. 2016; Norton et al. 2017).

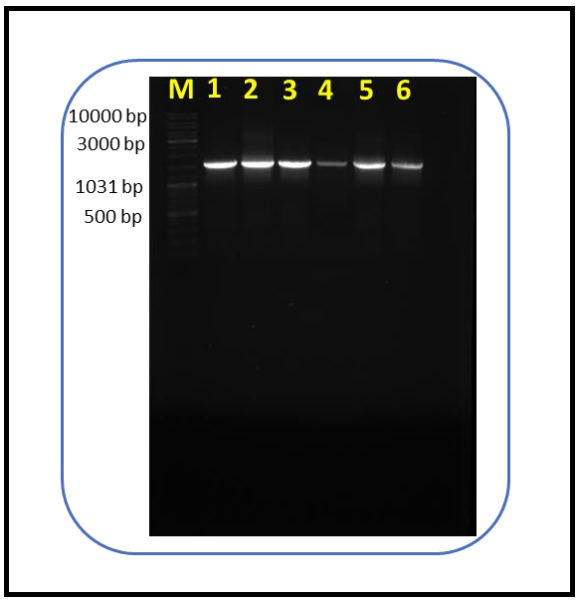


**Fig. 6** Gel profile depicting unsuccessful incorporation of *ABC1*-GFP donor DNA into the genome of the transformants. A band size of ~1389 bp representing a region within the unmodified *ABC1* loci was obtained (lanes 2 – 6), this corresponds to what was obtained for the wildtype strain (lane 1). M represents the DNA ladder.

### 4.4.2 Influence of arachidonic acid and fluconazole on Abc1p expression

Although the mechanism of intrinsic resistance to FLC in *C. krusei* has been chiefly attributed to alterations in FLC target, Erg11p, which consequently result in the decreased susceptibility of this target towards FLC (Venkateswarlu et al. 1997; Orozco et al. 1998; Fukuoka et al. 2003), the role of efflux pump transporters, including Abc1p, remains controversial. Efflux pumps are transport proteins that pump toxic compounds, including antimicrobial agents, out of the cell, and their overexpression results in a multidrug-resistance phenotype in pathogenic microbes (Webber and Piddock 2003; Lamping et al. 2009). The ATP-Binding Cassette (ABC) and Major Facilitator Superfamily (MFS) are the main transporter families in fungal species (Wirsching et al. 2001; White et al. 2002). The hydrolysis of ATP powers the ABC transporters' members; however, the MFS transporters rely on energy from the proton-motive force (Pao et al. 1998; Cannon et al. 2009; Rees et al. 2009; Redhu et al. 2016). Although four ABC transporters (Abc1p, Abc2p, Abc11p, Abc12p) have been identified in *C. krusei* (Lamping et

al. 2017; Douglass et al. 2018), Abc1p (Cdr1p) has proven to be the main transporter, and its overexpression results in resistance to antifungal drugs, including the azoles (Tsao et al. 2009; Lamping et al. 2009). Inhibitors of this efflux pump are limited, and PUFAs (e.g. AA) known to cause membrane disorganisation may represent potential inhibitors of this transporter (Avis and Belanger 2001; Pohl et al. 2011; Mishra et al. 2014).

However, since we were unable to obtain an *ABC1*-GFP mutant, we sought to assess the influence of AA and FLC on the expression of this transporter using SDS-PAGE and western blot analyses. This was performed by exposing biofilms of *C. krusei* UFS Y-0277 to AA (0.1 mM or 1 mM) and FLC (32 µg/ml) alone, and in combination, extracting total protein from these biofilms, and then assessing the expression of Abc1p using an anti-Cdr1 antibody. As shown in **Figure 7**, when compared to the control (DE), there was no apparent difference in the protein profile obtained when *C. krusei* biofilm was exposed to either AA or FLC singly, or in combination. Moreover, a protein with a size of almost 180 kDa, which may represent Abc1p (172 kDa), was identified in all treatments, including the DE control.

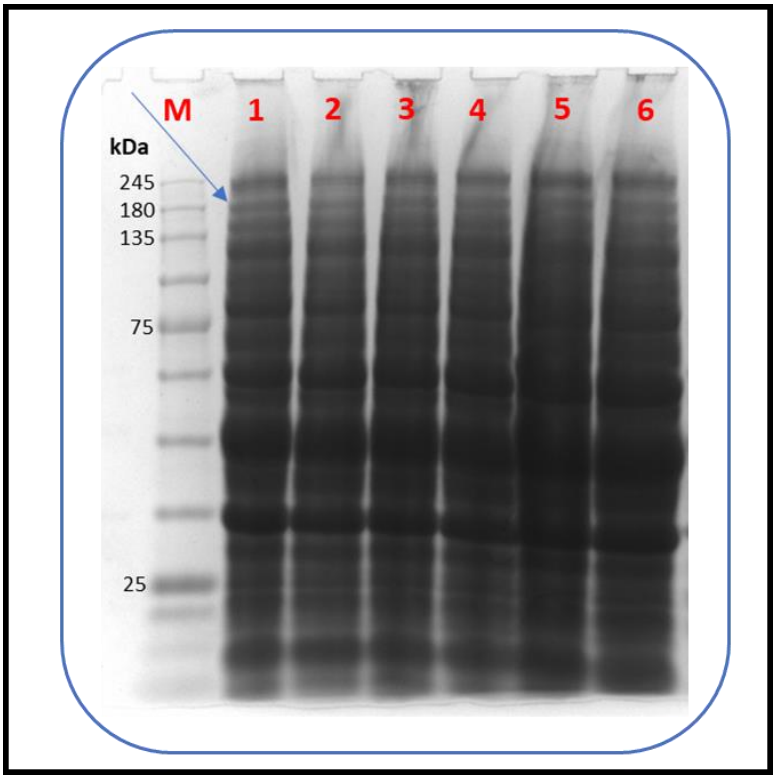


**Fig. 7** SDS-PAGE profile of proteins from *Candida krusei* biofilms following exposure to various treatments. **1**: DE (DMSO and ethanol) control, **2**: 32 µg/ml fluconazole (FLC), **3**: 0.1 mM Arachidonic acid (AA), **4**: combination of 0.1 mM AA and FLC, **5**: 1 mM AA, **6**: combination of 1 mM AA and FLC. M represents SDS-PAGE Pre-stained Protein Ladder (3.5 to 245 kDa). Arrow indicates a band corresponding to expected protein size of 172 kDa.

Additionally, western blot analysis was done using an anti-Cdr1 antibody to confirm this protein's identity as Abc1p and assess its expression levels. As depicted in **Figure 8**, a band which may represent Abc1p and suggest its expression was identified only in the presence of DE (control) and FLC. This may mean that Abc1p is constitutively expressed in this particular strain (Lamping et al. 2009), and overexpressed in the presence of FLC only. Its expression was however abrogated in all treatments with AA regardless of the concentration. However, these results are not entirely definitive, and future research would consider corroborating it with other analyses, such as quantitative western blot analysis and enzyme-linked immunosorbent assay, to measure the expression levels of Abc1p (Taylor and Posch 2014; Finger et al. 2018).

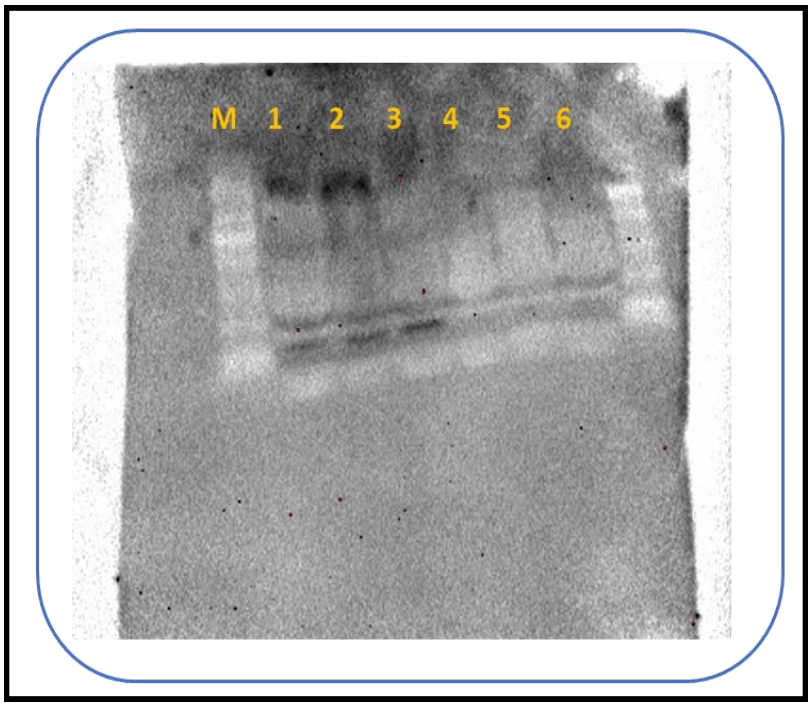


**Fig. 8** Confirmation of Abc1p protein and assessment of its expression level with western blot analysis following exposure to various treatments. **1**: DE (DMSO and ethanol) control, **2**: 32 µg/ml fluconazole (FLC), **3**: 0.1 mM Arachidonic acid (AA), **4**: combination of 0.1 mM AA and FLC, **5**: 1 mM AA, **6**: combination of 1 mM AA and FLC. Lanes 1 and 2 show expected band. M represents SDS-PAGE Pre-stained Protein Ladder (3.5 to 245 kDa).

### 4.4.3 Abc1p activity is increased by fluconazole but extenuated by arachidonic acid in a dose-dependent manner

We also evaluated the influence of AA and FLC on the functionality of Abc1p using Rhodamine 6G efflux assay. Rhodamine 6G is a substrate of ABC transporters, and its efflux is mediated by these transporters (Nakamura et al. 2001; Mukherjee et al. 2003; Tsao et al. 2009). Amongst these transporters, Cdr1p (Abc1p) is the primary transporter; hence Rh6G efflux was used to monitor its activity. To examine the influence of AA and FLC on the activity of Abc1p, Rh6G was allowed to passively diffuse into de-energised biofilms, the biofilms were then exposed to either AA (0.1 mM or 1 mM) or FLC alone, or in combination, after which the biofilms were re-energised with glucose, and the efflux of Rh6G was assessed.

As shown in **Figure 9A**, at a concentration of 0.1 mM, AA alone and in combination with FLC, could not inhibit the efflux of Rh6G. Remarkably, the activity of Abc1p was significantly extenuated in the presence of a higher concentration of AA (1 mM), either alone or in combination with FLC (**Fig. 9B**). This observation correlates with an earlier reported finding of dissipated activity of *C. albicans* efflux pump (Cdr1) in the presence of a high concentration (1 mM) of AA (Fourie 2020, Kuloyo 2020). Further, the diminished functionality of Abc1p observed in the presence of 1 mM AA may be due to the mislocalisation of Abc1 transporter from the cellular membranes (Fourie 2020). A similar study by Shareck and co-workers (2011) also demonstrated the mislocalisation of a membrane-bound protein, Ras1p, by conjugated linoleic acid. Furthermore, interference with ATP synthesis (ATP is essential for Abc1p activity) and/or mitochondrial dysfunction may also contribute to the reduced activity (Fourie 2020). Notably, the functionality of Abc1p was enhanced in the presence of FLC alone compared to the negative control (DE), and this may suggest that this transporter plays a role in FLC resistance in this strain; however, this needs to be further investigated (**Fig. 9**).

Conclusively, we observed the overexpression and increased functionality of Abc1p in the presence of FLC, and its diminished activity in the presence of 1 mM AA (but not 0.1 mM AA), either alone or in combination with FLC. Taken together, these findings suggest that AA influences the activity of Abc1 transporter in a dose-dependent manner and that this transporter plays a role in FLC resistance in this strain.

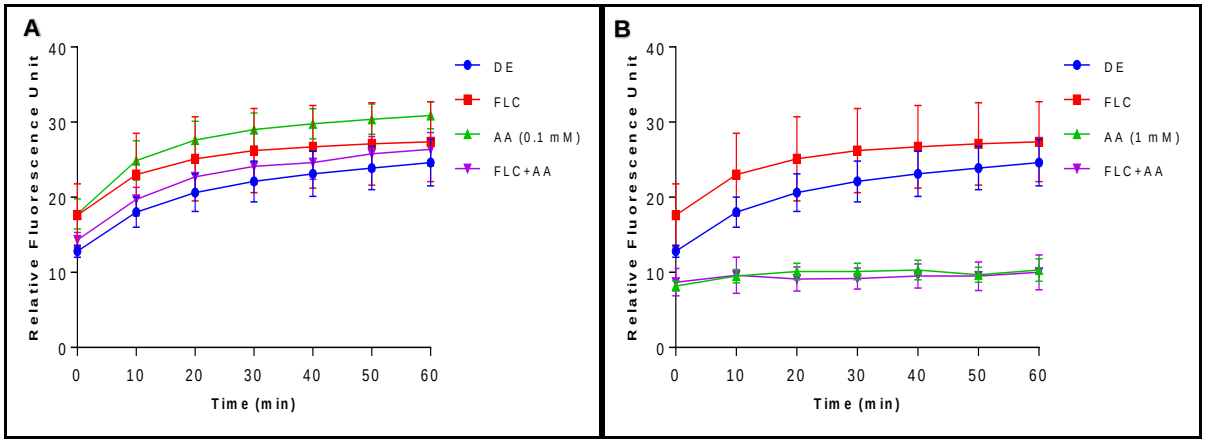


**Fig. 9** Rhodamine 6G efflux in *C. krusei* UFS Y-0277 biofilms after treatment with 0.1 mM arachidonic acid (**A**) and 1 mM arachidonic acid (**B**) in the presence or absence of fluconazole (32 µg/ml). Values are means of three independent experiments and error bars indicate standard deviation. **DE**: DMSO+Ethanol (control), **FLC**: fluconazole, **LA**: linoleic acid, **GLA**: gamma-linolenic acid.

## 4.5 Conclusions

This chapter's main objective was to assess the influence of AA and FLC on the localisation, expression, and activity of Abc1p in *C. krusei*. An initial attempt to fulfil this objective involved tagging Abc1p with GFP using CRISPR-Cas9 system, allowing its fluorescence (expression and localisation) to be assessed under various treatments; however, this was unsuccessful after several attempts. The influence of AA and FLC on the expression and activity of Abc1p was instead examined using western blot analysis and Rh6G efflux assay, respectively. Although Abc1 transporter was overexpressed in the presence of FLC, its expression was abrogated and undetected in all treatments with AA. Additionally, the functionality of Abc1p was enhanced in the presence of FLC; however, this was severely extenuated upon exposure to 1 mM AA, either alone or in combination with FLC. Although the mechanism by which AA diminishes the activity of Abc1 transporter was not investigated, our results do indicate that AA inhibits the expression of Abc1p. These findings demonstrate AA as a potential dose-dependent inhibitor of Abc1p and lent credence to the role of this transporter in FLC resistance.

## 4.6 References

Avis TJ, Belanger RR (2001) Specificity and mode of action of the antifungal fatty acid cis-9-heptadecenoic acid produced by *Pseudozyma flocculosa*. Applied and Environmental Microbiology 67:956–960. https://doi.org/10.1128/aem.67.2.956-960.2001

Cannon RD, Lamping E, Holmes AR, et al (2009) Efflux-mediated antifungal drug resistance. Clinical Microbiology Reviews 22:291–321. https://doi.org/10.1128/cmr.00051-08

Doench JG, Hartenian E, Graham DB, et al (2014) Rational design of highly active sgRNAs for CRISPR-Cas9–mediated gene inactivation. Nature Biotechnology 32:1262–1267. https://doi.org/10.1038/nbt.3026

Douglass AP, Offei B, Braun-Galleani S, et al (2018) Population genomics shows no distinction between pathogenic *Candida krusei* and environmental *Pichia kudriavzevii*: One species, four names. PLoS Pathogens 14:e1007138. https://doi.org/10.1371/journal.ppat.1007138

Ells R, Kemp G, Albertyn J, et al (2013) Phenothiazine is a potent inhibitor of prostaglandin $E_2$ production by *Candida albicans* biofilms. FEMS Yeast Research 13:849–855. https://doi.org/10.1111/1567-1364.12093

Fairbanks G, Steck TL, Wallach DFH (1971) Electrophoretic analysis of the major polypeptides

of the human erythrocyte membrane. Biochemistry 10:2606–2617. https://doi.org/10.1021/bi00789a030

Finger PF, Pepe MS, Dummer LA, et al (2018) Combined use of ELISA and western blot with recombinant N protein is a powerful tool for the immunodiagnosis of avian infectious bronchitis. Virology Journal 15:189. https://doi.org/10.1186/s12985-018-1096-2

Forastiero A, Garcia-Gil V, Rivero-Menendez O, et al (2015) Rapid development of *Candida krusei* echinocandin resistance during caspofungin therapy. Antimicrobial Agents and Chemotherapy 59:6975–6982. https://doi.org/10.1128/aac.01005-15

Fourie R (2020) Investigating the influence of arachidonic acid on Candida albicans and its interaction with *Pseudomonas aeruginosa*. Ph.D. Thesis, University of the Free State, Bloemfontein, South Africa

Fukuoka T, Johnston DA, Winslow CA, et al (2003) Genetic basis for differential activities of fluconazole and voriconazole against *Candida krusei*. Antimicrobial Agents and Chemotherapy 47:1213–1219. https://doi.org/10.1128/aac.47.4.1213-1219.2003

Guinea J, Sánchez-Somolinos M, Cuevas O, et al (2006) Fluconazole resistance mechanisms in *Candida krusei*: The contribution of efflux-pumps. Medical Mycology 44:575–578. https://doi.org/10.1080/13693780600561544

He X, Zhao M, Chen J, et al (2015) Overexpression of both *ERG11* and *ABC2* genes might be responsible for itraconazole resistance in clinical isolates of *Candida krusei*. PLoS ONE 10:e0136185. https://doi.org/10.1371/journal.pone.0136185

Hsu PD, Scott DA, Weinstein JA, et al (2013) DNA targeting specificity of RNA-guided Cas9 nucleases. Nature Biotechnology 31:827–832. https://doi.org/10.1038/nbt.2647

Jamiu AT, Albertyn J, Sebolai OM, Pohl CH (2020) Update on *Candida krusei*, a potential multidrug-resistant pathogen. Medical Mycology 59:14-30. https://doi.org/10.1093/mmy/myaa031

Janke C, Magiera MM, Rathfelder N, et al (2004) A versatile toolbox for PCR-based tagging of yeast genes: new fluorescent proteins, more markers and promoter substitution cassettes. Yeast 21:947–962. https://doi.org/10.1002/yea.1142

Katiyar SK, Edlind TD (2001) Identification and expression of multidrug resistance related ABC transporter genes in *Candida krusei*. Medical Mycology 39:109–116.

https://doi.org/10.1080/mmy.39.1.109.116

Kuloyo OO (2020) Investigation into the mechanism of arachidonic acid increased fluconazole susceptibility in *Candida albicans* biofilms and application to drug repurposing. Ph.D. Thesis, University of the Free State, Bloemfontein, South Africa

Lamping E, Ranchod A, Nakamura K, et al (2009) Abc1p is a multidrug efflux transporter that tips the balance in favor of innate azole resistance in *Candida krusei*. Antimicrobial Agents and Chemotherapy 53:354–369. https://doi.org/10.1128/aac.01095-08

Lamping E, Zhu J, Niimi M, Cannon RD (2017) Role of ectopic gene conversion in the evolution of a *Candida krusei* pleiotropic drug resistance transporter family. Genetics 205:1619–1639. https://doi.org/10.1534/genetics.116.194811

Lee PY, Costumbrado J, Hsu CY, Kim YH (2012) Agarose gel electrophoresis for the separation of DNA fragments. Journal of Visualized Experiments: https://doi.org/10.3791/3923

Maesaki S, Marichal P, Bossche HV, et al (1999) Rhodamine 6G efflux for the detection of *CDR1*-overexpressing azole-resistant *Candida albicans* strains. Journal of Antimicrobial Chemotherapy 44:27–31. https://doi.org/10.1093/jac/44.1.27

Mansfield BE, Oltean HN, Oliver BG, et al (2010) Azole drugs are imported by facilitated diffusion in *Candida albicans* and other pathogenic fungi. PLoS Pathogens 6:e1001126. https://doi.org/10.1371/journal.ppat.1001126

Mishra NN, Ali S, Shukla PK (2014) Arachidonic acid affects biofilm formation and $PGE_2$ level in *Candida albicans* and non-*albicans* species in presence of subinhibitory concentration of fluconazole and terbinafine. The Brazilian Journal of Infectious Diseases 18:287–293. https://doi.org/10.1016/j.bjid.2013.09.006

Mukherjee PK, Chandra J, Kuhn DM, Ghannoum MA (2003) Mechanism of fluconazole resistance in *Candida albicans* biofilms: Phase-specific role of efflux pumps and membrane sterols. Infection and Immunity 71:4333–4340. https://doi.org/10.1128/iai.71.8.4333-4340.2003

Mukhopadhyay K, Kohli A, Prasad R (2002) Drug susceptibilities of yeast cells are affected by membrane lipid composition. Antimicrobial Agents and Chemotherapy 46:3695–3705. https://doi.org/10.1128/aac.46.12.3695-3705.2002

Nakamura K, Niimi M, Niimi K, et al (2001) Functional expression of *Candida albicans* drug efflux pump Cdr1p in a *Saccharomyces cerevisiae* strain deficient in membrane transporters. Antimicrobial Agents and Chemotherapy 45:3366–3374. https://doi.org/10.1128/aac.45.12.3366-3374.2001

Nguyen N, Quail MMF, Hernday AD (2017) An efficient, rapid, and recyclable system for CRISPR-mediated genome editing in *Candida albicans*. mSphere 2:e00149-17. https://doi.org/10.1128/mSphereDirect.00149-17

Norton EL, Sherwood RK, Bennett RJ (2017) Development of a CRISPR-Cas9 system for efficient genome editing of *Candida lusitaniae*. mSphere 2:e00217-17 https://doi.org/10.1128/mSphere.00217-17

Orozco AS, Higginbotham LM, Hitchcock CA, et al (1998) Mechanism of fluconazole resistance in *Candida krusei*. Antimicrobial Agents and Chemotherapy 42:2645–2649. https://doi.org/10.1128/aac.42.10.2645

Pao SS, Paulsen IT, Saier MH (1998) Major facilitator superfamily. Microbiology and molecular biology reviews: MMBR 62:1–34

Pappas PG, Kauffman CA, Andes DR, et al (2016) Executive summary: Clinical practice guideline for the management of candidiasis: 2016 update by the Infectious Diseases Society of America. Clinical Infectious Diseases 62:409–417. https://doi.org/10.1093/cid/civ1194

Perea S, Lopez-Ribot JL, Kirkpatrick WR, et al (2001) Prevalence of molecular mechanisms of resistance to azole antifungal agents in *Candida albicans* strains displaying high-level fluconazole resistance isolated from human immunodeficiency virus-infected patients. Antimicrobial Agents and Chemotherapy 45:2676–2684. https://doi.org/10.1128/aac.45.10.2676-2684.2001

Pohl CH, Kock JLF, Thibane VS (2011) Antifungal free fatty acids. In: Science Against Microbial Pathogens: Communicating Current Research and Technological Advances. Formatex Research Center, Spain

Prasad R, Banerjee A, Khandelwal NK, Dhamgaye S (2015) The ABCs of *Candida albicans* Multidrug Transporter Cdr1. Eukaryotic Cell 14:1154–1164. https://doi.org/10.1128/ec.00137-15

Prasad R, De Wergifosse P, Goffeau A, Balzi E (1995) Molecular cloning and characterization

of a novel gene of *Candida albicans*, *CDR1*, conferring multiple resistance to drugs and antifungals. Current Genetics 27:320–329. https://doi.org/10.1007/bf00352101

Ramage G, Walle KV, Wickes BL, López-Ribot JL (2001) Standardized method for *in vitro* antifungal susceptibility testing of *Candida albicans* biofilms. Antimicrobial Agents and Chemotherapy 45:2475–2479. https://doi.org/10.1128/AAC.45.9.2475-2479.2001

Redhu AK, Shah AH, Prasad R (2016) MFS transporters of *Candida* species and their role in clinical drug resistance. FEMS Yeast Research 16:fow043. https://doi.org/10.1093/femsyr/fow043

Rees DC, Johnson E, Lewinson O (2009) ABC transporters: the power to change. Nature reviews Molecular cell biology 10:218–27. https://doi.org/10.1038/nrm2646

Ricardo E, Miranda IM, Faria-Ramos I, et al (2014) *In vivo* and *in vitro* acquisition of resistance to voriconazole by *Candida krusei*. Antimicrobial Agents and Chemotherapy 58:4604–4611. https://doi.org/10.1128/aac.02603-14

Robbins N, Caplan T, Cowen LE (2017) Molecular evolution of antifungal drug resistance. Annual Review of Microbiology 71:753–775. https://doi.org/10.1146/annurev-micro-030117-020345

Sanglard D, Odds FC (2002) Resistance of *Candida* species to antifungal agents: Molecular mechanisms and clinical consequences. The Lancet Infectious Diseases 2:73–85. https://doi.org/10.1016/s1473-3099(02)00181-0

Shareck J, Nantel A, Belhumeur P (2011) Conjugated linoleic acid inhibits hyphal growth in *Candida albicans* by modulating Ras1p cellular levels and downregulating *TEC1* expression. Eukaryotic Cell 10:565–577. https://doi.org/10.1128/ec.00305-10

Szczepaniak J, Cieślik W, Romanowicz A, et al (2017) Blocking and dislocation of *Candida albicans* Cdr1p transporter by styrylquinolines. International Journal of Antimicrobial Agents 50:171–176. https://doi.org/10.1016/j.ijantimicag.2017.01.044

Szczepaniak J, Łukaszewicz M, Krasowska A (2015) Estimation of *Candida albicans* ABC transporter behavior in real-time via fluorescence. Frontiers in Microbiology 6: https://doi.org/10.3389/fmicb.2015.01382

Tavakoli M, Zaini F, Kordbacheh M, et al (2010) Upregulation of the *ERG11* gene in *Candida krusei* by azoles. Daru: journal of Faculty of Pharmacy, Tehran University of Medical

Sciences 18:276–80

Taylor SC, Posch A (2014) The design of a quantitative western blot experiment. In: BioMed Research International. https://www.hindawi.com/journals/bmri/2014/361590/

Tsao S, Rahkhoodaee F, Raymond M (2009) Relative contributions of the *Candida albicans* ABC transporters Cdr1p and Cdr2p to clinical azole resistance. Antimicrobial Agents and Chemotherapy 53:1344–1352. https://doi.org/10.1128/aac.00926-08

Venkateswarlu K, Denning DW, Kelly SL (1997) Inhibition and interaction of cytochrome P450 of *Candida krusei* with azole antifungal drugs. Medical Mycology 35:19–25. https://doi.org/10.1080/02681219780000821

Wang Y, Wei D, Zhu X, et al (2016) A 'suicide' CRISPR-Cas9 system to promote gene deletion and restoration by electroporation in *Cryptococcus neoformans*. Scientific Reports 6:1–13. https://doi.org/10.1038/srep31145

Webber MA, Piddock L (2003) The importance of efflux pumps in bacterial antibiotic resistance. Journal of Antimicrobial Chemotherapy 51:9–11. https://doi.org/10.1093/jac/dkg050

Whaley SG, Berkow EL, Rybak JM, et al (2017) Azole antifungal resistance in *Candida albicans* and emerging non-*albicans Candida* species. Frontiers in Microbiology 7:2173. https://doi.org/10.3389/fmicb.2016.02173

White TC, Holleman S, Dy F, et al (2002) Resistance mechanisms in clinical isolates of *Candida albicans*. Antimicrobial Agents and Chemotherapy 46:1704–1713. https://doi.org/10.1128/aac.46.6.1704-1713.2002

Wirsching S, Moran GP, Sullivan DJ, et al (2001) *MDR1*-mediated drug resistance in *Candida dubliniensis*. Antimicrobial Agents and Chemotherapy 45:3416–3421. https://doi.org/10.1128/aac.45.12.3416-3421.2001

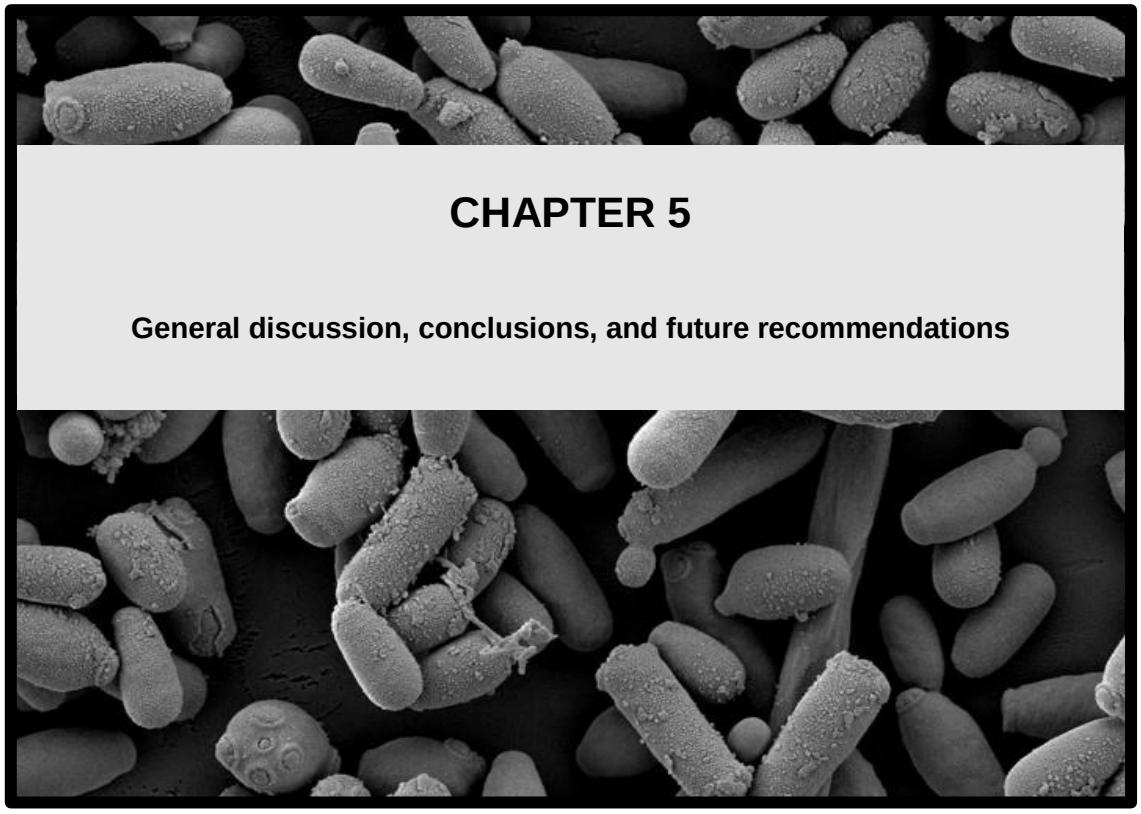

# CHAPTER 5

**General discussion, conclusions, and future recommendations**

## 5.1 Influence of polyunsaturated fatty acids on *in vitro* fluconazole susceptibility of *C. krusei*

The epidemiology of invasive candidiasis is changing, with an increasing number of infections being attributed to non-*albicans Candida* (NAC) species with reduced antifungal susceptibility (Chi et al. 2011; da Silva et al. 2013; Sadeghi et al. 2018). However, the number of antifungal agents available to treat these infections remains limited. This is, in part, due to the eukaryotic nature of both fungi and humans (Campoy and Adrio 2017). For example, the clinical use of polyenes, which target fungal ergosterol, is hindered by nephrotoxicity because of the slight affinity of these drugs for cholesterol, an ergosterol homolog found in humans (Paterson et al. 2003; Lemke et al. 2005). Fluconazole (FLC) remains the drug of choice for the treatment of many fungal infections, especially in resource-limited settings, due to its affordability, amongst other factors. However, NAC species are generally less susceptible to this drug, with 35% of *C. glabrata* and 10-25% of *C. tropicalis* isolates exhibiting either a primary or secondary resistance (Whaley et al. 2017). More worrisome, up to 97% of *C. krusei* isolates are considered inherently resistant to FLC (Whaley et al. 2017). This yeast also rapidly displays adaptive resistance to other antifungals, including the echinocandins (Forastiero et al. 2015). Consequently, other therapeutic approaches are being explored, including combination therapy, which has been harnessed against infectious agents in various forms, including the combination of conventional drugs with appropriate non-antimicrobial compounds (e.g. fatty acids, phytochemicals) (Ells et al. 2009; Jia et al. 2019). Combination therapy may provide greater benefits, including increased microbicidal activity, reduced toxicity, and decreased rate of resistance development (Chang et al. 2017; Prasad et al. 2017).

The antifungal property of unsaturated fatty acids against certain *Candida* spp. has been reported by previous studies (Thibane et al. 2010; Kim et al. 2020; Muthamil et al. 2020). This was confirmed in the present study. The antifungal effect of the tested polyunsaturated fatty acids (PUFAs), including oleic acid (OA), linoleic (LA), gamma-linolenic acid (GLA), arachidonic acid (AA), and eicosapentaenoic (EPA), on *C. krusei* biofilms was dependent on the strain, as well as on the chain length and dose of the fatty acid. The mechanism of action of antifungal unsaturated fatty acids has previously been found to be mainly through their incorporation into fungal membranes – which consequently increases membrane fluidity and permeability, and ultimately elicits membrane disorganisation (Avis and Belanger 2001; Pohl et al. 2011; Mishra et al. 2014). The disruption of hyphal morphogenesis by antifungal PUFAs has also been noted in certain *Candida* spp. (Shareck et al. 2011). Notably, in the present study, the most resistant strain to the action of PUFAs was also the least susceptible to FLC, possibly indicating a shared mechanism of action.

Previous studies, using *Candida* spp. without intrinsic FLC resistance (i.e. *C. albicans* and *C. dubliniensis*), found that PUFAs, such as AA and stearidonic acid (SDA), increase the antifungal susceptibility of these yeasts to amphotericin B and clotrimazole (Ells et al. 2009; Thibane et al. 2012). However, it was unknown whether the same would apply to a pathogenic yeast with intrinsic resistance to an antifungal drug, as in the case of *C. krusei*. We found that either of the two PUFAs (LA or GLA) overcomes the intrinsic FLC resistance of *C. krusei* and potentiates the action of FLC. An initial attempt to dissect the mechanism responsible for this potentiating effect using scanning electron microscopy revealed that the combination treatments elicit the production of extracellular vesicles (EVs), cell membrane damage, and cell rupture. Biofilm-associated EV secretions, critical for antifungal resistance have been identified previously (Zarnowski et al. 2018). Moreover, these vesicles may act as decoys to protect yeast cells from the cytotoxic effect of antifungal agents (Zhao et al. 2019). These structures are also released upon exposure of yeast cells to known oxidative stress inducers (Nollin and Borgers 1975; Lemar et al. 2005), suggesting the induction of oxidative stress a possible mechanism of the combination treatments. Similar structures were found on biofilms cells exposed to a high concentration of marine PUFAs (Thibane et al. 2010; Thibane et al. 2012).

A membrane integrity assay with propidium iodide dye further confirmed the detrimental effect of the combination treatments on the cell membrane; this effect is possibly a direct influence of PUFA insertion into fungal membranes or an aftermath of increased reactive oxygen species (ROS) and lipid peroxidation. Additionally, the induction of cell rupture and loss of intracellular contents (hallmarks of necrosis) observed might have been a consequence of a two-step process: an initial cell membrane disorganisation, induced by the insertion of PUFA into the yeast membranes, followed by an enhanced plasma membrane distortion and increased oxidative stress within the already vulnerable cells facilitated by FLC. This ultimately results in cell rupture via necrosis. Further findings in the present study showed that the induction of oxidative stress contributes to the potentiating effects of the combination treatments, as known antioxidants [i.e. butylated hydroxytoluene and α-tocopherol polyethylene glycol succinate (TPGS)], could rescue the biofilms from the cytotoxic effects of these treatments. Our results also suggest that the increased oxidative stress might be due to lipid peroxidation in the cell membrane since a better antioxidative effect was observed for TPGS which localises to the plasma membrane (Li et al. 2015; Yehye et al. 2015).

Furthermore, it was necessary to assess the influence of these treatments on the functionality of efflux pumps due to their indispensable role in extruding antimicrobial agents and increasing antifungal resistance (Lamping et al. 2009). Since drug efflux pumps are localised in the cell membrane and unsaturated fatty acids have been reported to elicit membrane disruption (Avis and Belanger 2001; Pohl et al. 2011; Mishra et al. 2014), the observed inhibition of efflux pump activity by the combination treatments may be due to the mislocalisation of efflux pumps, following

membrane disorganisation. Additionally, all the presently characterised efflux pumps in *C. krusei* are ATP-binding cassette (ABC) transporters which are dependent on the hydrolysis of ATP to function (Lamping et al. 2017; Douglass et al. 2018). Hence, the abrogated functionality of the efflux pumps might have been facilitated by ATP deficit, since antimicrobial fatty acids could disrupt oxidative phosphorylation (Yoon et al. 2018).

In summary, PUFAs show potential as antifungal-potentiating agents against an intrinsically-resistant yeast. Based on the aforementioned and above-discussed mechanisms of action, the possible sequence of events responsible for this effect could be "direct" or "indirect". The direct effect involves the incorporation of PUFA into cellular lipids and membranes. Such insertion increases the unsaturation index, directly alters membrane fluidity and stability, and ultimately results in membrane perturbation (Avis and Belanger 2001; Pohl et al. 2011; Mishra et al. 2014). As for the indirect influence, ROS production is enhanced following the incorporation of an exogenous unsaturated fatty acid (due to the presence of carbon-carbon double bonds) (Ayala et al. 2014). Next, oxidative degradation of lipids (lipid peroxidation) occurs due to the actions of free radicals (ROS) (Fuchs et al. 2014). At this point, lipid peroxidation results in either cell membrane disruption, oxidative stress, or a combination thereof. When the "membrane disruption" pathway is followed, the disruption of membrane protein functions occurs, and this pathway ultimately results in regulated and/or uncontrolled cell deaths (Yang and Stockwell 2016; Gaschler and Stockwell 2017). On the other hand, the pathway involving "oxidative stress" in most cases directly results in oxidative damage, which ultimately results in cell death via apoptosis, necrosis, or a combination thereof (Repetto et al. 2012; Pizzino et al. 2017). Notably, although both of these pathways could induce regulated (apoptosis) and uncontrolled (necrosis) cell death, the occurrence of necrotic cell death was more likely in this study due to the identification of some of its hallmarks, including cell rupture and loss of intracellular contents, in cells within the combination-treated biofilms (Eisenberg et al. 2010).

## 5.2 Influence of polyunsaturated fatty acids on the survival and fungal burden of infected *C. elegans*

In drug discovery, the *in vitro* antimicrobial activity of lead compounds does not always translate to a corresponding *in vivo* efficacy. In addition to providing valuable information on the correlation between findings of *in vitro* and *in vivo* assays, animal models are also employed to gain better insights into the progression and characterisation of diseases in humans, since many virulence traits and immune reactions are only induced *in vivo* (Marsh and May 2012). Because of this, we took a step further by evaluating the potentiating effects of the combination treatments in a *Caenorhabditis elegans* infection model. This model organism has been used for genetic analysis (Watts and Browse 2002), lipid and fatty acid metabolism studies (Bouyanfif et al. 2019; Mokoena et al. 2020), and certain drug discovery research (Madende et al. 2020). Moreover, the ability of

*C. krusei* to infect and kill this particular strain has been documented (Scorzoni et al. 2013). A study by Breger and co-workers (2007), demonstrated that FLC (at 32 µg/ml) could not prolong the survival of nematodes exposed to a FLC-resistant strain of *C. krusei*, and had a toxic effect on the nematodes. This was not the case in the present study, where it was able to slightly extend the median lifespan of *C. elegans*, one explanation for this is that its antifungal efficacy against the *C. krusei* strain used in this study outweighs its toxicity, if any, on infected nematodes. Our findings further demonstrated that each of the fatty acids (LA or GLA) alone was able to slightly extend the survival and reduce the intestinal fungal burden of infected nematodes. However, a superior overall activity was noted with the combination treatments. The mechanism for this *in vivo* potentiating effect was not investigated. However, it may be due to a direct effect on *C. krusei*, as found *in vitro*, or possibly due to improved immunity of *C. elegans* in the presence of these PUFAs*,* since there is evidence that endogenous and exogenous PUFAs, such as GLA and SDA, are required for *C. elegans* immunity (Nandakumar and Tan 2008). This, however, needs to be investigated. Conclusively, our *in vivo* findings correlate with the observed *in vitro* susceptibility profiles of the combination treatments; however, future studies should consider exploiting higher model animals.

## 5.3 Establishment of a CRISPR-Cas9 genome editing tool for *C. krusei*

The serendipitous discovery of and elaborate research on a bacterial and archaeal adaptive system known as Clustered Regularly Interspaced Short Palindromic Repeats (CRISPR) led to the development of a CRISPR-Cas9 mediated genome editing tool. This tool is superior to the earlier gene-editing endonucleases, including zinc-finger nucleases and transcription activator-like effector nucleases, owing to its affordability, simplicity – simple to design, but effective for answering complex genomic questions, flexibility, versatility, and high targeting and editing efficiency (Khadempar et al. 2019; Saha et al. 2019). A functional CRISPR-Cas9 editing system has been designed and utilised for gene-editing in *Candida albicans* (Vyas et al. 2015). Moreover, similar systems are also available for recalcitrant non-*albicans Candida* (NAC) species, such as *C. glabrata* and *C. auris* (Grahl et al. 2017; Lombardi et al. 2017). Indeed, the use of this tool in medical mycology has improved the understanding of the roles of various genes in virulence and resistance. However, no such system is available for *C. krusei*. The lack of such a facile and precise tool for genome engineering in this yeast has hindered molecular understanding of its resistance mechanisms. In the present study, a CRISPR-Cas9 system was developed for this *C. krusei* by adapting a HIS-FLP type *C. albicans*-specific system of Nguyen and co-workers (2017). Plasmids for this system were obtained from Addgene. Relevant fragments were replaced with corresponding homologs from *C. krusei* genome. The resulting optimised system is made up of a *CAS9* gene (which encodes the molecular scissor- Cas9 protein), placed under the control of *C. krusei ENO1* promoter; and a gRNA (under an *SNR52* promoter), which is adaptable to target

and edit any gene within this yeast's genome. The full CRISPR system integrates at the *HIS1* locus and possesses an intact (dominant) nourseothricin N-acetyltransferase (*NAT*) marker gene, which allows transformants to exhibit a nourseothricin-resistance phenotype. This system is recyclable and upon gene-editing, it is removed from the genome via growth on a maltose-containing medium accomplished by flippase (*FLP*) recombinase.

In literature, the efficacy of gene-editing tools is often assessed by targeting auxotrophic marker genes, since their disruption (or deletion) either prevents the growth of an auxotrophic mutant (in the case of *URA3* gene) or results in the production of a distinctive phenotype in the absence of an essential nutrient (red colonies in the case of *ADE2* gene) (Lacroute 1968; Poulter and Rikkerink 1983). By using our optimised system with relevant donor DNA (dDNA), we successfully targeted and deleted *URA3* and *ADE2*, to generate *ura3Δ/Δ* and *ade2Δ/Δ* mutants, respectively. The engineering efficiency of our system for *URA3* and *ADE2* deletion was between 10% – 16%. However, in the future, this system's toolbox will be strengthened by codon-optimising *CAS9* gene for expression in *C. krusei* (Weninger et al. 2016; Raschmanová et al. 2018), and placing the gRNA under a promoter that is specific for this yeast (Enkler et al. 2016; Morio et al. 2020). Strikingly, in comparison with the wildtype strain, the obtained auxotrophic mutants (*ade2Δ/Δ*, *ura3Δ/Δ*) demonstrated a reduced-filamentation phenotype. This may possibly suggest their reduced virulence. However, virulence studies, particularly in an intractable and simple host like *C. elegans*, are warranted (Madende et al. 2020). Similar studies have reported reduced virulence of mutants of *C. albicans* with disrupted *URA3* and *ADE2* (Kirsch and Whitney 1991; Donovan et al. 2001; Staab and Sundstrom 2003). To the best of our knowledge, this is the first development and usage of the CRISPR-Cas9 system for genome engineering in *C. krusei*.

## 5.4 Influence of arachidonic acid and fluconazole on the expression and function of Abc1p

Although the role of FLC target, Erg11p, in the intrinsic FLC resistance of *C. krusei* has been established (Venkateswarlu et al. 1997; Orozco et al. 1998; Fukuoka et al. 2003). The role of efflux pump transporters, including Abc1p (the homolog of Cdr1 protein in *C. albicans*), in this resistance remains obscure. Two earlier studies by Katiyar and Edlind (2001) and Guinea and co-workers (2006) have documented that no ABC transporters are involved in this yeast's innate FLC resistance. However, a later study noted a possible role of Abc1p in this resistance (Lamping et al. 2009). Despite their roles in antifungal resistance, no class of antifungal targets the efflux pumps. Interestingly, AA (a type of PUFA), has been demonstrated as a potential inhibitor of Abc1p homolog (Cdr1p) in *C. albicans* (Fourie 2020; Kuloyo 2020). The construction of a Green Fluorescent Fusion (GFP) fusion of Abc1p, using the adapted CRISPR-Cas9 system was attempted in order to gain valuable insights into the influence of AA and FLC on the localisation, expression, and activity of Abc1p in *C. krusei*. However, this was unsuccessful, possibly due to

the failure of the yeast to incorporate the supplied *ABC1*-GFP fusion donor DNA, after the creation of double-strand breaks (DSBs) by the Cas9 nuclease. Furthermore, with the use of alternative analytical techniques (western blot analysis and efflux pump assay), FLC was found to enhance both the expression and functionality of Abc1p. This may possibly indicate that this transporter plays a role in FLC resistance. Similar studies have reported the mechanism of resistance to itraconazole and voriconazole to be, in part, due to the overexpression of Abc1p and Abc2p (Tavakoli et al. 2010; Ricardo et al. 2014; He et al. 2015). However, AA (at a higher concentration), reduces the expression of Abc1p, and consequently extenuates its functionality, even in the presence of FLC. Together, these preliminary findings demonstrate AA as a potential inhibitor of Abc1p and lent credence to the role of this transporter in FLC resistance.

## 5.5 References


Avis TJ, Belanger RR (2001) Specificity and mode of action of the antifungal fatty acid cis-9-heptadecenoic acid produced by *Pseudozyma flocculosa*. Applied and Environmental Microbiology 67:956–960. https://doi.org/10.1128/aem.67.2.956-960.2001

Ayala A, Muñoz MF, Argüelles S (2014) Lipid peroxidation: Production, metabolism, and signaling mechanisms of malondialdehyde and 4-hydroxy-2-nonenal. Oxidative Medicine and Cellular Longevity 2014:1–31. https://doi.org/10.1155/2014/360438

Bouyanfif A, Jayarathne S, Koboziev I, Moustaid-Moussa N (2019) The nematode *Caenorhabditis elegans* as a model organism to study metabolic effects of ω-3 polyunsaturated fatty acids in obesity. Advances in Nutrition 10:165–178. https://doi.org/10.1093/advances/nmy059

Breger J, Fuchs BB, Aperis G, et al (2007) Antifungal chemical compounds identified using a *C. elegans* pathogenicity assay. PLoS Pathogens 3:e18. https://doi.org/10.1371/journal.ppat.0030018

Campoy S, Adrio JL (2017) Antifungals. Biochemical Pharmacology 133:86–96. https://doi.org/10.1016/j.bcp.2016.11.019

Chang YL, Yu SJ, Heitman J, et al (2017) New facets of antifungal therapy. Virulence 8:222–236. https://doi.org/10.1080/21505594.2016.1257457

Chi HW, Yang YS, Shang ST, et al (2011) *Candida albicans* versus non-*albicans* bloodstream infections: The comparison of risk factors and outcome. Journal of Microbiology, Immunology and Infection 44:369–375. https://doi.org/10.1016/j.jmii.2010.08.010

da Silva CR, de Andrade Neto JB, Sidrim JJC, et al (2013) Synergistic effects of amiodarone and fluconazole on *Candida tropicalis* resistant to fluconazole. Antimicrobial Agents and Chemotherapy 57:1691–1700. https://doi.org/10.1128/aac.00966-12

Donovan M, Schumuke JJ, Fonzi WA, et al (2001) Virulence of a phosphoribosylaminoimidazole carboxylase-deficient *Candida albicans* strain in an immunosuppressed murine model of systemic candidiasis. Infection and Immunity 69:2542–2548. https://doi.org/10.1128/iai.69.4.2542-2548.2001

Douglass AP, Offei B, Braun-Galleani S, et al (2018) Population genomics shows no distinction between pathogenic *Candida krusei* and environmental *Pichia kudriavzevii*: One species, four names. PLoS Pathogens 14:e1007138. https://doi.org/10.1371/journal.ppat.1007138

Eisenberg T, Carmona-Gutierrez D, Büttner S, et al (2010) Necrosis in yeast. Apoptosis 15:257–268. https://doi.org/10.1007/s10495-009-0453-4

Ells R, Kock JLF, Van Wyk PWJ, et al (2009) Arachidonic acid increases antifungal susceptibility of *Candida albicans* and *Candida dubliniensis*. Journal of Antimicrobial Chemotherapy 63:124–128. https://doi.org/10.1093/jac/dkn446

Enkler L, Richer D, Marchand AL, et al (2016) Genome engineering in the yeast pathogen *Candida glabrata* using the CRISPR-Cas9 system. Scientific Reports 6:1–12. https://doi.org/10.1038/srep35766

Forastiero A, Garcia-Gil V, Rivero-Menendez O, et al (2015) Rapid development of *Candida krusei* echinocandin resistance during caspofungin therapy. Antimicrobial Agents and Chemotherapy 59:6975–6982. https://doi.org/10.1128/aac.01005-15

Fourie R (2020) Investigating the influence of arachidonic acid on *Candida albicans* and its interaction with *Pseudomonas aeruginosa*. Ph.D. Thesis, University of the Free State, Bloemfontein, South Africa

Fuchs P, Perez-Pinzon MA, Dave KR (2014) Cerebral ischemia in diabetics and oxidative stress. Diabetes: Oxidative Stress and Dietary Antioxidants 15–23. https://doi.org/10.1016/b978-0-12-405885-9.00002-4

Fukuoka T, Johnston DA, Winslow CA, et al (2003) Genetic basis for differential activities of fluconazole and voriconazole against *Candida krusei*. Antimicrobial Agents and Chemotherapy 47:1213–1219. https://doi.org/10.1128/aac.47.4.1213-1219.2003

Gaschler MM, Stockwell BR (2017) Lipid peroxidation in cell death. Biochemical and Biophysical Research Communications 482:419–425. https://doi.org/10.1016/j.bbrc.2016.10.086

Grahl N, Demers EG, Crocker AW, Hogan DA (2017) Use of RNA-protein complexes for genome editing in non-*albicans* *Candida* species. mSphere 2:e00218-17 https://doi.org/10.1128/msphere.00218-17

Guinea J, Sánchez-Somolinos M, Cuevas O, et al (2006) Fluconazole resistance mechanisms in *Candida krusei*: The contribution of efflux-pumps. Medical Mycology 44:575–578. https://doi.org/10.1080/13693780600561544

He X, Zhao M, Chen J, et al (2015) Overexpression of both *ERG11* and *ABC2* genes might be responsible for itraconazole resistance in clinical isolates of *Candida krusei*. PLoS ONE 10:e0136185. https://doi.org/10.1371/journal.pone.0136185

Jia C, Zhang J, Zhuge Y, et al (2019) Synergistic effects of geldanamycin with fluconazole are associated with reactive oxygen species in *Candida tropicalis* resistant to azoles and amphotericin B. Free Radical Research 53:618–628. https://doi.org/10.1080/10715762.2019.1610563

Katiyar SK, Edlind TD (2001) Identification and expression of multidrug resistance related *ABC* transporter genes in *Candida krusei*. Medical Mycology 39:109–116. https://doi.org/10.1080/mmy.39.1.109.116

Khadempar S, Familghadakchi S, Motlagh RA, et al (2019) CRISPR-Cas9 in genome editing: Its function and medical applications. Journal of Cellular Physiology 234:5751–5761. https://doi.org/10.1002/jcp.27476

Kim YG, Lee JH, Park JG, Lee J (2020) Inhibition of *Candida albicans* and *Staphylococcus aureus* biofilms by centipede oil and linoleic acid. Biofouling 36:126–137. https://doi.org/10.1080/08927014.2020.1730333

Kirsch DR, Whitney RR (1991) Pathogenicity of *Candida albicans* auxotrophic mutants in experimental infections. Infection and Immunity 59:3297–3300

Kuloyo OO (2020) Investigation into the mechanism of arachidonic acid increased fluconazole susceptibility in *Candida albicans* biofilms and application to drug repurposing. Ph.D. Thesis, University of the Free State, Bloemfontein, South Africa

Lacroute F (1968) Regulation of pyrimidine biosynthesis in *Saccharomyces cerevisiae*. Journal of Bacteriology 95:824–832

Lamping E, Ranchod A, Nakamura K, et al (2009) Abc1p Is a multidrug efflux transporter that tips the balance in favor of innate azole resistance in *Candida krusei*. Antimicrobial Agents and Chemotherapy 53:354–369. https://doi.org/10.1128/aac.01095-08

Lamping E, Zhu J, Niimi M, Cannon RD (2017) Role of ectopic gene conversion in the evolution of a *Candida krusei* pleiotropic drug desistance transporter family. Genetics 205:1619–1639. https://doi.org/10.1534/genetics.116.194811

Lemar KM, Passa O, Aon M, et al (2005) Allyl alcohol and garlic (*Allium sativum*) extract produce oxidative stress in *Candida albicans*. Microbiology 151:3257–3265. https://doi.org/10.1099/mic.0.28095-0

Lemke A, Kiderlen AF, Kayser O (2005) Amphotericin B. Applied Microbiology and Biotechnology 68:151–62. https://doi.org/10.1007/s00253-005-1955-9

Li L, Naseem S, Sharma S, Konopka JB (2015) Flavodoxin-like proteins protect *Candida albicans* from oxidative stress and promote virulence. PLoS Pathogens 11:e1005147. https://doi.org/10.1371/journal.ppat.1005147

Lombardi L, Turner SA, Zhao F, Butler G (2017) Gene editing in clinical isolates of *Candida parapsilosis* using CRISPR/Cas9. Scientific Reports 7:1–11. https://doi.org/10.1038/s41598-017-08500-1

Madende M, Albertyn J, Sebolai O, Pohl CH (2020) *Caenorhabditis elegans* as a model animal for investigating fungal pathogenesis. Medical Microbiology and Immunology 209:1–13. https://doi.org/10.1007/s00430-019-00635-4

Marsh EK, May RC (2012) *Caenorhabditis elegans*, a model organism for investigating immunity. Applied and Environmental Microbiology 78:2075–2081. https://doi.org/10.1128/aem.07486-11

Mishra NN, Ali S, Shukla PK (2014) Arachidonic acid affects biofilm formation and $PGE_2$ level in *Candida albicans* and non-*albicans* species in presence of subinhibitory concentration of fluconazole and terbinafine. The Brazilian Journal of Infectious Diseases 18:287–293. https://doi.org/10.1016/j.bjid.2013.09.006

Mokoena NZ, Sebolai OM, Albertyn J, Pohl CH (2020) Synthesis and function of fatty acids

and oxylipins, with a focus on *Caenorhabditis elegans*. Prostaglandins & Other Lipid Mediators 148:106426. https://doi.org/10.1016/j.prostaglandins.2020.106426

Morio F, Lombardi L, Butler G (2020) The CRISPR toolbox in medical mycology: State of the art and perspectives. PLoS Pathogens 16:e1008201. https://doi.org/10.1371/journal.ppat.1008201

Muthamil S, Prasath KG, Priya A, et al (2020) Global proteomic analysis deciphers the mechanism of action of plant derived oleic acid against *Candida albicans* virulence and biofilm formation. Scientific Reports 10:1–17. https://doi.org/10.1038/s41598-020-61918-y

Nandakumar M, Tan MW (2008) Gamma-linolenic and stearidonic acids are required for basal immunity in *Caenorhabditis elegans* through their effects on p38 MAP kinase activity. PLoS Genetics 4:e1000273. https://doi.org/10.1371/journal.pgen.1000273

Nguyen N, Quail MMF, Hernday AD (2017) An efficient, rapid, and recyclable system for CRISPR-mediated genome editing in *Candida albicans*. mSphere 2:e00149-17. https://doi.org/10.1128/mSphereDirect.00149-17

Nollin SD, Borgers M (1975) Scanning electron microscopy of *Candida albicans* after *in vitro* treatment with miconazole. Antimicrobial Agents and Chemotherapy 7:704–711. https://doi.org/10.1128/AAC.7.5.704

Orozco AS, Higginbotham LM, Hitchcock CA, et al (1998) Mechanism of fluconazole resistance in *Candida krusei*. Antimicrobial Agents and Chemotherapy 42:2645–2649. https://doi.org/10.1128/aac.42.10.2645

Paterson PJ, Seaton S, Prentice HG, Kibbler CC (2003) Treatment failure in invasive aspergillosis: Susceptibility of deep tissue isolates following treatment with amphotericin B. Journal of Antimicrobial Chemotherapy 52:873–876. https://doi.org/10.1093/jac/dkg434

Pizzino G, Irrera N, Cucinotta M, et al (2017) Oxidative stress: Harms and benefits for human health. Oxidative Medicine and Cellular Longevity 2017:1–13. https://doi.org/10.1155/2017/8416763

Pohl CH, Kock JLF, Thibane VS (2011) Antifungal free fatty acids. In: Science Against Microbial Pathogens: Communicating Current Research and Technological Advances. Formatex Research Center, Spain

Poulter RT, Rikkerink EH (1983) Genetic analysis of red, adenine-requiring mutants of *Candida albicans*. Journal of Bacteriology 156:1066–1077. https://doi.org/10.1128/jb.156.3.1066-1077.1983

Prasad R, Banerjee A, Shah A (2017) Resistance to antifungal therapies. Essays in Biochemistry 61:157–166. https://doi.org/10.1042/ebc20160067

Raschmanová H, Weninger A, Glieder A, et al (2018) Implementing CRISPR-Cas technologies in conventional and non-conventional yeasts: Current state and future prospects. Biotechnology Advances 36:641–665. https://doi.org/10.1016/j.biotechadv.2018.01.006

Repetto M, Semprine J, Boveris A (2012) Lipid peroxidation: Chemical mechanism, biological implications and analytical determination. Lipid Peroxidation. https://doi.org/10.5772/45943

Ricardo E, Miranda IM, Faria-Ramos I, et al (2014) *In vivo* and *in vitro* acquisition of resistance to voriconazole by *Candida krusei*. Antimicrobial Agents and Chemotherapy 58:4604–4611. https://doi.org/10.1128/aac.02603-14

Sadeghi G, Ebrahimi-Rad M, Mousavi SF, et al (2018) Emergence of non-*Candida albicans* species: Epidemiology, phylogeny and fluconazole susceptibility profile. Journal de Mycologie Médicale 28:51–58. https://doi.org/10.1016/j.mycmed.2017.12.008

Saha SK, Saikot FK, Rahman MS, et al (2019) Programmable molecular scissors: Applications of a new tool for genome editing in biotech. Molecular Therapy - Nucleic Acids 14:212–238. https://doi.org/10.1016/j.omtn.2018.11.016

Scorzoni L, de Lucas MP, Mesa-Arango AC, et al (2013) Antifungal efficacy during *Candida krusei* infection in non-conventional models correlates with the yeast *in vitro* susceptibility profile. PLoS ONE 8:e60047. https://doi.org/10.1371/journal.pone.0060047

Shareck J, Nantel A, Belhumeur P (2011) Conjugated linoleic acid inhibits hyphal growth in *Candida albicans* by modulating Ras1p cellular levels and downregulating *TEC1* expression. Eukaryotic Cell 10:565–577. https://doi.org/10.1128/ec.00305-10

Staab JF, Sundstrom P (2003) *URA3* as a selectable marker for disruption and virulence assessment of *Candida albicans* genes. Trends in Microbiology 11:69–73. https://doi.org/10.1016/s0966-842x(02)00029-x

Tavakoli M, Zaini F, Kordbacheh M, et al (2010) Upregulation of the *ERG11* gene in *Candida krusei* by azoles. Daru: journal of Faculty of Pharmacy, Tehran University of Medical Sciences 18:276–80

Thibane VS, Kock JLF, Ells R, et al (2010) Effect of marine polyunsaturated fatty acids on biofilm formation of *Candida albicans* and *Candida dubliniensis*. Marine Drugs 8:2597–2604. https://doi.org/10.3390/md8102597

Thibane VS, Kock JLF, Van Wyk PWJ, et al (2012) Stearidonic acid acts in synergism with amphotericin B in inhibiting *Candida albicans* and *Candida dubliniensis* biofilms *in vitro*. International Journal of Antimicrobial Agents 40:284–285. https://doi.org/10.1016/j.ijantimicag.2012.05.021

Venkateswarlu K, Denning DW, Kelly SL (1997) Inhibition and interaction of cytochrome P450 of *Candida krusei* with azole antifungal drugs. Medical Mycology 35:19–25. https://doi.org/10.1080/02681219780000821

Vyas VK, Barrasa MI, Fink GR (2015) A *Candida albicans* CRISPR system permits genetic engineering of essential genes and gene families. Science Advances 1:e1500248. https://doi.org/10.1126/sciadv.1500248

Watts JL, Browse J (2002) Genetic dissection of polyunsaturated fatty acid synthesis in *Caenorhabditis elegans*. Proceedings of the National Academy of Sciences of the United States of America 99:5854–5859. https://doi.org/10.1073/pnas.092064799

Weninger A, Hatzl AM, Schmid C, et al (2016) Combinatorial optimization of CRISPR/Cas9 expression enables precision genome engineering in the methylotrophic yeast *Pichia pastoris*. Journal of Biotechnology 235:139–149. https://doi.org/10.1016/j.jbiotec.2016.03.027

Whaley SG, Berkow EL, Rybak JM, et al (2017) Azole antifungal resistance in *Candida albicans* and emerging non-*albicans Candida* species. Frontiers in Microbiology 7:2173. https://doi.org/10.3389/fmicb.2016.02173

Yang WS, Stockwell BR (2016) Ferroptosis: Death by lipid peroxidation. Trends in Cell Biology 26:165–176. https://doi.org/10.1016/j.tcb.2015.10.014

Yehye WA, Rahman NA, Ariffin A, et al (2015) Understanding the chemistry behind the antioxidant activities of butylated hydroxytoluene (BHT): A review. European Journal of Medicinal Chemistry 101:295–312. https://doi.org/10.1016/j.ejmech.2015.06.026

Yoon B, Jackman J, Valle-González E, Cho NJ (2018) Antibacterial free fatty acids and monoglycerides: Biological activities, experimental testing, and therapeutic applications. International Journal of Molecular Sciences 19:1114. https://doi.org/10.3390/ijms19041114

Zarnowski R, Sanchez H, Covelli AS, et al (2018) *Candida albicans* biofilm–induced vesicles confer drug resistance through matrix biogenesis. PLoS Biology 16:e2006872. https://doi.org/10.1371/journal.pbio.2006872

Zhao K, Bleackley M, Chisanga D, et al (2019) Extracellular vesicles secreted by *Saccharomyces cerevisiae* are involved in cell wall remodelling. Communications Biology 2:305 https://doi.org/10.1038/s42003-019-0538-8

# APPENDIX A: ETHICAL CLEARANCE FORM

UNIVERSITY OF THE FREE STATE
UNIVERSITEIT VAN DIE VRYSTAAT
YUNIVESITHI YA FREISTATA

UFS·UV
RESEARCH DEVELOPMENT
NAVORSINGSONTWIKKELING

**Environmental & Biosafety Research Ethics Committee**

11-Jul-2019

Dear **Mr Abdullahi Jamiu**

Project Title: **Influence of polyunsaturated fatty acids on fluconazole susceptibility and drug efflux in Candida krusei**

Department: **Microbial Biochemical and Food Biotechnology Department (Bloemfontein Campus)**

**APPLICATION APPROVED**

This letter confirms that this research proposal was given ethical clearance by the Biosafety & Environmental Research Ethics Committee of the University of the Free State.

Your ethical clearance number, to be used in all correspondence is: **UFS-ESD2019/0029**

**Please note the following:**

1. **This ethical clearance is valid for one year from the issuance of this letter.**
2. **If the research takes longer than one year to complete, please submit a Continuation Report to the Ethics Committee before ethical clearance expires.**
3. **If any changes are made during the research process (including a change in investigators), please inform the Ethics Committee by submitting an Amendment.**
4. **When the research is concluded, please submit a Final Report to the Ethics Committee.**

Thank you for your application and we wish you well in all of your research endeavours.

Yours Sincerely

Prof. RR (Robert) Bragg
Chairperson: Biosafety & Environmental Research Ethics Committee
University of the Free State

Directorate: Research Development
T: +27 (0)51 401 9398 | +27 (0)51 401 2075 | E: smitham@ufs.ac.za
Johannes Brill Building, Room 106D, First Floor
205 Nelson Mandela Drive | Park West, Bloemfontein 9301 | South Africa
P.O. Box 339 | Bloemfontein 9300 | South Africa | www.ufs.ac.za

# APPENDIX B: DEPOSITED MUTANTS' FORMS

**THE UFS UNESCO MIRCEN YEAST CULTURE COLLECTION**

Accession Form **No.** _____

UFS Collection Number: **UOFS Y-** _____ / _____

Received from: _____

_____

Date received: _____

Store: -70°C: _____ -196°C: _____

pr: _____ : _____ done by: _____

NOMENCLATURE DATA :

Species: Candida krusei (Pichia kudriavzevii)

Your Strain Number/Equivalent numbers: ade2Δ/Δ (Parental is C. krusei UFS Y-0217)

HISTORY [if previously received from a different source]:

[received from] The parental strain C. krusei UFS Y-0217 was

[address] received from the Yeast Culture Collection, University of the Free State, Bloemfontein, South Africa.

ISOLATION:

Isolated by:

_____ Date: _____

Isolated or derived from [please give all detail of habitat]: _____

_____

Sample collected by: _____

Identified by: _____ Date of ID: _____

Special characteristics for identification: _____

_____

**THE UFS UNESCO MIRCEN YEAST CULTURE COLLECTION**

Accession Form **No.** _____

UFS Collection Number: **UOFS Y-** _____ / _____

Received from: _____

_____

Date received: _____

Store: -70°C: _____ -196°C: _____

pr: _____ : _____ done by: _____

NOMENCLATURE DATA :

Species: Candida krusei (Pichia kudriavzevii)

Your Strain Number/Equivalent numbers: ura3 Δ/Δ (Parental strain: C. krusei UFS ~~Y-0217~~)

HISTORY [if previously received from a different source]:

[received from] Parental strain was (C. krusei UFS Y-0217) was

[address] received from the Yeast Culture Collection,
University of the Free State, Bloemfontein

ISOLATION:

Isolated by:

_____ Date: _____

Isolated or derived from [please give all detail of habitat]: _____

_____

Sample collected by: _____

Identified by: _____ Date of ID: _____

Special characteristics for identification: _____

_____